

Estudi de l'especificitat metà-llica i del papers dels lligands sulfur en metal-lotioneïnes (MTS) de diversos organismes

Rubén Orihuela García

Memòria presentada per aspirar al Grau de Doctor per Rubén Orihuela García

Vist i plau

Dra. Mercè Capdevila Vidal

Dr. Roger Bofill Arasa

Bellaterra, 10 de Juliol del 2009

Agraïments

Torno la vista enrere, ara fa uns quatre anys, tot just quan acabava la carrera i s'obrien davant meu dos camins: el primer portava cap al món laboral, ple d'incerteses, i el segon cap al món de la recerca. El destí va escollir per a mi i em vaig embarcar en aquest món que tantes alegries m'ha donat.

Principalment m'agradaria donar les gràcies als meus directors, a la Dra. Mercè Capdevila, per obrir-me la ment a noves idees i acollir-me en aquesta petita família, i al Dr. Roger Bofill, per ensenyar-me a ser crític i mostrar-me el camí per arribar (algun dia) a ser un bon científic. Gràcies a tots dos per fer possibles aquests meravellosos quatre anys, tant en l'aspecte professional com en el personal.

Gràcies també al Dr. Joan Sola per posar-me en contacte amb el que ara i sempre serà el meu grup i sobretot per la seva humilitat i bones maneres.

Gràcies a tot el meu grup de recerca, al Dr. Òscar Palacios, el “monstre” de l'espectrometria de masses, amb el que he compartit uns molt bons moments tant dintre com fora del laboratori. Als antics membres del laboratori, els autèntics “seniors”: al Dr. Fernando Novio, per la seva ajuda constant en tot moment, a la Dra. Laura Villarreal, amb la que comparteixo l'afició als gats i que em va passar el relleu en el camp de les MTs, a la Dra. Montserrat Serra, una altra “emetera”, la persona amb la que més he arribat a discutir articles durant aquests anys, i per últim a la properament Dra. Cristina Rodríguez, per ser tan “dissenyosa” i haver-me ajudat tantes vegades.

Un agraïment especial es mereixen les noves adquisicions del grup: l'Ester, la Cata i la Sívia. Gràcies per donar-li vida a aquest laboratori amb la seva “cháchara”.

A la Dra. Sívia Atrian, treballadora incansable i indispensable en aquest tàndem Genètica-Química, gràcies per haver-me iniciat en el meravellós món de la genètica. Gràcies a tots els companys del grup de Genètica, especialment a en Freddy, que encara que només va estar un any amb nosaltres li estic molt agraït per tota l'ajuda que em va donar; a la Míriam, per ser tan simpàtica i treballadora; i al Dr. Jordi Domènech, per la seva excel·lència en la investigació.

Al grup del “LEM”, en especial al Dr. Gonzalo Guirado, per contagiar-me el seu entusiasme per la recerca i a tots els “lemeros” menors, l'Hugo, la Gemma, la Laura i la Conní.

També m'agradaria agrair l'ajuda i recolzament de tots els membres de la Unitat de Química Inorgànica, als presents i als passats: el “nanofreak”, l'Ori, en Dani, en Josep, el Nachete, en Fran, el “mallorquí”, en Sergi, en Toni, en Sergio, la Meri... i un llarg etcètera, moltes gràcies a tots, us trobaré a faltar.

Als membres del Servei d'Anàlisi Química de la UAB, en especial al Dr. Ignasi Villaroya, per la seva col·laboració i ajuda en les mesures de DC i UV-Vis, i a la Dra. Alba Eustaquio, pel suport en les mesures d'ESI-TOF-MS.

Als Serveis Científico-Tècnics de la UB, en especial a la Dra. Elionor Pellfort, per la seva ajuda en mesures d'emissió atòmica.

I per últim donar les gràcies a la meva companya de vida, per “aguantar-me” i acompanyar-me en aquest trajecte durant aquests darrers 5 anys.

ABREUJAMENTS i ACRÒNIMS

3D: tridimensional

ΔHisCeMT2: Pèptid mutant derivat de CeMT2 corresponent a la deleció de la seva His terminal

ε: Coeficient d'extinció molar

C18: Pèptid mutant derivat de QsMT corresponent al domini C-terminal

CeMT1: Metal-lotioneïna MT1 del nematode *Caenorhabditis elegans*

CeMT2: Metal-lotioneïna MT2 del nematode *Caenorhabditis elegans*

Ct-CeMT1: Pèptid mutant derivat de CeMT1 corresponent al domini C-terminal

Ct-CeMT2: Pèptid mutant derivat de CeMT2 corresponent al domini C-terminal

Cup1: Metal-lotioneïna del llevat *Saccharomyces cerevisiae*

Cys: Cisteïna

DC: Dicroisme Circular

DEPC: Pirocarbonat de dietil

DNA: Àcid desoxiribonucleic

e_{aq}⁻: Electrò aquós o electró solvatat

Eq: Equivalent molar

ESI-MS: Espectroscòpia de masses amb ionització per electrosprai

FPLC: *Fast protein liquid chromatography* (cromatografia líquida d'alta resolució)

GC-FPD: Cromatografia de gasos amb detector fotomètric de flama

GSH: Glutatió reduït

GSSG: Glutatió oxidat

H[•]: Radical hidrogen

His: Histidina

ICP-AES: Espectroscòpia d'emissió atòmica de plasma acoblat per inducció

KO: genoanul-lat (*knockout*)

L: Lligand

Lys: Lisina

M: Metall

MeMT: Metal-lotioneïna MT-10-IV del mol·lusc *Mytilus edulis*

Met: Metionina

MT/ MTs: Metal-lotioneïna / metal-lotioneïnes

n1-Cd-Cup1: Metal-lotioneïna nativa Cup1 purificada mitjançant columnes d'intercanvi iònic i d'exclusió per mida

n2-Cd-Cup1: Metal-lotioneïna nativa Cup1 purificada únicament mitjançant columnes d'exclusió per mida.

N25: Pèptid mutant derivat de QsMT corresponent al domini N-terminal

N25-C18: Pèptid mutant derivat de QsMT corresponent a la substitució del seu espaiador per quatre glicines

NHis: Nitrogen histidínic

Nt-CeMT1: Pèptid mutant derivat de CeMT1 corresponent al domini N-terminal

Nt-CeMT2: Pèptid mutant derivat de CeMT2 corresponent al domini N-terminal

OH[•]: Radical hidroxil

PDB: Base de dades de proteïnes amb estructura tridimensional coneguda

POPC: 1-palmitoil-2-oleifosfatidilcolina

QsMT: Metal-lotioneïna de l'alzina surera *Quercus Suber*

RMN: Ressonància Magnètica Nuclear

SCys: Sofre cisteínic

Tris: Tris(hidroximetil)aminometà

Tyr: Tirosina

UV-Vis: Espectres d'absorció UV-visible

ÍNDEX

1. INTRODUCCIÓ	3
1.1 Característiques generals de les metal-lotioneïnes.....	3
1.2 Mètodes d'obtenció de les metal-lotioneïnes	4
1.3 Estructura de les metal-lotioneïnes	6
1.4 Classificació de les metal-lotioneïnes	8
1.5 Lligands no proteics en les metal-lotioneïnes	11
1.5.1 Anions clorur	11
1.5.2 Anions sulfur.....	11
1.6 Funcions de les metal-lotioneïnes	13
1.7 Les metal-lotioneïnes en els organismes vius.....	15
1.7.1 El sistema MT en <i>Mytilus edulis</i>	16
1.7.2 El sistema MT en <i>Quercus suber</i>	18
1.7.1 El sistema MT en <i>Caenorhabditis elegans</i>	19
1.7.2 El sistema MT <i>Saccharomyces cerevisiae</i>	21
2. OBJECTIUS	27
3. RESULTATS I DISCUSSIÓ.....	31
3.1 Estudi de la capacitat coordinant de la metal-lotioneïna MeMT del mol·lusc <i>Mytilus edulis</i>.....	32
3.1.1 Comportament de MeMT envers Zn(II) i Cd(II)	33
3.1.2 Comportament de MeMT envers Cu(I)	35
3.2 Estudi de la capacitat coordinant de la metal-lotioneïna QsMT de l'alzina surera <i>Quercus suber</i>.....	37
3.2.1 Comportament de QsMT envers Zn(II) i Cd(II)	38
3.3 Estudi de la capacitat coordinant de les metal-lotioneïnes CeMT1 i CeMT2 del nematode <i>Caenorhabditis elegans</i>.....	43
3.3.1 Comportament de CeMT1 envers Zn(II) i Cd(II)	44
3.3.2 Comportament de CeMT2 envers Zn(II) i Cd(II)	45
3.3.3 Comportament de CeMT1 envers Cu(I).....	47
3.3.4 Comportament de CeMT2 envers Cu(I).....	48
3.3.5 Estudi del paper de les His en la coordinació metàl·lica en CeMT1 i CeMT2.....	49

3.3.5.1	Estudi del paper coordinant de la His terminal de CeMT2.....	50
3.3.5.2	Estudi de la reactivitat de les His de CeMT1 i CeMT2 envers el DEPC.....	52
3.4	Estudi de la capacitat coordinant de la metal-lotioneïna Cup1 del llevat <i>Saccharomyces cerevisiae</i>.....	54
3.4.1	Comportament de Cup1 recombinant envers Zn(II) i Cd(II).....	55
3.4.2	Comportament de Cup1 recombinant envers Cu(I).....	57
3.4.3	Purificació i caracterització de la metal-lotioneïna nativa Cup1 en presència de Cd(II)	58
3.5	Estudi del comportament de les metal-lotioneïnes envers l'estrés reductor.....	61
3.5.1	Reactivitat de QsMT envers els radicals lliures	62
3.6	Vers una nova proposta de classificació de les MTs	66
4.	CONCLUSIONS	75
5.	PROCEDIMENT EXPERIMENTAL I TÈCNIQUES UTILITZADES	81
5.1	Obtenció i caracterització de la proteïna	81
5.2	Espectrometria de masses (ESI-MS-TOF)	82
5.3	Espectroscòpia d'emissió atòmica amb plasma acoblat per inducció (ICP-AES)	83
5.4	Espectroscòpia d'absorció ultraviolat-visible (UV-Vis).....	84
5.5	Espectroscòpia de dicroisme circular (DC)	85
5.6	Cromatografia de gasos amb detecció fotomètrica de flama (GC-FPD).....	86
5.7	Valoracions de les formes Zn-MT amb solucions de Cd(II) i Cu(I)	86
5.7.1	Agent valorant de Cd(II).....	86
5.7.2	Agent valorant de Cu(I).....	87
5.8	Acidificació-reneutralització de les formes Cd-MT	87

6. BIBLIOGRAFIA	93
7. ANNEX	
Article 1.....	103
“The metal binding features of the recombinant mussel <i>Mytilus edulis</i> MT-10-IV metallothionein”	
Article 2.....	121
“The Cd ^{II} -binding abilities of recombinant <i>Quercus suber</i> metallothionein: bridging the gap between phytochelatins and metallothioneins”	
Article 3.....	149
“ <i>C.elegans</i> metallothionein isoform specificity: metal-binding abilities and histidine role in CeMT1 and CeMT2”	
Article 4.....	169
“Cup1 revisited: divalent metal ion binding analysis unveils the presence of acid-labile sulfide (S ²⁻) ligands in native complexes”	
Article 5	181
“Zinc and cadmium complexes of a plant metallothionein under radical stress: desulfurization reactions associated with the formation of <i>trans</i> lipids in model membranes”	

1. Introducció

1. INTRODUCCIÓ

1.1 Característiques generals de les metal-lotioneïnes

Les metal-lotioneïnes, MTs, són unes metal-loproteïnes molt particulars que es caracteritzen per la seva elevada capacitat per coordinar i bescanviar ions metàl·lics. Oficialment van ser descobertes l'any 1957 per Margoshes i Vallee a partir de còrtex renal de cavall com a proteïnes associades a zinc i cadmi.¹ En aquell moment aquests autors les van anomenar metal-lotioneïnes degut al seu elevat contingut en metall i en residus de cisteïna. Les MTs constitueixen una gran família de proteïnes, presents en una àmplia gamma d'organismes vius -s'han trobat tant en organismes unicel·lulars (cianobacteris, llevats, protozous i recentment micobacteris²) com en pluricel·lulars (vertebrats, invertebrats i plantes).

Totes les MTs presenten les següents característiques comunes:

- Baix pes molecular (2-12 kDa).
- Elevat contingut en cisteïna (aproximadament el 30% dels aminoàcids).
- Elevada capacitat per coordinar i bescanviar ions metàl·lics.
- Baix contingut en residus hidrofòbics.
- Absència, en general, de residus aromàtics.
- Motius cisteínics característics: Cys-X-Cys, Cys-Cys o Cys-Cys-Cys (essent X un aminoàcid diferent a la cisteïna).

L'alt contingut en residus de cisteïna és el que més caracteritza aquestes proteïnes, ja que les Cys són les responsables principals de la coordinació metàl·lica, si bé de vegades els residus de His també poden coordinar metalls. El característic grup tiolat de les Cys actua com una base tova, de manera que té tendència a coordinar àcids de Lewis tous com el Cd(II) o el Cu(I) i àcids intermedis com el Zn(II). En els organismes vius, les MTs natives es troben enllaçades a metalls essencials com el Zn(II) i el Cu(I), així com també a metalls tòxics com Cd(II), Hg(II), Ag(I) o Pb(II).³ Addicionalment, estudis realitzats *in vitro* demostren que les MTs també poden enllaçar-se a altres ions metàl·lics com Au(III), Bi(III), Fe(II), Ni(II), Pt(II) i Tc(IV).⁴

1.2 Mètodes d'obtenció de les metal-lotio-neïnes

El procediment tradicional d'obtenció de MTs, i el més utilitzat fins a la dècada dels 90, es basa en la inducció de la seva síntesi en éssers vius per diferents vies i el seu posterior aïllament i purificació a partir dels teixits on més s'expressa la proteïna. Les MTs es veuen induïdes per un gran nombre de factors, com per exemple la presència d'ions metàl·lics, agents radicals oxidants, exposició a radiació UV o determinades hormones. Aquest mètode permet obtenir les MTs en forma nativa presents en els diferents teixits d'animals o plantes; ara bé, aquest mètode comporta dos grans inconvenients: a) el llarg i difícil procediment de purificació i b) la baixa concentració i pureza de les MTs natives obtingudes.⁵

Un mètode alternatiu per pal·liar els inconvenients de l'anterior però força menys utilitzat és la síntesi química de cadenes peptídiques sobre suport sòlid per produir apo-MT, és a dir, la seqüència de la proteïna sense enllaçar cap ió metàl·lic. Aquesta metodologia ha permès caracteritzar MTs de fongs^{6,7} i els dominis per separat d'algunes MTs de mamífer.⁶⁻¹¹ Aquesta metodologia, però, també presenta les seves limitacions, com són la dificultat de sintetitzar cadenes peptídiques llargues o la necessitat de protegir els residus cisteínics per evitar la seva oxidació.

Una alternativa òptima i més actual són les tècniques d'enginyeria genètica, més conegudes com a tècniques de l'ADN recombinant.¹² Es tracta d'aprofitar els mecanismes cel·lulars propis de síntesi de proteïnes en bacteris per a obtenir quantitats elevades d'un producte que normalment no es sintetitzaria en aquestes cèl·lules (producte heteròleg). Per aconseguir-ho s'ha d'introduir al bacteri un ADN que contingui tota la informació per a la síntesi de MT, els senyals de transcripció i traducció adequats i també la informació genètica addicional que garanteixi que la molècula de l'ADN que conté tots aquests elements es mantingui estable dins la cèl·lula i es transmeti als descendents (Figura 1). L'ADN que porta aquesta informació es denomina *vector*, la cèl·lula emprada per a la síntesi de la molècula heteròloga *hoste* i la proteïna així obtinguda *proteïna recombinant*. Aquesta tècnica permet obtenir quantitats elevades de MTs recombinants d'una pureza molt elevada i de propietats idèntiques a les MTs natives.¹³ D'altra banda, l'enginyeria genètica també permet modificar les seqüències d'ADN per a obtenir proteïnes modificades a nivell d'estructura primària en les posicions desitjades (mutagènesi dirigida). Aquesta tècnica permet introduir mutacions puntuals d'aminoàcids en els punts d'interès, fet

que no és possible mitjançant el mètode d'obtenció tradicional a partir de teixits d'animals o plantes.

El conjunt d'avantatges exposats ha fet que actualment el mètode de l'ADN recombinant sigui el mètode més utilitzat per a la obtenció de MTs i el que s'ha emprat per a obtenir les MTs estudiades en aquesta Tesi Doctoral.

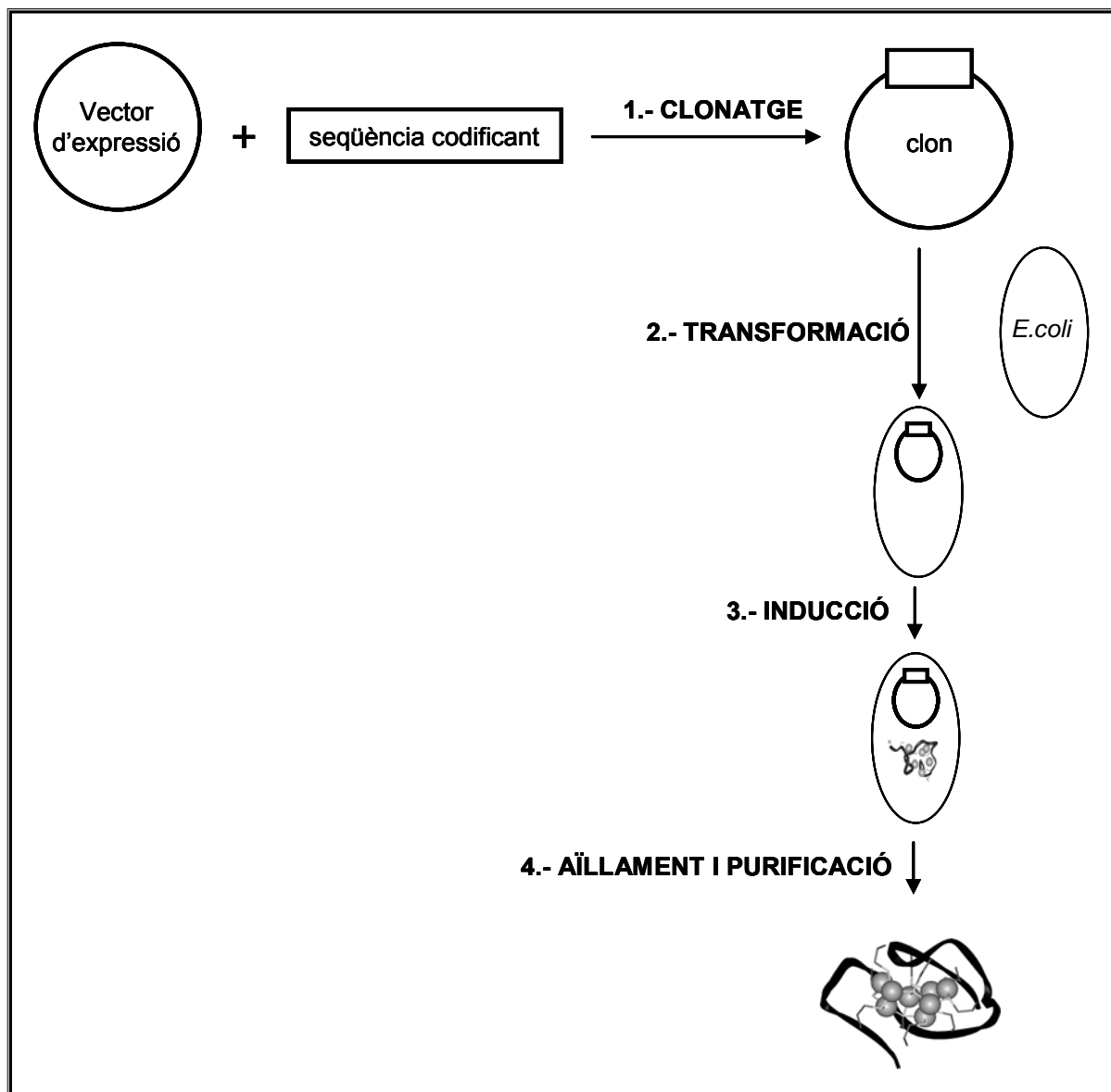


Figura 1.- Esquema general d'obtenció i purificació d'una proteïna recombinant.

1.3 Estructura de les metal-lotioneïnes

És ben conegut que les MTs només adopten un plegament tridimensional estable i ben definit quan coordinen ions metà·lics, majoritàriament via enllaços metall-SCys (o bé metall-NHis). Així doncs, la coordinació dels ions metà·lics és el que determina com serà el plegament de les MTs, ja que gràcies a la gran flexibilitat de la cadena peptídica aquesta pot disposar espacialment els tiolats cisteínics de manera que puguin satisfer els diferents entorns de coordinació preferits dels diferents ions metà·lics, fins i tot encara que difereixin força en el seu radi atòmic.⁴ En canvi, les metal-lotioneïnes en la seva forma demetal·lada, que es coneixen amb el nom d'apometal-lotioneïnes (apo-MT), presenten una estructura desordenada (*random coil*).^{14,15}

Degut a la flexibilitat de la cadena polipeptídica i a la fluctuació dinàmica dels ions metà·lics coordinats a aquesta, fins al moment només s'han resolt unes poques estructures tridimensionals de MTs amb tècniques de ressonància magnètica multinuclear (RMN) o per difracció de raigs X (Taula 1).

Organisme	Metal-lotioneïna	Tècnica
Mamífer (humà, rata i conill)	Cd ₇ -MT2	RMN ¹⁶⁻¹⁸ ,
Mamífer (rata)	Zn ₂ Cd ₅ -MT2	Difracció de raigs X ¹⁹
Mamífer (ratolí)	Cd ₇ -MT1	RMN ²⁰
Mamífer (ratolí i humà)	Cd ₄ -αMT-3	RMN ^{21,22}
Peix (<i>N.coriiceps</i>)	Cd ₇ - ncMT	RMN ²³
Crustaci (<i>C.sapidus</i>)	Cd ₆ -MT1	RMN ²⁴
Crustaci (<i>H.americanus</i>)	Cd ₆ -MT1	RMN ²⁵
Equinoderm (<i>S.Purpuratus</i>)	Cd ₇ -MTA	RMN ²⁶
Llevat (<i>S.cerevisiae</i>)	Cu ₇ -MT, Ag ₇ -MT	RMN ^{27,28}
Llevat (<i>S.cerevisiae</i>)	Cu ₈ -MT	Difracció de raigs X ²⁹
Bacteri (<i>Synechococcus</i>)	Cd ₄ -SmtA	RMN ³⁰
Fong (<i>N.crassa</i>)	Cd ₆ -NcMT	RMN ³¹

Taula 1.- MTs amb l'estructura tridimensional inclosa en el *Protein Data Bank* (PDB).

Tret de la MT SmtA de cianobacteri, que només presenta un sol domini,³⁰ totes les estructures tridimensionals resoltes de MTs amb metalls divalents -Zn(II) i Cd(II)- presenten una estructura dividida en dos dominis separats, cadascun amb un clúster metall-tiolat. Així, per exemple, en la MT de mamífer,¹⁶⁻²² el seu domini N-terminal (domini β) està format per 3 ions divalents enllaçats tetraèdricament a 9 tiolats cisteínics ($M_3(SCys)_9$) i el seu domini C-terminal (domini α) forma un clúster amb 4 ions divalents també coordinats tetraèdricament a 11 residus de cisteïna ($M_4(SCys)_{11}$) (Figura 2.a).

L'any 2001 el grup dirigit pel Prof. Sadler va descriure per primera vegada una metal-lotioneïna de cianobacteri formada per un sol clúster metall-MT, similar al que presenta el domini α de mamífer, però en el que el lloc ocupat per dues cisteïnes correspon ara a dues histidines, formant un clúster $[M_4(SCys)_9(NHis)_2]$ (Figura 2.b). Quan aquesta MT s'obté unida a ions Zn(II) un d'aquests és inert enfront a la substitució per ions Cd(II), de manera que s'ha associat SmtA a les proteïnes conegudes com a dits de zinc (*zinc fingers*).³⁰

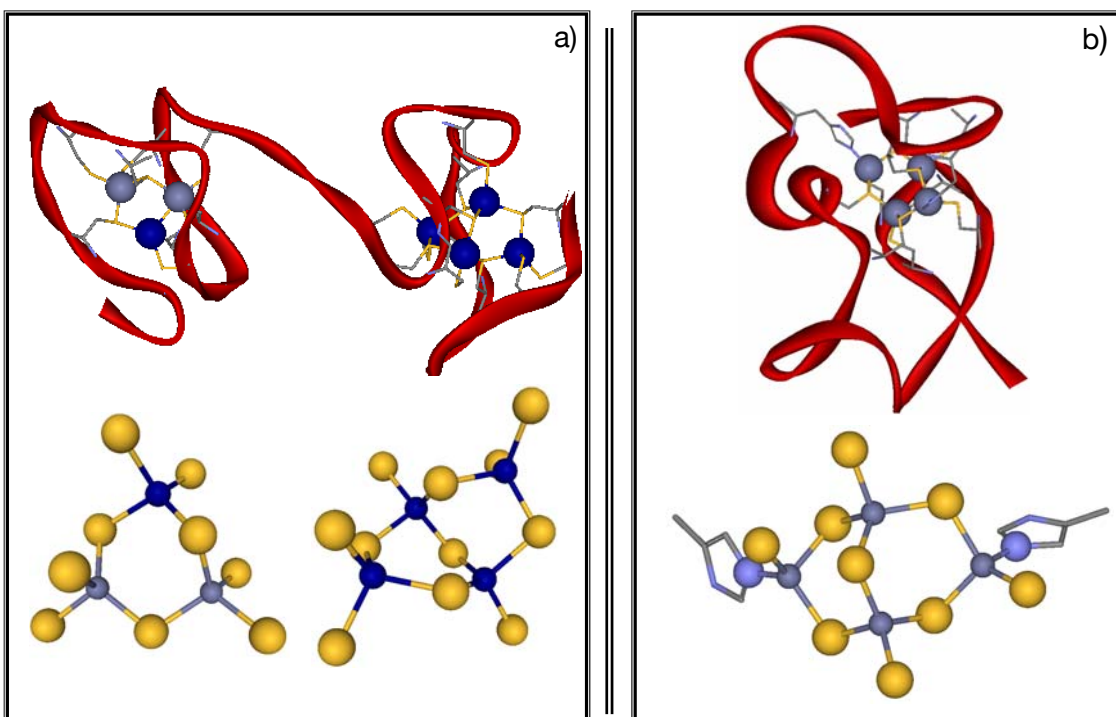


Figura 2.- Estructures tridimensionals, resoltes per RMN, de MTs enllaçades a ions divalents: a) Zn_2Cd_5 -MT2 de mamífer (rata) resolta per difracció de raigs X i els seus dominis β i α formats pels agregats $Cd_1Zn_2-(SCys)_9$ i $Cd_4-(SCys)_{11}$, respectivament i b) Zn_4 -SmtA de cianobacteri (MT de *Synechococcus*) i l'agregat $Zn_4-(SCys)_9(NHis)_2$ que forma.

Pel que fa als metalls monovalents, quan les MTs coordinen Cu(I) ho fan mitjançant dos o tres lligands cisteíncs, amb geometria lineal o trigonal-plana.^{4,14,32} En tots els casos el coure enllaçat es troba en estat d'oxidació +1, ja que el Cu(II) és capaç d'oxidar la cisteïna formant cistina³³ (un pont disulfur entre dues cisteïnes) tot reduint-se a Cu(I).

La informació estructural dels agregats que formen les MTs amb el Cu(I) és molt escassa principalment degut a la manca d'activitat en la RMN (moment quadrupolar del Cu(I)=5/2) i a la dificultat d'obtenir monocristalls d'aquests complexos aptes per a la difracció de raigs X.²⁹ Tot i així, s'ha aconseguit resoldre l'estructura de la MT de llevat *Saccharomyces cerevisiae* (Cup1) tant per difracció de raigs X²⁹ com per RMN^{27,28} (Figura 3) i la de la MT del fong *Neurospora crassa* (Nc-MT) per RMN.³¹ En ambdós casos la proteïna forma un únic clúster metàl·lic donant lloc a les formes Cu₈-Cup1 i Cu₆-NcMT, respectivament.

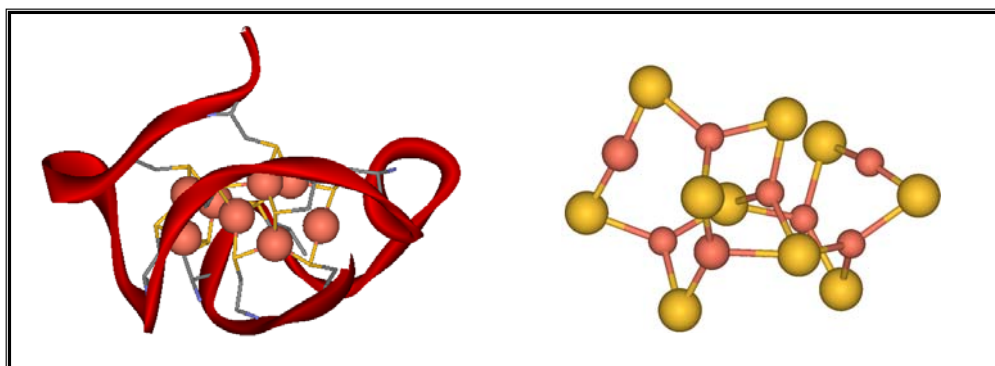


Figura 3.- Estructura tridimensional de Cu₈-Cup1 de llevat (*Saccharomyces cerevisiae*) resolta per difracció de raigs X i agregat Cu₈-(SCys)₁₀ que forma.

1.4 Classificació de les metal-lotioneïnes

Normalment les proteïnes es classifiquen segons la seva funcionalitat (proteases, oxigenases, reductases, etc). En el cas de les MTs, no s'ha pogut fer d'aquesta manera ja que avui dia encara es discuteix quina pot ser la seva funció fisiològica principal. Per aquest motiu s'han fet diverses propostes de classificació en funció de les seves homologies de seqüència i característiques estructurals.

La primera classificació es va proposar l'any 1985 durant el Segon Congrés Internacional de Metal-lotioneïnes, on es va establir una subdivisió de les mateixes en tres grans grups en funció de la seva estructura primària:³⁴

- **Classe I**, MTs amb una alta homologia de seqüència amb la isoforma MT1 de ronyó de cavall i estructurades en dos dominis. Contenen entre 59 i 63 aminoàcids, dels quals al voltant de 20 són Cys. Aquests tipus de MTs es troben en la majoria de vertebrats i en alguns invertebrats.
- **Classe II**, MTs que presenten una gran heterogeneïtat de seqüències i són no alineables ni entre si ni amb la isoforma MT1 de cavall. Aquestes MTs es troben en plantes, fongs, invertebrats i alguns bacteris. La majoria estan constituïdes per un únic domini.
- **Classe III**, les anomenades cadistines, fitoquelatines (PCs) i altres polipèptids de fórmula general (γ -Glu-Cys)_nGly, de síntesi enzimàtica, que es troben principalment en vegetals i organismes unicel·lulars. Les PCs coordinen ions metàl·lics divalents mitjançant cisteïnes i anions sulfur, formant estructures en les que el recobriment proteic embolcalla un microcristall de sulfur metàl·lic (Figura 4), que rep el nom de *crystallite*.³⁵

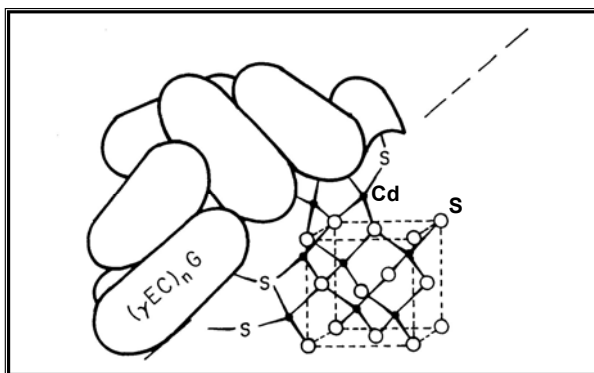
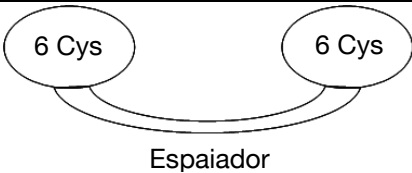
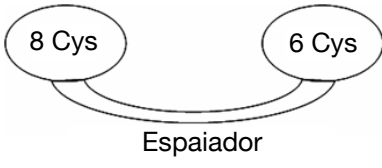
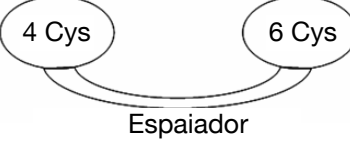
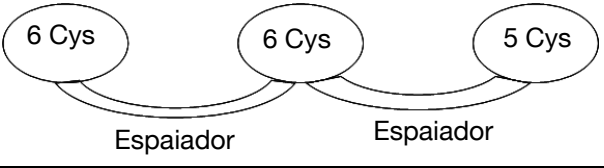


Figura 4.- En els agregats metall-MT de les PCs la proteïna recobreix els microcristalls de CdS (*crystallites*), els quals s'uneixen a la PC mitjançant enllaços Cd-SCys (extret de Winge *et al.*³⁵).

L'any 1999 els investigadors Binz i Kägi van proposar un nou sistema d'ordenació en base a similituds de seqüència globals. Aquesta classificació, molt més detallada, divideix les MTs en famílies, subfamílies, subgrups, isoformes i subisoformes, pràcticament donant lloc a tants tipus de MTs com grups taxonòmics es coneixen.^{36,37}

Un exemple particular d'aquesta classificació és el cas de les MTs de planta. Aquesta família de MTs es caracteritza per la presència de com a mínim un domini sense cisteïnes (*espaiador*) entre dos dominis rics en aquest aminoàcid. Cobbet i Goldsbrough van completar la classificació general proposada per Binz i Kägi

classificant les MTs de planta en 4 tipus diferents (Taula 2) en funció del nombre de cisteïnes que conté cada domini.³⁸

Tipus 1	
Tipus 2	
Tipus 3	
Tipus 4	

Taula 2.- Representació esquemàtica dels diferents tipus de MTs de planta (adaptada de Cobbet i Goldsbrough³⁸).

En qualsevol cas, cap de les dues classificacions esmentades proporciona informació funcional o evolutiva de les MTs, ja que únicament es basen en la similitud de seqüència. Per aquest motiu l'any 2001 el grup de recerca on s'ha realitzat aquesta Tesi va proposar un nou model de classificació de les MTs, basat tant en la seva seqüència aminoacídica com en la seva preferència envers els ions metàl·lics essencials Zn(II) i Cu(I).³⁹ Si els ions metàl·lics coordinats a les MTs determinen la seva estructura, sembla probable que Zn(II) i Cu(I), amb característiques coordinants pròpies, donin lloc a agregats metall-MT diferents. En conseqüència, i en base a les relacions estructura/funció, cal esperar que estructures diferents també determinin funcions diferents per a aquestes metal-loproteïnes. Així, per a classificar-les, cal avaluar la seva capacitat coordinant envers aquests dos metalls essencials, cosa que es fa mitjançant la seva producció recombinant en medis de cultiu enriquits amb aquests ions metàl·lics, l'estudi de la substitució Zn^{II}/Cd^{II} i Zn^{II}/Cu^I *in vitro* del Zn(II) inicialment coordinat *in vivo* i l'anàlisi qualitativa i quantitativa de la composició i estructura dels agregats metàl·lics formats. D'aquesta manera les MTs es poden classificar com a:

- **Zn-tioneïna:** Aquella MT que en medis rics en Cu(II) dóna lloc a espècies heterometà·liques Zn,Cu-MT i que per tant requereix Zn(II) per a estructurar-se *in vivo* en presència de Cu(I).
- **Cu-tioneïna:** Aquella MT que en medis rics en Cu(II) dóna lloc a espècies homometà·liques Cu-MT i que per tant no requereix Zn(II) per a estructurar-se *in vivo* en presència de Cu(I).

1.5 Lligands no proteïcs en metal-lotioneïnes

A part dels aminoàcids cisteïna i histidina, en la bibliografia es troben exemples de lligands inorgànics formant part dels complexos metall-MT. D'entre aquests, els més importants són els anions clorur i els anions sulfur, ambdós descrits pel grup de recerca on s'emmarca aquesta Tesi Doctoral.^{40,41}

1.5.1 Anions clorur

La participació de lligands clorur en MTs va ser proposada per primera vegada l'any 2002 per part del grup de recerca del Dr. Vallee quan estudiava la interacció de les metal-lotioneïnes amb l'ATP.⁴² En aquest estudi es va observar que els anions clorur actuaven com a lligands en les MTs, enllaçant-se als residus de lisina. Posteriorment, el grup de recerca en el qual s'ha emmarcat aquesta Tesi Doctoral va proposar també la participació d'anions clorur en els agregats metall-MT.⁴¹ Tot i que la presència d'aquest anió ha estat demostrada mitjançant estudis espectroscòpics (DC, UV, Raman) avui en dia encara no s'ha aconseguit caracteritzar espectromètricament cap complex metall-MT amb anions clorur coordinats.

1.5.2 Anions sulfur

La presència d'ions sulfur (S^{2-}) va ser inicialment descrita en els agregats metà·lics d'uns pèptids molt propers a les MTs^{43 - 45} anomenats fitoquelatines (inicialment considerades com a metal-lotioneïnes de tipus 3, vegi's apartat 1.3). Aquests polipèptids de síntesi enzimàtica coordinen metalls mitjançant cisteïnes i anions sulfur àcid-làbils.³⁵ L'any 2005 el grup de recerca en el qual he treballat durant

aquesta Tesi Doctoral va descriure per primera vegada la presència d'aquests lligands en MTs recombinants produïdes en *E.coli*.⁴⁰ Fins al moment s'han detectat anions sulfur àcid-làbils en els complexos Zn-MT i Cd-MT, essent en aquests últims molt més abundants.^{40,46,47} En les MTs estudiades, els resultats indiquen la coexistència en una mateixa mostra d'agregats metall-MT amb ions sulfur i sense, encara que la presència d'aquests no sembla incrementar la capacitat coordinant dels pèptids. En la Figura 5 es mostren els espectres representatius de DC de diverses formes Cd-MT obtingudes recombinantment que contenen en els seus complexos lligands sulfur àcid-làbils.

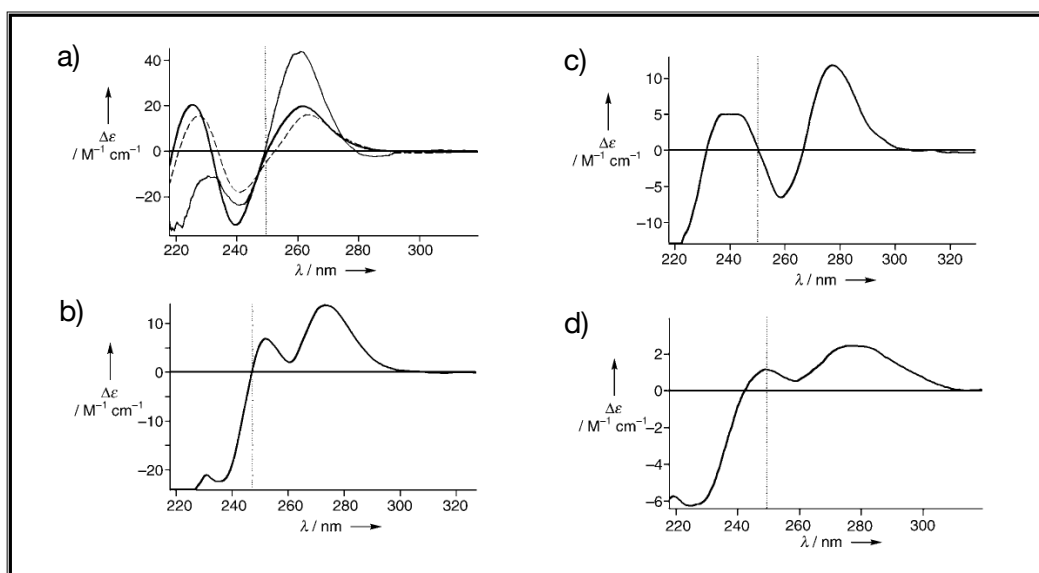


Figura 5.- Espectres de DC representatius d'algunes Cd-MTs que contenen ions sulfur. Tots els espectres mostren les absorcions de DC característiques dels cromòfors Cd-(SCys)₄ a 250 nm ja sigui en forma de gaussiana (d) com en forma de derivada (a,b,c). En tots quatre espectres s'observen absorcions en la zona de 280 nm atribuïbles a la presència d'enllaços Cd-S²⁻ (adaptació de Capdevila *et al.*⁴⁰).

La presència d'aquests anions en les MTs ha suscitat una gran controvèrsia entre els diferents especialistes en el camp.⁴⁸ Per exemple, alguns autors suggereixen que la presència de sulfur en MTs recombinants és deguda al propi metabolisme dels bacteris. En aquest sentit, en la bibliografia es troben estudis on es descriu la producció de nanopartícules de CdS per part d'*E.coli* només afegint al medi de cultiu CdCl₂ i Na₂S.⁴⁹

Així doncs, un dels objectius d'aquesta Tesi Doctoral serà determinar si les MTs natives provinents d'altres organismes que no siguin *E.coli* també presenten en els seus agregats lligands sulfur àcid-làbils, demostrant així que aquests lligands sulfur no són artefactes provinents del metabolisme dels bacteris.

1.6 Funcions de les metal-loproteïnes

Després de més de mig segle d'ençà del seu descobriment i amb uns 20000 articles científics relacionats, la comunitat científica encara debat quines són les funcions de les MTs.

La funció més acceptada entre els investigadors és la capacitat destoxicadora de les MTs davant de metalls pesants basant-se en: a) l'augment de la sensibilitat enfront de la contaminació amb cadmi dels organismes i cèl·lules que han estat modificades genèticament i que no poden sintetitzar MT⁵⁰⁻⁵² i en b) l'efecte inductor que tenen els metalls tòxics com Ag(I), Cd(II) i Hg(II) sobre els gens que codifiquen per a aquestes proteïnes.⁵²⁻⁵⁶ Ara bé, donat que la contaminació per Cd(II) és un fenomen recent en la nostra societat i que l'estructura primària de les MTs està altament conservada entre els diferents organismes, és molt probable que la destoxicació de metalls pesants com el Cd(II) no correspongui a cap funció evolutiva de les MTs. Per tant, aquestes propietats destoxicadores semblarien ser més una conseqüència indirecta del seu elevat contingut en residus coordinants que no pas conseqüència directa del seu procés evolutiu.

Una altra funció atribuïda a les MTs és l'homeòstasi d'ions Zn(II) i Cu(I).^{57,58} Per exemple, en mamífers el zinc és l'element de transició més abundant després del ferro, i el coure és un oligoelement indispensable per a la vida, ja que forma part de molts centres actius en diferents metal-loproteïnes. Actualment no es té gaire informació sobre els transportadors d'aquests metalls i les interaccions amb els diferents components intracel·lulars, però alguns estudis suggereixen que les MTs podrien estar relacionades en la regulació de l'absorció de Zn(II) i Cu(I), la seva distribució i emmagatzematge i el seu alliberament.^{50,54}

S'ha proposat també que les MTs podrien actuar com a carrabines moleculars (*chaperones*) per a la síntesi de metal-loproteïnes i de factors de transcripció dependents de metall, actuant com a reservori de zinc i transferint-lo a aquests.⁵⁹ Aquesta funció seria duta a terme pels grups tiol de les MTs, els quals s'oxidarien davant el glutatió oxidat (GS-SG), formant ponts disulfur (cistina) i glutatió reduït (GSH), amb el consegüent alliberament de metall. En definitiva, les MTs es veurien implicades en un cicle redox, tal i com es mostra en la Figura 6.⁶⁰

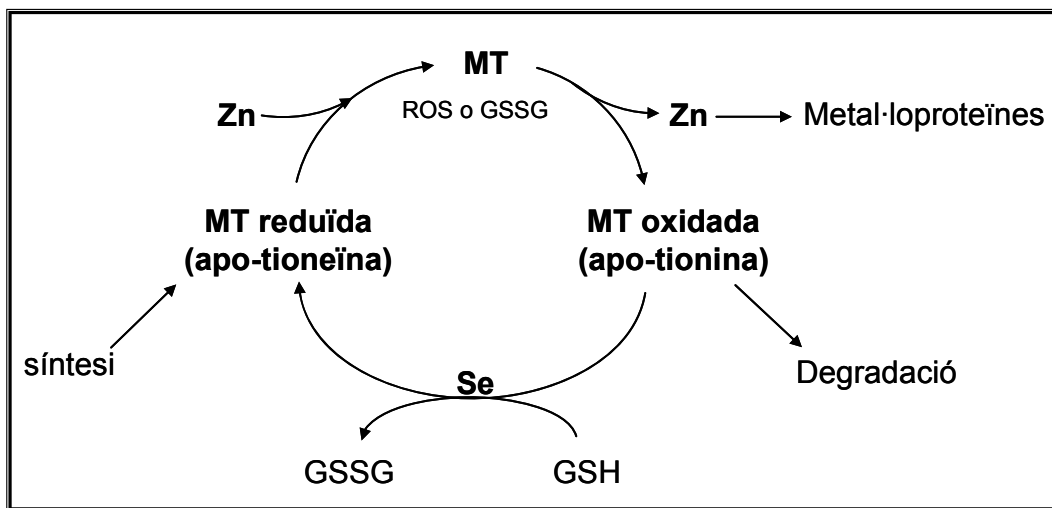


Figura 6.- Representació esquemàtica del cicle redox proposat per a les MTs. El Zn(II) unit a la MT s'alliberaria quan la cisteïna és oxidada. Aquesta MT oxidada podria ser degradada o bé reduïda en presència de glutatí (GSH) amb l'ajut de catalitzadors de seleni (glutatí peroxidasa). En presència de Zn(II), la MT reduïda seria ràpidament reconstituïda, tancant-se d'aquesta manera el cicle (adaptació de Kang⁶⁰).

El paper de les MTs com a agents antioxidants també ha estat àmpliament estudiat.⁶¹ La presència d'espècies reactives d'oxigen (ROS) a la cèl·lula és una de les causes principals de l'apoptosi (mort cel·lular autoprogamada)^{62,63} i s'ha comprovat que aquesta augmenta en les cèl·lules on no es sintetitza MT. Així doncs, s'ha proposat que les MTs podrien participar en el procés d'eliminació dels radicals lliures hidroxil, peròxid o superòxid,^{60,64,65} reaccionant-hi directament i oxidant-se, formant ponts disulfur o bé cedint ions zinc o coure a enzims antioxidants, com per exemple la superòxid dismutasa (SOD).^{66,67}

D'altra banda, els estudis amb organismes on s'ha suprimit l'expressió gènica de les MTs (MT *knockout* o MT KO) també han permès aprofundir en el coneixement que es té sobre les MTs.^{68,69} Així, s'ha vist com els ratolins MT-KO tenen tendència a patir obesitat, de manera que les MTs podrien estar implicades en la regulació del balanç energètic cel·lular.⁷⁰

Així doncs, les funcions més importants atribuïdes a les MTs serien:

- paper destoxicador de metalls tòxics.
- homeòstasi de Zn(II) i Cu(I).
- Actuar de carrabines moleculars per a la síntesi de metal-loproteïnes.
- propietats antioxidants i antiapoptòtiques.
- control metabòlic de la producció d'energia.

1.7 Les metal-lotioneïnes en els organismes vius

Les MTs es troben presents en la pràctica totalitat dels éssers vius i avui dia es coneixen més de 250 metal-lotioneïnes procedents del regne animal, vegetal i procariota.³⁷ D'aquestes, les més conegudes i estudiades han estat les MTs de mamífer i fong i darrerament les de planta. En la bibliografia es poden trobar una gran varietat de treballs tant a nivell biològic (purificació, patrons d'expressió, estudis genètics...) com químic (reactivitat, estructuració, estudis espectroscòpics...).

En mamífer s'han aïllat fins a quatre gens codificant de MT (isoformes MT1, MT2, MT3 i MT4) i on alguna isoforma pot presentar subisoformes (MT1a, MT1b...), com és el cas de l'isoforma MT1 de l'esser humà, de la que se'n coneixen 13 subisoformes. Aquestes quatre isoformes presenten similitud de seqüència i 20 cisteïnes en posicions totalment conservades, encara que existeixen diferències en el seu patró d'expressió. Així, mentre que MT1 i MT2 es sintetitzen constitutivament i ubiqua, MT3 només es sintetitzada en el sistema nerviós central i MT4 en l'epiteli escamós estratificat.^{71,72}

Al contrari, les MTs d'invertebrats constitueixen una família molt heterogènia i en general menys estudiada des del punt de vista químic o estructural.⁷³ Es coneixen estudis en sistemes MT en insectes,⁷⁴ crustacis,⁷⁵⁻⁷⁷ equinoderms,²⁶ mol·luscos,⁷⁸ i nematodes.^{79,80} D'altra banda, la majoria del treballs realitzats sobre invertebrats aquàtics, tant mol·luscs com crustacis o anèl·lids, han consistit en analitzar el paper fisiològic de les MTs i el seu potencial ús com a biomarcadors de la contaminació d'una regió.⁵⁴

Pel que fa a les MTs de planta, la primera indicació de la seva existència es dóna l'any 1987, quan Kennedy i col·laboradors⁸¹ van aïllar i seqüenciar parcialment una proteïna de la llavor de blat que contenia grans quantitats de Zn(II) i que van anomenar EC protein (*Early Cysteine-labelled protein*). Des d'aleshores s'han descrit un gran nombre de gens de MTs en diferents espècies i s'han efectuat estudis d'expressió que els relacionen principalment amb l'homeòstasi del coure, especialment en processos de senescència d'òrgans i teixits vegetals.^{82,83} En general, però, aquestes proteïnes han estat tant des del punt de vista estructural com funcional molt poc estudiades.

Donat que en aquesta Tesi Doctoral s'aprofundirà en el coneixement de metal-lotioneïnes d'invertebrats (el mol·lusc *Mytilus edulis* i el nematode *Caenorhabditis elegans*), planta (*Quercus suber*) i llevat (*Saccharomyces cerevisiae*), a

continuació es presenta, amb més detall un resum dels coneixements actuals dels sistemes MT en aquests organismes.

1.7.1 El sistema MT en *Mytilus edulis*



M. edulis és el nom científic del musclo atlàctic o musclo comú. En aquest organisme s'han identificat fins al moment 10 isoformes de MT dividides en dues grans famílies, MT10 i MT20³⁷ (Figura 7.a). La síntesi de les isoformes MT10 s'indueix per la presència de zinc o per baixes concentracions de cadmi, en canvi la síntesi de les isoformes MT20 només és induïda a altes concentracions de cadmi. Això ha fet que fins ara s'hagi atribuït un paper homeostàtic a les primeres i un paper destoxicador a les darreres.⁸⁴⁻⁸⁷ Gràcies a aquestes propietats, des de fa uns anys la síntesi de MT en *M.edulis* (i en altres invertebrats aquàtics com l'ostra *Crassostrea gigas*⁸⁸ o la cloïssa *Ruditapes decussatus*⁸⁹) s'ha fet servir com a biomarcador de la presència de metalls tòxics en ecosistemes aquàtics.⁵⁴

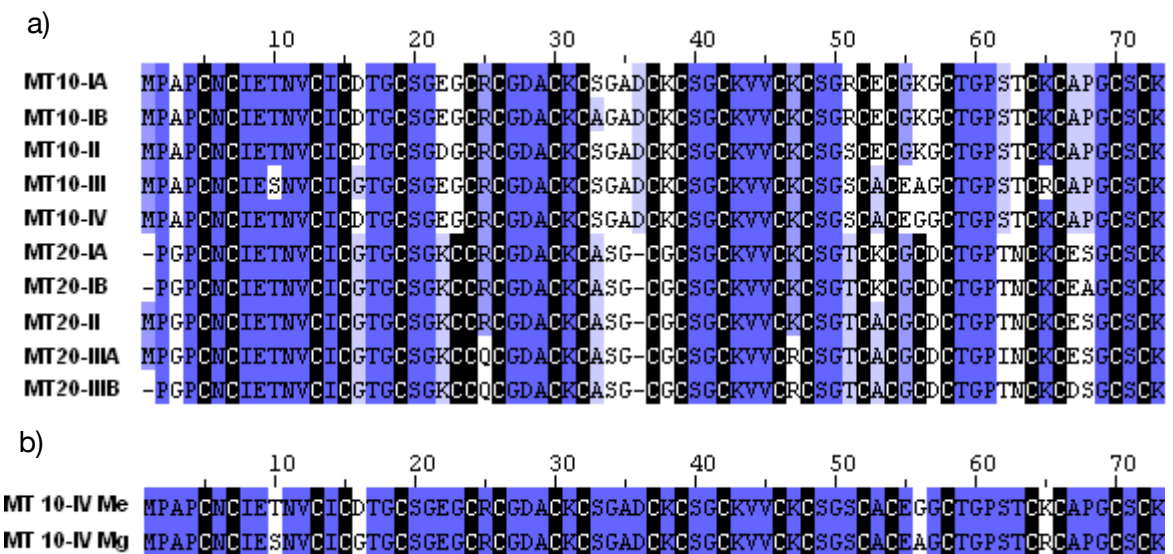


Figura 7.- Alineament en base a similituds de seqüència mitjançant l'aplicació ClustalW de: a) totes les isoformes de MT de *M.edulis* i b) la isoforma MT10-IV de *M.edulis* i la isoforma MT10-IV de *M.galloprovincialis*. En negre s'observen els residus de cisteïna.

Respecte l'estruccura primària d'aquestes MTs, les isoformes MT10 estan formades per 73 aminoàcids, dels quals 21 són Cys, mentre que les isoformes MT20 contenen 23 Cys d'entre un total de 71 o 72 aminoàcids. Degut a la semblança amb

les MTs de vertebrat, les MTs de mol·lusc es consideren com de tipus I o de la família 3 segons Binz i Kägi.

Malgrat tots els estudis realitzats en l'àmbit de l'ecotoxicologia, en la bibliografia no existeixen estudis de caracterització dels agregats metall-MT de les metal-lotioneïnes de *M.edulis*. Els únics estudis estructurals realitzats es centren en les isoformes MT10 i MT20 de *Mytilus galloprovincialis*, molt similars a les de *M.edulis*, tal i com s'observa en la Figura 7.b. En aquests estudis, mitjançant la reconstitució d'apo-MT i en base a mesures d'absorció atòmica, es proposen les espècies Cd₇-MT10 i Cd₇-MT20.^{90,91} Segons la resolució parcial de l'estructura tridimensional de la isoforma Cd₇-MT10 s'ha determinat que aquesta adopta un plegament en dos dominis independents, amb els clústers metall-MT invertits respecte la MT de mamífer, tal i com s'indica en la Figura 8.⁹²

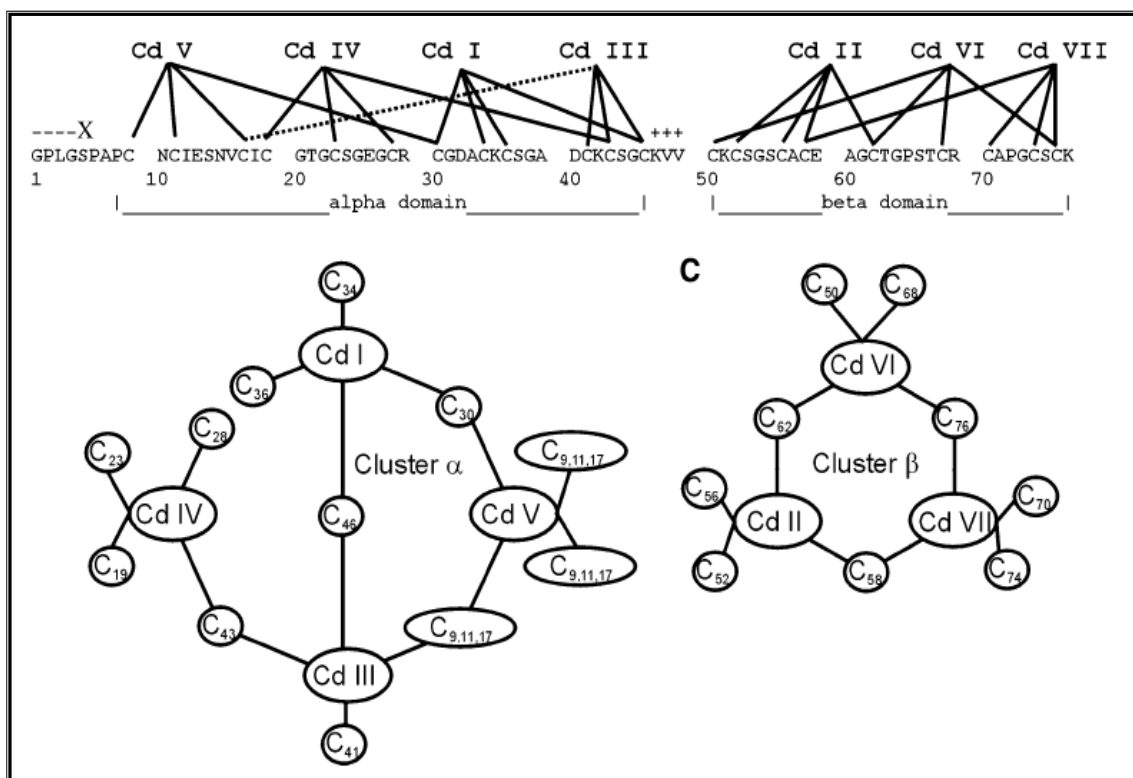


Figura 8.- Estructura primària de Cd₇-MT10 de *M.galloprovincialis* amb la connectivitat dels clústers metall-MT determinats per RMN de ¹H i ¹¹³Cd (extret de Digilio *et al.*⁹²).

1.7.2 El sistema MT en *Quercus suber*



La metal-lotioneïna d'alzina surera (*Quercus suber* MT) va poder ser aïllada per primer cop a partir d'una cerca en una llibreria de cDNA de fel·lema⁹³ gràcies a una col·laboració del nostre grup de recerca amb el grup de la Dra. Marisa Molinas, investigadora del Departament de Biologia de la Universitat de Girona. Així, es va determinar que el gen que codifica per a QsMT s'indueix sota condicions d'estrés oxidatiu i que participa en el metabolisme del coure. El fet que la seva estructura primària contingui 8 residus de Cys en el domini N-terminal i 6 en el domini C-terminal, i que ambdós dominis estiguin separats entre si per un espaiador, ha permès classificar-la com a MT de planta de tipus 2 segons la classificació de Cobbet i Goldsbrough³⁸ (Taula 2).

En aquesta col·laboració amb el grup de la Dra. Molinas, es va descriure l'aïllament i caracterització de QsMT en ser obtinguda en medis rics en Cu(II), Zn(II) i Cd(II), que van permetre classificar-la com a Cu-tioneïna a causa de la seva preferència envers el Cu(I). Sorprendentment, quan QsMT es biosintetitzava en presència de Zn(II) s'obtenien uns complexos amb unes estequiometries inferiors que quan s'obtenia en medis rics en amb Cd(II) (4 ions de Zn(II) *vs.* 6 ions de Cd(II)).⁹³ Aquestes diferències en l'estequiometria eren degudes a la presència de lligands àcid-làbils presents en els complexos Cd-QsMT que es podien eliminar en acidificar la mostra. La detecció d'aquests lligands àcid-làbils és el que va propiciar que un any després es descrigués per primera vegada la presència de lligands sulfur en les metal-lotioneïnes recombinants.⁴⁰

Amb posterioritat, i amb l'objectiu d'estudiar el possible model de plegament de QsMT en coordinar els ions essencials Cu(I) i Zn(II), es van biosintetitzar els dominis per separat d'aquesta MT, juntament amb un pèptid mutant on l'espaiador era substituït per 4 residus de glicina.⁴⁷ És important destacar que encara no existeix cap estructura tridimensional resolta d'una MT de planta, si bé en la bibliografia s'han proposat dos models de plegament de MT de planta diferents: per una banda, un model on els dos dominis rics en cisteïna formarien dos clústers independents, formant una estructura anomenada en forma de pesa^{94,95} (Figura 9.a), i per altra banda, un model on ambdós dominis interactuarien formant un únic clúster (Figura 9.b), generant una estructura en forma de pinça.^{96,97} En el cas de QsMT, l'estudi dels seus

dominis per separat va permetre proposar un model de plegament en forma de pinça en coordinar els ions Zn(II) i Cu(I).⁴⁷

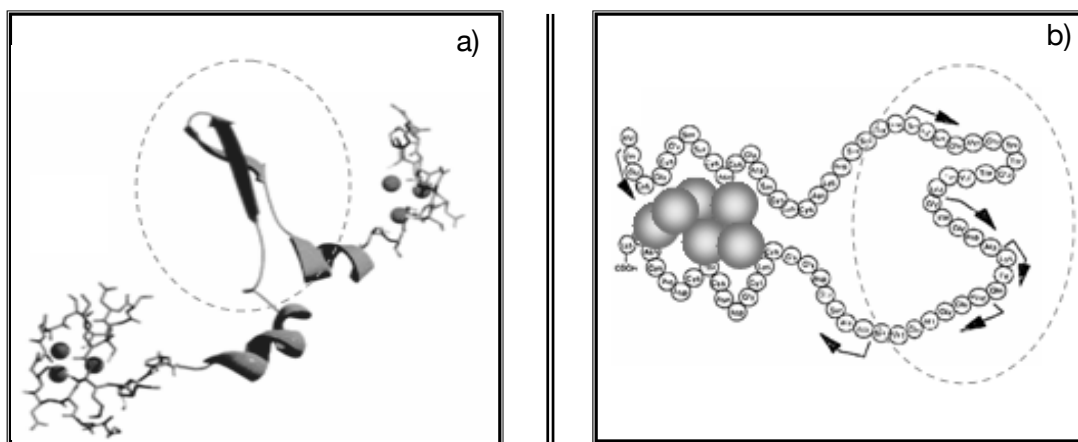


Figura 9.- Models estructurals proposats per a les MTs de planta: a) model en forma de pesa d'acord amb les dades publicades per a *T.durum*.⁹⁴ i b) model en forma de pinça, proposat per a la MT de *P.sativum*.⁹⁶ Les zones corresponents a l'espaiador es mostren encerclades.

1.7.3 El sistema MT en *Caenorhabditis elegans*



C.elegans és un nematode compost de 959 cèl·lules i, gràcies a la seqüènciació del seu genoma⁹⁸ l'any 1998, actualment és emprat com un organisme model per a l'estudi dels aspectes de desenvolupament d'organismes eucariotes i dels fenòmens de toxicitat envers els metalls de transició.⁷⁹

C.elegans conté dos gens que codifiquen respectivament per dues isoformes de MT, anomenades CeMT1 i CeMT2, els quals s'expressen de manera independent i no mitjançant factors de transcripció. El gen de la isoforma 1 (CeMT1) s'expressa constitutivament en la faringe, mentre que ambdós gens s'expressen en presència de cadmi a l'intestí.⁹⁹ Crida l'atenció que la síntesi de CeMT1 i de CeMT2 no s'indueix en presència ni de zinc ni de coure, reafirmant el paper proposat per a algunes MTs com a agents destoxicadors de metalls xenobiòtics.

Pel que fa a l'estructura primària de CeMT1 i CeMT2 (Figura 10), la isoforma 1 conté 75 aminoàcids, dels quals 19 són Cys, 4 His i 1 és un residu aromàtic (tirosina). En canvi CeMT2 és més curta degut a la deleció de 15 aminoàcids en l'extrem

C-terminal. També presenta una Cys de menys (18 Cys en total) i només una His terminal.

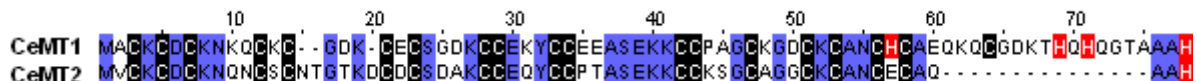


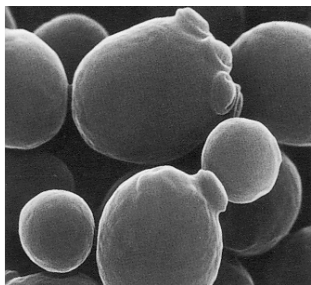
Figura 10.- Alineament en base a similitud de seqüència de les isoformes CeMT1 i CeMT2 del nematode *C.elegans* mitjançant l'aplicació ClustalW. En negre s'observen els residus de cisteïna i en vermell els d'histidina.

Ambdós pèptids presenten una seqüència molt diferent a les de les altres MTs d'invertebrats¹⁰⁰ així com algunes altres característiques inusuals. Per exemple, la divergència entre les dues isoformes és molt superior a la que hi ha entre isoformes de vertebrat i la seva estructura primària conté aminoàcids atípics, com Tyr i His. Degut a aquestes peculiaritats, tradicionalment s'han classificat com a metal-lotioneïnes de tipus II o del grup 6 segons Binz i Kägi.

Les dades que es tenen actualment respecte la coordinació metàl·lica de les MTs de *C.elegans* es centren principalment en la isoforma CeMT2. Concretament es sap que CeMT2 coordina *in vivo* 6 àtoms de cadmi, tant en ser induïda per cadmi en l'organisme com quan es produueix heteròlogament.¹⁰¹ En canvi, les úniques dades que existeixen en la bibliografia per a la isoforma CeMT1 en forma nativa indiquen que aquesta conté un 20% de zinc quan és purificada.⁸⁰

Pel que fa als estudis amb organismes MT-KO, aquests mostren una major sensibilitat davant la intoxicació per cadmi, però també deficiències en paràmetres biològics com per exemple el volum del cos o el número de descendents. Aquestes deficiències són veuen més accentuades en mutants Δ CeMT1 que en els Δ CeMT2, suggerint la possibilitat que la isoforma 1 tingui alguna funció important en el metabolisme a part de la destoxicació de metalls pesants.¹⁰² Tot i així, llur comportament coordinant envers metalls fisiològics com el Zn(II) i el Cu(I) o metalls tòxics com el Cd(II) no ha estat estudiat.

1.7.4 El sistema MT en *Saccharomyces Cerevisiae*



Saccharomyces cerevisiae és un llevat unicel·lular i un dels organismes model d'eucariota més intensament estudiats en biologia molecular i cel·lular. Conté dos gens que codifiquen per a dues MTs diferents, Cup1 i Crs5, relacionades amb la destoxicació de coure, ja que són regulades transcripcionalment per aquest ió. De fet, Cup1 ha estat tradicionalment considerada la Cu-tioneïna de referència. Des que va ser aïllada i caracteritzada,¹⁰³ el seu estudi ha donat lloc a un gran nombre de treballs. Cal destacar que Cu-Cup1 ha estat la primera i única Cu-MT de la qual s'ha resolt l'estructura tant per RMN¹⁰⁴ com per difracció de raigs X.²⁹ Aquest extens estudi ha permès conèixer amb detall aquesta MT, que *in vivo* enllaça entre 7 i 8 ions Cu(I) mitjançant 10 de les seves 12 Cys.²⁷ Experiments amb agents quelatants específics de Cu(I) van demostrar la presència de dos ions coure molt làbils,¹⁰⁵ cosa que explica les diferents relacions Cu/MT trobades. Aquesta labilitat diferencial dels Cu(I) enllaçats a Cup1 s'ha atribuït als diferents entorns de coordinació (6 Cu trigonals i 2 de digonals) que presenta el Cu(I) en la proteïna. Estudis *in vitro* de reconstitució des de la forma apo-MT han demostrat que aquesta proteïna també pot enllaçar Cd(II) i Zn(II) en una relació de 4 metalls per MT.¹⁰⁶

El gen que codifica per Crs5 no es va descobrir fins l'any 1994, quan s'intentaven identificar factors addicionals en MT de llevat que contribuïssin a l'homeòstasi i destoxicació del Cu.¹⁰⁷ Curiosament, aquesta proteïna presenta similituds de seqüència amb nombroses MTs de mamífer i d'invertebrats, mentre que comparteix poques homologies amb Cup1 (Figura 11). La diferència en el nombre de Cys entre les dues MTs de *S.cerevisiae* comporta també diferents capacitats de coordinació metàl·lica, les quals són majors en el cas de Crs5, que enllaça entre 10 i 12 ions Cu(I) i entre 6 i 7 ions Cd(II).⁴⁶ Aquest alt contingut metàl·lic juntament amb la presència d'un segment dins la seqüència de Crs5 de 8 residus aminoacídics deficient en Cys, suggereix l'organització de la proteïna en dos dominis, tal i com es descriu per les MTs de mamífer, mentre que Cup1 mostra una disposició monodominical.²⁷



Figura 11.- Alineament en base a similituds de seqüència mitjançant l'aplicació ClustalW de les isoformes del llevat *S.cerevisiae* Crs5 i Cup1. En negre s'observen els residus de cisteïna i en vermell els d'histidina.

Pel que fa a la funcionalitat d'ambdues isoformes, Crs5 ha estat relacionada amb els processos d'homeòstasi i destoxicació del coure, si bé es creu que Cup1 seria la responsable principal de la tolerància envers aquestió en *S.cerevisiae*, ja que els ions coure enllaçats a aquesta proteïna són cinèticament més inertes i, probablement, termodinàmica més estables que els units a Crs5. Per altra part, Crs5 podria tenir una funció tamponadora de Cu(I), degut a la seva labilitat d'enllaç a aquest metall.¹⁰⁸ Addicionalment, s'ha arribat a relacionar Crs5 amb l'homeòstasi del zinc, tal i com suggereixen els estudis realitzats amb aquesta proteïna per part del nostre grup de recerca.⁴⁶

2. Objectius

2. OBJECTIUS

Aquesta Tesi Doctoral té com a objectiu principal l'aprofundiment en la relació estructura/funció de les metal-lotioneïnes. Per tal de poder assolir-lo es proposa seguir els punts següents:

1. Ampliar els escassos coneixements actuals sobre el comportament coordinant d'algunes MTs, com són les del nematode *Caenorhabditis elegans*, la del mol·lusc *Mytilus edulis* i la de l'arbre *Quercus suber*, tot estudiant el possible paper coordinant dels residus d'histidina d'aquelles isoformes que en continguin.
2. Provar que les MTs natives també contenen lligands sulfur àcid-làbils, demostrant així que aquests lligands no són artefactes provinents del metabolisme d'*E.coli*, i estudiar la participació dels lligands sulfur en les metal-lotioneïnes tant recombinats com natives.
3. Estudiar la reacció de les MTs envers els radicals lliures.
4. Per últim, refinar la classificació de les metal-lotioneïnes en Zn- i Cu-tioneïnes.

3. Resultats i discussió

3. RESULTATS I DISCUSSIÓ

En aquest apartat es dóna una visió global del treball, exposant de manera resumida els resultats obtinguts i fent-ne una discussió general. Els resultats s'han dividit en 6 blocs. En els 3 primers, es discutiran les propietats coordinants d'algunes MTs d'organismes que no han estat estudiats anteriorment des d'un punt de vista espectroscòpic i espectromètric; com són: la metal-lotioneïna MT-10-IV del mol·lusc *Mytilus edulis* (Apartat 3.1, Article 1), la metal-lotioneïna QsMT de l'alzina surera *Quercus suber* (Apartat 3.2, Article 2) i les metal-lotioneïnes CeMT1 i CeMT2 del nematode *Caenorhabditis elegans* (Apartat 3.3, Article 3). Aquests treballs han donat lloc a dos articles científics publicats i un altre actualment en revisió. Tots tres, s'han inclòs en l'annex d'aquesta Tesi Doctoral.

En l'apartat 3.4, i amb l'objectiu de demostrar la presència d'anions sulfur àcid-làbils en les metal-lotioneïnes natives, es descriu la purificació i caracterització de la metal-lotioneïna nativa Cup1, obtinguda a partir de cultius del llevat *Saccharomyces Cerevisiae* que s'han fet créixer en medis enriquits en Cd(II). Addicionalment, s'ha caracteritzat aquesta mateixa metal-lotioneïna Cup1 obtinguda recombinantment a partir de cultius d'*E.coli*. L'article corresponent a aquests estudis actualment es troba en procés de redacció i s'ha inclòs en l'annex d'aquesta Tesi Doctoral en format d'article (Article 4).

En el cinquè bloc (Apartat 3.5) s'ha utilitzat la metal-lotioneïna QsMT per tal d'estudiar la reactivitat de les MTs envers les espècies radicalàries reactives. Aquest treball ha donat lloc a una publicació que també s'ha inclòs en l'annex (Article 5).

Per últim, en l'apartat 3.6 es proposa un refinament de la classificació de les MTs en Zn- i Cu-tioneïnes presentada fa uns anys pel nostre grup de recerca.

En tots els casos les proteïnes recombinants estudiades han estat sintetitzades pel grup de recerca dirigit per la Dra. Sílvia Atrian, Catedràtica del Departament de Genètica de la Facultat de Biologia de la Universitat de Barcelona (vegi's apartat 5.1).

3.1 Estudi de la capacitat coordinant de la metal-lotioneïna MeMT del mol·lusc *Mytilus edulis*

És un fet d'àmplia actualitat avui en dia l'ús de MTs d'organismes aquàtics invertebrats com a biomarcadors de la contaminació per metalls pesants, encara que gairebé no existeixen estudis sobre les seves propietats coordinants. Com ja s'ha comentat en l'apartat 1.7.1, el mol·lusc *M.edulis* presenta diferents isoformes de MT probablement especialitzades en l'homeòstasi de Zn(II) i en la destoxicació de Cd(II).⁸⁴⁻⁸⁷ Per aquest motiu, s'ha considerat interessant estudiar la isoforma MT-10-IV (MeMT) del mol·lusc *M.edulis*, la qual ha estat relacionada amb l'homeòstasi de Zn(II) per diversos autors. Així, aquest treball constitueix el primer estudi sobre el comportament coordinant de la isoforma MT-10-IV del mol·lusc *M.edulis* envers els ions metà·lics Zn(II), Cd(II) i Cu(I).

El procediment utilitzat per a l'estudi de la capacitat coordinant *in vivo* de MeMT envers Zn(II), Cd(II) i Cu(I) ha consistit en una primera etapa de síntesi recombinant per dos sistemes d'expressió diferents –però completament anàlegs– en medis enriquits en Zn(II), Cd(II) o Cu(II). Els complexos metall-MT obtinguts s'han caracteritzat mitjançant les tècniques espectroscòpiques i espectromètriques habituals (ICP-AES, DC, UV-Vis i ESI-MS).

L'estudi del comportament *in vitro* de MeMT s'ha efectuat seguint tres estratègies diferents: a) mitjançant processos de desplaçament Zn/Cd i Zn/Cu de l'espècie Zn₇-MeMT, b) mitjançant la reconstitució amb Cd(II) des de la forma apo-MT, i c) mitjançant acidificacions-reneutralitzacions de l'espècie Cd-MT obtinguda *in vivo*. Tots els complexos metà·lics formats al llarg dels estudis *in vitro* s'han caracteritzat, tot determinant el seu grau d'estructuració i el seu contingut metà·lic, mitjançant les tècniques de DC, UV-Vis i ESI-MS, i posteriorment s'han comparat les espècies obtingudes *in vitro* i *in vivo*.

Els estudis de caracterització de la metal-lotioneïna MeMT s'han realitzat en col·laboració amb el grup del Dr. Jeremias H. R. Kägi, del Biochemisches Institut de la Universitat de Zürich. A continuació es presenten i comenten els resultats obtinguts.

3.1.1 Comportament de MeMT envers Zn(II) i Cd(II)

En la biosíntesi de MeMT en medis enriquits en Zn(II) i Cd(II) s'han obtingut espècies amb l'estequiometria esperada per a una metal-lotioneïna amb 21 residus de Cys, *i.e.*, M₇-MeMT (on M= Zn o Cd, Taula 3). Les dades d'ESI-MS i de DC mostren que aquestes MTs s'obtenen *in vivo* com a espècies homometàl·liques, amb un alt grau d'estructuració (Figures 2.A i 2.B, Article 1).

Proteïna	Zn-MeMT	Cd-MeMT
[conc.]	$1 \cdot 10^{-4}$ M	$1 \cdot 10^{-4}$ M
ICP-AES	7.0 Zn/prot	7.3 Cd/prot
ESI-MS	Zn ₇ -MeMT	Cd ₇ -MeMT

Taula 3.- Resultats de la caracterització dels complexos metall-MeMT obtinguts per enginyeria genètica mitjançant la seva biosíntesi en medis rics en Zn(II) i Cd(II).

Precisament, el grup de recerca del Dr. Viarengo ha resolt parcialment l'estructura de la metal-lotioneïna Cd₇-MT10 del musclo *M.galloprovincialis*, la qual es plega en dos dominis independents.⁹² Donat que aquesta MT presenta una alta similitud de seqüència amb MeMT (Figura 7.b) i ambdues, en expressar-se com a Cd-MTs, donen lloc a complexos de la mateixa estequiometria i amb propietats espectroscòpiques gairebé idèntiques (Figura 12), es pot assumir que MeMT adopta un plegament bidominial anàleg al de *M.galloprovincialis*, coordinant 4 metalls divalents en el domini N-terminal i 3 metalls en el domini C-terminal.

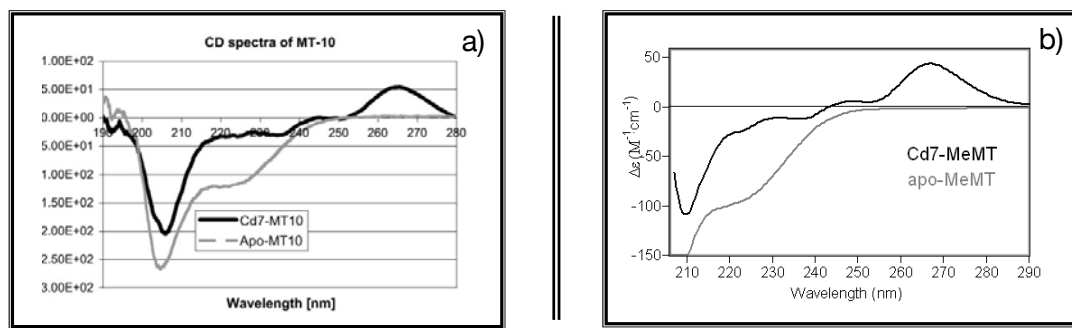


Figura 12.- Espectres de DC de les formes demetal·lades (apo) i de les espècies obtingudes en presència de Cd(II) de a) MT10 de *M.galloprovincialis* (extret de Viarengo *et al.*⁹¹) i b) MT-10-IV de *M.edulis*.

Els estudis *in vitro* dels complexos Cd-MeMT han posat de manifest la dificultat de reproduir tant espectroscòpicament com espectromètrica l'espècie Cd₇-MeMT obtinguda *in vivo*. Així, els estudis de desplaçament Zn/Cd realitzats a partir de l'espècie Zn₇-MeMT han revelat que es necessita un gran excés de metall, entre 11 i 15 equivalents, per desplaçar totalment el Zn inicialment enllaçat a la metal-lotioneïna i obtenir una espècie majoritària homometàlica Cd₇-MeMT (Taula 3, article 1). Encara que aquesta observació podria semblar indicar la presència d'algun Zn(II) estructural en el clúster metàl·lic, l'obtenció d'una espècie homometàlica altament estructurada en la biosíntesi de MeMT en medis enriquits en Cd(II) descarta aquesta hipòtesi. Així, la reticència a l'intercanvi complet de Zn(II) per Cd(II) molt probablement és deguda al plegament de la proteïna al voltant del clúster metàl·lic, fet que dificultaria l'accés dels ions Cd(II) als tiolats cisteínicos més interns. A més, la impossibilitat d'obtenir *in vitro* espècies Cd₇-MeMT isoestequiomètriques a les obtingudes *in vivo* amb propietats espectropolarimètriques idèntiques a les de les espècies biosintetitzades indica que la metal-lotioneïna MeMT pot adoptar un plegament diferent al voltant dels agregats metàl·lics dependent de si s'obté en condicions *in vivo* o *in vitro*.

Pel que fa als experiments d'acidificació-reneutralització, un fet a destacar és que l'acidificació de Cd₇-MeMT provoca la precipitació del 75% de la proteïna. Malgrat aquest fet, s'ha pogut observar que la reneutralització de la mostra dóna lloc a espècies Cd-MeMT de propietats espectroscòpiques anàlogues a les de les espècies obtingudes tant per desplaçament Zn/Cd (Figura 5, Article 1) com a les de les espècies resultants després de reconstituir la forma apo-MeMT amb Cd(II) (Figura 3, Article 1). Aquestes dades indiquen que totes les espècies Cd-MeMT obtingudes *in vitro* s'estructuren igual però de diferent manera a com ho fa la proteïna *in vivo*.

Així mateix, la precipitació observada podria estar relacionada amb un procés de biomineralització que s'ha descrit que té lloc en alguns organismes invertebrats com cucs i mol·luscos.^{109,110} Durant aquest procés el Cd(II) s'enllaça a uns grànuls rics en sulfur i queda emmagatzemat en uns orgànuls similars als lisosomes anomenats cadmosomes, per a ser excretats amb posterioritat. Els estudis indiquen que aquest grànuls rics en sulfur provenen de la hidròlisi àcida de proteïnes riques en Cys, com són les metal-lotioneïnes.¹¹¹

3.1.2 Comportament de MeMT envers Cu(II)

A diferència del que succeeix en el cas de les síntesis en presència de Cd(II) i de Zn(II), la similitud de pes atòmic entre el Zn (65.38 uma) i el Cu (63.55 uma) i l'interval de confiança obtingut en les mesures d'ESI-MS fan que mitjançant aquesta tècnica no sigui possible determinar la relació Zn:Cu:MT de les espècies obtingudes *in vivo* i/o *in vitro* en presència de Cu a pH neutre. Així, en tots els casos, les espècies detectades per ESI-MS es denoten com a M_n -MT on M pot ser indistintament Cu(I) o Zn(II). Per resoldre aquest problema les mostres són analitzades a pH 2.5, per tal de determinar-ne el contingut en Cu, ja que en aquest pH els enllaços Cu-tiolat encara són estables, a diferència del que succeeix amb els enllaços Zn-tiolat.

La metal-lotioneïna MeMT s'ha sintetitzat diverses vegades en medis rics en Cu(II). Aquestes síntesis recombinants han donat lloc a dos tipus de produccions diferents, les anomenades produccions de Tipus 1 i les de Tipus 2 (Taula 4). Les síntesis de Tipus 1 han donat lloc a una mescla d'espècies heterometàl·liques Zn,Cu-MT amb un contingut en Zn(II) significatiu i on M_8 -MeMT és l'espècie majoritària. Per la seva part, les síntesis de Tipus 2 donen lloc a una barreja d'espècies heterometàl·liques on M_{12} -MeMT és l'espècie majoritària i en les que el contingut en Cu(I) és major que en les espècies de Tipus 1.

Proteïna	Cu-MeMT tipus 1	Cu-MeMT tipus 2
[conc.]	$0.9 \cdot 10^{-4}$ M	$0.5 \cdot 10^{-4}$ M
ICP-AES	3.3 Zn/prot 4.6 Cu/prot	1.4 Zn/prot 9.2 Cu/prot
ESI-MS	M_8 -MeMT (M) M_9 -MeMT M_{10} -MeMT (m)	M_{12} -MeMT (M) M_{11} -MeMT M_{13} -MeMT (m)

Taula 4.- Resultats de la caracterització dels complexos metall-MeMT obtinguts per enginyeria genètica mitjançant la seva biosíntesi en medis rics en Cu(II). Les espècies estan ordenades segons la seva abundància en solució. (M) representa l'espècie majoritària i (m) la minoritària.

Aquestes diferències en les produccions es poden explicar per la major/menor presència d'oxigen durant la biosíntesi, tal i com aquest grup ja havia descrit en

treballs anteriors.⁴⁶ En aquests, es va observar que la quantitat de Zn(II) en el bacteri productor de la MT és independent del grau d'oxigenació, mentre que la concentració de Cu total disminueix significativament quan s'ha oxigenat el medi de cultiu. Així doncs, molt probablement durant la biosíntesi de les produccions de Tipus 1 la quantitat d'oxigen en el medi de cultiu de *E.coli* va ser més elevada que durant la biosíntesi de les produccions de Tipus 2.

Tal com ja s'ha descrit en les valoracions amb Cd(II), en els estudis de desplaçament Zn/Cu duts a terme *in vitro* amb Zn₇-MeMT també és necessari un gran excés de Cu(I) per tal de desplaçar totalment els ions Zn(II) inicialment enllaçats a MeMT. En aquest cas, a més, la reticència a l'intercanvi Zn/Cu és fins i tot més elevada que en el cas del Cd(II). Així, per exemple, per tal de generar espècies anàlogues a les de les produccions biosintetitzades en medis enriquits en Cu fa falta l'addició respectiva al medi de 14 i 26 equivalents de Cu(I) per tal de reproduir les produccions de Tipus 1 o 2, i no és fins que s'han afegit 30 equivalents de Cu(I) que es generen espècies homometà·liques Cu₁₂-MeMT. Tal i com succeïa en el cas del Cd(II), la dificultat per a un intercanvi total de Zn/Cu ha d'estar relacionat amb el plegament que adopta la proteïna en coordinar Zn(II) més que no pas amb l'especificitat envers els diferent ions metà·lics, ja que l'ordre d'afinitat metà·lica de les MTs s'ha descrit que segueix el mateix ordre proposat per als tiolats inorgànics:¹¹²

$$\text{Hg}^{2+} > \text{Ag}^+ \approx \text{Cu}^+ > \text{Cd}^{2+} > \text{Zn}^{2+}.$$

Resumint, la isoforma aquí estudiada, MT-10-IV, es sintetitza en l'organisme viu basalment i la seva síntesi augmenta en resposta a la presència de Zn(II) o a baixes concentracions de Cd(II). En aquest sentit, els estudis realitzats posen de manifest (a) l'elevada capacitat d'aquesta metal-lotioneïna per coordinar ions metà·lics divalents. A més, (b) els complexos Zn₇-MeMT mostren una elevada reticència a intercanviar els ions Zn(II) per Cd(II) o Cu(I), probablement a causa del plegament que adopta la cadena peptídica en coordinar el Zn(II). Així mateix, (c) els complexos Cd₇-MT són molt estables i no es descarta que puguin participar en la formació dels anomenats cadmosomes. Per altra banda, el coure, que no és un metall inductor de la síntesi de MeMT en l'organisme viu, (d) provoca la formació de complexos heterometà·lics Zn/Cu-MT *in vivo*. Així doncs, aquest conjunt de resultats ha portat a (e) classificar MeMT com a Zn-tioneïna, ja que s'ha trobat una bona correlació entre les diferents funcions proposades per a aquesta MT i les seves habilitats coordinants.

3.2. Estudi de la capacitat coordinat de la metal-lotioneïna QsMT de l'alzina surera *Quercus suber*

Els estudis de la metal-lotioneïna d'alzina surera van ser iniciats fa uns anys en aquest grup de recerca i van donar lloc a dues publicacions.^{47,93} En aquells treballs es va descriure l'aïllament i caracterització de QsMT quan s'obté en medis rics en Cu(II), Zn(II) i Cd(II), es va proposar un model de plegament en forma de pinça per a Cu-QsMT i Zn-QsMT on l'espaiador no participava en la coordinació metàl·lica i es va classificar QsMT com a Cu-tioneïna. Addicionalment, es van descriure diferències estequiomètriques entre les formes Zn-QsMT i Cd-QsMT obtingudes *in vivo*, així com la presència d'un alt contingut en anions sulfur àcid-làbils en Cd-QsMT.

En vistes a aquests resultats, s'ha considerat adient aprofundir en el coneixement de QsMT envers Cd(II), estudiar el paper dels anions sulfur com a lligands en aquests complexos i proposar un model de plegament per a Cd-QsMT. Per tal d'assolir aquests objectius, s'han biosintetitzat en presència de Zn(II) i Cd(II) QsMT i tres pèptids mutants de QsMT: el domini N-terminal (N25, amb 8 Cys), el domini C-terminal (C18, amb 6 Cys) i un pèptid idèntic a QsMT però on l'espaiador ha estat substituït per 4 residus de glicina (N25-C18) - vegi's Figura 13. Així mateix, també s'han estudiat els processos de desplaçament Zn/Cd *in vitro* dels 4 pèptids seguint el procediment descrit en l'apartat 3.1. L'interès de l'estudi del pèptid truncat N25-C18 rau en el fet que de la seva comparació amb el pèptid QsMT sencer es podrà deduir el paper de l'espaiador en la coordinació i en la destoxicació de Cd(II).

Aquest treball s'ha efectuat en col·laboració amb el grup de recerca dirigit per la Dra. Marisa Molinas, del Departament de Biologia de la Universitat de Girona.



Figura 13.- Seqüència d'aminoàcids de QsMT i dels seus fragments constitutius. El pèptid N25 correspon al domini N-terminal, el pèptid C18 correspon al domini C-terminal i N25-C18 a un pèptid que conté els dos dominis i on l'espaiador ha estat substituït per 4 residus de glicina. Els residus de Cys estan marcats en vermell i la His de l'espaiador en blau.

3.2.1 Comportament de QsMT envers Zn(II) i Cd(II)

Les produccions *in vivo* dels 4 pèptids en presència de Zn(II)^{47,93} han donat lloc a les mateixes estequiometries Zn:proteïna que les obtingudes en treballs anteriors. Addicionalment, però, a diferència dels treballs anteriors, s'han detectat espècies sulfurades minoritàries en Zn-QsMT, Zn-N25-C18 i Zn-N25, mentre que C18 ha estat l'únic pèptid en el que no s'ha detectat sofre inorgànic, ni per GC-FPD ni per ESI-MS (Taula 5).

Proteïna	Zn-QsMT	Zn-N25-C18	Zn-N25	Zn-C18
[conc.]	$0.9 \cdot 10^{-4}$ M	$1.3 \cdot 10^{-4}$ M	$3.2 \cdot 10^{-4}$ M	$3.3 \cdot 10^{-4}$ M
ICP-AES	3.5 Zn/prot	3.6 Zn/prot	2.2 Zn/prot	1.8 Zn/prot
GC-FPD	1.3 S ²⁻ /prot	1.0 S ²⁻ /prot	0.3 S ²⁻ /prot	N.D.
ESI-MS	Zn ₄ -QsMT (M) Zn ₃ -QsMT Zn ₄ S ₂ -QsMT (m)	Zn ₄ -N25-C18 (M) Zn ₄ S ₁ -N25-C18 Zn ₃ S ₁ -N25-C18 (m)	Zn ₂ -N25 (M) Zn ₃ -N25 Zn ₇ S ₁ -(N25) ₂ (m)	Zn ₂ -C18 (M) Zn ₁ -C18 Zn ₅ -(C18) ₂ (m)

Taula 5.- Resultats de la caracterització dels complexos metall-QsMT i dels seus fragments constitutius obtinguts per enginyeria genètica mitjançant la seva biosíntesi en medis rics en Zn(II). Les espècies estan ordenades segons la seva abundància en solució. (M) representa l'espècie majoritària i (m) la minoritària. N.D. indica contingut en S²⁻ no detectable.

La biosíntesi de QsMT en medis enriquits en Cd(II) ha donat lloc a tres tipus de preparacions homometàl·liques de Cd(II) diferents, anomenades (1), (2) i (3) respectivament, les quals difereixen espectroscòpicament, (Figura 1A, Article 2), encara que mostren una especiació comparable segons les dades d'ESI-MS (Taula 6).

Proteïna	Cd-QsMT (1)	Cd-QsMT (2)	Cd-QsMT (3)	Cd-N25-C18
[conc.]	$0.8 \cdot 10^{-4}$ M	$0.6 \cdot 10^{-4}$ M	$1.3 \cdot 10^{-4}$ M	$1.0 \cdot 10^{-4}$ M
ICP-AES	6.7 Cd/prot	6.3 Cd/prot	5.3 Cd/prot	5.9 Cd/prot
GC-FPD	2.9 S ²⁻ /prot	2.4 S ²⁻ /prot	2.2 S ²⁻ /prot	2.4 S ²⁻ /prot
ESI-MS	Cd ₆ S ₄ -QsMT (M) Cd ₇ S ₄ -QsMT Cd ₅ -QsMT (m)	Cd ₆ S ₄ -QsMT (M) Cd ₇ S ₄ -QsMT Cd ₅ -QsMT (m)	Cd ₅ -QsMT (M) Cd ₆ S ₄ -QsMT (m)	Cd ₆ S ₄ -N25-C18 (M) Cd ₅ -N25-C18 (m)

Taula 6.- Resultats de la caracterització dels complexos metall-QsMT i metall-N25-C18 obtinguts per enginyeria genètica mitjançant la seva biosíntesi en medis rics en Cd(II). Les espècies estan ordenades segons la seva abundància en solució. (M) representa l'espècie majoritària i (m) la minoritària.

Pel que fa al pèptid Cd-N25-C18, i tal i com succeeix en la biosíntesi amb Zn(II) (Taula 5), la seva biosíntesi en medis rics en Cd(II) dóna lloc a complexos espectromètricament anàlegs als de les produccions de la proteïna sencera, encara que amb propietats espectropolarimètriques diferents (Figura 14).

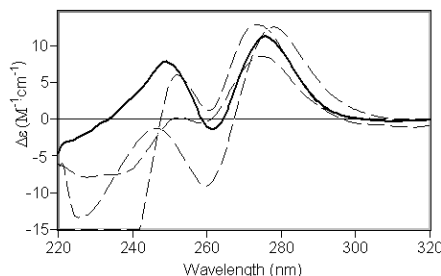


Figura 14.- Comparació entre els espectres de DC de Cd-N25-C18 (línia contínua) i les 3 produccions de Cd-QsMT (línies discontinuades).

Aquesta dada ens indica que encara que el paper de l'espaiador en la coordinació metàl·lica sigui menyspreable, sí que pot influir en l'estructura i per tant tenir algun paper funcional. Aquest fet queda també de manifest en experiments efectuats amb soques de llevat on s'ha induït la síntesi dels diferents pèptids per separat en medis enriquits en Cd(II). Les soques que presenten una major resistència a la intoxicació per Cd(II) són aquelles que sintetitzen QsMT sencera, fet que implica que la capacitat de destoxicar d'aquesta proteïna està íntimament relacionada amb la presència de l'espaiador i la forma com aquesta MT es replega al voltant del clúster metàl·lic (Figura 15).

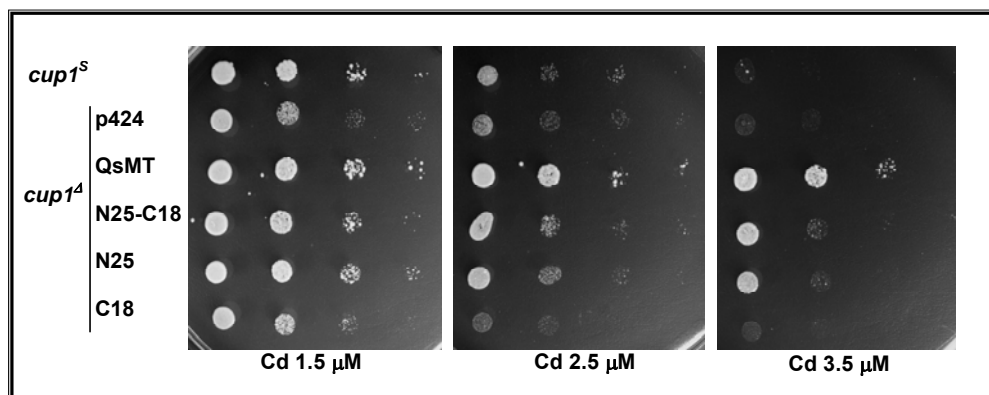


Figura 15.- Experiment d'inducció dels 4 pèptids d'aquest treball en soques de llevat. Cada primera columna correspon al cultiu inicial i les columnes següents corresponen a dilucions 1:10 de l'anterior. CUP 1^s correspon a una soca de llevat amb la seva pròpia MT. p424 és el nom del plàsmid emprat per a la inserció dels diversos pèptids en les soques i correspon, doncs, a soques que no sintetitzen cap MT. Es mostra el creixement de les diferents soques en medis amb 3 concentracions diferents de Cd(II).

Additionalment, i amb l'objectiu d'estudiar les diferències entre els 3 tipus diferents de preparacions Cd-QsMT, s'ha procedit a llur acidificació controlada (Figura 16). Així en el cas concret de la producció Cd-QsMT (1), s'observa que l'espectre de DC es manté constant entre pH 7.0 i aproximadament pH 4.5, mentre que l'espectre de DC de la producció (3) perd la banda gaussiana centrada a *ca.* 255 nm i evoluciona cap a un espectre anàleg al de la producció Cd-QsMT (2) a pH 7.0, per acabar generant a pH 4.5 un espectre de DC pràcticament idèntic al de les preparacions Cd-QsMT (1). En la bibliografia hi ha estudis que suggereixen que absorcions de DC a uns 250 nm poden ser atribuïbles a la coordinació Cd-His.¹¹³ Conseqüentment, una participació diferent en la coordinació metàl·lica de la His en les diferents preparacions Cd-QsMT seria consistent amb el fet que totes presentessin inicialment un espectre de DC diferent a pH 7.0 (Figura 1A, Article 2) i acabessin generant un mateix espectre a pH 4.5 després de la protonació del nitrogen imidazòlic de la His (Figura 16.c). Així doncs, els resultats indiquen que Cd-QsMT (3), amb un contingut en sofre inorgànic menor que les altres produccions (Taula 6), estaria majoritàriament composta per una espècie Cd₅-QsMT de baixa nuclearitat on la histidina participa en la coordinació a Cd(II). En canvi, les produccions Cd-QsMT (1), més riques en lligands sulfur, contenen espècies de major estequiomètria (Cd₆ i Cd₇-QsMT) de manera que la His ja no participaria en la coordinació metàl·lica. Per altra banda, la producció Cd-QsMT (2) no seria més que una mescla de les preparacions de tipus (1) i (3). Així doncs, quan Cd-QsMT es sintetitza *in vivo* el residu de His de l'espatador participaria o no en la coordinació al Cd(II) en funció del contingut en sulfur de la proteïna, determinant alhora l'estequiomètria, l'estructura i probablement la funcionalitat dels agregats metàl·lics finals que es formaran.

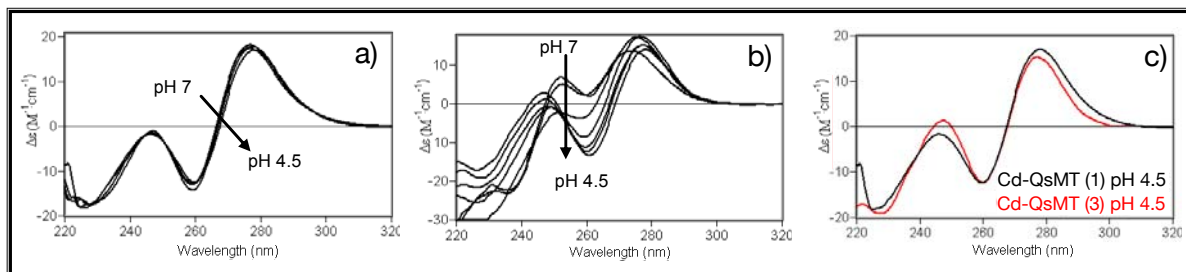


Figura 16.- Acidificació de les diferents produccions de Cd-QsMT. a) Espectres de DC des de pH 7.0 fins a pH 4.5 de Cd-QsMT (1). b) Espectres de DC des de pH 7.0 fins a pH 4.5 de Cd-QsMT (3). c) Comparació dels espectres de DC de Cd-QsMT (1) i (3) a pH 4.5.

Pel que fa als fragments de QsMT, tant N25 com C18 es sintetitzen com a espècies dimèriques homometà-líques en medis enriquits en Cd(II) (Taula 7). Per un costat, N25 dóna lloc a l'espècie dimèrica majoritària $\text{Cd}_7\text{S}_4\text{-(N25)}_2$, fet que estaria d'acord amb l'alt contingut en sulfur detectat per GC-FPD, mentre que els complexos de Cd-C18 s'obtenen com una mescla de les espècies dimèriques $\text{Cd}_4\text{-(C18)}_2$ (majoritària) i $\text{Cd}_5\text{-(C18)}_2$ (minoritària). En qualsevol cas, és important destacar que els fragments constitutius de QsMT sempre formen dímers quan coordinen Cd(II) en condicions *in vivo*. La tendència que presenten els fragments aïllats a dimeritzar per donar lloc a estequiomètries Cd/prot similars a les de QsMT, indica que és precisament la proteïna sencera la que presenta major capacitat destoxicadora de Cd(II), d'acord amb els resultats d'inducció d'aquests pèptids en soques de llevat (Figura 15).

Proteïna	Cd-N25	Cd-C18
[conc.]	$1.2 \cdot 10^{-4}$ M	$2.8 \cdot 10^{-4}$ M
ICP-AES	3.8 Cd/prot	2.3 Cd/prot
GC-FPD	$2.8 \text{ S}^{2-}/\text{prot}$	$0.5 \text{ S}^{2-}/\text{prot}$
ESI-MS	$\text{Cd}_7\text{S}_4\text{-(N25)}_2$ (M) $\text{Cd}_6\text{-(N25)}_2$ (m)	$\text{Cd}_4\text{-(C18)}_2$ (M) $\text{Cd}_5\text{-(C18)}_2$ (m)

Taula 7.- Resultats de la caracterització dels fragments constitutius N25 i C18 de QsMT obtinguts per enginyeria genètica mitjançant la seva biosíntesi en medis rics en Cd(II). Les espècies estan ordenades segons la seva abundància en solució. (M) representa l'espècie majoritària i (m) la minoritària

Pel que fa als estudis de desplaçament Zn/Cd realitzats *in vitro* a partir de les formes Zn-MT, s'ha revelat que, d'acord amb el contingut en sulfur de tots els pèptids excepte en el cas del mutant C18, la substitució del Zn(II) per Cd(II) no permet generar *in vitro* espècies Cd-MTs anàlogues a les biosintetitzades *in vivo* (Taules S1-S4, Article 2), sinó que les espècies que s'obtenen sense afegir sulfur al medi són sempre d'una estequimetria inferior. Així, per a QsMT i N25-C18 s'obtenen els complexos Cd_4^- i Cd_5^- , mentre que per al pèptid N25 sempre s'obté l'espècie monomèrica $\text{Cd}_3\text{-N25}$. Amb la posterior addició de Na_2S a aquestes espècies, els sulfurs s'incorporen com a lligands als diferents complexos, tal i com es pot observar en els espectres de DC i UV (Figura 2, Article 2). És important destacar el cas del pèptid N25, on la capacitat de dimeritzar està estretament relacionada amb la disponibilitat d'anions sulfur en el medi, ja que si aquests lligands són absents o es troben en baixes

concentracions, les espècies dimèriques no es poden formar. Pel que fa al pèptid C18, el fet que l'espècie Zn-C18 de partida no contingui anions sulfur ha permès reproduir perfectament a partir dels estudis de desplaçament Zn/Cd *in vitro* l'espècie Cd-C18 obtinguda *in vivo* (Figura S5, Article 2).

Per altra banda, el major contingut metàl·lic de Cd-QsMT *vs* el de Zn-QsMT ha estat relacionat amb el major contingut en sulfur del primer. Aquest fet fa que QsMT constitueixi l'únic cas conegut d'una MT amb diferents capacitats coordinants enfront dels metalls divalents Zn(II) i Cd(II).

Respecte al model de plegament de QsMT en presència de Cd(II), es proposa un model en forma de pinça en base als següents fets. Per un costat, els espectres de DC del final de la covaloració (valoració conjunta dels pèptids Zn-N25 i Zn-C18 amb Cd(II), Figura 9, Article 2) no reproduïxen cap dels espectres de DC de les 3 preparacions Cd-QsMT mentre que, en la covaloració sí que podem reproduir la suma dels espectres de les valoracions amb Cd(II) dels pèptids N25 i C18 per separat. Aquests fets indiquen que en la covaloració aquests pèptids es comporten independentment, al contrari del que passa en Cd-QsMT, on els dominis estarien interactuant. Per un altre costat, si *in vivo* la tendència dels pèptids N25 i C18 és la de dimeritzar quan coordinen Cd(II), el més plausible és que QsMT es plegui en forma de pinça per a complir aquest requeriment.

3.3 Estudi de la capacitat coordinat de les metal-lotioneïnes CeMT1 i CeMT2 del nematode *Caenorhabditis elegans*

Una part del treball aquí presentat s'ha dedicat a l'estudi de les dues isoformes CeMT1 i CeMT2 del nematode *C.elegans*. Com ja s'ha comentat en l'apartat 1.7.3, aquestes dues proteïnes semblen tenir bàsicament una funció destoxicadora en l'organisme, encara que hi ha indicis que la isoforma CeMT1 també podria estar implicada en processos metabòlics.¹⁰²

La dissimilitud entre aquestes dues isoformes (Figura 17), la presència de residus atípics (His i Tyr) en la seva seqüència i la manca d'una caracterització acurada dels complexos als que donen lloc amb Zn(II), Cd(II) i Cu(I) ens ha portat a estudiar les seves propietats de coordinació metàl·lica per tal de determinar-ne les similituds i diferències. Així doncs, en aquest apartat es recullen els resultats de la caracterització dels complexos metàl·lics de CeMT1 i CeMT2, així com de la dels seus dominis putatius, mitjançant metodologies anàlogues a les descrites per la metal-lotioneïna MeMT. Addicionalment, s'ha comparat el diferent comportament coordinant de les dues isoformes i s'ha estudiat el possible paper dels residus de His en la coordinació metàl·lica.

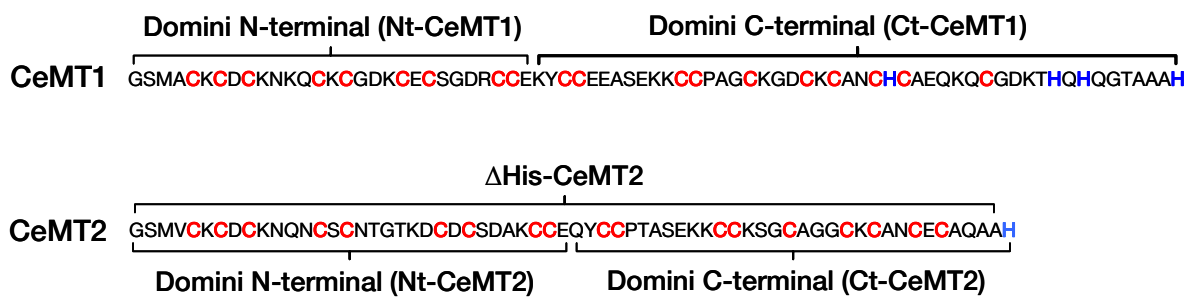


Figura 17.- Seqüència d'aminoàcids de CeMT1 i CeMT2 així com dels seus fragments constitutius. Els pèptids Nt-CeMT1 i Nt-CeMT2 corresponen als dominis N-terminals, els pèptids Ct-CeMT1 i Ct-CeMT2 corresponen als dominis C-terminals i ΔHis-CeMT2 correspon a un pèptid mutant derivat de CeMT2 on s'ha suprimit la His terminal. Els residus de Cys estan marcats en vermell i les His en blau. Noteu la gran similitud de seqüència d'ambdós dominis N-terminal, amb 9 Cys cadascun, mentre que els dominis C-terminal difereixen significativament: mentre que la isoforma 2 conté 9 Cys i 1 His terminal, la isoforma 1, més llarga, conté 1 Cys i 3 His més que la isoforma 2.

3.3.1 Comportament de CeMT1 envers Zn(II) i Cd(II)

La isoforma CeMT1 s'expressa en medis enriquits en Zn(II) com a una única espècie homometàl·lica Zn₇-CeMT1. En canvi, la biosíntesi dels seus dominis per separat dóna lloc a una mescla d'espècies homometàl·liques per al domini N-terminal, on les espècies majoritàries són Zn₃- i Zn₁-NtCeMT1, i un complex Zn₄-CtCeMT1 majoritari per al domini C-terminal (Taula 8.a). La suma dels espectres de DC dels dos fragments aïllats no permet reproduir l'espectre original de Zn₇-CeMT1. Aquestes dades, juntament amb els resultats d'ESI-MS, suggereixen que els dos dominis interaccionen en el pèptid sencer en coordinar Zn(II). Per altra banda, quan CeMT1 i el seu fragment C-terminal són biosintetitzats en presència de Cd(II), s'obtenen espècies heterometàl·liques: Cd₆Zn₁-CeMT1 i Cd₃Zn₁-CtCeMT1. En canvi, en aquestes condicions, el domini N-terminal dóna lloc a una espècie majoritària homometàl·lica Cd₃-NtCeMT1 (Taula 8.b). A partir d'aquestes dades es pot concloure que el Zn(II) present en CeMT1 en ser sintetitzada en medis rics en Cd(II) està situat en el seu fragment C-terminal.

	Proteïna	Zn-CeMT1	Zn-NtCeMT1	Zn-CtCeMT1
a)	[conc.]	1.5·10 ⁻⁴ M	2.1·10 ⁻⁴ M	1.0·10 ⁻⁴ M
	ICP-AES	6.5 Zn/prot	1.8 Zn/prot	2.1 Zn/prot
	ESI-MS	Zn ₇ -CeMT1	Zn ₃ -NtCeMT1 Zn ₁ -NtCeMT1	Zn ₄ -CtCeMT1 (M) Zn ₂ -CtCeMT1 Zn ₁ -CtCeMT1 (m)

	Proteïna	Cd-CeMT1	Cd-NtCeMT1	Cd-CtCeMT1
b)	[conc.]	0.6·10 ⁻⁴ M	0.4·10 ⁻⁴ M	0.2·10 ⁻⁴ M
	ICP-AES	6.5 Cd/prot 0.9 Zn/prot	2.9 Cd/prot 0.1 Zn/prot	2.9 Cd/brot 0.6 Zn/prot
	ESI-MS	Cd ₆ Zn ₁ -CeMT1	Cd ₃ -NtCeMT1 (M) Cd ₃ Zn ₁ -NtCeMT1 (m)	Cd ₃ Zn ₁ -CtCeMT1

Taula 8.- Resultats de la caracterització dels complexos metall-CeMT1 i dels seus fragments obtinguts per enginyeria genètica mitjançant la seva biosíntesi en medis rics a) en Zn(II) i b) en Cd(II). Les espècies estan ordenades segons la seva abundància en solució. (M) representa l'espècie majoritària i (m) la minoritària.

L'estudi del comportament *in vitro* de CeMT1 i dels seus fragments envers Cd(II) s'ha efectuat de manera anàloga a com ja s'ha descrit per al pèptid MeMT (apartat 3.1). Els estudis de desplaçament Zn/Cd realitzats *in vitro* amb l'espècie Zn₇-CeMT1 han revelat que l'addició de 6 equivalents de Cd(II) permet reproduir a la perfecció, tant espectroscòpicament com espectromètrica, l'espècie Cd₆Zn₁-CeMT1 obtinguda *in vivo* (Figura 4, Article 3). Aquesta espècie heterometàlica continua essent l'espècie majoritària fins i tot després d'addicionar al medi un excés de Cd(II) (12-14 equivalents). Els mateixos estudis de desplaçament s'han efectuat per als pèptids N-terminal i C-terminal i en ambdós casos l'addició de 3 equivalents de Cd(II) permet reproduir les espècies obtingudes *in vivo* (Cd₃-NtCeMT1 i Cd₃Zn₁-CtCeMT1). Addicionalment, per tal d'estudiar amb més profunditat el paper d'aquest ió Zn(II) present en el domini C-terminal, s'ha intentat substituir afegint diferents equivalents de Cd(II) als pèptids Zn,Cd-CeMT1 i Zn,Cd-CtCeMT1 obtinguts *in vivo*. Els resultats d'ESI-MS obtinguts després de diversos equivalents afegits indiquen que les espècies majoritàries continuen essent heterometàliques. Així doncs, tal i com succeeix en el cas de la metal-lotioneïna de bacteri SmtA,³⁰ l'ió de Zn(II) situat al domini C-terminal de CeMT1 tindria un paper estructural i no es descarta la possibilitat que algun o tots els residus de His de l'estructura primària de CeMT1 participin en la coordinació metàlica, donada la seva major preferència envers el Zn(II) que envers el Cd(II).

3.3.2 Comportament de CeMT2 envers Zn(II) i Cd(II)

La isoforma CeMT2 i els seus dominis N-terminal (9 Cys) i C-terminal (9 Cys i 1 His) s'han biosintetitzat i caracteritzat de forma anàloga a CeMT1. Addicionalment, amb l'objectiu d'estudiar el possible paper coordinant de la His terminal present tant en el pèptid CeMT1 com en CeMT2, s'ha produït un pèptid mutant que presenta la delecio del residu de la His terminal de CeMT2 (Δ HisCeMT2). La caracterització i comparació d'aquest pèptid mutant amb la forma silvestre CeMT2 es discutirà amb més profunditat en l'apartat 3.3.5.

A diferència del que succeeix amb CeMT1, la biosíntesi de CeMT2 en medis enriquits en Zn(II) dóna lloc a una mescla d'espècies homometàliques, on la majoritària és Zn₆-CeMT2 (Figura 1, Article 3). Els seus fragments constitutius també s'expressen com a una mescla d'espècies homometàliques on la majoritària conté 3 Zn(II) (Taula 9.a).

En aquest cas, i tal com succeeix amb Zn-CeMT1, la suma dels espectres de DC dels dominis per separat no reproduieixen l'espectre de DC de la proteïna sencera, fet que indicaria que els dominis N-terminal i C-terminal de CeMT2 també interactúen en coordinar Zn(II).

	Proteïna	Zn-CeMT2	Zn-NtCeMT2	Zn-CtCeMT2
a)	[conc.]	$1.5 \cdot 10^{-4}$ M	$1.9 \cdot 10^{-4}$ M	$0.34 \cdot 10^{-4}$ M
	ICP-AES	5.0 Zn/prot	2.6 Zn/prot	2.2 Zn/prot
	ESI-MS	Zn ₆ -CeMT2 (M) Zn ₅ -CeMT2 Zn ₄ -CeMT2 (m)	Zn ₃ -NtCeMT2 (M) Zn ₂ -NtCeMT2 (m)	Zn ₃ -CtCeMT2 (M) Zn ₂ -CtCeMT2 (m)

	Proteïna	Cd-CeMT2	Cd-NtCeMT2	Cd-CtCeMT2
	[conc.]	$0.3 \cdot 10^{-4}$ M	$0.2 \cdot 10^{-4}$ M	$2.7 \cdot 10^{-4}$ M
	ICP-AES	5.7 Cd/prot	2.3 Cd/prot 0.1 Zn/prot	2.9 Cd/prot
	ESI-MS	Cd ₆ -CeMT2	Cd ₃ -NtCeMT2 (M) Cd ₃ Zn ₁ -NtCeMT2 (m)	Cd ₃ -CtCeMT2

Taula 9.- Resultats de la caracterització dels complexos metall-CeMT2 i dels seus fragments obtinguts per enginyeria genètica mitjançant la seva biosíntesi en medis rics a) en Zn(II) i b) en Cd(II). Les espècies estan ordenades segons la seva abundància en solució. (M) representa l'espècie majoritària i (m) la minoritària.

En la biosíntesi de CeMT2 en presència de Cd(II) s'obté una única espècie homometàlica d'estequiometria Cd₆-CeMT2 i tant NtCeMT2 com CtCeMT2 es sintetitzen com una mescla d'espècies on la majoritària conté 3 ions Cd(II) (Taula 9.b).

L'estudi del comportament de CeMT2 i dels seus fragments envers Cd(II) mitjançant estudis de desplaçament Zn/Cd *in vitro* posen de manifest la facilitat de reproduir les espècies Cd-MT obtingudes *in vivo*. Així, l'addició de 6 equivalents de Cd(II) a l'espècie Zn₆-CeMT2 i de 3 equivalents als complexos Zn-NtCeMT2 i Zn-CtCeMT2 permeten generar les espècies Cd₆-CeMT2, Cd₃-NtCeMT2 i Cd₃-CtCeMT2 respectivament, amb les mateixes propietats espectroscòpiques i espectromètriques que les espècies Cd-MTs obtingudes *in vivo* (Figura 4, Article 3).

En resum, els resultats indiquen que les diferències entre les capacitats coordinants de les isoformes CeMT1 i CeMT2 són degudes a les diferències entre els respectius fragments C-terminals, ja que els dominis N-terminal d'ambdós pèptids presenten gairebé la mateixa seqüència primària i es comporten de la mateixa manera quan coordinen ions divalents. Per tant, el més probable és que la presència del Zn(II) estructural present en el domini C-terminal de CeMT1 estigui relacionat amb la presència de 1 Cys extra i/o als 3 residus addicionals de His que presenta aquesta isoforma, fet que justificaria la presència del Zn(II) extra en les espècies Zn₄- i Cd₃Zn₁-CtCeMT1 respecte les espècies Zn₃- i Cd₃-CtCeMT2.

3.3.3 Comportament CeMT1 envers Cu(II)

Independentment del grau d'oxigenació dels cultius, la biosíntesi de CeMT1 en medis enriquits en Cu dóna sempre lloc a la mateixa mescla d'espècies heterometà·liques Zn,Cu-MT. Així, l'espècie majoritària obtinguda és M₈-CeMT1 a pH 7.0 i Cu₄-CeMT1 a pH 2.4 (Taula 10). Cal destacar que les estequiometries obtingudes són menors de les esperades per a una MT amb 19 residus de Cys (CeMT1 té la capacitat de coordinar 7 metalls divalents). Aquest fet estaria d'acord amb l'especificitat d'aquesta isoforma per als ions divalents. El mateix fenomen té lloc per el fragment C-terminal, que dóna lloc a una espècie heterometà·lica, tal i com mostren els resultats d'ESI-MS realitzats a diferents pHs (M₅-MT a pH 7 i Cu₄-MT a pH àcid) (Taula 10). En canvi, el fragment NtCeMT1 mostraria clarament un caràcter de Cu-tioneïna, ja que quan és produït en medis enriquits en Cu el seu contingut en Zn(II) es menyspreable. Anàlogament al que té lloc per a la proteïna sencera, per ambdós fragments el grau d'oxigenació dels cultius no afecta les espècies obtingudes durant la biosíntesi en presència de Cu(II). El fet que el fragment C-terminal presenti major caràcter de Zn-tioneïna que el N-terminal i per tant major preferència envers els metalls divalents precisament permetria explicar per què el fragment NtCeMT1 forma espècies amb estequiometria superior al C-terminal (Cu₅-NtCeMT1 *vs.* Cu₄-CtCeMT1) tot i el seu menor nombre de residus potencials coordinants (9 Cys per al N-terminal *vs.* 10 Cys i 4 His per al C-terminal).

Proteïna	Cu-CeMT1	Cu-NtCeMT1	Cu-CtCeMT1
[conc.]	$0.6 \cdot 10^{-4}$ M	$0.4 \cdot 10^{-4}$ M	$0.6 \cdot 10^{-4}$ M
ICP-AES	2.2 Zn/prot 4.6 Cu/prot	4.4 Cu/prot	0.8 Zn/prot 3.7 Cu/prot
ESI-MS	pH 7.0	M_8 -CeMT1 (M) M_9 -CeMT1 (M) M_6 -CeMT1 (m) M_5 -CeMT1 (m)	Cu_5 -NtCeMT1 M_4 -CtCeMT1 (M) M_5 -CtCeMT1 (m)
	pH 2.4	Cu_4 -CeMT1 (M) Cu_8 -CeMT1 (m)	Cu_5 -NtCeMT1 Cu_4 -CtCeMT1

Taula 10.- Resultats de la caracterització dels complexos metall-CeMT1 i dels seus fragments obtinguts per enginyeria genètica mitjançant la seva biosíntesi en medis rics en Cu(II). Les espècies estan ordenades segons la seva abundància en solució. (M) representa l'espècie majoritària i (m) la minoritària.

3.3.4 Comportament de CeMT2 envers Cu(II)

La isoforma CeMT2 quan es sintetitzada en medis enriquits en Cu(II) en condicions d'oxigenació normals dóna lloc a la mateixa mescla d'espècies heterometàl·liques Zn,Cu-MT que les obtingudes per CeMT1, on l'espècie majoritària és M_8 -CeMT2 (Taula 11). En canvi, quan es sintetitzada en condicions de baixa oxigenació s'obtenen espècies pràcticament homometàl·liques de Cu(I). Pel que fa als fragments constitutius de CeMT2, en la biosíntesi en qualsevol condició d'oxigenació s'obté l'espècie homometàl·lica Cu_5 -NtCeMT2 i l'heterometàl·lica M_4 -CtCeMT2 (Taula 11). Així doncs, el domini N-terminal es comportaria de la mateixa manera en ambdues isoformes (CeMT1 i CeMT2), presentant un fort caràcter de Cu-tioneïna, mentre que els respectius dominis C-terminal d'ambdues isoformes presentarien tan sols lleus diferències pel que fa a la coordinació del Cu(I).

En conclusió, tant el contingut metàl·lic com les estequiometries obtingudes en la biosíntesi de CeMT2, CeMT1 i els seus fragments en presència de Cu són molt similars. L'única diferència rau en que la isoforma CeMT2 és comportaria millor en presència de Cu(I) en condicions de baixa oxigenació, el que és indicatiu que la isoforma CeMT1 tindria un caràcter més elevat de Zn-tioneïna que no pas la isoforma 2, possiblement degut al major número de residus de His. No obstant, les diferències

apreciades en coordinar metalls divalents no són tan accentuades quan aquestes MTs coordinen ions monovalents com Cu(I) ja que totes dues isoformes es sintetitzen en medis enriquits en Cu(II) com a espècies amb estequiomètries del tipus M₈-MT. Per aquest motiu, podem suposar que els possibles residus coordinants addicionals presents en el fragment CtCeMT1 (1 Cys i 3 His), encara que no incrementen la capacitat coordinant d'aquesta isoforma envers el Cu(I), són determinants a l'hora d'establir l'especificitat metàl·lica de la isoforma CeMT1 per als ions divalents.

Proteïna	Cu-CeMT2 (\approx) ^[a]	Cu-CeMT2 (\downarrow) ^[a]	Cu-NtCeMT2	Cu-CtCeMT2
[conc.]	0.7·10 ⁻⁴ M	0.1·10 ⁻⁴ M	1.0·10 ⁻⁴ M	0.6·10 ⁻⁴ M
ICP-AES	2.5 Zn/prot 4.3 Cu/prot	0.5 Zn/prot 6.6 Cu/prot	4.2 Cu/prot	0.5 Zn/prot 3.5 Cu/prot
ESI-MS	pH 7.0	M ₈ -CeMT2 (M) M ₉ -CeMT2 (M) M ₆ -CeMT2 (m) M ₅ -CeMT2 (m)	M ₈ -CeMT2 (M) M ₉ -CeMT2 (m) M ₄ -CeMT2 (m)	Cu ₅ -NtCeMT2
	pH 2.5	Cu ₄ -CeMT2 (M) Cu ₈ -CeMT2 (m)	Cu ₈ -CeMT2 (M) Cu ₄ -CeMT2 (M)	Cu ₅ -NtCeMT2
				M ₈ -CtCeMT2 (M) M ₉ -CtCeMT2 (M) M ₆ -CtCeMT2 (m) M ₅ -CtCeMT2 (m)
				Cu ₄ -CtCeMT2 (M) Cu ₈ -CtCeMT2 (m)

Taula 11.- Resultats de la caracterització dels complexos metall-CeMT2 i dels seus fragments obtinguts per enginyeria genètica mitjançant la seva biosíntesi en medis rics en Cu(II). [a] (\approx) indica condicions d'oxigenació normals i (\downarrow) condicions de baixa oxigenació. Les espècies estan ordenades segons la seva abundància en solució. Les espècies estan ordenades segons la seva abundància en solució. (M) representa l'espècie majoritària i (m) la minoritària.

3.3.5 Estudi del paper de les His en la coordinació metàl·lica en CeMT1 i CeMT2

Com s'ha comentat anteriorment, les majors diferències entre les isoformes CeMT1 i CeMT2 es troben en el fragment C-terminal. El domini C-terminal de CeMT1 presenta una inserció de 15 aminoàcids respecte a CeMT2, que inclou 3 residus de His i una Cys addicionals (Figura 18). En la bibliografia s'han descrit MTs que contenen residus de His participant en la coordinació metàl·lica, com per exemple la MT de bacteri Zn₄-SmtA³⁰ (Figura 2.b). Així, a causa de l'alt contingut en residus de His de la isoforma 1 s'ha volgut determinar si aquestes poden participar en la coordinació metàl·ica.

Ct-CeMT1 GSKY**CC**EEASEKK**CC**PAG**CK**G**DCK**CAN**CHC**AEQK**QC**GD**KTHQH**QGTAAA**H**
 Ct-CeMT2 GSQ**YCC**PTASEKK**CC**KSGCAGG**CK**CANCE**CAQ**----- AA**H**

Figura 18.- Comparació de seqüències dels fragments C-terminal de les metal-lotioneïnes CeMT1 i CeMT2. Els residus de Cys estan marcats en vermell, les His en blau i la Tyr en verd.

Per tal d'efectuar aquest estudi s'han seguit dues estratègies diferents. Per una banda, s'ha biosintetitzat per enginyeria genètica un pèptid mutant de CeMT2 on s'ha suprimit el residu de His terminal (Δ HisCeMT2) i s'han estudiat les diferències espectroscòpiques i espectromètriques envers la coordinació metàl·lica de Zn(II), Cd(II) i Cu(I) entre aquest pèptid i la forma silvestre CeMT2. Per altra banda, degut a la complexitat de realitzar pèptids mutants de CeMT1 deficientes en His en alguna de les seves posicions, s'ha optat per a fer reaccionar ambdues isoformes amb un reactiu que presenta una alta especificitat per a les His lliures i accessibles¹¹⁴ (pirocarbonat de dietil, DEPC) i determinar per ESI-MS el número de carboxietilacions formades (Figura 19).

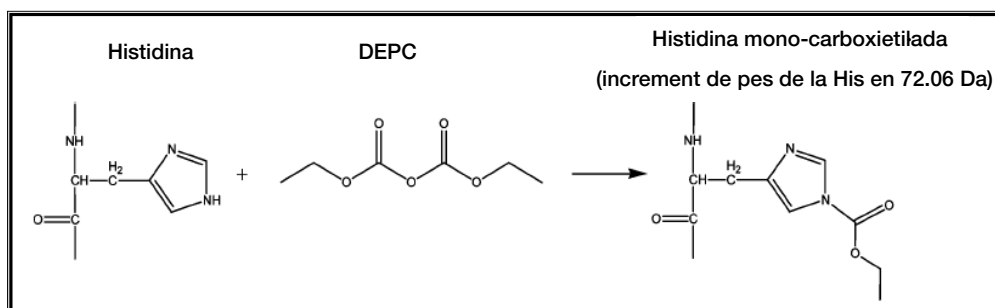


Figura 19.- Reacció entre el DEPC i un residu de His accessible per a formar His mono-carboxietilada.

3.3.5.1 Estudi del paper coordinant de la His terminal de CeMT2

La biosíntesi de Δ HisCeMT2 en medis enriquits en Zn(II) i Cd(II) ha donat lloc a uns complexos amb unes propietats espectromètriques idèntiques a les de CeMT2 (Taula 12). Així doncs, la delecio de la His terminal present en CeMT2 no sembla afectar les seves habilitats coordinants ni en condicions *in vivo* ni *in vitro*. En canvi, els espectres de DC d'ambdós pèptids presenten lleugeres diferències (Figura 2, Article 3), fet que podria indicar algun tipus d'interacció entre la His terminal i els metalls. Amb tot, aquesta His terminal no incrementa la capacitat coordinant de CeMT2 així com probablement tampoc la de CeMT1, donada la identitat de seqüències

d'ambdues isoformes en la part final del domini C-terminal (aminoàcids AAH, Figura 18).

Proteïna	Zn-CeMT2	Zn-ΔHisCeMT2	Cd-CeMT2	Cd-ΔHisCeMT2
[conc.]	$1.5 \cdot 10^{-4}$ M	$0.7 \cdot 10^{-4}$ M	$0.3 \cdot 10^{-4}$ M	$0.2 \cdot 10^{-4}$ M
ICP-AES	5.0 Zn/prot	4.7 Zn/prot	5.7 Cd/prot	5.5 Cd/prot
ESI-MS	Zn ₆ -CeMT2 (M) Zn ₅ -CeMT2 Zn ₄ -CeMT2 (m)	Zn ₆ -ΔHisCeMT2 (M) Zn ₅ -ΔHisCeMT2 Zn ₄ -ΔHisCeMT2 (m)	Cd ₆ -CeMT2	Cd ₆ -ΔHisCeMT2

Taula 12.- Resultats de la caracterització dels complexos metall-CeMT2 i metall-ΔHisCeMT2 mitjançant la seva biosíntesi en medis rics en Zn(II) i Cd(II). Les espècies estan ordenades segons la seva abundància en solució. (M) representa l'espècie majoritària i (m) la minoritària.

En canvi, el pèptid mutant ΔHisCeMT2 s'ha sintetitzat diverses vegades en medis enriquits en Cu(II), tant en condicions de baixa oxigenació com en condicions normals, i en tots els casos s'han obtingut sempre espècies homometàl·liques Cu₈-ΔHisCeMT2 (Taula 13), tant a pH 7.0 com a pH àcid, mentre que la isoforma CeMT2 dóna lloc, en aquestes condicions, a espècies heterometàl·liques. Així doncs, la presència de His en els pèptids estudiats és la que determina la formació d'espècies homometàl·liques de Cu o heterometàl·liques Zn,Cu, i per tant les responsables de conferir un determinat caràcter de Zn-tioneïna o de Cu-tioneïna, encara que no augmenten la capacitat coordinant d'aquests pèptids.

Proteïna	Cu-CeMT2 (\approx) ^[a]		Cu-CeMT2 (\downarrow) ^[a]	Cu-ΔHisCeMT2(\approx) ^[a]
[conc.]	$0.7 \cdot 10^{-4}$ M		$0.1 \cdot 10^{-4}$ M	$0.4 \cdot 10^{-4}$ M
ICP-AES	2.5 Zn/prot 4.3 Cu/prot		0.5 Zn/prot 6.6 Cu/prot	8.7 Cu/prot
ESI-MS	pH 7.0	M ₈ -CeMT2 (M) M ₉ -CeMT2 (M) M ₆ -CeMT2 (m) M ₅ -CeMT2 (m)	M ₈ -CeMT2 (M) M ₉ -CeMT2 (m) M ₄ -CeMT2 (m)	Cu ₈ -ΔHisCeMT2 (M) Cu ₉ -ΔHisCeMT2 (m)
	pH 2.5	Cu ₄ -CeMT2 (M) Cu ₈ -CeMT2 (m)	Cu ₈ -CeMT2 (M) Cu ₄ -CeMT2 (M)	Cu ₈ -ΔHisCeMT2 (M) Cu ₉ -ΔHisCeMT2 (M)

Taula 13.- Resultats de la caracterització dels complexos metall-CeMT2 i metall-ΔHisCeMT2 mitjançant la seva biosíntesi en medis rics en Cu(II). [a] (\approx) indica condicions d'oxigenació normals i (\downarrow) condicions de baixa oxigenació. Les espècies estan ordenades segons la seva abundància en solució. (M) representa l'espècie majoritària i (m) la minoritària.

3.3.5.2 Estudi de la reactivitat de les His de CeMT1 i CeMT2 envers el DEPC

El reactiu DEPC no és útil a l'hora de quantificar el nombre de His que participen en la coordinació metàl·lica, sinó que més aviat serveix per conèixer el nombre de His que no hi participen, ja que aquelles His que, degut al plegament de la proteïna, són inacessibles al reactiu no són modificades per aquest. A més a més, el DEPC no només pot reaccionar amb les His lliures, sinó que també ho pot fer (amb menys afinitat) amb d'altres aminoàcids com són per exemple les Cys, Tyr o l'extrem amino-terminal de les proteïnes.¹¹⁵ Així doncs, per tal de poder determinar el nombre real de His modificades en els pèptids CeMT1 i CeMT2, cal almenys fer servir com a blanc altres pèptids que no continguin residus de Tyr ni de His, ja que tant en CeMT1 com en CeMT2, a part dels residus de His, contenen un residu de Tyr. En la Taula 14 es mostren tots els resultats obtinguts en els experiments d'incubació amb DEPC. Així, el mutant ΔHisCeMT2 només presenta 1 modificació i per tal de determinar si aquesta és deguda a la Tyr o a l'extrem amino-terminal, s'ha utilitzat el pèptid NtCeMT1 com a blanc, ja que aquest no conté en la seva seqüència cap residu de Tyr ni de His. Els resultats indiquen que NtCeMT1 també presenta una sola modificació, i que per tant aquesta només pot ser atribuïble a l'extrem amino-terminal en ambdós casos, de manera que la Tyr en CeMT2 no és carboxietilada pel DEPC.

Per als complexos de CeMT1 i CeMT2 obtinguts en presència de Zn(II) i Cd(II) així com pels seus respectius fragments Cd-Cterminals, s'obtenen sempre 2 modificacions amb el DEPC, que forçosament només poden ser degudes a la His terminal i l'extrem amino-terminal. Per tant, la His terminal de CeMT2, i probablement també la de CeMT1, no participarien de manera important en la coordinació metàl·lica ni de Zn(II) ni de Cd(II) i les 3 His extres de CeMT1 o bé podrien estar participant en la coordinació metàl·lica o bé no són accessibles al DEPC, donat que només 1 de les seves 4 His són modificades.

Per resumir, en aquest treball s'han caracteritzat les metal-lotioneïnes CeMT1 i CeMT2 d'un nematode. S'ha comprovat que les dues tenen una elevada afinitat per coordinar metalls divalents i que la isoforma CeMT1 és la que presenta major especificitat per al Zn(II), tal i com mostren les diferents espècies obtingudes en la biosíntesi d'aquests pèptids en medis enriquits en Zn(II): mescla d'espècies per a Zn-CeMT2 en contraposició a una única espècie Zn₇-CeMT1 molt estable i que conté un Zn(II) estructural en el domini C-terminal de difícil substitució per Cd(II). Paral·lelament,

s'ha estudiat el paper de les His en la coordinació metàl·lica i s'ha observat que en CeMT2 i CeMT1 la His terminal no incrementa la capacitat coordinant envers el Zn(II) i el Cd(II) i que en CeMT1 podrien haver-hi 3 His participant en la coordinació de Zn(II) i Cd(II). Precisament, l'increment en el nombre de residus coordinants en CeMT1 explicaria l'elevada preferència d'aquesta isoforma envers el Zn(II). Això suggereix que aquesta MT podria presentar alguna diferència funcional en l'organisme a part de destoxicar Cd(II) que potser explicaria les variacions detectades en el volum corporal i en el nombre de descendents citades en la introducció.¹⁰² Per últim, gràcies als estudis efectuats amb el pèptid mutant ΔHisCeMT2, s'ha comprovat que els residus de His són els que determinen el caràcter de Zn-tioneïna en els pèptids CeMT1 i CeMT2.

Proteïna	DEPC/MT ^[a]	Nº de modificacions ^[b]	Nº His modificades ^[c]
Cd-NtCeMT1	5	1	0
Zn-ΔHisCeMT2	5	1	0
Zn-CeMT2	5	2	1
Cd-CeMT2	5	2	1
Cd-CtCeMT2	1.5	2	1
Zn-CeMT1	8	2	1
Cd-CeMT1	8	2	1
Cd-CtCeMT1	6	2	1

Taula 14.- Dades analítiques obtingudes en els experiments d'incubació de diverses MTs amb DEPC. a) Relació entre el número d'equivalents de DEPC/MT, b) nombre de carboxietilacions detectades per ESI-MS, c) nombre probable de His carboxietilades.

3.4 Estudi de la capacitat coordinant de la metal-lotioneïna Cup1 del llevat *Saccharomyces cerevisiae*

Aquest grup de recerca va descriure per primera vegada la presència de lligands sulfur en els complexos metà·lics de metal-lotioneïnes recombinants l'any 2005.⁴⁰ D'ençà, aquests lligands inorgànics s'han trobat en moltes de les metal-lotioneïnes recombinants estudiades.^{46,47} Com a norma general, els lligands sulfur es troben en quantitats més elevades quan la MT es sintetitza en medis rics en Cd(II) que no pas en Zn(II) o Cu(II), i són especialment abundants en aquelles MTs amb un elevat caràcter de Cu-tioneïna (com per exemple en Cd-QsMT). Cal tenir en compte, però, que fins aquest moment l'única metodologia emprada per a la síntesi de MTs per part del nostre grup de recerca ha estat la de l'ADN recombinant, és a dir, que les MTs han estat obtingudes a partir de cèl·lules d'*E.coli*. Ara bé, com s'havia descrit que els bacteris poden sintetitzar nanopartícules de CdS dintre de les seves cèl·lules només afegint una sal de Cd(II) i Na₂S al medi de cultiu,⁴⁹ vàrem creure necessari descartar la hipòtesi que els lligands sulfur dels complexos metà·lics de les metal-lotioneïnes recombinants fossin deguts al propi metabolisme del bacteri. Per això, es va decidir purificar i caracteritzar els complexos de Cd(II) d'una Cu-tioneïna nativa (és a dir, no recombinant) per esbrinar si aquests contenien anions sulfur que actuessin com a lligands i, en cas que els tinguessin, poder quantificar-los. Amb aquest objectiu, s'ha obtingut la metal-lotioneïna nativa Cup1 a partir del llevat *S.cerevisiae*. Aquesta MT només es sintetitza en presència d'excés de Cu de manera que per tal de poder obtenir els complexos Cd-Cup1 s'ha treballat amb una soca mutant d'aquest llevat (anomenada N301). Aquesta presenta una mutació en el factor de transcripció que regula la síntesi de la proteïna i que a més confereix a les cèl·lules una elevada resistència al Cd(II), fets que permeten que Cup1 es pugui sintetitzar en llevats crescuts en medis rics en Cd(II).

Paral·lelament a aquest treball, s'ha caracteritzat espectroscòpicament i espectromètrica, mitjançant les tècniques habituals (DC, UV-Vis, ESI-MS, ICP-AES, GC-FPD), la metal-lotioneïna recombinant Cup1 obtinguda a partir de cultius d'*E.coli* enriquits en medis enriquits en Zn(II), Cd(II) i Cu(II). D'aquesta manera, s'han estudiat les similituds i diferències existents entre la metal-lotioneïna Cup1 nativa i la recombinant.

3.4.1 Comportament de Cup1 recombinant envers Zn(II) i Cd(II)

Quan la metal-lotioneïna recombinant Cup1 és biosintetitzada en medis enriquits en Zn(II) s'obté una mescla d'espècies on Zn_4 -Cup1 és l'espècie majoritària (Taula 15). Per altra banda, en la biosíntesi en medis enriquits en Cd(II), s'obté una mescla d'agregats homometàl·lics, amb un contingut en metall superior al de la producció Zn-Cup1 (5.9 ions Cd(II) vs. 2.8 Zn(II)), i on l'espècie majoritària inicialment presenta l'estequiometria Cd_5 -Cup1, acompanyada d'altres espècies que presenten lligands sulfur àcid-làbils amb relacions Cd:MT superiors, *i.e.* Cd_6S_1 - i Cd_7S_4 -Cup1 (Taula 15).

Proteïna	Zn-Cup1	Cd-Cup1
[conc.]	$1.9 \cdot 10^{-4}$ M	$1.1 \cdot 10^{-4}$ M
ICP-AES	2.8 Zn/prot	5.9 Cd/prot
GC-FPD	N.D	$1.7 S^{2-}/prot$
ESI-MS	Zn_4 -Cup1 (M) Zn_3 -Cup1 Zn_5 -Cup1 (m)	Cd_5 -Cup1 (M) Cd_6S_1 -Cup1 Cd_6S_4 -Cup1 (m)

Taula 15.- Resultats de la caracterització dels complexos metall-Cup1 obtinguts per enginyeria genètica mitjançant la seva biosíntesi en medis rics en Zn(II) i Cd(II). Les espècies estan ordenades segons la seva abundància en solució. (M) representa l'espècie majoritària i (m) la minoritària. N.D. indica contingut en S^{2-} no detectable.

De manera molt interessant, i sense precedents en la bibliografia fins al moment, en aquest treball s'ha constatat que les espècies inicialment presents en les preparacions Cd-Cup1 no són termodinàmicament estables, de manera que evolucionen amb el temps cap a un estat més favorable. Això provoca una modificació de la distribució molecular i conseqüentment de l'abundància de les espècies presents en solució. Així, en la Figura 20.c es pot observar com l'espècie inicialment majoritària, Cd_5 -Cup1, esdevé minoritària fins gairebé desaparèixer al cap d'un temps mentre que l'abundància de les espècies riques en sulfur, i inicialment minoritàries, va augmentant amb el temps. Evidentment, aquesta evolució comporta una reestructuració de l'estructura proteica, la generació de nous enllaços Cd- S^{2-} i la pèrdua d'enllaços Cd-SCys, observables per les espectroscòpies de DC i UV-Vis (Figura 20.a i 20.b).

Per altra banda, en els estudis de desplaçament Zn/Cd realitzats *in vitro*, i tal com succeeix en el cas de QsMT, no és possible generar les espècies sulfurades

inicialment obtingudes en la biosíntesi de Cd-Cup1 ni tan sols afegint diversos equivalents de Na_2S al final de les valoracions. Aquesta dificultat per a reproduir les espècies biosintetitzades també queda manifesta en els experiments d'acidificació-reneutralització. Després d'acidificar i reneutralitzar les preparacions Cd-Cup1, l'espècie majoritària en solució és $\text{Cd}_5\text{-Cup1}$, la qual presenta unes propietats espectropolarimètriques molt similars a les de les espècies obtingudes durant els estudis de desplaçament Zn/Cd realitzats *in vitro* a partir de l'espècie $\text{Zn}_4\text{-Cup1}$. Amb tot, l'addició de Na_2S després de l'acidificació-reneutralització de l'espècie $\text{Cd}_5\text{-Cup1}$ permet formar espècies sulfurades, detectables per ESI-MS, però en cap cas no es poden reproduir les espècies obtingudes inicialment en la biosíntesi de Cd-Cup1.

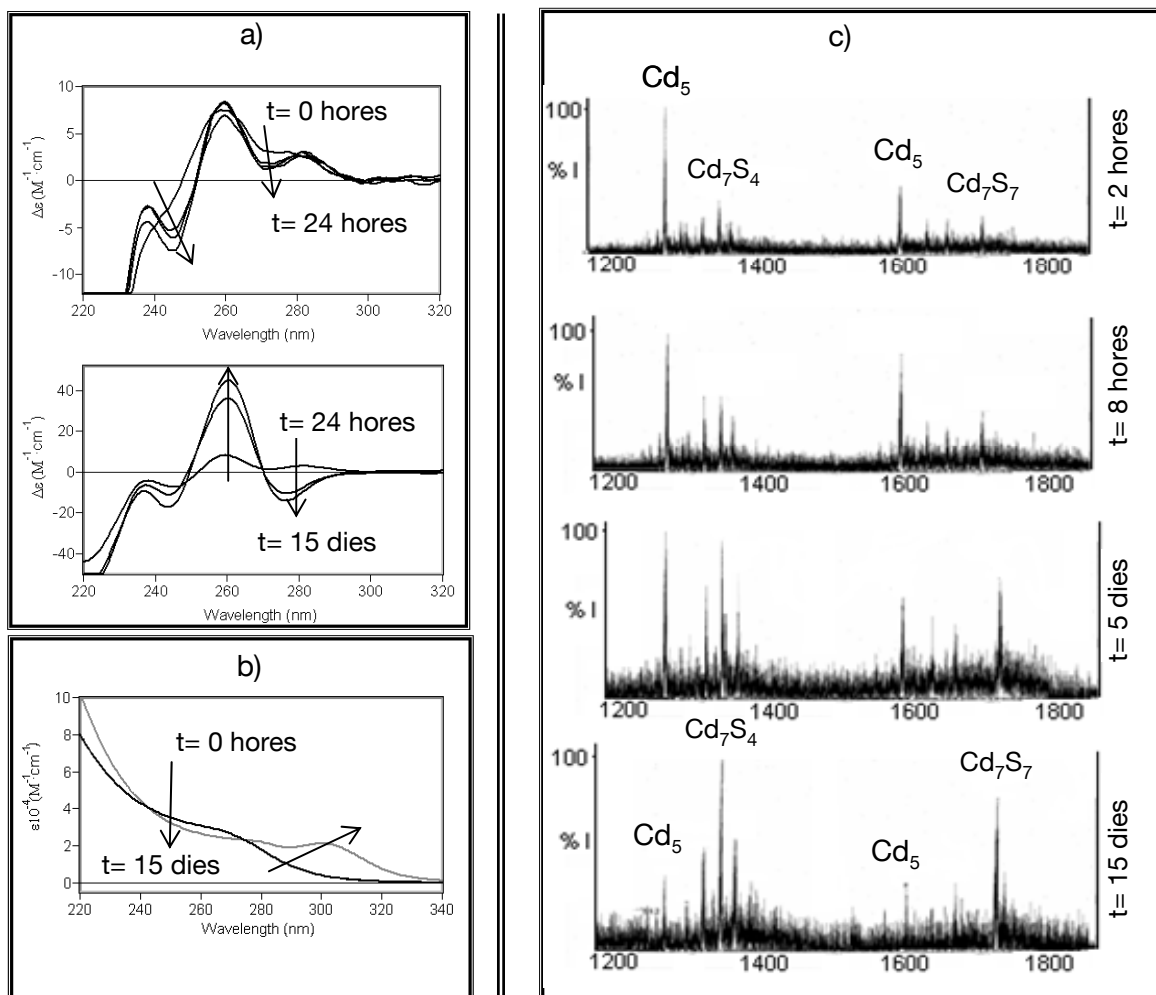


Figura 20.- Canvis espectroscòpics i espectromètrics de la preparació Cd-Cup1 obtinguda *in vivo* amb el temps. a) Canvis produïts en els espectres de DC des de $t = 0$ h fins a $t = 15$ dies, b) Espectres de UV-Vis mesurats a $t = 0$ h (línia negra) i a $t = 15$ dies (línia gris), c) Evolució de la distribució molecular d'espècies presents en solució en diferents dies (des de $t = 0$ h fins a $t = 15$ dies) mesurada per ESI-MS.

3.4.2 Comportament de Cup1 recombinant envers Cu(I)

La biosíntesi de la metal-lotioneïna recombinant Cup1 en medis enriquits en Cu(II) en condicions de baixa oxigenació dóna lloc a pràcticament una única espècie homometàlica Cu₈-Cup1 acompanhada d'una espècie dimèrica molt minoritària, Cu₁₆-(Cup1)₂ (Taula 16). La presència d'aquestes espècies dimèriques ja ha estat proposada en la bibliografia en estudis que suggereixen que Cup1 podria dimeritzar fent servir dues de les seves Cys que no participen en la coordinació metàlica.¹¹⁶ En canvi, quan Cup1 és obtinguda en condicions d'oxigenació normals també s'obté una espècie majoritària homometàlica Cu₈-Cup1, però en aquest cas acompanhada d'altres espècies molt minoritàries d'estequiometries inferiors.

Proteïna	Cu-Cup1 (↓) ^[a]	Cu-Cup1 (≈) ^[a]
[conc.]	0.6·10 ⁻⁴ M	1.8·10 ⁻⁴ M
ICP-AES	8.0 Cu/prot	7.0 Cu/prot
ESI-MS	pH 7.0	Cu ₈ -Cup1 (M) Cu ₁₆ -(Cup1) ₂ (m)
	pH 2.5	Cu ₈ -Cup1 (M) Cu ₁₆ -(Cup1) ₂ (m)

Taula 16.- Resultats de la caracterització dels complexos metall-Cup1 obtinguts per enginyeria genètica mitjançant la seva biosíntesi en medis rics en Cu(II). [a] (≈) indica condicions d'oxigenació normals i (↓) condicions de baixa oxigenació. Les espècies estan ordenades segons la seva abundància en solució. (M) representa l'espècie majoritària i (m) la minoritària.

Pel que fa als estudis de desplaçament Zn/Cu realitzats *in vitro* a partir de l'espècie Zn₄-Cup1, l'addició de 7-8 equivalents de Cu(I) permet reproduir tant espectroscòpicament com espectromètrica la preparació Cu-Cup1 obtinguda *in vivo* en condicions d'oxigenació normals. A més, s'observa per DC i per ESI-MS, i tal i com està descrit en la bibliografia,¹¹⁷ que el procés per a la formació de l'espècie Cu₈-MT és cooperatiu. Així, quan només s'han addicionat 4 equivalents de Cu(I) a l'espècie Zn₄-Cup1, l'espècie Cu₈-Cup1 ja es troba present en solució.

3.4.3 Purificació i caracterització de la metal-lotioneïna nativa Cup1 en presència de Cd(II)

Una part d'aquest treball ha consistit en la purificació i caracterització de la metal-lotioneïna nativa (Cup1) obtinguda a partir d'una soca mutant del llevat *Saccharomyces cerevisiae* (N301) que s'ha fet créixer en un medi de cultiu ric en Cd(II). L'objectiu era comprovar si aquesta dóna lloc a la formació de complexos metall-Cup1 que incorporin anions sulfur àcid-làbils com a lligands, tal i com succeeix en el cas de les metal-lotioneïnes recombinants.

Tradicionalment, en el procés de purificació de metal-lotioneïnes natives a partir de teixits s'utilitza un gran nombre de columnes cromatogràfiques, tant d'exclusió per mida com d'intercanvi iònic.¹¹⁸ En el nostre cas, la purificació de la metal-lotioneïna nativa Cup1 s'ha realitzat seguint dues metodologies diferents que s'han dut a terme en paral·lel (Figura 21).

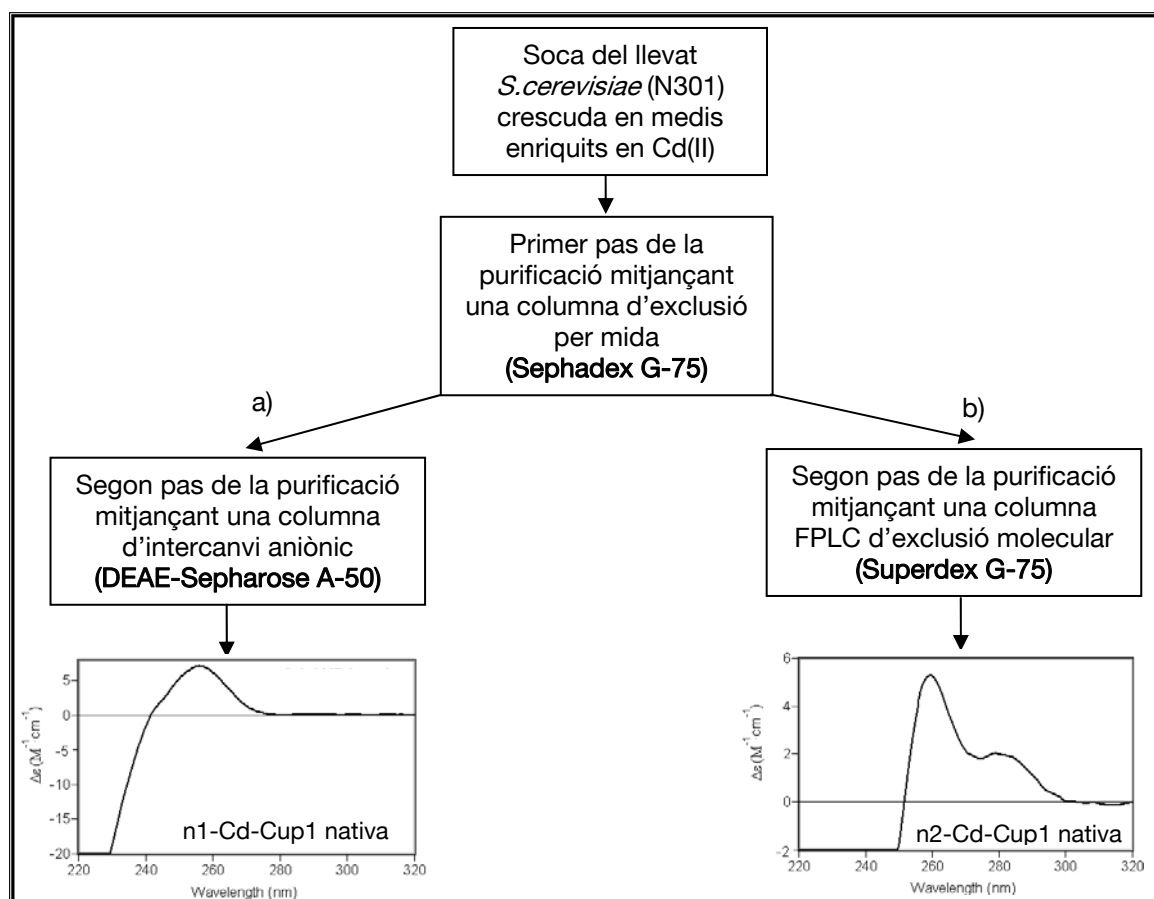


Figura 21.- Esquema general de la purificació de la metal-lotioneïna nativa Cup1 mitjançant dues metodologies diferents. a) Utilitzant columnes de bescanvi iònic b) Sense utilitzar columnes d'intercanvi iònic.

En el primer mètode, s'ha repetit el protocol universalment utilitzat de purificació de MTs natives consistent en una primera purificació amb una columna cromatogràfica d'exclusió per mida, seguida d'una columna d'intercanvi aniónic. Mitjançant aquest procés de purificació de la Cup1 nativa, la metal-lotioneïna recuperada no conté anions sulfur detectables per ESI-MS, DC, o GC-FPD. Aquesta preparació nativa (anomenada n1-Cd-Cup1) conté Cd₅-Cup1 com a espècie majoritària i d'altres espècies hetero- (Zn,Cd-) i homometàl·liques (Cd-Cup1) minoritàries (Taula 17), la qual mostra unes propietats espectroscòpiques i una especiació per ESI-MS molt similars a les obtingudes durant els estudis de desplaçament Zn/Cd realitzats *in vitro* amb l'espècie Zn₄-Cup1 recombinant (Figura 22.a). Aquestes semblances entre les dades *in vivo* i *in vitro* no són d'estranyar donat que en cap dels dos casos les mostres de partida (n1-Cd-Cup1 i Zn-Cup1 recombinant) no contenen lligands sulfur àcid-làbils. La hipòtesi que permetria explicar els resultats de n1-Cd-Cup1 és que amb la utilització de columnes d'intercanvi iònic probablement els lligands sulfur interaccionarien i quedarien retinguts pels grups catiònics de la columna (en aquest cas dietilaminoetil) de tal manera que les espècies finalment eluídes no contindrien aquest tipus de lligand (Taula 17).

Proteïna	n1-Cd-Cup1	n2-Cd-Cup1
[conc.]	0.8·10 ⁻⁴ M	0.9·10 ⁻⁴ M
ICP-AES	4.2 Cd/prot	4.4 Cd/prot
GC-FPD	N.D	2.3 S ²⁻ /prot
ESI-MS*	Cd ₅ -Cup1 (M) Cd ₄ Zn ₁ -Cup1 Cd ₆ -Cup1 (m)	Cd ₅ -Cup1 (M) Cd ₆ S ₁ -Cup1 Cd ₆ S ₄ -Cup1 Cd ₄ Zn ₁ -Cup1(m)

Taula 17.- Resultats de la caracterització dels complexos natius metall-Cup1 obtinguts en medis rics en Cd. Les espècies estan ordenades segons la seva abundància en solució. (M) representa l'espècie majoritària i (m) la minoritària.

Per aquest motiu, en el segon mètode emprat per a purificar la metal-lotioneïna nativa Cup1, s'ha suprimit l'ús de les columnes d'intercanvi iònic i tan sols s'han emprat columnes cromatogràfiques d'exclusió per mida. En aquest cas la proteïna purificada també s'obté com una mescla de complexos heterometàl·lics (Zn,Cd-), però ara també es troben presents tant espècies sulfurades minoritàries (detectades per ESI-MS, DC i GC-FPC), com espècies homometàl·liques i heterometàl·liques no sulfurades (Taula 17). Així, la Cd-Cup1 nativa purificada mitjançant aquest mètode

(anomenada n2-Cd-Cup1) dóna lloc a una espècie majoritària Cd₅-Cup1 acompanyada d'altres espècies minoritàries, Cd₄Zn₁- i Cd₆S₁-Cup1. Aquesta preparació presenta propietats espectropolarimètriques molt similars a les espècies Cd-Cup1 recombinants (Figura 22.b).

Així doncs, es pot concloure que: a) la forma nativa Cd-Cup1 conté anions sulfur àcid-làbils que actuen com a lligands en els seus agregats; b) la presència d'aquests lligands no és un artefacte generat pel metabolisme d'*E.coli*; c) la preparació nativa Cd-Cup1 conté espècies minoritàries heterometàl·liques Zn,Cd-Cup1, fet que no té lloc quan aquesta MT es produeix de forma recombinant i d) només s'aïllen espècies sulfurades quan es suprimeix l'ús de columnes cromatogràfiques de bescanvi anònic. Aquest últim fet pot explicar fàcilment per què fins al moment no s'havia detectat la presència d'aquest lligands en els complexos metall-MT natius purificats a partir d'organismes vius.

Així doncs, hem desenvolupat un mètode de purificació que ha permès demostrar la presència de lligands S²⁻ en preparacions Cd-MT natives. Aquest mètode, a més, podria ser emprat per a purificar altres proteïnes que continguin aquests anions.

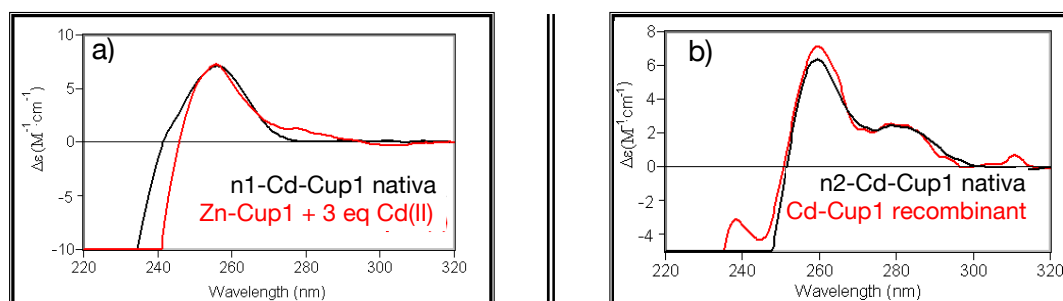


Figura 22.- Comparació entre els espectres de DC de: a) n1-Cd-Cup1 i l'espectre obtingut després d'afegir 3 equivalents de Cd(II) a l'espècie Zn₄-Cup1 recombinant i de b) Cd-Cup1 recombinant a temps 0 i n2-Cd-Cup1.

3.5 Estudi del comportament de les metal-lotioneïnes envers l'estrés reductor

Com ja s'ha comentat en l'apartat 1.6, una de les funcions atribuïdes a les MTs és la de protecció contra les espècies reactives d'oxigen (ROS). Donada la importància de l'estrés oxidatiu sobre els organismes vius, en la bibliografia es troben una gran quantitat de treballs adreçats a aquest tema i actualment es coneix que les espècies reactives d'oxigen reaccionen amb les cisteïnes de les MTs, donant lloc a ponts disulfur i alliberant el metall coordinat.⁶¹ En canvi, l'efecte de l'estrés reductor en les MTs no ha estat tant estudiat. Entre les espècies causants d'estrés reductor, les més habituals són el radical H[•] i els electrons solvatats (e_{aq}⁻). Aquestes espècies poden produir danys en biomolècules mitjançant la desulfurització dels grups tiol dels aminoàcids Cys i Met.^{119,120} Durant aquests processos de desulfurització el residu de Met es transforma en àcid α-aminobutíric (Aba) i l'aminoàcid Cys en alanina (Ala), generant-se els radicals metanotiil (CH₃S[•]) i sulfidril (S^{•-}), respectivament (Figura 23). Els radicals tiil tenen la capacitat de migrar a les membranes cel·lulars, on transformen la disposició *cis* del doble enllaç dels seus àcids grassos a disposició *trans* (Figura 24.b). Aquesta *trans*-isomerització comporta un increment de la rigidesa de les membranes que en fa variar les seves propietats físiques, com la viscositat o la permeabilitat, i, per tant, les seves propietats fisiològiques.¹²¹ A causa del contingut en residus de Cys i Met i en anions sulfur àcid-làbils de les MTs, s'ha considerat adient efectuar un estudi sobre l'efecte de l'estrés reductor en aquestes proteïnes. Aquest treball s'ha efectuat en col·laboració amb el grup de recerca dirigit pel Dr. Chrysostomos Chatgilialoglu del ISOF, Consiglio Nazionale delle Ricerche (Bolonya), i en el marc de l'acció CM0603 del COST.

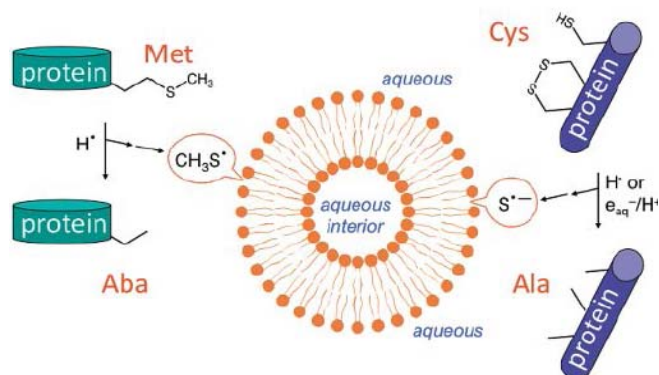


Figura 23.- Esquema general dels danys produïts en lípids i proteïnes per radicals reductors. Els aminoàcids Met i Cys es converteixen en àcid α-aminobutíric (Aba) i alanina (Ala), respectivament, generant-se radicals CH₃S[•] i S^{•-} capaços de migrar a la bicapa lipídica i induir la *trans*-isomerització dels àcids grassos insaturats (extret de Atrian *et al.*¹²²).

3.5.1. Reactivitat de QsMT envers els radicals lliures

En el treball que es presenta aquí s'ha estudiat tant la reactivitat dels complexos Zn(II)- i Cd(II)-QsMT envers espècies radicalàries reactives com els canvis estructurals que pateixen les MTs com a conseqüència de l'exposició a aquests radicals. La generació de les espècies reactives s'ha dut a terme mitjançant la radiòlisi de l'H₂O amb radiació gamma (Figura 24.a), i el percentatge de *trans*-isomerització produït pels radicals s'ha mesurat fent servir uns models biomimètics de membranes cel·lulars (el POPC), aprofitant la capacitat dels radicals tiil generats en els processos de desulfurització per a *trans*-isomeritzar els àcids grassos que les formen.

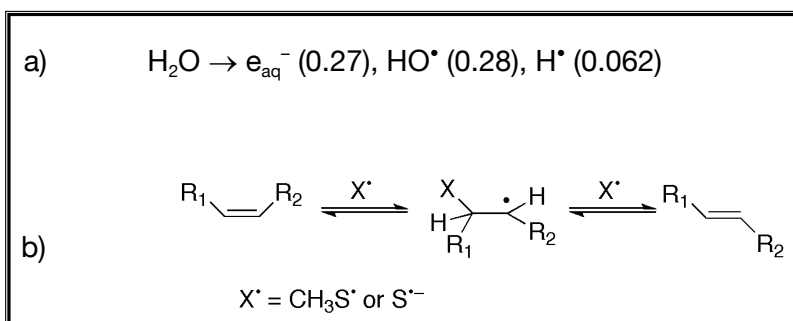


Figura 24.- a) Reacció corresponent a la radiòlisi de l'H₂O. Entre parèntesi es mostra el rendiment de radiació química en unitats de $\mu\text{M}\cdot\text{J}^{-1}$. b) Mecanisme de reacció de la *trans*-isomerització catalitzada per radicals CH₃S[•] o S^{•-}.

L'estudi de l'efecte de les espècies reactives en les MTs s'ha efectuat en quatre condicions diferents, variant el tipus i les concentracions de les diferents espècies reactives en solució (mètodes A1, A2, B1 i B2, Figura 25). Per una banda, s'ha estudiat la reactivitat de les MTs envers els radicals quan en el medi hi ha presents tant espècies radicalàries reactives d'oxigen (OH[•]) com espècies reactives reductores (e_{aq}⁻ i H[•]) (mètodes A1 i A2). En el mètode A2, la concentració de radical hidroxil és superior a la del mètode A1 gràcies a l'addició de N₂O, que transforma els e_{aq}⁻ en radicals hidroxil (Equació 4, Article 5). En els mètodes B1 i B2 s'ha estudiat la reactivitat de les MTs únicament davant les espècies reductores. Mitjançant l'addició de tBuOH al medi, es neutralitzen els radicals hidroxil i únicament queden presents en solució els radicals H[•] i els electrons solvatats (Equació 5, Article 5). En el mètode B2, i tal i com té lloc en el mètode A2, l'addició de N₂O transforma els e_{aq}⁻ en radicals hidroxil, que a la seva vegada són neutralitzats pel tBuOH, deixant en solució únicament els radicals H[•].

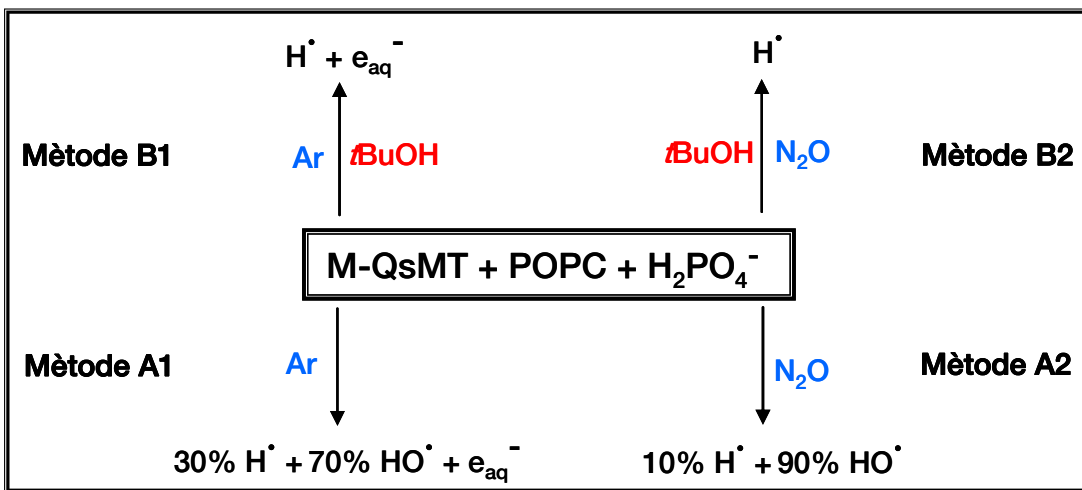


Figura 25.- Esquema general dels quatre tipus diferents d'experiments realitzats variant el tipus i la concentració de les espècies reactives en el medi.

D'aquest conjunt d'experiments realitzats cal destacar dos aspectes importants:

- per una banda, que la formació de radicals tiil és molt més elevada en el mètode B, quan no hi ha radicals hidroxil en el medi (Figura 26).
- per altra banda, la major capacitat de Cd-QsMT respecte de Zn-QsMT per a induir la *trans*-isomerització dels àcids grassos, tant en el mètode A com en el mètode B (Figura 26).

Pel que fa a les diferències observades entre els mètodes A i el B, la generació d'espècies radicalàries tiil és molt més abundant en el mètode B, quan només hi ha presents en solució els radicals H[•] i els electrons solvatats. Aquest fet és fàcil d'explicar, ja que és ben conegut que els radicals OH[•] (resents en el mètode A) tenen la capacitat de reaccionar amb els grups tiol de les Cys de les MTs, oxidant-los i formant ponts disulfur,⁶⁰ competint d'aquesta manera amb la generació de radicals tiil. A més, també s'observa que quan en el medi hi ha presents tant radicals H[•] com e⁻_{aq} (mètode B1), la formació d'isòmers *trans* en les membranes és superior que quan només hi ha radicals H[•] (mètode B2). Aquest fet és indicatiu de la capacitat dels electrons aquosos per a generar espècies radicalàries tiil capaces d'arribar a les membranes.

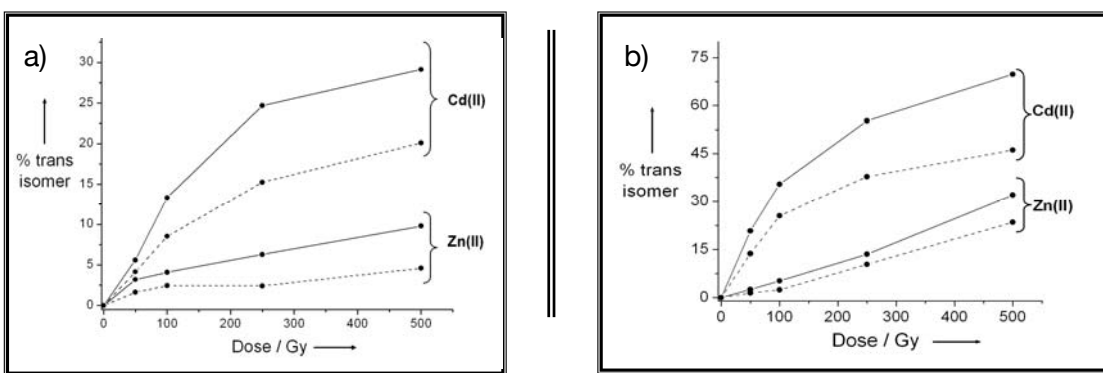


Figura 26.- Estudi del percentatge de trans-isomerització del POPC produït per Zn-QsMT i Cd-QsMT en funció de la quantitat d'irradiació aplicada. a) mètodes A1 (línia contínua) i A2 (línia discontínua) i b) mètodes B1 (línia contínua) i B2 (línia discontínua).

Pel tal d'explicar les diferents capacitats dels pèptids Zn-QsMT i Cd-QsMT per a induir la *trans*-isomerització en les membranes cel·lulars, s'ha de tenir en compte que, encara que tant la forma Zn-QsMT com Cd-QsMT contenen en la seva estructura primària 14 Cys i 3 Met susceptibles de patir una desulfurització, aquestes contenen diferents quantitats de lligands sulfur àcid-làbils en els seus agregats, essent aquesta més elevada en la forma Cd-QsMT (Taula S1, Article 5). En estudis anteriors,¹²³ s'ha descrit com els anions sulfur poden formar també radicals tii de la forma $\text{HS}^\bullet/\text{S}^{\bullet-}$. Així doncs, les espècies H^\bullet i e_{aq}^- no solament atacarien les Met i Cys, sinó que també serien capaces de generar altres radicals tii a partir de l'atac als lligands sulfur. Per tal de demostrar la capacitat d'aquests lligands sulfur que formen part dels agregats metall-MT per a produir radicals tii, s'ha mesurat la reactivitat dels compostos CdS i ZnS envers les diferents espècies reactives i s'ha observat com aquests també generen aquest tipus de radicals capaços d'isomeritzar els àcids grassos de les membranes (Figures S1 i S2, Article 5). Així doncs, és obvi que Cd-QsMT, amb un contingut en sofre inorgànic més elevat que Zn-QsMT, tingui una capacitat superior per a *trans*-isomeritzar els àcids grassos de les membranes.

Per tal d'estudiar l'efecte causat per les espècies H^\bullet i e_{aq}^- en l'estructura de Zn- i Cd-QsMT, s'ha analitzat espectroscòpicament i espectromètrica (DC, Raman i ESI-MS) l'efecte de la irradiació sobre aquests pèptids. Les dades obtingudes per espectroscòpia Raman indiquen que mentre que en el pèptid Cd-QsMT els residus més afectats per la radiació són els residus de Met i els lligands sulfur, en Zn-QsMT ho són els tiolats cisteíncs. Aquestes diferències en la reactivitat possiblement són degudes al diferent plegament que adopten els dos pèptids en presència d'aquests

metalls. Encara que tots dos adopten un plegament en forma de pinça, en el cas de Cd-QsMT l'espaiador té un paper fonamental en el plegament. Així doncs, l'espaiador és possiblement qui determina la diferent reactivitat dels pèptids, ja que les dades d'ESI-MS del pèptid Cd-QsMT indiquen que l'atac de les espècies radicalàries té lloc principalment en l'espaiador, causant la seva fragmentació (Figura 7, Article 5). A més, també s'ha observat que el nombre de fragmentacions de la cadena peptídica és directament proporcional a la intensitat de la radiació aplicada.

Paradoxalment, en els estudis d'espectroscòpia Raman s'observa que el residu d'His present en ambdós pèptids participa en la coordinació metàl·lica després de la irradiació d'aquests. En canvi, els espectres de DC de Cd-QsMT abans i després d'irradiar sugereixen justament el contrari, la pèrdua de la capacitat de coordinació metàl·lica de la His (Figura 6, Article 5). L'explicació d'aquest fet podria ser deguda al tractament aggressiu aplicat a les mostres abans de fer les anàlisis d'espectroscòpia Raman. Durant aquestes preparacions, la mostra és dialitzada i liofilitzada, de manera que el plegament del pèptid podria variar, i per tant es podrien obtenir resultats diferents dels obtinguts en solució, fet que explicaria els diferents resultats obtinguts mitjançant les dues tècniques.

En resum, en aquest estudi s'ha demostrat que les MTs no protegeixen contra l'estrés reductor, ja que les d'espècies radicalàries reductores poden produir la desulfurització dels aminoàcids Met i Cys en les metal-lotioneïnes i generar radicals tills amb capacitat de migrar cap a les membranes i causar danys dintre de la cèl·lula. A més, els estudis realitzats demostren que els lligands sulfur àcid-làbils també poden causar processos de *trans*-isomerització en les membranes, fet molt important ja que en l'entorn intracel·lular existeixen altres proteïnes que contenen lligands sulfur àcid-làbils, com per exemple les proteïnes ferro-sofre.¹²⁴

3.6 Vers una nova proposta de classificació de les MTs

D'acord amb el comentat en l'apartat 1.4, fins al moment s'han proposat tres tipus de classificacions per a les MTs. La classificació més recent, proposada per aquest grup de recerca, divideix les MTs en Zn-tioneïnes i Cu-tioneïnes. Les Zn-tioneïnes són aquelles MTs que en medis rics en Cu(II) donen lloc a espècies heterometà·liques Zn,Cu-MT. En canvi, les Cu-tioneïnes són aquelles MTs que en medis rics en Cu(II) donen lloc a espècies homometà·liques Cu-MT. Darrerament, i en treballs del nostre grup de recerca, s'ha pogut observar que la major o menor oxigenació dels cultius d'*E.coli*, productors de les MTs recombinants, poden determinar la naturalesa homo- o heteronuclear dels complexos metall-MT finals.⁴⁶ Aquest fet, sumat al fet que els lligands sulfur àcid-làbils es troben bàsicament en les MTs tradicionalment classificades com a Cu-tioneïnes,^{46,47} ens ha portat a revisar i actualitzar la nostra proposta de classificació de les MTs en Cu-tioneïnes i Zn-tioneïnes. Així doncs, revisant totes les MTs estudiades per aquest grup de recerca en els darrers 15 anys, s'ha pogut demostrar que existeix una gradació en les propietats de les MTs que permet ordenar-les entre les que hem anomenat Cu-tioneïnes genuïnes i Zn-tioneïnes genuïnes. Aquests dos extrems de MTs convergeixen en una classe central de MTs que presenta unes característiques intermèdies (Taula 18). Per tal d'establir aquesta gradació s'han considerat els següents factors:

- La presència o absència de Zn(II) en els complexos metall-MT biosintetitzats en medis enriquits en Cu(II) (sota diferents graus d'oxigenació dels cultius d'*E.coli*).
- La presència o absència de lligands sulfur en les formes Cd-MT obtingudes *in vivo*.
- La presència o absència de Zn(II) en les formes Cd-MT biosintetitzades.
- El grau de reticència a l'intercanvi Zn/Cd *in vitro* de les Zn-MTs obtingudes *in vivo*.
- La relació entre el nombre de Cys i el nombre d'equivalents de Cu(I) necessaris per tal de reproduir *in vitro* les espècies Cu-MT obtingudes *in vivo*.

MTs	Zn-MT <i>in vitro</i> ^[a]	Cd-MT <i>in vitro</i> ^[a]	Zn-MT + excés de Cd(II) ^[a]	Cu-MT <i>in vitro</i> ^{[a][b]}	Cys/Cu(I) ^[c]
CeMT1	Zn ₇	Cd ₆ Zn ₁	Cd ₆ Zn ₁ , Cd ₇ Zn ₁ , Cd ₈ Zn ₁	↑ M ₈ , M ₉ , M ₅ , M ₆ (2.2 Zn, 4.6 Cu)	4.8
MeMT	Zn ₇	Cd ₇	Cd ₆ Zn ₁ , Cd ₇ , Cd ₅ Zn ₂	↑ M ₈ , M ₉ , M ₁₀ (3.3 Zn, 4.6 Cu)	3.5
MT1	Zn ₇	Cd ₇ , Cd ₇ Zn ₁	Cd ₅ , Cd ₆ Zn ₂ , Cd ₅ Zn ₂ , Cd ₆ Zn ₁ , Cd ₇ Zn ₁	↑ Cd ₇ Zn ₃ (2.4 Zn, 7.2 Cu)	2.9
HpCdMT	Zn ₆ , Zn ₅ , Zn ₄ , Zn ₃	Cd ₆ , Cd ₆ Zn ₁ , Cd ₅	Cd ₆ , Cd ₆ Zn ₁	↑ M ₅ , M ₄ , M ₆ , M ₇ , M ₈ , M ₃ (2.6 Zn, 1.9 Cu) ↓ M ₁₀ , M ₁₁ , M ₁₂ , M ₈ , M ₉ (0.8 Zn, 8.3 Cu)	3.0
TpyMT1	Zn ₁₁ , Zn ₁₁ S ₁ , Zn ₁₀	Cd ₁₁ , Cd ₁₁ S ₁	Cd ₁₁ , Cd ₁₁ S ₁	↑ M ₉ , M ₁₀ , M ₈ , M ₁₁ , M ₁₂ (2.9 Zn, 5.3 Cu) ↓ M ₁₀ (0.4 Zn, 7.3 Cu)	3.1
SpMTA	Zn ₇ , Zn ₆ S ₂ , Zn ₃ , Zn ₄	Cd ₇ , Cd ₆ S ₂ , Cd ₅ S ₁	Cd ₈ , Cd ₆ , Cd ₁₀	↑ M ₈ , M ₄ , M ₆ (2.2 Zn, 5.0 Cu) ↓ M ₄ , M ₈ (3.0 Zn, 5.5 Cu)	2.9
CkMT	Zn ₅ , Zn ₅ S ₁	Cd ₅ , Cd ₅ S ₂	Cd ₅ , Cd ₅ S ₁	↑ Cd ₇ Zn ₃ (2.5 Zn, 7.4 Cu)	2.9
MTH	Zn ₆ , Zn ₇	-----	Cd ₆ , Cd ₆ Zn ₂ , Cd ₆ Zn ₁	↑ M ₈ , M ₁₁ , M ₉ , M ₁₀ (1.6 Zn, 10.8 Cu)	2.3
CeMT2	Zn ₆ , Zn ₅ , Zn ₄ , Zn ₃	Cd ₆ , Cd ₆ S ₁	Cd ₆ , Cd ₅ , Cd ₈	↑ M ₈ , M ₉ , M ₅ , M ₆ , M ₇ (2.5 Zn, 4.3 Cu)	2.3
Crs5	Zn ₆ , Zn ₇ , Zn ₅ , Zn ₇ S ₂	Cd ₇ , Cd ₆ S ₂ , Cd ₆ , Cd ₅ S ₂	Cd ₅ , Cd ₅ S ₄	↑ M ₈ , M ₉ , M ₁₀ , M ₁₁ , M ₁₂ (1.8 Zn, 5.7 Cu) ↓ Cd ₁₀ , Cd ₁₀ , Cu ₁₁ , Cu ₁₂ , Cu ₈ , Cu ₁₃	2.1
MT4	Zn ₅ , Zn ₅ S ₁	Cd ₄ Zn ₄ Cd ₂ Zn ₄ X ₂ Cd ₄ Zn ₂ X (X=S ₂ /Zn)	Cd ₅ , Cd ₆ Zn ₁	↑ Cd ₇ Zn ₃ (2.7 Zn, 7.3 Cu) ↓ Cd ₁₀	2.0
QsMT	Zn ₄ , Zn ₃ , Zn ₂ , Zn ₄ S ₂	Cd ₄ S ₄ , Cd ₅ S ₄ , Cd ₅	Cd ₄ , Cd ₅ , Cd ₃ , Cd ₆	↑ M ₈ , M ₄ , M ₉ (1.7 Zn, 5.5 Cu)	2.0
HpCuMT	Zn ₆ , Zn ₅ , Zn ₄ , Zn ₃	Cd ₆ , Cd ₇ , Cd ₆ S ₂ , Cd ₆ S ₂	Cd ₅ , Cd ₆ , Cd ₈ , Cd ₆ Zn ₁ , Cd ₇ Zn ₁ , Cd ₅ Zn ₁	↑ M ₁₀ , M ₈ , M ₆ , M ₅ , M ₇ , M ₁₂ , M ₄ (2.8 Zn, 3.1 Cu) ↓ Cd ₁₂ , Cd ₁₃	1.8
MtnA	Zn ₄ , Zn ₃	Cd ₄ , Cd ₃ , Cd ₅ S ₂	Cd ₄ , Cd ₃	↑ Cd ₈ , Cd ₇	1.7
MtnB	Zn ₄ , Zn ₃ , Zn ₅	Cd ₄ , Cd ₄ S ₁ , Cd ₅ , Cd ₅ S ₁	Cd ₄ , Cd ₅	↑ Cd ₉ , Cd ₈	1.3
Cup1	Zn ₄ , Zn ₃ , Zn ₅	Cd ₅ , Cd ₆ S ₁ , Cd ₅ S ₄	Cd ₅ , Cd ₄	↑ Cd ₈ , Cd ₄ ↓ Cd ₈ , Cd ₁₆ -dimer	1.2

Taula 18.- Esquema de gradació del caràcter Zn-/Cu-tioneïna de les MTs. En la part superior es troben les Zn-tioneïnes genuïnes i en la part inferior les Cu-tioneïnes genuïnes.

[a] Dades d'ESI-MS. Les espècies majoritàries estan marcades en negreta i les espècies sulfurades estan marcades en blau.

[b] (↔) indica condicions d'oxigenació normals i (↓) indica condicions de baixa oxigenació. El contingut en Zn i Cu obtingut per ICP-AES s'ha indicat en tòtes les espècies heterometàl·liques.

[c] Nombre de Cys respecte el nombre d'equivalents de Cu(II) necessaris per tal de reproduir *in vitro* els complejos obtinguts durant la biosíntesi de les espècies Cu-MT en condicions d'oxigenació normals.

Així, s'ha observat que les Zn-tioneïnes genuïnes sempre s'obtenen com a espècies heterometà·liques en ser biosintetitzades en medis enriquits en Cu(II), sigui quin sigui el grau d'oxigenació dels cultius. Aquest fet és indicatiu de l'essencialitat del Zn(II) per al correcte plegament de la proteïna en coordinar *in vivo* ions Cu(I). Per altra banda, les Cu-tioneïnes genuïnes donen lloc a espècies homometà·liques de Cu(I) sota qualsevol grau d'oxigenació dels cultius. Per contra, les MTs amb propietats intermèdies poden donar lloc a espècies homometà·liques o heterometà·liques dependent del grau d'oxigenació dels cultius d'*E.coli*.

Un punt important a l'hora d'efectuar aquesta nova proposta de classificació ha estat la presència o absència de lligands sulfur en els complexos Cd-MT obtinguts *in vivo*. S'ha comprovat que la quantitat de lligands sulfur és proporcional al caràcter de Cu-tioneïna d'una determinada MT i que aquests es troben totalment absents en els complexos formats per les Zn-tioneïnes genuïnes. Aquests lligands sulfur (tret dels casos de QsMT i Cup1) semblen no incrementar la capacitat coordinant de les MTs estudiades, ja que les espècies sulfurades obtingudes són sempre espècies minoritàries o presenten la mateixa estequiomètria metall-MT que les espècies majoritàries. Aquestes observacions indiquen que les MTs amb un elevat caràcter de Zn-tioneïna no requeririen lligands addicionals per a coordinar ions divalents, mentre que les Cu-tioneïnes, especialment dissenyades per a coordinar ions monovalents, quan són obligades a coordinar metalls divalents, i especialment Cd(II), fan ús dels anions sulfur. Per altra banda, les Zn-tioneïnes genuïnes, en ser biosintetitzades en medis enriquits en Cd(II) donen lloc a espècies heterometà·liques Zn,Cd-MT, com és el cas de CeMT1, MT1 o HpCdMT (Taula 18), i precisament aquestes MTs són les que presenten una major reticència *in vitro* a intercanviar completament el Zn(II) per Cd(II).

Un altre factor determinant per elaborar aquesta classificació ha estat la relació entre els equivalents de Cu(I) necessaris per reproduir les espècies Cu-MT biosintetitzades en condicions normals d'oxigenació, i el total de residus cisteíncics de cadascuna de les MTs considerades (n° Cys/eq Cu(I)). Així, encara que en tots els casos estudiats es poden reproduir les espècies sintetitzades *in vivo* per addició de diversos eq de Cu(I) a les corresponents formes Zn-MT, en les Cu-tioneïnes genuïnes la ratio Cys/Cu(I) és menor que en les Zn-tioneïnes genuïnes. Aquest fet estaria d'accord amb la hipòtesi que inicialment dintre de les cèl·lules les metal·tioneïnes es produirien com a Zn-MTs i, posteriorment, aquest metall seria substituït per Cu(I) dependent de les necessitats de la cèl·lula. En el cas de les Cu-tioneïnes, en que tot el Zn(II) és substituït per Cu(I), la quantitat de Cu(I) necessària per a efectuar aquesta substitució serà més gran que en el cas de les Zn-tioneïnes, en què la substitució

només és parcial, fet que justificaria la disminució del valor Cys/Cu(I) al llarg de la Taula 18.

En base a aquesta gradació, les proteïnes estudiades en aquesta Tesi Doctoral abastarien tot l'espectre, des de les isoformes CeMT1 i MeMT (Zn-tioneïnes genuïnes) fins a Cup1 (Cu-tioneïna genuïna), passant per CeMT2 i QsMT, ambdues amb característiques intermèdies (Taules 18 i 19).

Zn-tioneïnes genuïnes	Cu-tioneïnes genuïnes
Es sintetitzen com a una única espècie quan són bioproduïdes en medis enriquits en Zn(II) i com a mescla d'espècies en medis enriquits en Cu(II)	Es sintetitzen com a mescla d'espècies quan són bioproduïdes en medis enriquits en Zn(II) i com a una única espècie en medis enriquits en Cu(II)
Contenen Zn(II) en ser bioproduïdes en medis enriquits en Cd(II)	Contenen lligands S ²⁻ en ser produïdes en medis enriquits en Cd(II)
Reticència a l'intercanvi Zn/Cd <i>in vitro</i>	No mostren cap reticència a l'intercanvi de Zn/Cd <i>in vitro</i>
S'obtenen com a espècies heterometà·liques en ser bioproduïdes en medis enriquits en Cu(II), independentment del grau d'oxigenació del cultiu	S'obtenen com a espècies homometà·liques en ser bioproduïdes en medis enriquits en Cu(II), independentment del grau d'oxigenació del cultiu

Taula 19.- Comparació de els propietats de les Zn-tioneïnes i les Cu-tioneïnes genuïnes.

Aquesta gradació, a més, posa de manifest la relació existent entre les diferents capacitats de coordinació metà·lica de les MTs i les seves funcions fisiològiques. Per exemple, Cup1, que forma espècies homometà·liques de Cu amb una elevada especificitat per aquest metall, únicament es sintetitza en llevat com a resposta a un excés de Cu o Ag. En canvi, les isoformes CeMT1 i MeMT, que en els organismes vius es sintetitzen basalment, són les que presenten la major especificitat per al Zn(II). Per contra, les MTs on s'ha proposat que podrien participar tant en el metabolisme del Cu(I) com en el del Zn(II), com és el cas CkMT¹²⁵ o Crs5,⁴⁶ es troben situades al mig de la taula de gradació, mostrant unes propietats intermèdies entre les Zn- i les Cu-tioneïnes genuïnes. Aquesta especificitat de les MTs envers un metall en particular té el seu màxim exponent en les isoformes del cargol *Helix pomatia*. Ambdues, amb el mateix nombre de residus aminoacídics i amb el mateix nombre de Cys i situades en les mateixes posicions (Figura 27), mostren una preferència d'enllaç

metàl·lic completament diferent.^{100,126} Aquest fet indica que l'especificitat metàl·lica de les MTs no només ve determinada pels seus residus cisteínics, sinó que la resta d'aminoàcids també participen a l'hora de fer que una determinada MT tingui caràcter de Zn- o Cu-tioneïna.

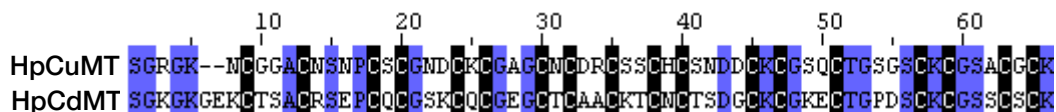


Figura 27.- Alineament en base a similitud de seqüència de les isoformes HpCuMT i HpCdMT del cargol *Helix pomatia* mitjançant l'aplicació ClustalW. En negre s'observen els residus de cisteïna.

4. Conclusions

4. CONCLUSIONS

El treball realitzat en el marc d'aquesta Tesi Doctoral ha permès arribar a un conjunt de conclusions, les quals s'exposen a continuació agrupades d'acord amb els diferents objectius proposats.

➤ *Comportament coordinant de la isoforma MeMT del mol·lusc *M.edulis**

- MeMT es classifica com una Zn-tioneïna genuïna. Aquests resultats estan d'acord amb el seu possible paper en l'homeòstasi de Zn(II), tal i com suggereixen els diferents patrons d'inducció dels gens MT en el musclo.
- MeMT presenta una elevada capacitat coordinant envers els ions divalents, especialment per al Zn(II). A més, el plegament que adopta aquesta MT en coordinar Zn(II) fa que alguns d'aquests ions siguin difícilment substituïbles per Cd(II) o Cu(I).
- MeMT pot adoptar un plegament diferent quan coordina Cd(II) depenent de si el complex Cd-MeMT s'obté *in vivo* o *in vitro*.

➤ *Comportament coordinant de la isoforma QsMT de l'alzina *Q.suber**

- La síntesi de QsMT en medis rics en Zn(II) i Cd(II) dóna lloc a complexos metall-MT no isoestequiomètrics i conseqüentment no isoestructurals.
- Els lligands sulfur en les espècies Cd-QsMT així com en els pèptids mutants Cd-N25-C18 i Cd-N25 són imprescindibles per assolir el plegament correcte dels pèptids. A més, aquests lligands addicionals incrementen la capacitat coordinant d'aquests proteïnes.
- QsMT adopta un plegament en forma de pinça en coordinar Cd(II), en el qual l'espaiador probablement desenvolupa un rol indispensable per a l'estructuració correcta de l'agregat, tot i no participar directament en la coordinació metàl·lica. Addicionalment, s'ha comprovat la importància de l'espaiador a l'hora de conferir propietats destoxicadores a la proteïna.

➤ *Comportament coordinant de les isoformes CeMT1 i CeMT2 del nematode C.elegans*

- CeMT1 es classifica com a Zn-tioneïna genuïna i presenta un major caràcter de Zn-tioneïna que CeMT2, fet que suggereix l'existència d'una funció biològica per a CeMT1 addicional a la de destoxicació.
- CeMT1 presenta un Zn(II) estructural situat en el domini C-terminal, el qual probablement està coordinat per algun residu d'histidina. Addicionalment, s'ha comprovat que la histidina terminal en el pèptid CeMT2 no participa de manera important en la coordinació a metalls divalents.
- CeMT1 i CeMT2 es comporten de manera anàloga quan coordinen Cu(I), i encara que les histidines extres presents en CeMT1 no participen en la coordinació metàl·lica d'aquest ió, són les que determinen el caràcter de Zn-tioneïna d'aquest pèptid.

➤ *Estudi del paper dels lligands sulfur en les metal-lotioneïnes*

- Excepte casos puntuals, els lligands sulfur no incrementen la capacitat coordinant de les metal-lotioneïnes.
- Els lligands sulfur àcid-làbils són més abundants quan les MTs s'obtenen com a Cd-MTs i la seva abundància és proporcional al caràcter de Cu-tioneïna del polipèptid.
- S'ha demostrat que les metal-lotioneïnes natives contenen lligands sulfur àcid-làbils en els seus complexos (cas de Cd-Cup1), fet que indica que l'obtenció de MTs recombinants riques en lligands sulfur no és un artefacte provocat pel metabolisme dels bacteris. Aquest resultat obre noves perspectives, tant estructurals com funcionals, en el camp de les MTs i de les bionanopartícules.
- L'obtenció de complexos metall-MT natius rics en sulfur només és possible quan no s'empren columnes d'intercanvi iònic, donat que aquestes provoquen la pèrdua dels lligands sulfur dels complexos Cd-MT.

- *Estudi de la reactivitat de les metal-lotioneïnes envers els radicals lliures*
 - A diferència del que succeeix amb els radicals oxidants, les MTs no semblen protegir els organismes envers els radicals reductors, sinó més aviat al contrari, ja que la desulfurització dels aminoàcids metionina i cisteïna pot causar danys en l'entorn cel·lular via la *trans*-isomerització dels àcids grassos que constitueixen les membranes cel·lulars. A més, la presència de lligands sulfur addicionals en les MTs incrementa els processos de desulfurització i conseqüentment la generació de radicals tòxics.
- *Nova proposta de classificació de les metal-lotioneïnes*
 - S'ha demostrat que existeix una gradació entre les que hem anomenat Cuttonioneïnes genuïnes i les Zn-tioneïnes genuïnes, convergint en una classe central de MTs amb característiques intermèdies.
 - L'especificitat de les MTs envers els diferents ions metà·lics no només pot ser atribuïda als tiolats cisteíncs, sinó que la resta d'aminoàcids també desenvolupen un paper fonamental a l'hora de determinar les preferències metà·liques d'una determinada MT.

5. Procediment experimental i tècniques utilitzades

5. PROCEDIMENT EXPERIMENTAL I TÈCNIQUES UTILITZADES

En aquest apartat es fa un recull de les tècniques i dels procediments utilitzats per dur a terme l'obtenció i caracterització de totes les proteïnes emprades en aquesta Tesi Doctoral.

Tot el material de vidre utilitzat ha estat rentat inicialment amb HNO_3 20% (v/v) i després amb aigua mili-Q abundant. La finalitat d'aquest procediment de rentat ha estat la d'eliminar els possibles ions metà·lics presents en el material de vidre. En tots els experiments portats a terme s'ha utilitzat aigua mili-Q i les solucions emprades han estat de qualitat espectroscòpica. El material de plàstic utilitzat ha estat d'un sol ús.

5.1 Obtenció i caracterització de la proteïna

La síntesi i purificació de totes les metal-lotioneïnes recombinants estudiades en aquesta Tesi Doctoral ha estat duta a terme pel grup de recerca dirigit per la Dra. Sílvia Atrian, Catedràtica de Genètica de la Universitat de Barcelona. Les MTs han estat produïdes mitjançant la tècnica de l'ADN recombinant a través de la introducció del gen que les codifica en cèl·lules del bacteri *E.coli*. Totes han estat produïdes en presència de Zn(II), Cd(II) i Cu(II) i posteriorment han estat purificades i eluídes en tampó Tris-HCl 50 mM a pH 7.0. En tots els casos les proteïnes han estat obtingudes amb una pureza superior al 95% i unes concentracions elevades ($\approx 10^{-4}$ M).^{14,127} Cal esmentar que el coure que es troba present en les MTs presenta únicament l'estat d'oxidació +1, tot i que la sal que s'introdueix en el medi de cultiu és CuSO_4 , ja que les cèl·lules d'*E.coli* només permeten l'entrada de Cu(II) i no de Cu(I) en el seu interior. Ara bé, un cop dins la cèl·lula existeixen diversos mecanismes de reducció de Cu(II) que asseguren la formació correcta dels complexos Cu^I-MT. Pel que fa a la Cd-Cup1 nativa aïllada del llevat *S.cerevisiae*, la seva síntesi i purificació, descrites en l'apartat 3.4.3 d'aquest treball, han estat dutes a terme personalment pel present candidat al títol de Doctor conjuntament amb el senyor Fredy Monteiro, doctorant del Departament de Genètica de la UB.

El primer pas a l'hora de caracteritzar les MTs obtingudes és comprovar la integritat de la cadena peptídica. L'anàlisi per espectrometria de masses a pH àcid (forma apo) permet la determinació del seu pes molecular i per tant la confirmació de

la integritat de la mateixa. Els passos que es duen a terme a continuació són: la determinació, mitjançant ESI-MS a pH 7.0, del nombre i estequiomètria de les diferents espècies metall-lades, la mesura de la concentració de la proteïna i de la relació global metall/proteïna, via la determinació del sofre total, zinc, cadmi i coure per ICP-AES, l'estudi del plegament de la proteïna per dicroisme circular, la determinació de les absorcions en l'UV-Vis, i en el cas on es detecten per ESI-MS espècies que contenen lligands sulfur àcid-làbils o si existeix divergència entre els resultats de l'ICP-AES convencional i àcid, la quantificació de sulfur per GC-FPD. A continuació es resumeixen els principis bàsics relatius a les tècniques utilitzades per a la caracterització de les proteïnes.

5.2 Espectrometria de masses (ESI-MS-TOF)

L'espectrometria de masses (MS), amb ionització per electrosprai (ESI) i analitzador de temps de vol (TOF) és una tècnica ideal per a poder determinar l'estequiomètria i massa de les espècies metall-MT realment presents en solució. Per un costat el mètode d'ionització és molt suau i no provoca la pèrdua dels ions metàl·lics dels complexos metall-MT. Per l'altre, l'analitzador TOF d'alta resolució permet determinar relacions massa/càrrega (m/z) de manera molt acurada. A més a més, el fet de tenir acoblada una bomba de HPLC permet treballar amb diferents solucions tampó. En el nostre cas s'ha treballat a dos valors de pH diferents: pH 7.0, on les espècies metall-MT es mantenen inalterades, i a pH 2.0-2.5, condicions en les quals tot el Zn(II) i/o Cd(II) es desenllaça de les MTs, observant-se així únicament les espècies apo-MT (provinents de les formes Zn- i/o Cd-MT) i les espècies Cu-MT (provinents de els formes Zn,Cu-MT).

Els espectres de masses s'han enregistrat en l'espectròmetre Micro Tof-Q de Brucker, del Servei d'Anàlisi Química de la UAB, calibrat amb una solució de NaI (200 ppm NaI en H₂O/isopropanol 1:1). Les condicions experimentals per analitzar MTs contenint metalls divalents (Zn, Cd) han estat: 20 µL de proteïna injectada; voltatge del capil·lar de 5000 V; temperatura zona d'asseccament (dry temp.) 90-110 °C; gas d'asseccament (dry gas) 6 L/min; rang de m/z 800-2000. La fase mòbil consisteix en una mescla 95:5 d'acetat amònic/amoníac 15 mM : acetonitril a pH 7.0.

Les mostres que contenen coure han estat analitzades injectant 20 µL de proteïna; voltatge del capil·lar de 4000 V; temperatura zona d'asseccament (dry temp.) 80 °C; gas d'asseccament (dry gas) 6 L/min; rang de m/z 800-2000. La fase mòbil

consisteix en una mescla 90:10 d'acetat amònic/amoníac 15 mM : acetonitril a pH 7.0. Per a l'anàlisi a pH àcid, les condicions utilitzades han estat les mateixes que les emprades en el cas de metalls divalents, excepte en la composició de la fase mòbil, que en aquest cas és una mescla 95:5 d'àcid fòrmic : acetonitril a pH 2.0-2.4. Totes les mostres han estat injectades com a mínim per duplicat per tal d'assegurar la reproductibilitat.

5.3 Espectroscòpia d'emissió atòmica amb plasma acoblat per inducció (ICP-AES)

L'anàlisi per ICP-AES d'una MT permet determinar-ne simultàniament el contingut total de metalls (Zn, Cd, Cu) i de sofre. Aquest es realitza com a mínim per duplicat per a cada mostra. Totes les mesures es preparen prenent entre 100 i 500 µL de proteïna i s'enrasa amb HNO₃ al 2% en matrassos aforats de 2 o 5 mL. Les rectes de calibrat dels 4 elements es realitzen mitjançant la preparació de patrons de diferent concentració a partir de patrons estandarditzats de 1000 ppm. Cal dir que el contingut en sofre en aquest cas inclou tant el sofre de les cisteïnes i metionines com el provinent dels ions sulfur àcid-làbils. Aquesta metodologia s'ha anomenat en aquesta Tesi Doctoral “ICP-AES convencional”. Ara bé, precisament a causa de la possible presència de lligands sulfur àcid-làbils en alguns dels agregats metàl·lics de les MTs, els resultats obtinguts per ICP-AES convencional s'han confrontat amb els obtinguts mitjançant la variant anomenada “ICP-AES àcid”, en la qual la mostra és incubada a 65°C amb HClO₄ concentrat abans de la mesura per ICP-AES. D'aquesta manera la concentració de sofre mesurada dependrà únicament de la quantitat de cisteïna i metionina, ja que els possibles ions sulfur presents en solució s'hauran alliberat en forma d'àcid sulfhídric gasós. La mesura del contingut en sofre total permet calcular la concentració de proteïna en solució en base a la seva seqüència. Per a efectuar aquestes mesures s'ha utilitzat l'equip Thermo Jarrell Ash Polyscan 611, dels Serveis Científicotècnics de la UB, treballant en les longituds d'ona 182.04 nm, 213.85 nm, 324.75 nm i 228.80 nm per a mesurar S, Zn, Cu i Cd, respectivament.

5.4 Espectroscòpia d'absorció ultraviolat-visible (UV-Vis)

A diferència d'altres proteïnes, la gran majoria de les MTs no contenen aminoàcids aromàtics en la seva seqüència. Per això la seva forma demetal·lada és totalment incolora i, en conseqüència, transparent a longituds d'ona superiors a 220 nm. D'altra banda, quan la proteïna es coordina a centres metàl·lics ho fa, en general, mitjançant residus de Cys, de manera que totes les absorcions presents a longituds d'ona superiors a 220 nm seran degudes a la coordinació del metall a les Cys. Ara bé, tot i que l'espectroscòpia d'absorció UV-Vis permet determinar la naturalesa dels àtoms donadors i l'estereoquímica de coordinació en els complexos de metalls de transició, això no és possible en el cas dels metalls amb configuració electrònica d^{10} . Tot i així, en absència de bandes d-d és possible que depenen de la naturalesa del lligand puguin aparèixer bandes de transferència de càrrega (TC), com és el cas dels lligands tiolat. La relació de les bandes TC, força amples i d'elevada energia, amb l'estereoquímica de coordinació esdevé, però, força més complexa. Així, els agregats metall(d^{10})-MT són comparables a complexos polinuclears $[M_y(SR)_x]$ i són capaços de presentar bandes de TC lligand \rightarrow metall, o TCLM, les quals poden proporcionar informació sobre la naturalesa del cromòfor, tot i que sovint es requereix informació addicional per poder extreure'n conclusions significatives. Per aquest motiu, ens interessa més observar l'evolució del conjunt d'espectres que s'obtenen al llarg d'una valoració en la qual es van substituint progressivament els metalls inicialment enllaçats a la proteïna per part de l'altre ió metàl·lic (agent valorant). D'aquesta manera, es generen posteriorment els espectres de diferència corresponents a addicions consecutives (p.ex.: 6-5 equivalents de Cd(II) afegits, que s'expressa com a 6-5, es mesura l'efecte provocat únicament per aquest sisè ió Cd(II) afegit). Els espectres de diferència ens informaran de la formació o desaparició de determinats cromòfors provocats únicament per l'addició de l'equivalent considerat.

Els espectres d'absorció UV-Vis s'han enregistrat en l'espectrofotòmetre *HP8452A* de *diode array* del Servei d'Anàlisi Química de la UAB, amb 15 segons de temps d'integració i emprant una cubeta de quars amb d'1 cm de pas de llum. Com a blanc s'ha emprat una solució de la mateixa concentració de tampó que les mostres. Tots els espectres s'han tractat amb el programa informàtic GRAMS/32.

5.5 Espectroscòpia de dicroisme circular (DC)

L'espectroscòpia de DC es basa en l'absorció per part d'un cromòfor òpticament actiu d'una llum incident polaritzada en un pla. Es pot considerar que una llum polaritzada linealment està formada per dos feixos de llum polaritzats circularment en sentits oposats. L'absorció desigual dels dos feixos de llum per part d'un cromòfor òpticament actiu es tradueix en l'existència de dos coeficients d'extinció molar, ϵ_e i ϵ_d , és a dir, la llum polaritzada circularment en el sentit esquerre (e) és absorbida amb diferent intensitat que la del sentit dret (d). La variació dels coeficients d'extinció molar, $\Delta\epsilon = |\epsilon_e - \epsilon_d|$, en funció de la longitud d'ona de la radiació incident constitueix la base dels espectres de dicroisme circular. Les bandes dels espectres de DC poden ser de dos tipus diferents: gaussianes i en forma de derivada. Una banda gaussiana indica l'existència de cromòfors idèntics però independents. En canvi, quan dos o més cromòfors idèntics, connectats per enllaços σ , s'orienten adequadament per establir interaccions mútues, apareix un acoblament anomenat *exciton coupling*, que transforma la banda gaussiana en una altra banda en forma de primera derivada.

En el cas de les MTs, els cromòfors $[M(SR)_x]$ esdevenen òpticament actius gràcies a la transferència de la quiralitat pròpia de la cadena peptídica (L-aminoàcids) als centres metàl·lics. D'aquesta manera el senyal de DC dóna informació directa de l'entorn de coordinació del metall, essent la intensitat de les bandes dicroiques una mesura del grau de plegament o d'estructuració de la proteïna. Malgrat això, la presència de diferents entorns de coordinació en una mateixa espècie metall-MT, la possible coexistència de diferents graus de metal·lació per una mateixa proteïna i la presència de més d'un metall són factors limitants en aquesta tècnica.

Els espectres DC de les mostres s'han enregistrat en l'espectropolarímetre *Jasco-715*, del Servei d'Anàlisi Química de la UAB, a 50 nm/min, 0.5 nm de resolució i utilitzant una cubeta de quars segellada d'1 cm de pas de llum. Com a blanc s'ha emprat una solució de la mateixa concentració de Tris-HCl que les mostres enregistrades. Tots els espectres s'han tractat amb el programa informàtic GRAMS/32.

5.6 Cromatografia de gasos amb detecció fotomètrica de flama (GC-FPD)

Aquest tipus de cromatografia està especialment indicada per a la detecció d'anions sulfur àcid-làbils a baixes concentracions i permet la quantificació del nombre de S²⁻ per molècula de MT en aquelles preparacions en les quals els resultats d'ICP-AES convencional i àcid presentin resultats diferents o s'hagin detectat espècies sulfurades per ESI-MS. En aquesta tècnica s'acidifica prèviament la mostra, la qual allibera H₂S, que queda retingut en un *head-space* i que posteriorment és cromatografiat i detectat per un detector fotomètric de flama (FPD).

Per a aquestes mesures s'ha utilitzat el cromatógraf *HP5890* sèrie II acoblat a un detector *FPD80 CE* (Thermo Finningan), dels Serveis Científicotècnics de la UB. Els patrons requerits s'han preparat a partir de solucions de Na₂S·9H₂O estandarditzades iodometricament.⁴⁰

5.7 Valoracions de les formes Zn-MT amb solucions de Cd(II) i Cu(I)

Les formes Zn-MT obtingudes per enginyeria genètica han estat valorades amb solucions aquoses de Cd(II) i Cu(I) (vegeu a continuació). Aquestes valoracions s'han dut a terme a 25 °C sota atmosfera d'argó dins d'una cel·la de quars d'1 cm de pas de llum amb tap i han estat seguides mitjançant les tècniques de DC i UV-Vis. Tant la solució proteica com l'agent valorant han estat bombollejats amb argó després de cada equivalent de metall valorant afegit per tal d'evitar la presència d'oxigen. Addicionalment, alíquots escollides en punts destacats de les valoracions han estat analitzades també per ESI-MS.

5.7.1 Agent valorant de Cd(II)

L'agent valorant de Cd(II) s'ha preparat per dilució en aigua mili-Q d'una solució estàndard de 1000 ppm de CdCl₂. La concentració de la solució final s'ha determinat en l'espectrofotòmetre d'absorció atòmica de flama Perkin Elmer 2100, del Servei d'Anàlisi Química de la UAB. Els patrons de calibració han estat preparats per dilució en HNO₃ al 2% d'una solució estàndard de CdCl₂.

5.7.2 Agent valorant de Cu(I)

L'agent valorant de Cu(I) que s'ha utilitzat ha estat una solució del complex $[\text{Cu}(\text{CH}_3\text{CN})_4]\text{ClO}_4$ en 30% de CH₃CN. S'ha escollit aquest compost atenent al fet que és una sal molt resistent a l'oxidació a l'aire i que l'anion ClO₄⁻ no interfereix en els estudis *in vitro* de les MTs ja que és molt poc coordinant.

La síntesi del complex de Cu(I) es duu a terme sota una atmosfera de nitrogen i es basa en la publicada per Kubas, Monzyc i Crumbliss.¹²⁸ Sobre una suspensió de 4.0 g de Cu₂O en 80 mL de CH₃CN s'hi addicionen lentament 24.6 mL de HClO₄ 4.6 M. La barreja resultant es deixa refluir a 100°C sota agitació magnètica. El sòlid blanc que havia començat a precipitar es redissol ràpidament i la solució adquireix una tonalitat blau pàl·lid que correspon a la presència de trases de Cu(II). Un cop no s'observa gens de sòlid blanc es filtra la solució en calent. El filtrat es deixa refredar a temperatura ambient, després a la nevera i per últim al congelador tota la nit. Passat aquest temps es recullen els cristalls blancs de $[\text{Cu}(\text{CH}_3\text{CN})_4]\text{ClO}_4$. Es renten amb 3 porcions de 5-10 mL de Et₂O, s'assequen al buit i es guarden sota atmosfera d'argó al dessecador. Finalment, la solució utilitzada de Cu(I) que s'emprarà per a valorar es prepara en atmosfera d'argó per dilució de la sal en una solució aquosa al 30% en volum de CH₃CN. La concentració de Cu de la solució es determina en l'espectrofotòmetre d'absorció atòmica de flama Perkin Elmer 2100, del Servei d'Anàlisi Química de la UAB. Els patrons de calibració es preparen per dilució en HNO₃ al 2% d'una solució estàndard de CuCl₂. Cal afegir també que abans de poder emprar aquest agent valorant cal verificar l'absència d'ions Cu(II) en solució mitjançant mesures d'EPR. Aquestes mesures s'han dut a terme amb l'espectròmetre de ressonància paramagnètica electrònica Brucker ESP 300 E amb sistema criogènic de nitrogen líquid, de l'ICMAB-CSIC.

5.8 Acidificació-reneutralització de les formes Cd-MT

Les formes Cd-MT obtingudes per enginyeria genètica han estat acidificades des de pH 7.0 fins a pH 1.0 amb solucions aquoses d'àcid clorhídric de concentració variable (1-1·10⁻³M). Un cop a pH 1.0, la solució proteica es bombollejada amb argó durant 20 minuts. Acte seguit, la solució es reneutralitza fins a pH 7 mitjançant una solució aquosa de NaOH de concentració variable (1-1·10⁻³M). En el cas on els complexos de partida Cd-MT continguin lligands sulfur, s'addicionen diversos equivalents d'una

solució Na₂S estandarditzada iodomètricament. Els processos d'acidificació-reneutralització s'han dut a terme a temperatura ambient sota atmosfera d'argó dins d'una cel·la de quars d'1 cm de pas de llum amb tap i han estat seguides mitjançant les tècniques de DC i UV-Vis. Sempre que ha estat possible, alíquots de l'inici i del final dels experiments s'han analitzat per ESI-MS.

6. Bibliografia

6. BIBLIOGRAFIA

- 1.- Margoshes, M.; Vallee, B., *J. Am. Chem. Soc.*, **(1957)**, 79, 4813-4814.
- 2.- Gold, B.; Deng, H.; Bryk, R.; Vargas, D.; Eliezer, D.; Roberts, J.; Jiang, X.; Nathan, C., *Nat. Chem. Bio.*, **(2008)**, 4, 609-616.
- 3.- Kay, J.; Cryer, A.; Darke, B.M.; Killer, P.; Lees, W.E.; Norey, C.G.; Stark, J.M., *Int. J. Biochem.*, **(1991)**, 23, 1-5.
- 4.- Stillman, M.J., *Coord. Chem. Rev.*, **(1995)**, 144, 461-511.
- 5.- Riordan, J.F.; Vallee, B.L., *Methods Enzymol.*, **(1991)**, 205, 616-626.
- 6.- Kull, F.J.; Reed, M.F.; Elgren, T.E.; Ciardelli, T.L.; Wilcox, D.E., *J. Am. Chem. Soc.*, **(1990)**, 112, 2291-2298.
- 7.- Nishiyama, Y.; Nakayama, S.; Okada, Y.; Min, K.S.; Onosaka, S.; Tanaka, K., *Chem. Pharm. Bull.*, **(1990)**, 38, 2112-2117.
- 8.- Okada, Y.; Ohta, N.; Iguchi, S.; Tsuda, Y.; Sasaki, H.; Kitagawa, T.; Yagyu, M.; Min, K.S.; Onosaka, S.; Tanaka, K., *Chem. Pharm. Bull.*, **(1986)**, 34, 986-998.
- 9.- Hartmann, H.J.; Li, Y.J.; Weser, U., *Biometals*, **(1992)**, 5, 187-191.
- 10.- Li, Y.J.; Weser, U., *Inorg. Chem.*, **(1992)**, 31, 5526-5533.
- 11.- Sewell, A.K.; Jensen, L.T.; Erikson, J.C.; Palmiter, R.D.; Winge, D.R., *Biochemistry*, **(1995)**, 34, 4740-4747.
- 12.- Cols. N., *Tesi Doctoral*, Dept. Genètica, Universitat de Barcelona, **(1996)**.
- 13.- Capdevila, M.; Cols, N.; Romero-Isart, N.; González-Duarte, R.; Atrian, S.; González-Duarte, P., *Cell. Mol. Life Sci.*, **(1997)**, 53, 681-688.
- 14.- Romero-Isart, N.; Vašák, M., *J. Inorg. Biochem.*, **(2002)**, 88, 388-396.
- 15.- Cobine, P.A.; McKay, R.T.; Zangger, K.; Dameron, C.T.; Armitage, I.M., *Eur. J. Biochem.*, **(2004)**, 271, 4213-4221.
- 16.- Schultze, P.; Worgötter, E.; Braun, W.; Wagner, G.; Vašák, M.; Kägi, J.H.; Wüthrich, K., *J. Mol. Biol.*, **(1988)**, 203, 251-268.
- 17.- Aseniev, A.; Schultze, P.; Wörgötter, E.; Braun, W.; Wagner, G.; Vašák, M.; Kägi, J.H.; Wüthrich, K., *J. Mol. Biol.*, **(1988)**, 201, 637-657.
- 18.- Messerle, B.A.; Schäffer, A.; Vašák, M.; Kägi, J.H.; Wüthrich, K., *J. Mol. Biol.*, **(1990)**, 214, 765-779.
- 19.- Robbins, A.H.; McRee, D.E.; Williamson, M.; Collet, S.A.; Xuong, N.H.; Furey, W.F.; Stout, C.D., *J. Mol. Biol.*, **(1991)**, 221, 1269-1293.
- 20.- Zangger, K.; Öz, G.; Otvos, J.D.; Armitage, I.M., *Protein Sci.*, **(1999)**, 8, 2630-2638.
- 21.- Öz, G.; Zangger, K.; Armitage, I.M., *Biochemistry*, **(2001)**, 40, 11433-11441.
- 22.- Robbins, A.H.; McRee, D.E.; Williamson, M.; Collet, S.A.; Xuong, N.H.; Furey, W.F.; Stout, C.D., *J. Mol. Biol.*, **(1991)**, 221, 1269-1293.
- 23.- Capasso, C.; Carginak, V.; Crescanzi, O.; Di Maro D.; Parisi, E.; Spadaccini, R.; Temussi, P.A., *Structure*, **(2003)**, 11, 435-443.
- 24.- Narula, S.S.; Brouwer, M.; Hua, Y.; Armitage, I.M., *Biochemistry*, **(1995)**, 34, 620-631.
- 25.- Muñoz, A.; Försterling, F.H.; Shaw III, C.F.; Petering, D.H., *J. Biol. Inorg. Chem.*, **(2002)**, 7, 713-724.
- 26.- Riek, R.; Prêcheur, B.; Wang, Y.; Mackay, E.A.; Wider, G.; Güntert, P.; Liu, A.; Kägi, J.H.; Wüthrich, K., *J. Mol. Biol.*, **(1999)**, 291, 417-428.
- 27.- Bertini, I.; Hartmann, H.J.; Klein, T.; Liu, G.; Luchinat, C.; Weser, U., *Eur. J. Biochem.*, **(2000)**, 267, 1008-1018.
- 28.- Peterson, C.W.; Narula, S.S.; Armitage, I.M., *FEBS lett.*, **(1996)**, 379, 85-93.
- 29.- Calderone, V.; Dolderer, B.; Hartmann, H.J.; Echner, H.; Luchinat, C.; Del Bianco, C.; Mangani, S.; Weser, U., *Proc. Natl. Acad. Sci. USA*, **(2005)**, 102, 51-56.
- 30.- Blindauer, C.A.; Harrison, M.D.; Parkinson, J.A.; Robinson, A.K.; Cavet, J.S.; Robinson, N.J.; Sadler, P.J., *Proc. Natl. Acad. Sci. USA*, **(2001)**, 98, 9593-9598.
- 31.- Smith, T.A.; Lerch, K.; Hodgson, K.O., *Inorg. Chem.*, **(1986)**, 25, 4677-4680.
- 32.- Vašák, M., *Encyclopedia of Inorganic Chemistry*, **(1994)**, IV, 2229-2241.
- 33.- Jocelyn, P.C., *Eur. J. Biochem.*, **(1967)**, 2, 327-331.
- 34.- Fowler, B.A.; Hildebrand, C.E.; Kojima, Y.; Webb, M., dins: *Metallothionein II*, Kägi, J.H.; Kojima, Y.; Birkhäuser, V., **(1987)**, 52, 19-22.

- 35.- Winge, D.; Dameron, C.T.; Mehra, R.K., dins: *Metallothioneins*, Stillman, M.J.; Shaw III, F.C.; Suzuki, K.T., (1992), 11, 257-270.
- 36.- Binz, P.A.; Kägi, J.H., dins: *Metallothionein IV*, Birkhäuser, V., (1999), 7-13.
- 37.- <http://www.unizh.ch/~mtpage/classif.html>
- 38.- Cobbett, C.; Goldsborough, P., *Ann. Rev. Pl. Biol.*, (2002), 53, 159-182.
- 39.- Valls, M.; Bofill, R.; González-Duarte, R.; González-Duarte, P.; Capdevila, M.; Atrian, S., *J. Biol. Chem.*, (2001), 276, 32835-32843.
- 40.- Capdevila, M.; Domenech, J.; Pagani, A.; Tío, L.; Villarreal, L.; Atrian, S., *Angew. Chem. Int. Ed.*, (2005), 44, 4618-4622.
- 41.- Villarreal, L.; Tio, L.; Atrian. S.; Capdevila. M., *Arch. Biochem. Biophys.*, (2005), 435, 331-335.
- 42.- Maret, W.; Heffron, G.; Hill, H.A.; Djuricic, D.; Jiang, L.J.; Vallee, B.L.; *Biochemistry*, (2002), 41, 1689-1694.
- 43.- Reese, R.N.; Winge, D.R., *J. Biol. Chem.*, (1988), 263, 12832-12835.
- 44.- Weber, D.N.; Shaw III, F.; Petering, D.H., *J. Biol. Chem.*, (1987), 262, 6962-6964.
- 45.- Reese, R.N.; Mehra, R.M.; Tarbet, E.B.; Winge, D.R., *J. Biol. Chem.*, (1988), 263, 4186-4192.
- 46.- Pagani, A.; Villarreal, L.; Capdevila, M.; Atrian, S., *Mol. Microbiol.*, (2007), 63, 256-269.
- 47.- Domènec, J.; Mir, G.; Huguet, G.; Capdevila, M.; Molinas, M.; Atrian, S.; *Biochimie*, (2006), 88, 583-593.
- 48.- Freisinger, E., *Dalton Trans.*, (2008), 47, 6663-6675.
- 49.- Sweeney, R.Y.; Mao, C.; Gao, X.; Burt, J.L.; Belcher, A.M.; Georgiou, G.; Iverson, B.L., *Chem. Biol.*, (2004), 11, 1553-1559.
- 50.- Palmiter, R.D., *Proc. Natl. Acad. Sci. USA*, (1998), 95, 8428-8430.
- 51.- Mastersm B.A.; Kelly, E.J.; Quaife, C.J.; Brinster, R.L.; Palmitier, R.D., *Proc. Natl. Acad. Sci. USA*, (1994), 91, 584-588.
- 52.- Klaassen, C. D.; Liu, J.; Choudhuri, S., *Annu. Rev. Pharmacol. Toxicol.*, (1999), 39, 267-294.
- 53.- Trinchella, F.; Riggio, M.; Filosa, S.; Volpe, M.G.; Parisi, E.; Scudiero, R., *Comp. Biochem. Physiol. C Toxicol. Pharmacol.*, (2006), 144, 272-278.
- 54.- Amiard, J.C.; Amiard-Triquet, C.S.; Pellerin, B.J.; Rainbow. P.S., *Aquat. Toxicol.*, (2006), 76, 160-202.
- 55.- Moltó, E.; Bonzón-Kulichenko, E.; del Arco, A.; López-Alañón, D.M.; Carrillo, O.; Gallardo, N.; Andrés, A., *Gene*, (2005), 361, 140-148.
- 56.- Yang, Z.B.; Zhao, Y.L.; Li,N.; Yang,J., *Arch. Environ. Contam. Toxicol.*, (2007), 52, 222-228.
- 57.- Kägi, J.H., *Methods Enzymol.*, (1991), 205, 613-626.
- 58.- Haq, F.; Mahoney, M.; Koropatnick, J., *Mutat. Res.*, (2003), 533, 211-226.
- 59.- Udom, A.O.; Brady, F.O., *Biochem. J.*, (1980), 187, 329-335.
- 60.- Kang, Y.J., *Exp. Biol. Med. (Maywood)*, (2006), 231, 1459-1467.
- 61.- Formigari, A.; Irato, P.; Santon, A., *Comp. Biochem. Physiol. C Toxicol. Pharmacol.*, (2007), 146, 443-459.
- 62.- Deng, D.X.; Chakrabarti, S.; Waalkes, M.P.; Cherian, M.G., *Histopathology*, (1998), 32, 340-347.
- 63.- Kondo, Y.; Rusnak, J.M.; Hoyt, D.G.; Settineri, C.E.; Pitt, B.R.; Lazo, J.S., *Mol. Pharmacol.*, (1997), 52, 195-201.
- 64.- Viarengo, A.; Burlando, B.; Ceratto, N.; Panfoli, I., *Cell. Mol. Biol.*, (2000), 46, 407-417.
- 65.- Quesada, A.R.; Byrnes, R.W.; Krezoski, S.O.; Petering, D.H., *Arch. Biochem. Biophys.*, (1996), 334, 241-250.
- 66.- Lazo, J.S.; Kondo, Y.; Dellapiazza, D.; Michalska, A.E.; Choo, K.H.; Pitt, B.R., *J. Biol. Chem.*, (1995), 270, 5506-5510.
- 67.- Buttké, T.M.; Sandstrom, P.A., *Immunol. Today*, (1994), 15, 7-10.
- 68.- Coyle, P.; Philcox, J.C.; Rofe, A.M., *J. Nutr.*, (1999), 129, 372-379.
- 69.- Ogra, Y.; Aoyama, M.; Suzuki, K.T., *Arch. Biochem. Biophys.*, (2006), 451, 112-118.
- 70.- Beattie, J.H.; Wood, A.M.; Newman, A.M.; Bremner, I.; Choo, K.H.; Michalska, A.E.; Duncan, J. S.; Trayhurn, P., *Proc. Natl. Acad. Sci. U S A*, (1998), 95, 358-363.
- 71.- Quaife, C.J.; Findley, S.D.; Erikson, J.C.; Froelick, G.J.; Kelly, E.J.; Zambrowicz, B.P.; Palmiter, R.D., *Biochemistry*, (1994), 33, 7250-7259.

- 72.- Liang, L.; Fu, K.; Lee, D.K.; Sobieski, R.J.; Dalton, T.; Andrews, G.K., *Mol. Rep. Dev.* **(1996)**, 43, 25-37.
- 73.- González-Duarte, P., dins: *Comprehensive Coordination Chemistry II*, McCleverty, J. A.; Meyer, T.J., **(2003)**, 8, 213-228.
- 74.- Egli, D.; Domènec, J.; Selvaraj, A.; Balamurugan, K.; Hua, H.; Capdevila, M; Georgiev, O.; Schaffner, W.; Atrian, S., *Genes to Cells*, **(2006)**, 11, 647-658.
- 75.- Narula, S.S.; Brouwer, M.; Hua, Y.; Armitage, I.M., *Biochemistry*, **(1995)**, 34, 620-631.
- 76.- Valls, M.; Bofill, R.; González-Duarte, R.; González-Duarte, P.; Capdevila, M.; Atrian, S., **(2001)**, *J. Biol. Chem.*, 276, 32835-32843.
- 77.- Lerch, K.; Ammer, D.; Olafson, R. W., *J. Biol. Chem.* **(1982)**, 257, 2420-2426.
- 78.- Ceratto, N.; Dondero, F.; Van de Loo, J.W.; Burlando, B.; Viarengo, A., *Comp. Biochem. Physiol. C*, **(2002)**, 131, 217-222.
- 79.- Liao, V.H-C.; Dong, J.; Freedman, J.H., *J. Biol. Chem.*, **(2002)**, 277, 42049-42059.
- 80.- Maruyama, K.; Hori, R. Nishihara, T., *Eisei Kagaku*, **(1986)**, 32, 22-27.
- 81.- Lane, B.; Kajioka, R.; Kennedy, T., *Biochem. Cell. Biol.*, **(1987)**, 65, 1001-1005.
- 82.- Murphy, A.; Taiz, L., *Plant. Physiol.* **(1995)**, 109, 945-954.
- 83.- Van Hoof, N.A.; Hassinen, V.H.; Hakvoort, H.W.J.; Ballintijn, K.F.; Schat, H.; Verkleij, J.A.C.; Ernst, W.H.G.; Karenlampi, S.O.; Tervahauta, A.I., *Plant. Physiol.*, **(2001)**, 126, 1519-1526.
- 84.- Lemoine, S.; Laulier, M.; *Mar. Pollut. Bull.*, **(2003)**, 46, 1450-1455.
- 85.- Ciocan, C.M.; Rotchell, J.M., *Environ. Sci. Technol.*, **(2004)**, 38, 1073-1078.
- 86.- Grattarola, M.; Carloni, M.; Dondero, F.; Viarengo, A.; Vergani, L., *Mol. Biol. Rep.*, **(2006)**, 33, 265-272.
- 87.- Barsyte, D.; White, K.N.; Lovejoy, D.A., *Comp. Biochem. Physiol. C*, **(1999)**, 122, 287-296.
- 88.- Geffard, A.; Amiard, J.C.; Amiard-Triquet, C., **(2002)**, *Biomarkers*, 7, 123-137.
- 89.- Hamza-Chaffai, A.; Amiard, J.C.; Pellerin, R.P.; Joux, L.; Berthet, B., *Comp. Biochem. Physiol. C*, **(2000)**, 127, 153-163.
- 90.- Vergani, L.; Grattarola, M.; Borghi, C.; Dondero, F.; Viarengo, A., *FEBS J.*, **(2005)**, 272, 6014-6023.
- 91.- Vergani, L.; Grattarola, M.; Grasselli, E.; Dondero, F.; Viarengo, A., *Arch. Biochem. Biophys.*, **(2007)**, 465, 247-253.
- 92.- Digilio, G.; Bracco, C.; Vergani, L.; Botta, M.; Osella, D.; Viarengo, A., *J. Biol. Inorg. Chem.*, **(2009)**, 14, 167-178.
- 93.- Mir, G.; Domènec, J.; Huguet, G.; Guo, W.J.; Goldsbrough, P.B.; Atrian, S.; Molinas, M., *J. Exp. Bot.*, **(2004)**, 55, 2483-2493.
- 94.- Bilecen, K.; Ozturk, U.H.; Adil, D.D.; Sutlu, T.; Petoukhov, M.V.; Svergun, D.I.; Koch, H.J.; Sezerman, U.O.; Cakmak, I.; Sayers, Z., *J. Biol. Chem.*, **(2005)**, 280, 13701-13711.
- 95.- Chunming Z.; Tun, L.; Riqing, Z.; Nanming, Z.; Jinyuan, L., *Chin. Sci. Bull.*, **(2000)**, 45, 1413-1417.
- 96.- Kille, P.; Winge, R.D.; Harwood, L.J.; Kay, J., *FEBS Lett.*, **(1991)**, 295, 171-175.
- 97.- Morris, C.A.; Nicolaus, B.; Sampson, V.; Harwood, J.L.; Kille, P., *Biochem. J.*, **(1999)**, 38, 553-560.
- 98.- The *C.elegans* Sequencing Consortium, *Science*, **(1998)**, 282, 2012-2018.
- 99.- Slice, L.W.; Freedman, J.H.; Rubin, C.S., *J. Biol. Chem.*, **(1990)**, 265, 256-263.
- 100.- Dallinger, R., *Comp. Biochem. Physiol.*, **(1996)**, 113C, 125-133.
- 101.- You, C.; Mackay, E.A.; Gehrig, P.M.; Hunziker, P.E.; Kagi, J.H., *Arch. Biochem. Biophys.*, **(1999)**, 372, 44-52.
- 102.- Hugues, S.; Stürzenbaum, S.R., *Environ. Pollut.*, **(2007)**, 145, 395-400.
- 103.- Prinz, R.; Weser, U., *Hoppe-Seyler's Z. Physiol. Chem.*, **(1975)**, 356, 767-776.
- 104.- Luchinat, C.; Dolderer, B.; Del Bianco, C.; Echner, H.; Hartmann, H.J.; Voelter, W.; Weser, U., *J. Biol. Inorg. Chem.*, **(2003)**, 8, 353-859.
- 105.- Weser, U.; Hartmann, H.J., *Biochim. Biophys. Acta.*, **(1988)**, 953, 1-5.
- 106.- Winge, D.R.; Nielson, K.B.; Gray, W.R.; Hamer, D.H., *J. Biol. Chem.*, **(1985)**, 260, 14464-14470.
- 107.- Culotta, V.C.; Howard, W.R.; Liu, X.F., *J. Biol. Chem.*, **(1994)**, 269, 25295-25302.
- 108.- Jensen, L.T.; Howards, W.R.; Strain, J.J.; Winge, D.R.; Culotta, V.C., *J. Biol. Chem.*, **(1996)**, 271, 18514-18519.

- 109.- George S.G., *Comp. Biochem. Physiol. C*, (1983), 76, 53-57.
- 110.- Morgan, A.J.; Morris, B., *Histochemistry*, (1982), 75, 269-285.
- 111.- Stürzenbaum, S.R.; Georgiev, O.; Morgan, A.J.; Kille, P., *Environ. Sci. Technol.* (2004), 38, 6283-6289.
- 112.- Vasák, M.; Romero-Isart, N., dins: *Encyclopedia of Inorganic Chemistry*, (2006), 5, 3208-3221.
- 113.- Romero-Isart, N.; Cols, N.; Termansen, J.L.; Gelpí, R.; Gonzalez-Duarte, R.; Atrian, S.; Capdevila, M.; Gonzalez-Duarte, P., *Eur. J. Biochem.*, (1999), 259, 519-527.
- 114.- Miles, E.W. *Methods Enzymol.*, (1977), 47, 431-442.
- 115.- Mendoza, V.L.; Vachet, R.W., *Anal. Chem.*, (2008), 80, 2895-2904.
- 116.- Peterson, C.W.; Narula, S.S.; Armitage, I.M., *FEBS Lett.*, (1996), 379, 85-93.
- 117.- Byrd, J.; Berger, R.M.; McMillin, D.R.; Wright, C.F.; Hamer, D.; Winge, D.N., *J. Biol. Chem.*, (1988), 263, 6688-6694.
- 118.- Weser, U.; Hartmann, H.J.; Fretzdorff, A.; Strobel, G.J., *Biochim. Biophys. Acta*, (1979), 493, 465-477.
- 119.- Chatgilialoglu, C.; Altieri, A.; Fischer, H., *J. Am. Chem. Soc.*, (2002), 124, 12816-12823.
- 120.- Chatgilialoglu, C.; Samadi, A.; Guerra, M.; Fischer, H., *Chem. Phys. Chem.*, (2005), 6, 286-291.
- 121.- Roberts, T.L.; Wood, D.A.; Riemersma, R.A.; Gallagher, P.J.; Lampe, F.C., *Lancet*, (1995), 345, 278-282.
- 122.- Atrian, S.; Bobrowski, K.; Capdevila, M.; Chatgilialoglu, C.; Ferreri, C.; Houée-L., Han-tal; Salzano, A.; Scaloni, A.; Torreggiani, A., *Chimia*, (2008), 62, 721-727.
- 123.- Ferreri, C.; Chatgilialoglu, C.; Torreggiani, A.; Salzano, A.M.; Renzone, G.; Scaloni, A., *J. Proteome Res.*, (2008), 7, 2007-2015.
- 124.- Johnson, D.C.; Dean, D.R.; Smith, A.D.; Johnson, M.K., *Annu. Rev. Biochem.*, (2005), 74, 247-281.
- 125.- Villarreal, L.; Tío, L.; Capdevila, M.; Atrian, S., *FEBS J.*, (2006), 273, 523-535.
- 126.- Dallinger, R.; Berger, B.; Hunziker, P.; Kägi J.H.R., *Nature*, (1997), 338, 237-238.
- 127.- Cols, N.; Romero-Isart, N.; Capdevila, M.; Oliva, B.; González-Duarte, P.; González-Duarte, R.; Atrian, S., *J. Inorg. Biochem.*, (1997), 68, 157-166.
- 128.- Kubas, G.J.; Monzyk, B.; Crumbliss, A.L., *Inorg. Synt.*, (1979), 19, 90-92.

7. ANNEX

Articles i manuscrits elaborats durant aquesta Tesi Doctoral

ARTICLE 1

The metal-binding features of the recombinant mussel *Mytilus edulis* MT-10-IV metallothionein

Journal of Biological Inorganic Chemistry, (2008), 13, 801-812

The metal-binding features of the recombinant mussel *Mytilus edulis* MT-10-IV metallothionein

Rubén Orihuela · Jordi Domènech · Roger Bofill ·
Chunhui You · Elaine A. Mackay · Jeremias H. R. Kägi ·
Mercè Capdevila · Sílvia Atrian

Received: 11 December 2007 / Accepted: 20 March 2008 / Published online: 4 April 2008
© SBIC 2008

Abstract In contrast with the paradigmatic mammalian metallothioneins (MTs), mollusc MT systems consist at least of a high-cadmium induced form, possibly involved in detoxification, and another isoform either constitutive or regulated by essential metals and probably associated with housekeeping metabolism. With the aim of providing a deeper characterization of the coordination features of a molluscan MT peptide of the latter kind, we have analyzed here the metal-binding abilities of the recombinant MeMT-10-IV isoform of *Mytilus edulis* (MeMT). Also, comparison

with other MTs of this type has been undertaken. A synthetic complementary DNA was constructed, cloned and expressed into two *Escherichia coli* systems. Upon zinc coordination, MeMT folds in vivo into highly chiral and stable Zn₇ complexes, with an exceptional reluctance to fully substitute cadmium(II) and/or copper(I) for zinc(II). In vivo cadmium binding leads to homometallic Cd₇ complexes that structurally differ from any of the in vitro prepared Cd₇ complexes. Homometallic Cu–MeMT can only be obtained in vitro from Zn₇–MeMT after a great molar excess of copper(I) has been added. In vivo, two different heterometallic Zn,Cu–MeMT complexes are recovered, which nicely correspond to two distinct stages of the in vitro zinc/copper replacement. These MeMT metal-binding features are consistent with a physiological role related to basal/housekeeping metal, mainly zinc, metabolism, and confirm the correspondence between the *MeMT* gene response pattern and the functional properties of the encoded protein.

R. Orihuela and J. Domènech contributed equally to this work.

Electronic supplementary material The online version of this article (doi:10.1007/s00775-008-0367-6) contains supplementary material, which is available to authorized users.

R. Orihuela · R. Bofill · M. Capdevila
Departament de Química,
Facultat de Ciències,
Universitat Autònoma de Barcelona,
08193 Bellaterra, Barcelona, Spain

J. Domènech · S. Atrian (✉)
Departament de Genètica,
Facultat de Biologia,
Universitat de Barcelona,
Av. Diagonal 645,
08028 Barcelona, Spain
e-mail: satrian@ub.edu

C. You · E. A. Mackay · J. H. R. Kägi
Biochemisches Institut,
Universität Zürich,
8057 Zurich, Switzerland

M. Capdevila · S. Atrian
Institut de Biomedicina,
Universitat de Barcelona,
08028 Barcelona, Spain

Keywords Bivalve · Mollusca · Metal metabolism · MT-10-IV · Zinc, cadmium and copper binding

Introduction

Metallothioneins (MTs) are metal-chelating proteins reported in all animals, most plants and certain prokaryotes analyzed to date [1]. They do not constitute a monophyletic protein family, but rather a superfamily of heterogeneous low molecular weight Cys-rich peptides, for which definite homology relations can be only established inside broad taxonomic groups (cf. the Binz & Kägi classification criteria at <http://www.expasy.ch/cgi-bin/lists?metallo.txt>). Most current MT knowledge comes from vertebrate MTs, mainly from the paradigmatic mammalian MT1 and MT2

forms, which are composed of approximately 60 amino acids, including 20 Cys, and fold into two independent domains when coordinating divalent metal ions, as revealed by NMR [2] and X-ray crystallographic [3] analyses. The N-terminal segment, with nine Cys in Cys-X-Cys arrays, forms a β domain binding three M(II) ions, and the C-terminal segment, with 11 Cys, some of which in Cys-Cys tandems form an α domain, including four M(II) ions. This bidomain architecture is also exhibited by the Cd(II) complexes of MTs belonging to two groups of invertebrates: Echinodermata (sea urchin, *Strongylocentrotus purpuratus* MTA [4]) and Crustacea (blue crab, *Callinectes sapidus* [5], and American lobster, *Homarus americanus* [6]). Unfortunately, besides these two cases and the Arthropoda *Drosophila* MT system [7], few comprehensive metal-MT coordination studies have been carried out on invertebrates. Such studies are absolutely essential, bearing in mind that a lack of homology among invertebrates, and also with vertebrate MTs, precludes any homology-driven inference regarding their structural and functional properties.

In relation to their biological roles, invertebrate MTs provide numerous examples of the existence of two function-specific types: isoforms related to the homeostasis and handling of essential metal ions [Zn(II) and Cu(I)] and those involved in the detoxification of xenobiotic metals, such as Cd(II). This MT differentiation, which significantly differs from the scenario found in the paradigmatic mammalian MT system, has been identified and studied both at protein (metal-binding preferences) and at gene (induction-response) levels. Hence, following the denomination proposed in [8], the so-called Zn thioneins (or *divalent metal* MTs) share properties optimized for the coordination of divalent metal ions, especially Cd(II), and the corresponding genes respond to this stimulus. In contrast, the so-called Cu thioneins yield a pattern of optimized Cu(I) binding, which also correlates well with metal housekeeping functions, including basic Zn metabolism. The metal-binding abilities of the multiple MT isoforms have been well studied in Arthropoda (Crustacea [8, 9] and Diptera [7, 10, 11]) and additionally in terrestrial Mollusca (snail, *Helix pomatia* [12]). Paradoxically, little is known about the metal-binding properties of aquatic mollusc MTs, when considering the broadly accepted use of these organisms as biomonitoring for water metal contamination, and the wealth of literature consequently accumulated on toxicological and environmental areas (for a recent review, see [13]).

Among aquatic molluscs (particularly marine), species of *Mytilus* can be considered model organisms. In this genus, two families of MT polypeptides have been described according to their amino acid sequence characteristics: the MT-10 type, 73-residue-long peptides including 21 Cys

distributed mainly in Cys-X-Cys motives, and the MT-20 type, including 72-residue-long peptides, with two of their 23 Cys arranged in Cys-Cys doublets. The MT system is overrepresented in the *Mytilus edulis* species, with up to eight reported isoforms, six of the MT-10 type and two as MT-20 variants. The MT forms identified in other Mytilidae [14, 15] can also be classified in one of these two categories, which, according to DNA sequence comparisons, are considered homologous and to result from prespeciation duplication events conserving the intron/exon gene organization [16]. Gene expression and transcript distribution studies revealed that Zn and low concentrations of Cd mainly induce the synthesis of MT-10 isoforms, whereas the MT-20 isoforms respond to high Cd concentrations [17–20]. These different expression patterns strongly suggest that the MT-10 and MT-20 types would have evolved under specialization pressure to provide different physiological functions, namely, metal homeostasis and detoxification, respectively. Substantiation of this hypothesis requires a functional analysis of the mussel MT system at the protein level. Unfortunately, and contrasting with the far deeper understanding of the corresponding gene system on the one hand, and of the physiological and detoxification traits on the other, there is a considerable gap concerning the link between them, i.e., the functional properties of the *M. edulis* MT proteins in relation to metal coordination.

To shed light on this subject, we present in this study a thorough characterization of the Zn-, Cd- and Cu-binding abilities of the *M. edulis* MeMT-10-IV (MeMT) isoform, which has been related to metal housekeeping roles according to its transcriptional behavior. The comparative analysis of the MeMT metal-coordination features has revealed that MeMT has an unprecedented preference for Zn(II). This is consistent with its hypothesized role in mussel metal physiological function from gene-induction criteria [19, 21]. Furthermore, a comparison of the MeMT features with those of other MTs is provided.

Materials and methods

Complementary DNA and expression plasmid construction

A complementary DNA (cDNA) coding for the MeMT isoform (MeMT-cDNA) was synthetically constructed on the basis of the reverse translation of its amino acid sequence [22] (Fig. 1) following the *Escherichia coli* codon usage bias. The eight oligonucleotides shown in Fig. S1 (four corresponding to the sense strand and four to the antisense strand) were synthesized using an Applied Biosystems DNA synthesizer, purified by high-performance liquid chromatography according to manufacturer's

Me-10-IV	MPAPCN C IETNV---CICDTG-C S GEGCR C CGDACK C SGAD---CKC S GCKVV C KCSGSCA C E G GTGPST-C K CA P GSCK
Me-20-I	M P GP C N C IETNV---C I CGTG-C S GKCC R CGDACK C AS G ---C G CGCKV V CKCSGTCKCGCDCTGP T N-C K CE S CSCK
MTH	M P PGC-CKDK----CECAEGGGK-T C CKC-T S RCA-----PCEK C SGCKPSKDEAKT C SPK---CKCP
MT1	MDPNC S GTGGS---CTCTSS-C A CKNKC-T S CKKS-----CCSCCPVGGS---KCAQGCVKGAADKCTCCA
Crs5	MTVKICDCEGECKDSCHCGST-CL-P S CGEK C RDHSTGSPQCKSGERCK---CETTCTCEK-S-KCNCEK G
QsMT	MS C CGGN C CGT C CGSGCGCKMFPDI S EKT T TLIVGVAPQKTHFEGSEMGVGAENGCK C GSN C TC D PC N CK

Fig. 1 Amino acid sequence of the MT10-IV isoform of *Mytilus edulis* (MeMT) aligned, using ClustalW, with those metallothionein (MT) peptides with which it is compared in this work, except for the plant QsMT form, since its interfering Cys-devoid segment disrupts any comparison. Definitions and the UniProtKB/Swiss-Prot data bank accession numbers for these sequences are the following: Me-10-IV (P80249); MT-20-I (P80251), one of the *M. edulis* isoforms belonging

to the subfamily of MT-20-like mollusc MTs; MTH (P29499), crustacean MT of the American lobster *Homarus americanus*; MT1 (P02802), isoform 1 of the mouse *Mus musculus*; Crs5 (P41902), the second MT of baker's yeast *Saccharomyces cerevisiae*; QsMT (EMBL accession AJ277599.2), a plant MT isoform, isolated from the cork oak *Quercus suber*

instructions, assembled and annealed to yield the complete double-stranded cDNA. A number of restriction enzyme sites, not affecting the cDNA coding meaning, were introduced in this sequence to allow for construction, mapping (*FokI*, *MboI*, *Apal*, *ApII*, *MaeIII*, *DraIII*, *BglII* and *BanI*) and subcloning requirements (*Clal* and *EcoRI*).

The synthetic MeMT-cDNA, previously digested with *Clal/EcoRI*, was first subcloned into the expression vector pPWSu [23], which yielded the recombinant construct MeMT-pPWSu for production of MeMT as an independent protein under a heat-inducible promoter. For synthesis of MeMT as a GST-fusion protein, the same coding sequence was subcloned into the *BamHI/SalI* sites of the pGEX-4T2 plasmid (Amersham GE-HC) [24]. These two restriction sites were respectively added to the 5' and 3' ends of the previously described cDNA by PCR amplification, using the MeMT-pPWSu plasmid as a template and the following oligonucleotides as primers: 5'-CGGGGATCCATGCCCTG CACCG-3' (upstream) and 5'-ACGCGTCGACTTATTG GCAACT-3' (downstream). The 30-cycle amplification reaction was performed with the thermostable DNA polymerase Immolase (Bioline) under the following conditions: 45 s at 95 °C (denaturation), 30 s at 58 °C (hybridization) and 45 s at 72 °C (elongation). The final product was analyzed by agarose gel electrophoresis/ethidium bromide staining; the band with the expected size was excised and subcloned into the pGEX-4T2 plasmid.

The recombinant plasmids were transformed into *E. coli* JM105 for integrity and identity analysis, and into protease-deficient strains (MeMT-pPWSu in 1B392LonΔ1 and MeMT-pGEX in BL21) for protein synthesis. DNA sequence was determined using the ABI PRISM dye terminator-cycle sequencing ready reaction kit (PerkinElmer) in an Applied Biosystems ABI PRISM 310 automatic sequencer.

In vivo synthesis and purification of the recombinant metal-MeMT complexes

Recombinant MeMT was obtained from the MeMT-pPWSu construct essentially as described in [23]. Protein

synthesis was induced by a temperature shift from 30 to 42 °C. Cultures of 6–8 L of the transformed 1B392 LonΔ1 cells were supplemented with 300 μM CdCl₂ in order to stabilize the nascent protein; thus, MeMT was recovered complexed to Cd(II) from this expression system. Total bacterial protein extracts were sonicated in the presence of 1 mM phenylmethylsulfonyl fluoride and fractionated by ethanol/chloroform precipitation. Two chromatography steps were applied: first, gel filtration through a Sephadex G-50 column (2.5 cm × 180 cm) equilibrated with 20 mM Tris(hydroxymethyl)aminomethane hydrochloride (Tris-HCl), 0.15 M NaCl (pH 8.6); and second, anion exchange (Bio-gelA DEAE in a 5PW, 1.7 cm × 12.5 cm high-performance liquid chromatography column equilibrated with 20 mM Tris-HCl, pH 8.0) and eluted with a gradient of 10 mM Tris-HCl containing from 25 mM to 50 mM NaCl. Selected fractions were confirmed by 15% sodium dodecyl sulfate polyacrylamide gel electrophoresis and kept at –80 °C until further use.

The MeMT-GST fusion polypeptides were biosynthesized in 3-L cultures of transformed BL21 cells. Expression was induced with isopropyl β-D-thiogalactopyranoside and cultures were supplemented with 500 μM CuSO₄, 300 μM ZnCl₂ or 300 μM CdCl₂ and grown further for 3 h. Total protein extract was prepared from these cells as previously described in [24]. The MeMT-GST fusions were purified by glutathione-Sepharose 4B (Amersham Pharmacia) affinity. Metal complexes were recovered from the fusion constructs by thrombin cleavage and batch-affinity chromatography. After concentration using Centriprep Microcon 3 (Amicon), the metallopeptides were finally purified by fast protein liquid chromatography in a Superdex75 column (Pharmacia) equilibrated with 50 mM Tris-HCl, pH 7.0. Selected fractions were confirmed by 15% sodium dodecyl sulfate polyacrylamide gel electrophoresis and kept at –80 °C until further use. All procedures were performed using Ar (pure grade 5.6) saturated buffers, and all syntheses were performed at least twice to ensure reproducibility. As a consequence of the cloning requirements, two additional glutathione residues were present at the N-terminus of the MeMT polypeptides

obtained by this method; however, these had previously been shown not to alter the MT metal-binding capacities [25].

Analysis and characterization of the recombinant metal–MeMT complexes

Apo-MeMT samples of the MeMT preparations synthesized from MeMT–pPWRSu were obtained by acidification through a G-25 Sephadex column equilibrated with 10 mM HCl or 0.1% trifluoroacetic acid [26], and analyzed by reverse-phase chromatography on a C18, 22 cm × 4.6 mm column. The mercapto-group content of this material was assessed with 2,2'-dithiopyridine at pH 4.0, using a molar absorbance value of 7,000 M⁻¹ cm⁻¹ for thiopyridine [23]. The Cd content of the Cd–MeMT complexes formed after reconstitution with Cd(II) of this apo-MeMT was determined by atomic absorption spectrometry using a VIDEO 12 aa/ae spectrophotometer. Electronic absorption and circular dichroism (CD) measurements in these samples were, respectively, performed with a Cary 3 UV–vis and a JASCO model J-715 spectrophotometer equipped with a Compaq 633 computer.

The S, Zn, Cd and Cu content of the Zn–MeMT, Cd–MeMT and Cu–MeMT preparations obtained from the pGEX system was analyzed by means of inductively coupled plasma atomic emission spectroscopy (ICP–AES) using a Polyscan 61E (Thermo Jarrell Ash) spectrometer, measuring S at 182.040 nm, Zn at 213.856 nm, Cd at 228.802 nm and Cu at 324.803 nm. Samples were treated as in [27], but were alternatively incubated in 1 M HCl at 65 °C for 5 min prior to measurements in order to eliminate possible traces of labile sulfide ions, as otherwise described in [28]. Protein concentrations were calculated from the *acid* ICP–AES S measure, assuming that all S atoms were contributed by the MeMT peptide, that is, 22 S/mol MeMT (1 Met and 21 Cys residues). A JASCO spectropolarimeter (model J-715) interfaced to a computer (J700 software) was used for CD measurements at a constant temperature of 25 °C maintained by a Peltier PTC-351S apparatus. Electronic absorption measurements were performed with an HP-8453 diode-array UV–vis spectrophotometer. All spectra were recorded with 1-cm capped quartz cuvettes, corrected for the dilution effects and processed using the GRAMS 32 program.

In vitro Zn-, Cd- and Cu-binding studies of MeMT

The apo-MeMT, prepared as described already, was used to reconstitute the Cd complexes by addition of Cd(II) ions, as reported in [23] with sea urchin MT. The independent titrations of Zn–MeMT with Cd(II) or Cu(I) at pH 7 were carried out following the procedures described elsewhere

[24, 29]. Additionally, in vitro acidification/reneutralization experiments were performed by adapting a previously reported procedure [30]. Essentially, 10 µM Cd–MeMT preparations were acidified from neutral (7.0) to acid (2.0) pH with 10⁻³–1 M HCl depending on the stage of the titration. CD and UV–vis spectra were recorded at pH 7.0, 4.5, 4.0, 3.0 and 2.0 both immediately after acid addition and 10 min later, always with identical results. Finally, the samples were kept at pH 2.0 for 20 min and then they were reneutralized to pH 7.0 with 10⁻³–1 M NaOH, also depending on the stage of the titration. CD and UV–vis spectra were recorded at pH 2.0, 2.5 and 7.0. All the changes experienced by the sample during these experiments were corrected for dilution effects. During all experiments strict oxygen-free conditions were kept by saturation of the solution with Ar.

Electrospray ionization mass spectrometry analyses

Molecular masses of the proteins synthesized by the pPWRTSu system were analyzed with a SCIEX APIII instrument. For the Cd–MeMT complexes, the sample was injected in 5 mM ammonium acetate pH 6.5 at a concentration of 2 pmol/ml in 50% acetonitrile. For the corresponding apo forms, samples were injected in the same buffer, but containing 30% methanol and 1.1% (v/v) acetic acid.

Time-of-flight electrospray ionization mass spectrometry (ESI–MS) analyses of the metallopeptides recovered from the pGEX system were performed using an Ultima Micromass quadrupole time-of-flight instrument, controlled by MassLynx software and calibrated with NaI (0.2 g of NaI dissolved in 100 ml of a 1:1 H₂O/2-propanol mixture). Twenty microliters of the sample was injected at 40 µl/min under the following conditions: source temperature, 150 °C; desolvation temperature, 250 °C; capillary counter electrode voltage, 3.0 kV; cone potential, 80 V. Spectra were collected throughout an *m/z* range from 950 to 2,150 at a rate of 2 s per scan with an interscan delay of 0.1 s. The liquid carrier was a 10:90 mixture of acetonitrile and 5 mM ammonium acetate, pH 7. For the analysis of apo-MeMT obtained from recombinant Zn–MeMT, and of heterometallic Zn,Cu–MeMT species, 10 µl of the sample at pH 7 was injected under the same conditions described for the holo forms, with the following exceptions in order to release Zn(II) ions but not Cu(I) ions from the complexes: the liquid carrier was a 50:50 mixture of acetonitrile and ammonium formate/ammonia at pH 2.5; the source temperature was decreased to 100 °C and the desolvation temperature to 150 °C. In all cases, molecular masses were calculated in accordance with [31, 32]. All samples were injected at least twice in order to ensure reproducibility.

Results and discussion

Identity and integrity of the recombinant MeMT polypeptides

The construction of an artificial DNA sequence encoding the MeMT protein was successfully achieved using eight overlapping oligonucleotides that spanned the entire length of its coding region. This cDNA was cloned into two *E. coli* expression vectors (pPWRT and pGEX) and the results obtained when the recombinant constructs were expressed in Cd-enriched bacterial cultures were totally comparable, which validates the results achieved here with other metal ions.

From the pPWRT expression system, three subforms of MeMT were recovered and identified through ESI-MS by the molecular masses shown in Table 1. They corresponded to (1) the mature, methionine-less gene product, (2) the precursor form with the expected molecular mass for the encoded polypeptide and (3) the precursor form initiated by an *N*-formyl methionine residue. Recombinant synthesis from the pGEX expression system yielded an MT polypeptide whose identity, purity and integrity were also confirmed by ESI-MS, using the apo form obtained at pH 2.5 from the Zn-MeMT complexes. This analysis indicated the presence of a single polypeptide of the expected molecular mass (in this case, 7,254.40 Da, corresponding to the sequence shown in Fig. 1 with additional N-terminal Gly and Ser residues, due to its synthesis as a GST fusion construct). The MT portion was recovered at an approximate concentration of 1×10^{-4} – 2×10^{-4} M for Zn- and Cd-MeMT productions, and of 0.5×10^{-4} – 1×10^{-4} M for Cu-MeMT syntheses, this meaning an average of 1 mg of pure metal-MT complex per liter of bacterial culture.

Table 1 Molecular masses of the apo-MeMT obtained from both *Escherichia coli* expression systems

Expression system	$m_{\text{exp}}^{\text{a}}$	m_{th}^{b}
pPWRT	6,979.0 ^c	6,979.2 ^c
	7,110.6 ^d	7,110.4 ^d
	7,138.6 ^e	7,138.5 ^e
pGEX	7,254.9	7,254.4

MeMT MeMT-10-IV isoform of *Mytilus edulis*

^a Experimental molecular masses. Measurements were always performed in duplicate. All corresponding standard deviations were always less than 0.1%

^b Theoretical molecular mass of the corresponding species. In the case of Cu_xZn species, the molecular masses indicated correspond to the homometallic Cu_x and Zn_x species, respectively

^c Processed methionine-less MeMT; data reported in [33]

^d MeMT polypeptide with an initial methionine residue

^e MeMT polypeptide with an initial *N*-formyl methionine residue

Characterization of the in vivo synthesized Zn-MeMT and Cd-MeMT species

Recombinant (i.e., in vivo folded) Zn-MeMT complexes were obtained from the pGEX expression system. This yielded a predominant Zn₇-MeMT together with some very minor species (Zn₆-MeMT, Zn₇S₁-MeMT and Zn₈-MeMT), as shown by the ESI-MS results at pH 7.0 (Table 2, Fig. S2a), and consistently with an average content of 7.0 Zn(II) per MT, as measured by acid ICP-AES.

In vivo folded Cd-MeMT samples were available from the two expression systems, exhibiting totally equivalent stoichiometric and spectropolarimetric features. The molecular masses of the Cd species obtained from pPWRT (shown in Table 2) exactly corresponded to a load of seven Cd(II) ions to each of the three apo forms described above (Table 1) [33]. This stoichiometry was coincident with the 7.3 Cd(II) per MT ratio obtained from acid ICP-AES and with the detection of an almost unique ESI-MS peak corresponding to Cd₇-MeMT in the preparations from the pGEX system (Table 2, Fig. S2b). In this case, minor species were Cd₆S₂-MeMT, Cd₇S₁-MeMT and Cd₈-MeMT. Therefore, as expected on the basis of the similar number of Cys residues in MeMT and mammalian MTs (21 compared with 20), this protein gives rise to major Zn₇ and Cd₇ species when expressed in Zn- and Cd-rich media respectively, these data being in good concordance with those reported for MT-10 [34] and MT-20 *Mytilus galloprovincialis* isoforms [20].

Remarkably, the CD spectra of both recombinant Zn₇-MeMT and Cd₇-MeMT are highly dissimilar to those of homometallic forms of other MTs, showing that no typical CD spectra can be assumed to exist for all the MT complexes of a certain metal ion [28]. Hence, Zn-MeMT exhibited a wide, intense and asymmetric CD spectrum (Fig. 2a) centered at approximately 235 nm (positive), indicative of the presence of at least two different absorptions, one attributable to the well-defined Zn-thiolate chromophores (at approximately 240 nm) and the other to the putative participation of chloride ligands (at approximately 230 nm) in the Zn-thiolate clusters. The CD spectra of the Cd-MeMT preparations recovered from both expression plasmids (that of the pGEX preparation included in Fig. 2b) and showing an asymmetric and intense fingerprint were practically coincident, and highly similar to that recently reported for recombinant *M. galloprovincialis* Cd₇-MT-10 [35]. They could be interpreted as an exciton coupling centered at approximately 250 nm (Cd-thiolate chromophores) with the positive maximum at 266 nm and a faint contribution at approximately 280 nm (Cd-sulfide chromophores), and probably another exciton-coupling component centered at approximately 240 nm, which may

Table 2 Metal-to-protein ratios and molecular masses of the recombinant Zn(II)–MeMT, Cd(II)–MeMT and Cu(I)–MeMT complexes obtained from the pGEX expression system, unless indicated

Metal supplemented	M/MeMT (ICP–AES)	M–MeMT species ^f (ESI–MS)	$m_{\text{exp}}^{\text{a}}$	m_{th}^{b}	
Zn(II)	7.0	Zn₇–MeMT	7,698.0	7,698.0	
Cd(II)	7.3	Cd₇–MeMT	8,030.8	8,027.2	
Cd(II) (pPWRT)	–	Cd ₇ –MeMT	7,752.0 ^c	7,752.0 ^c	
		Cd ₇ –MeMT	7,885.0 ^d	7,883.2 ^d	
		Cd ₇ –MeMT	7,912.0 ^e	7,911.3 ^e	
Cu(I) type 1	3.3 (Zn) 4.6 (Cu)	M₈–MeMT M ₉ –MeMT M ₁₀ –MeMT	7,760.1 7,814.8 7,878.8	7,754.7–7,761.4 7,817.3–7,824.8 7,879.8–7,888.2	
Cu(I) type 2	1.4 (Zn) 9.2 (Cu)	pH 7 pH 2.5	M₁₂–MeMT M ₁₁ –MeMT M ₁₃ –MeMT Cu₈–MeMT Cu ₉ –MeMT Cu ₁₀ –MeMT	8,002.0 7,938.4 8,066.1 7,749.0 7,812.0 7,875.5	8,004.9–8,014.9 7,942.3–7,951.5 8,067.4–8,078.3 7,754.7 7,817.3 7,879.7

ICP–AES inductively coupled plasma atomic emission spectroscopy, ESI–MS electrospray ionization mass spectrometry

^a Experimental molecular masses. Measurements were always performed in duplicate. All corresponding standard deviations were always less than 0.1%

^b Theoretical molecular mass of the corresponding species. In the case of Cu,Zn species, the molecular masses indicated correspond to the homometallic Cu_x and Zn_x species, respectively

^c Processed methionine-less MeMT; data reported in [33]

^d MeMT polypeptide with an initial methionine residue

^e MeMT polypeptide with an initial N-formyl methionine residue

^f Species proposed according to the mass difference between holoprotein and apoprotein. Species in **bold** are the major components of the preparation. In the case of Zn,Cu mixed-metal species, the metal-to-protein stoichiometries deduced at pH 7.0 are indicated as M_x (M is Zn or Cu)

reflect chloride participation in the Cd₇–MeMT clusters. Assignment of the 235 nm (Zn) and 240 nm (Cd) CD absorptions to chloride ligand contributions is supported by previous works by our group [11, 36], as well as by Raman spectroscopy results on the Zn₇–MeMT species (unpublished results). Their presence is not detectable by ESI–MS, as previously reported for the mammalian Cd–MT complexes [36]. Alternatively, these CD features could also be interpreted by the contribution of a second exciton-coupled metal–thiolate ligand to metal charge transfer band.

The literature provides other examples of CD envelopes similar to those of MeMT [i.e., the Zn complexes of the MT of American lobster (*H. americanus*) and the second MT of *Saccharomyces cerevisiae* (Crs5), Fig. 2a; and the Cd complexes of the MT from cork oak (*Quercus suber*) and Crs5, Fig. 2b; cf. origin and sequence information of these MTs in Fig. 1], all of these clearly different from the paradigmatic mammalian MT corresponding complexes (also included in Fig. 2a, b). This confirms that diverse MT isoforms, owing to their dissimilar amino acid sequences, give rise to different metal–thiolate clusters (i.e., unequal structures) that produce patently different CD spectra and that could be related to their distinct functionalities.

Characterization of the in vitro prepared Cd–MeMT species

Cd₇–MeMT clusters were obtained in vitro by three distinct procedures: (1) reconstitution of the apo form with Cd(II) ions, (2) Cd(II) titration of the recombinant Zn₇–MeMT preparations and (3) acidification and subsequent renaturalization of the recombinant Cd₇–MeMT preparations.

In vitro Cd–MeMT reconstitution from the apo form

The set of CD and UV–vis absorption spectra recorded during the addition of Cd(II) to apo-MeMT (Fig. 3) illustrate the progressive absorption increase associated with the incorporation of the Cd(II) ions to the apo form, with a linear rise in amplitude up to about 7.6 equiv of Cd(II) added. The subsequent CD spectra show the re-emergence of the ellipticity maxima near 266 nm observed in the recombinant preparations. However, CD features below 260 nm clearly differ from those of the in vivo preparations, this indicating that the in vivo folded Cd–MeMT clusters cannot be obtained by direct binding of Cd(II) to the MeMT peptide.

Fig. 2 Comparison of the circular dichroism (CD) spectra of in vivo synthesized **a** Zn-MeMT (solid black line), Zn-MTH [8] (solid gray line), Zn-Crs5 [32] (dashed line) and Zn₇-MT1 [25] (dotted line); **b** Cd-MeMT (solid black line), Cd-QsMT [30] (solid gray line), Cd-Crs5 [32] (dashed line) and Cd₇-MT1 [47] (dotted line); and **c** Cu-MeMT type 1 (solid line) and type 2 (dashed line)

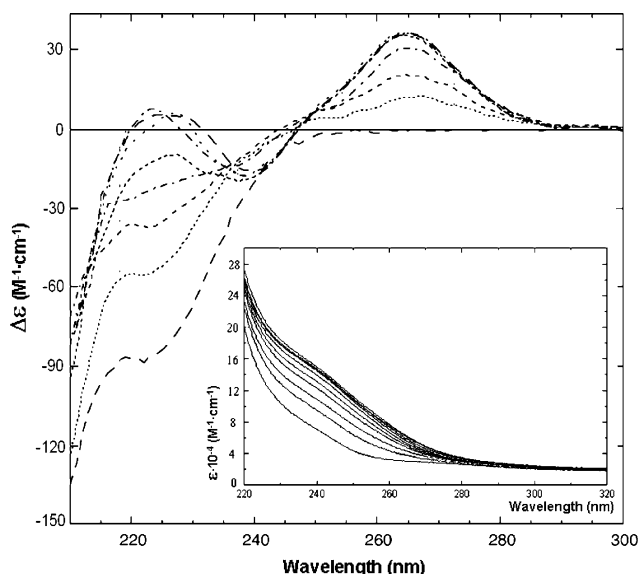
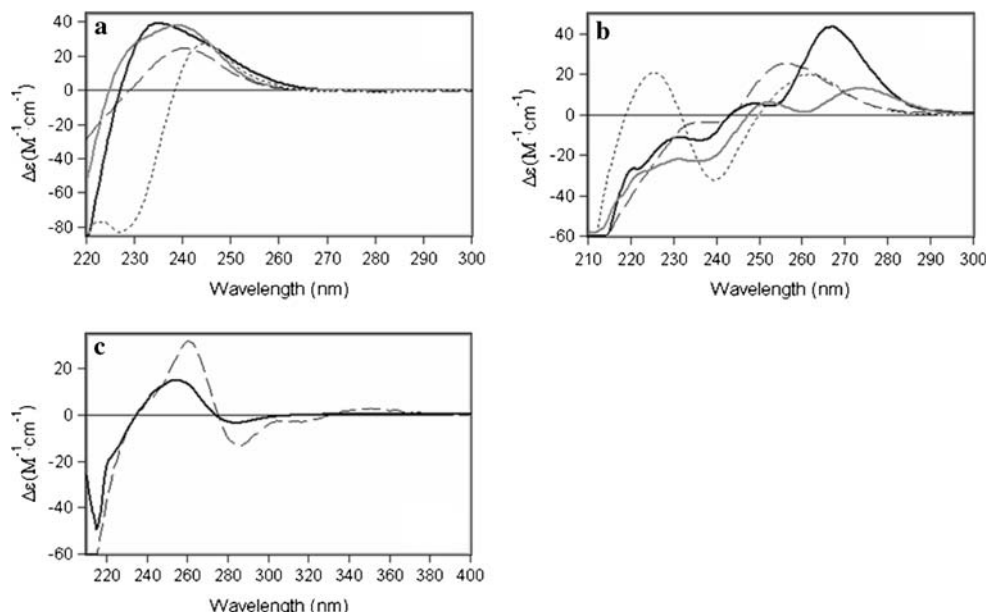


Fig. 3 Reconstitution of Cd-MeMT by addition of Cd(II) to the corresponding apo form followed by CD and UV-vis (inset) absorptions spectroscopies. The successive spectra, from bottom to top, resulted from the addition of 0, 2.5, 4.2, 5.9, 6.7, 7.6, 8.4, 9.2 and 10.1 equiv of Cd(II) to a 2.5 μ M solution of apo-MeMT in 20 mM 2-morpholinoethanesulfonic acid, pH 6.5

In vitro Cd(II) titration of Zn-MeMT

The spectroscopic (Fig. 4) and spectrometric (Table 3) data recorded during the titration of Zn₇-MeMT with Cd(II) are indicative of an initial, noncooperative replacement of Zn(II) by Cd(II) up to the seventh Cd(II) equivalent added. At this point, the sample, mainly consisting of Cd₆Zn₁-MeMT, shows an intense CD spectrum, analogous to that of the initial Zn₇-MeMT but redshifted,

indicating a similar folding of both complexes. This spectrum remains practically invariant between 7 and 9 equiv of Cd(II) added. For 9 equiv of Cd(II) added, the ESI-MS data reveal the coexistence of heterometallic Zn₂Cd₅ and Zn₁Cd₆ species with Cd₇-MeMT, which, significantly, is not yet the major species. After this titration point, the CD spectrum dramatically evolves to a new CD envelope, and consequently the initial Zn₇-MeMT and final Cd₇-MeMT species will definitely be nonisostructural. It is the addition of 11 equiv of Cd(II) that renders Cd₇-MeMT as the major species, but 15 equiv of Cd(II) is needed to fully avoid the presence of Zn,Cd heterometallic species, these data suggesting a certain reluctance of MeMT in the exchange of the last Zn(II) ions. At this stage a Cd₈-MeMT species, which represents the maximum Cd(II) load of MeMT, is also detected. Remarkably, the molecular distribution of the metal-MeMT species at this point of the titration nicely matched that of the in vivo Cd-MeMT preparations. However, both preparations exhibited definitely dissimilar CD spectra, with differences mainly in the 220–260 nm region (Fig. 5), due to the approximately 240 nm centered exciton-coupling band, developed with the addition of 9–15 equiv of Cd(II). According to the ESI-MS data, this band cannot be attributed to the presence of Zn in the Cd-MeMT complexes. Possible explanations could be related, as hypothesized for the in vivo preparations, to the participation of chloride counterions from the titrating agent (CdCl₂) in the Cd-MeMT complexes or to a second Cd-thiolate transition also giving rise to exciton coupling, as supported for the very large biphasic signal with crossover near 240 nm when Zn₇-MeMT has been exposed to 15 equiv of Cd(II) (Fig. 5, dotted line).

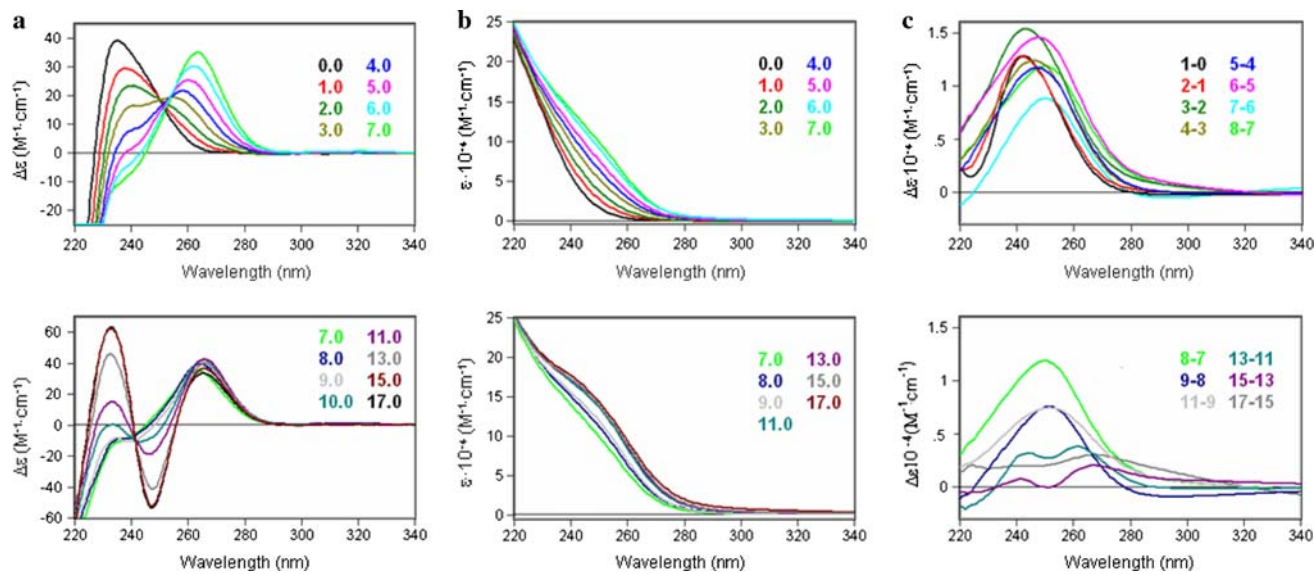


Fig. 4 **a** CD, **b** UV-vis and **c** UV-vis difference spectra corresponding to the titration of a 10 μ M solution of Zn₇–MeMT with Cd(II) at pH 7

Table 3 Metal–MeMT species detected by ESI–MS during the titration of a 10 μ M solution of Zn₇–MeMT with Cd(II) at pH 7

	Cd(II) equivalents added to Zn ₇ –MeMT							
	2	3	4	6	7	9	11	15
Zn ₇ Cd ₁ –MeMT	×							
Zn ₆ Cd ₁ –MeMT	×							
Zn ₆ Cd ₂ –MeMT	◆		◆					
Zn ₅ Cd ₂ –MeMT	✓	✗	◆					
Zn ₅ Cd ₃ –MeMT			◆					
Zn ₄ Cd ₃ –MeMT	✓	✓	◆					
Zn ₃ Cd ₄ –MeMT	✗	✗	✗					
Zn ₃ Cd ₅ –MeMT			◆					
Zn ₂ Cd ₅ –MeMT	◆	✓	◆	✗				
Zn ₁ Cd ₆ –MeMT			✗	✓	✓	✗		
Cd ₇ –MeMT				✗	✗	✓	✓	
Cd ₈ –MeMT							✗	

✓ denotes major species, ✗ denotes intermediate species, ◆ denotes minor species

In vitro acidification/reneutralization of in vivo Cd–MeMT

Acidification of the recombinant Cd–MeMT preparations unexpectedly led to a precipitation process in the samples despite the use of previously validated procedures [30]. Specifically, between pH 4 and 3 the solution becomes significantly turbid, in concordance with a massive precipitation of protein. In fact, reneutralization of the sample to pH 7 allowed recovery of only a quarter of the initial CD intensity, which indicates a loss of approximately 75% of the original protein (Fig. S3). Precipitation at acid pH

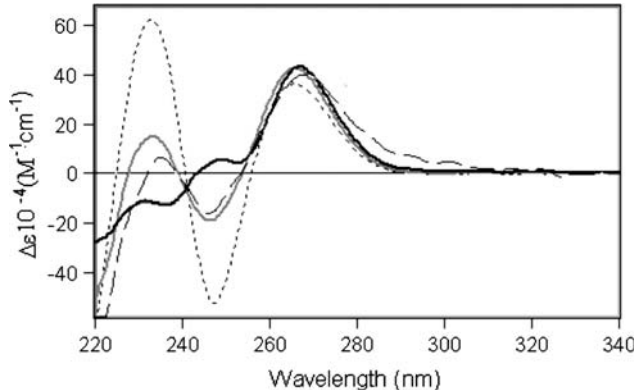


Fig. 5 Comparison of the CD spectrum of: the in vivo Cd–MeMT preparation (solid black line), the final solution obtained after adding 11 equiv (solid gray line) and 15 equiv (dotted line) of Cd(II) to Zn₇–MeMT; and the solution recovered after an acidification/reneutralization process of recombinant Cd–MeMT (dashed line). The intensities of the CD spectra were normalized for the sake of comparability

would be on the basis of the generation of the corpuscles called cadmosomes as further commented on in “Concluding remarks.” Despite the drawback of protein precipitation, normalization of the final CD spectrum allows its comparison with the fingerprint of the initial in vivo Cd–MeMT (Fig. 5), which is once again clearly different in the 220–260 nm region (see earlier). Therefore, the acidification/reneutralization of recombinant Cd₇–MeMT is not a fully reversible process, as the chromophores absorbing at approximately 240 nm seem at least to be inverting their chirality at some of the stages of the process.

Overall, the three in vitro strategies assayed for Cd₇–MeMT preparation [i.e., Cd(II) reconstitution of

apo-MeMT, Cd(II) titration of Zn₇–MeMT or direct acidification/reconstitution of Cd₇–MeMT] led to samples of the same speciation and that were spectroscopically (i.e., structurally) equivalent. Interestingly, none of these three procedures give rise to a sample with the spectroscopic features of the in vivo Cd₇–MeMT preparations. Consequently, it is clear that two different types of Cd₇–MeMT complexes are obtained depending on their in vitro or in vivo origin, and regardless of the *E. coli* expression system used. The failure to reproduce the recombinant in vivo forms documents that, in contrast to the situation with mammalian MTs, no pathway for suitable folding prevails under in vitro conditions. Since purification and characterization of Cd–MeMT complexes from mussel organisms has never been attained, at this stage of knowledge it is impossible to assess which of the two folds reported in this work would more closely reproduce that of the native form.

MeMT provides a clear example to disregard the early hypothesis that invertebrate MTs bind six divalent metal ions in contrast to vertebrate MTs binding seven divalent metal ions. In fact, the coordination capacity (in terms of the number of metal ions) in a metal–MT complex appears significantly related to the number of coordinating residues, i.e., mainly its Cys content. Thus, among invertebrates, *H. pomatia* (Gastropoda/Mollusca; 18 Cys [12]), *C. sapidus*, *H. americanus*, *Cancer pagurus*, and *Scylla serrata* (Crustacea; 18 Cys [5, 6, 37, 38]) and *Caenorhabditis elegans* (Nematoda; 19 Cys [39]) are known to harbor six divalent metal ions, whereas *S. purpuratus* (Echinodermata; 20 Cys [4]), *Lumbricus rubellus* (Annelida; 20 Cys [40]) and *M. edulis* (Bivalva/Mollusca; 21 Cys, this work) appear above the threshold allowing the coordination of seven divalent metal ions.

Characterization of the in vivo synthesized Cu–MeMT species

Cu–MeMT preparations were recovered from Cu-enriched cultures of *E. coli* transformants of the pGEX expression constructs. This invariably yielded two kinds of heterometallic MeMT productions containing different Zn(II) to Cu(I) ratios and denominated types 1 and 2 (Table 1). The composition of these preparations was analyzed by ESI–MS at two pH values, 7.0 and 2.5, since Cu(I)–thiolate but not Zn(II)–thiolate bonds persist at pH 2.5, while at pH 7.0 both metal ions are indiscernible owing to their close atomic masses. Hence, metal complexes identified in type 2 productions are of higher nuclearity and show higher Cu(I) and lower Zn(II) contents than those of type 1 (Table 1). The different CD features (Fig. 2c) of both types of syntheses were consistent with their distinct Zn(II) and Cu(I) content, since a higher CD intensity at approximately

240 nm—probably related to Zn–thiolate chromophores—is observed for the high Zn-containing productions (type 1).

Characterization of the in vitro prepared Cu–MeMT species

Cu–MeMT complexes were prepared in vitro by Cu(I) titration of recombinant Zn₇–MeMT under thermodynamic conditions. This reaction was followed by CD and UV–vis spectrophotopies (Fig. 6) as well as by ESI–MS at pH 7.0 and 2.5 (Table 4). From the initial steps of the titration, two main features become apparent. First, the progressive additions of Cu(I) to Zn₇–MeMT provoke the coexistence of multiple species, which allows cooperativeness throughout the titration to be discarded. Second, Zn₇–MeMT exhibits an ever-higher reluctance in the Zn/Cu than in the Zn/Cd replacement, if the number of Cu(I) equivalents required for Zn(II) displacement is taken into account. It should be recalled that (1) despite spectroscopic data suggesting Cu(I) binding during the first 6 equiv of Cu(I) added, ESI–MS results reveal that at this point Zn₇–MeMT is still the major species, and (2) formation of homometallic Cu₁₂–MeMT is not observed until 30 equiv of Cu(I) has been added to Zn₇–MeMT.

Comprehensive consideration of all the spectroscopic and spectrometric data recorded during this titration allows the proposal of three stages, which although almost isodichroic, lead to the coexistence of numerous heterometallic Zn,Cu–MeMT species. However, some kind of cooperativeness can be envisaged in light of the ESI–MS data at pH 2.5. Respectively, these show generation from Zn₇–MeMT of major complexes containing four Cu(I), direct conversion of the latter to complexes containing eight Cu(I) and, finally, production of a continuum of species extending up to 12 Cu(I); during the first [from 0 to 18 equiv of Cu(I) added], second [from 18 to 28 equiv of Cu(I) added] and third stages. It is worth noting that these homometallic or heterometallic Cu₁₂-containing species are only achievable under high excess Cu(I) (i.e., 30 equiv) in vitro conditions. The stepwise incorporation of Cu(I) into recombinant human apo-MT3 has already revealed cooperative formation of Cu₄ and Cu₈ clusters [41, 42] and addition of this metal ion to Zn–MT1 also rendered formation of Cu₄ clusters in the β domain [43, 44].

Interestingly, the scenarios attained at the end of the first and the second stages perfectly reproduced the features of the in vivo type 1 and type 2 preparations. Hence, for 14 equiv of Cu(I) added there is a coexistence of major M₈ and M₉ species showing a CD fingerprint (Fig. 7a) equivalent to that of the recombinant type 1 samples. Subsequently, for 26–28 equiv of Cu(I) added, the Zn/Cu replacement reaction reaches another stage that yields speciation and CD features comparable to those of

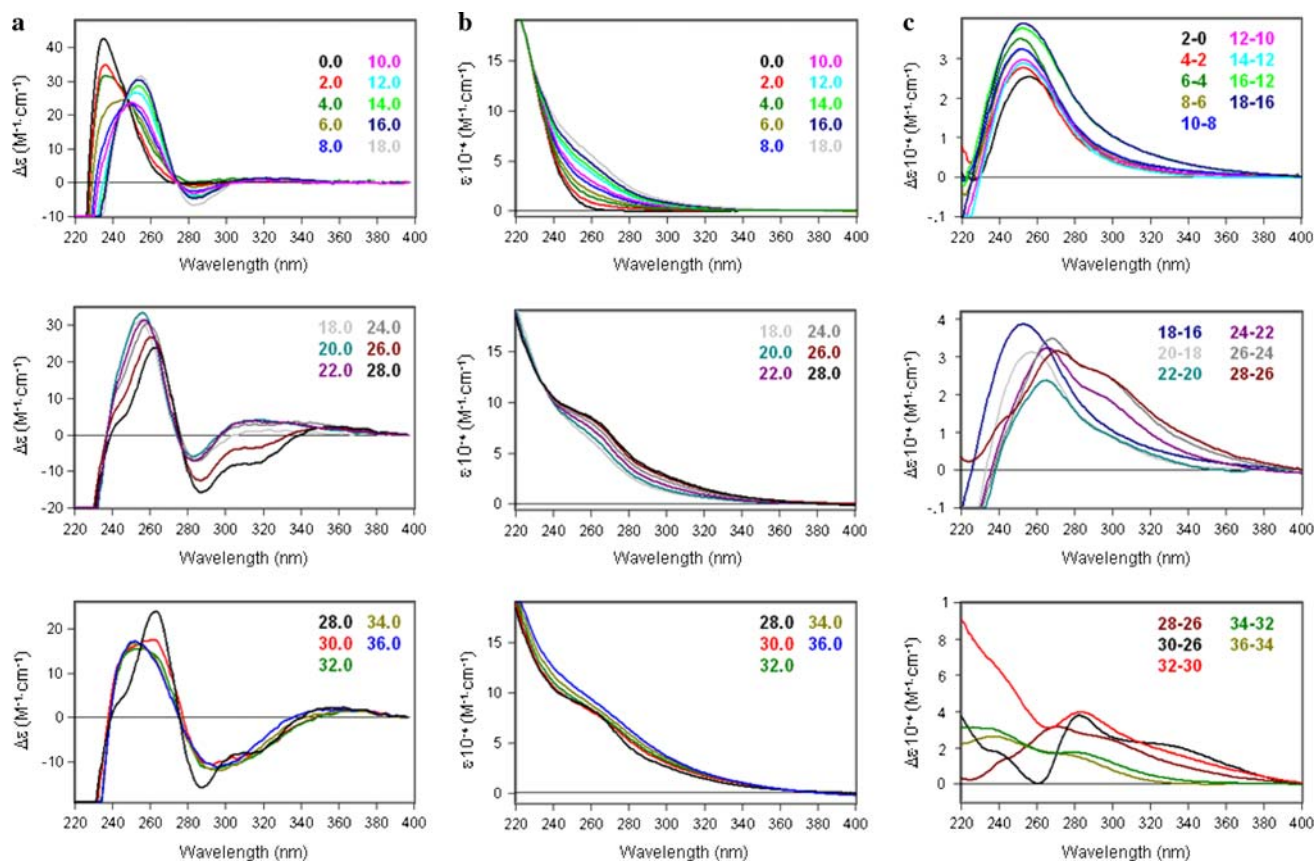


Fig. 6 **a** CD, **b** UV-vis and **c** UV-vis difference spectra obtained during the titration of a 10 μM solution of Zn₇–MeMT with Cu(I) at pH 7

Table 4 Metal–MeMT species detected by ESI–MS at pH 7 and at pH 2.5 during the titration of a 10 μM solution of Zn₇–MeMT with Cu(I) at pH 7 (M is Zn or Cu)

Species	Cu(I) equivalents added to Zn ₇ –MeMT (pH 7)						Species	Cu(I) equivalents added to Zn ₇ –MeMT (pH 2.5)						
	2	6	14	21	23	28		2	6	14	21	23	28	30
M ₇ –MeMT	✓	✗	◆				Apo-MeMT	✓	✓	✗				
M ₈ –MeMT	✓	✓	✓	✗	✗	✗	Cu ₄ –MeMT	◆	✓	◆				
M ₉ –MeMT	◆	✓	✗	✗	✗	✓	Cu ₈ –MeMT	✗	✓	✓	✗	✗	◆	
M ₁₀ –MeMT	✗	✓	✓	✓	✗	✗	Cu ₉ –MeMT	✗	✗	✓	✓	✓	✓	
M ₁₁ –MeMT	◆	✗	◆	◆	◆	✗	Cu ₁₀ –MeMT	◆	✓	✓	✓	✓	✓	
M ₁₂ –MeMT		✓	◆	◆	◆	✗	Cu ₁₁ –MeMT		✗		✓	✓	✓	
M ₁₃ –MeMT						✗	Cu ₁₂ –MeMT				✗	✓	✓	

✓ denotes major species, ✗ denotes intermediate species, ◆ denotes minor species

recombinant type 2 Cu–MeMT (Fig. 7b). At this point, probably most of the species are still heterometallic Zn,Cu–MeMT complexes together with species of up to M₁₃ mainly containing eight and nine Cu(I) ions (Tables 1, 4); however, the presence of certain Cu–MeMT homometallic species cannot be discarded. These results may perhaps reflect the existence of two thermodynamically stable steps in the Zn/Cu replacement reaction that are alternatively reached, depending on the conditions of the physiological environment in which the Cu complexes are

synthesized. This was clearly demonstrated for yeast Crs5, with the culture degree of oxygenation determining the step of the Zn/Cu displacement reaction reproduced *in vivo* [32].

Concluding remarks

The results of the comparative physicochemical study of the *in vivo* Zn(II)-, Cu(I)- and Cd(II)-binding abilities of

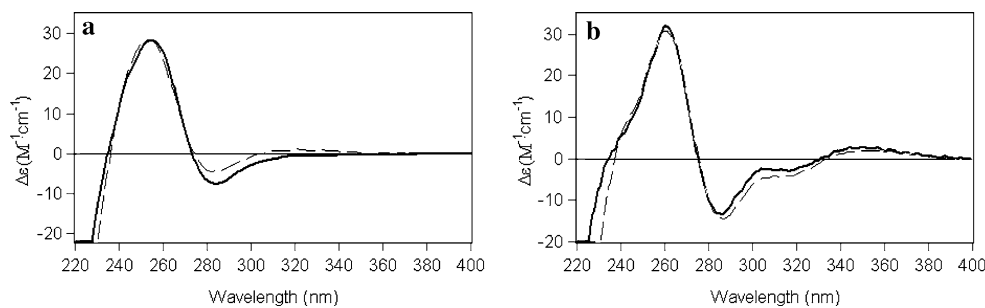


Fig. 7 Comparison of the normalized CD spectra of **a** the Cu–MeMT species obtained under in vitro [after 14 equiv of Cu(I) had been added, dashed line] and in vivo (type 1, solid line) conditions, and of

b the Cu–MeMT species obtained under in vitro [after 26 equiv of Cu(I) had been added, dashed line] and in vivo (type 2, solid line) conditions

the mussel MeMT reported here are consistent with the role of this isoform in the mussel basal/housekeeping metal metabolism suggested by the response of its encoding gene to metal induction, rather than with Cd(II) detoxification events. *Mytilus* sp. MT-10 genes are constitutively expressed, yielding significant amounts of the encoded proteins (that of *M. edulis* here called MeMT) at basal level, which only increase in response to Zn and to low amounts of Cd, unlike the MT-20 genes, which remain practically silent unless a high amount of Cd is present [19, 21]. Hence, MeMT is able to fold into highly chiral and stable complexes upon Zn coordination, precisely the optimal gene inducer, and what is more, these Zn complexes exhibit an uncommon high reluctance to in vitro fully substitute Cd and/or Cu for this metal ion. These Zn-binding features of MeMT depict a significantly different behavior in relation to its mammalian counterparts. In vivo Cd coordination leads to homometallic Cd₇–MeMT complexes, a stoichiometry that cannot be achieved in vitro by Zn/Cd displacement unless excess Cd(II) is used in a process that notably leads to nonisostructural complexes. Finally, when expressed in Cu-enriched media, two types of heterometallic Zn,Cu complexes are recovered, each of these exhibiting a different Cu load, which corresponds to two steps in the in vitro Zn/Cu replacement. Homometallic Cu complexes are only obtained in vitro after a great molar excess of Cu(I) has been added. In this scenario, the MT-20 system would probably provide more suitable means of excess metal detoxification; in relation to this idea, certain differences between the Cd complexes formed by both *M. galloprovincialis* isoforms have already been reported [35]. It is worth noting that our results showed unprecedented precipitation of the Cd–MeMT complexes at acid pH. This could be the basis for the formation of the characteristic Cd-containing granules called cadmosomes [45] detected in some organs (kidneys) of Cd-intoxicated mussels [46], since Cd–MT aggregates are usually targeted in the highly acidic lysosomal environments.

From a comparative evolutionary overview, most MeMT features are coincident with those of yeast Crs5 MT [32] and of mammalian MT4 [47], MT forms which are clearly associated with basal metal metabolism instead of metal detoxification processes. Coincidentally, all these MTs are at the base of the trees constructed from multialignment comparisons [32, 47], and seem to have given rise to the Cd-handling isoforms by duplication/differentiation events in taxonomic groups as distant as mammals or bivalve and gastropod molluscs (cf. *H. pomatia* [12]). This evolutionary strategy contrasts with that observed in Arthropoda, where two clearly defined forms have been described: Cu-thioneins and divalent metal-inducible thioneins [5, 8].

In summary, the best gene inducer (Zn) is the metal yielding the best fold and homogeneous Zn–MeMT complexes. Then, the second-best inducer (Cd, at low concentration) yields also homometallic Cd–MeMT complexes, but in vitro Zn/Cd replacement hardly removes the last Zn(II) ion from Zn–MeMT. Finally, Cu, which is not a MeMT gene inducer, renders mixed Zn,Cu–MeMT complexes, with an even higher reluctance towards Zn/Cu exchange. Interaction of MeMT with Cu should therefore rely on heterometallic species conformed by constitutively synthesized proteins.

Acknowledgments This work was supported by Spanish Ministerio de Ciencia y Tecnología grants BIO2006-14420-C02-01 for S.A. and BIO2006-14420-C02-02 for M.C. R.O. received a predoctoral fellowship from the Departament de Química, Universitat Autònoma de Barcelona. We thank the Serveis Científico-Tècnics, Universitat de Barcelona (gas chromatography–flame photometric detection, ICP–AES, ESI–MS, DNA sequencing) and the Servei d’Anàlisi Química (SAQ), Universitat Autònoma de Barcelona (CD, UV–vis) for allocating instrument time.

References

1. Kägi JHR (1993) In: Suzuki KT, Imura N, Kimura M (eds) Metallothionein III, biological roles and medical implications. Birkhäuser, Basel, pp 29–55

2. Arseniev A, Schultze P, Wörgötter E, Braun W, Wagner G, Vasák M, Kägi JHR, Wüthrich K (1988) *J Mol Biol* 201:637–657
3. Robbins AH, McRee DE, Williamson M, Collett SA, Xuong NH, Furey WF, Wang BC, Stout CD (1991) *J Mol Biol* 221:1269–1293
4. Riek R, Prêcheur B, Wang Y, Mackay EA, Wider G, Güntert P, Liu A, Kägi JHR, Wüthrich K (1999) *J Mol Biol* 291:417–428
5. Narula SS, Brouwer M, Hua Y, Armitage IM (1995) *Biochemistry* 34:620–631
6. Zhu Z, DeRose EF, Mullen GP, Petering DH, Shaw CF III (1994) *Biochemistry* 33:8858–8865
7. Egli D, Domènec J, Selvaraj A, Balamurugan K, Hua H, Capdevila M, Georgiev O, Schaffner W, Atrian S (2006) *Genes Cells* 11:647–658
8. Valls M, Bofill R, González-Duarte R, González-Duarte P, Capdevila M, Atrian S (2001) *J Biol Chem* 276:32835–32843
9. Syring RA, Hoexum-Brouwer T, Brouwer M (2000) *Comp Biochem Physiol C* 125:325–332
10. Valls M, Bofill R, Romero-Isart N, González-Duarte R, Abián J, Carrascal M, González-Duarte P, Capdevila M, Atrian S (2000) *FEBS Lett* 467:189–194
11. Domènec J, Palacios O, Villarreal L, González-Duarte P, Capdevila M, Atrian S (2003) *FEBS Lett* 533:72–78
12. Dallinger R, Berger B, Hunziker P, Kägi JHR (1997) *Nature* 338:237–238
13. Amiard J-C, Amiard-Triquet C, Barka S, Pellerin J, Rainbow PS (2006) *Aquat Toxicol* 76:160–202
14. Ceratto N, Dondero F, van de Loo J-W, Burlando B, Viarengo A (2002) *Comp Biochem Physiol C* 131:217–222
15. Hardivillier Y, Leignel V, Denis F, Uguen G, Cosson R, Laulier M (2004). *Comp Biochem Physiol C* 139:111–118
16. Leignel V, Laulier M (2006) *Comp Biochem Physiol C* 142:12–18
17. Baršte D, White KN, Lovejoy DA (1999) *Comp Biochem Physiol C* 122:287–296
18. Lemoine S, Laulier M (2003) *Mar Pollut Bull* 46:1450–1455
19. Ciocan CM, Rotchell JM (2004) *Environ Sci Technol* 38:1073–1078
20. Grattarola M, Carloni M, Dondero F, Viarengo A, Vergani L (2006) *Mol Biol Rep* 33:265–272
21. Lemoine S, Bigot Y, Sellos D, Cosson RP, Laulier M (2000) *Mar Biotechnol* 2:195–203
22. Mackay EA, Overnell J, Dunbar B, Davison I, Hunziker PE, Kägi JHR, Fothergill JE (1993) *Eur J Biochem* 218:183–194
23. Wang Y, Mackay EA, Kurasaki M, Kägi JHR (1994) *Eur J Biochem* 225:449–457
24. Capdevila M, Cols N, Romero-Isart N, González-Duarte R, Atrian S, González-Duarte P (1997) *Cell Mol Life Sci* 53:681–688
25. Cols N, Romero-Isart N, Capdevila M, Oliva B, González-Duarte P, González-Duarte R, Atrian S (1997) *J Inorg Biochem* 68:157–166
26. Vasák M (1991) *Methods Enzymol* 205:452–458
27. Bongers J, Walton CD, Richardson DE, Bell JU (1988) *Anal Chem* 60:2683–2686
28. Capdevila M, Domènec J, Pagani A, Tío L, Villarreal L, Atrian S (2005) *Angew Chem Int Ed* 44:4618–4622
29. Bofill R, Palacios O, Capdevila M, Cols N, González-Duarte R, Atrian S, González-Duarte P (1999) *J Inorg Biochem* 73:57–64
30. Domènec J, Orihuela R, Mir G, Molinas M, Atrian S, Capdevila M (2007) *J Biol Inorg Chem* 12:867–882
31. Fabris D, Zaia J, Hathout Y, Fesenlau C (1996) *J Am Chem Soc* 118:12242–12243
32. Pagani A, Villarreal L, Capdevila M, Atrian S (2007) *Mol Microbiol* 63:256–269
33. Gehrig PM, You C, Dallinger R, Gruber C, Brouwer M, Kägi JHR, Hunziker PE (2000) *Protein Sci* 9:395–402
34. Vergani L, Grattarola M, Borghi C, Dondero F, Viarengo A (2005) *FEBS J* 272:6014–6023
35. Vergani L, Grattarola M, Grasselli E, Dondero F, Viarengo A (2007) *Arch Biochem Biophys* 465:247–253
36. Villarreal L, Tío L, Atrian S, Capdevila M (2005) *Arch Biochem Biophys* 435:331–335
37. Otvos JD, Olafson RW, Armitage IM (1982) *J Biol Chem* 257:2427–2431
38. Overnell J, Good M, Vasák M (1988) *Eur J Biochem* 172:171–177
39. You C, Mackay EA, Gehrig PM, Hunziker PE, Kägi JHR (1999) *Arch Biochem Biophys* 372:44–52
40. Stürzenbaum SR, Winters C, Galay M, Morgan AJ, Kille P (2001) *J Biol Chem* 276:34013–34018
41. Jensen LT, Peltier JM, Winge DR (1998) *J Biol Inorg Chem* 3:627–631
42. Roschitzki B, Vasák M (2002) *J Biol Inorg Chem* 7:611–616
43. Bofill R, Capdevila M, Cols N, Atrian S, González-Duarte P (2001) *J Biol Inorg Chem* 6:405–417
44. Dolderer B, Echner H, Beck A, Hartmann HJ, Weser U, Luchinat C, Del Bianco C (2007) *FEBS J* 274:2349–2362
45. Morgan AJ, Morris B (1982) *Histochemistry* 75:269–285
46. George SG (1983) *Comp Biochem Physiol C* 76:53–57
47. Tío L, Villarreal L, Atrian S, Capdevila M (2004) *J Biol Chem* 279:24403–24413

The metal-binding features of the recombinant mussel *Mytilus edulis* MT-10-IV metallothionein

Rubén Orihuela, Jordi Domènech, Roger Bofill, Chunhui You, Elaine A. Mackay,
Jeremias H. R. Kägi, Mercè Capdevila and Sílvia Atrian

SUPPLEMENTARY MATERIAL

Figures

Fig. S1 Synthetic gene coding for mussel MeMT constructed from the eight oligonucleotides indicated.

The protein translation is shown under the cDNA sequence, with the Cys residues underlined.

Fig. S2 QTOF ESI-MS spectra corresponding to **a** *in vivo* Zn-MeMT and **b** *in vivo* Cd-MeMT preparations, both synthesized from the pGEX expression system.

Fig. S3. **a** CD, **b** UV-vis, and **c** UV-vis difference spectra corresponding to the acidification (first row) and reneutralization (second row) of a 10 µM solution of Cd₇-MeMT.

1
 CGATATATATGCCTGCACCGTGTAACTGTATTGAGACTAATGTGTGCATTTGCGACACA
 TATATATATACGGACGTGGCACATTGACATAACTCTGATTACACACGTAAACGCTGTGT
 5
 Met Pro Ala Pro Cys Asn Cys Ile Glu Thr Asn Val Cys Ile Cys Asp Thr

2
 GGGTGTTCGGGCGAGGGTTGCCGTTGTGGCGATGCGTGCAAGTGTCTGGTGCCGATTGC
 CCCACAAGCCCCTCCCAACGGAACACCCGCTACGCACGTTACAAGACCACGGCTAACG
 6
 Gly Cys Ser Gly Glu Gly Cys Arg Cys Gly Asp Ala Cys Lys Cys Ser Gly Ala Asp Cys

3
 AAGTGTTCGGATGCAAAGTGGTTGCAAATGTTCCGGATCTTGTGCGTGTGAGGGCGGT
 TTCACAAGACCTACGTTCACCAAACGTTACAAGGCCTAGAACACGCACACTCCCCCA
 7
 Lys Cys Ser Gly Cys Lys Val Val Cys Lys Cys Ser Gly Ser Cys Ala Cys Glu Gly Gly

4
 TGCACGGGCCCATCTACTTGCAAATGTGCACCGGGTTGCAGTTGCAAATAAG
 ACGTGCCCCGGTAGATGAACGTTACACGTGGCCCAACGTCAACGTTATTCTTAA
 8
Cys Thr Gly Pro Ser Thr Cys Lys Cys Ala Pro Gly Cys Ser Cys Lys End

Fig. S1 Synthetic gene coding for mussel MeMT constructed from the eight oligonucleotides indicated. The protein translation is shown under the cDNA sequence, with the Cys residues underlined.

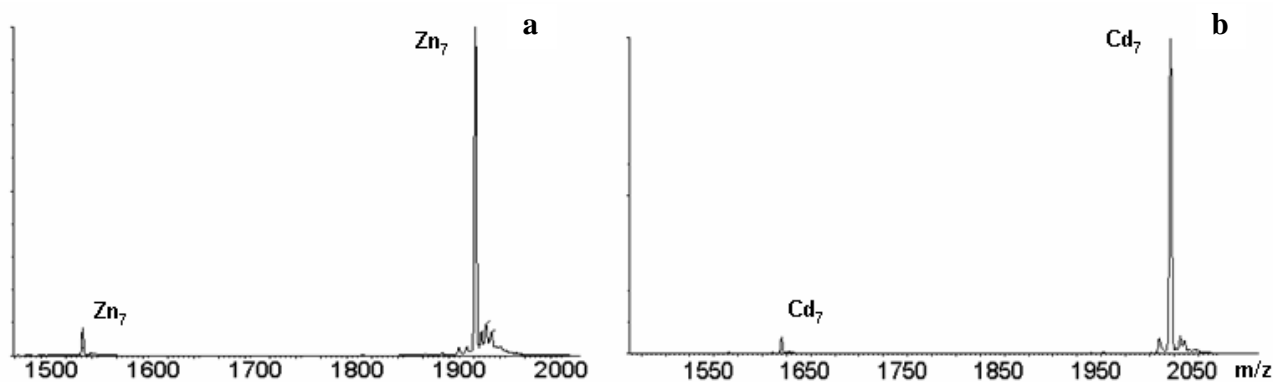


Fig. S2 QTOF ESI-MS spectra corresponding to **a** *in vivo* Zn-MeMT and **b** *in vivo* Cd-MeMT preparations, both synthesized from the pGEX expression system.

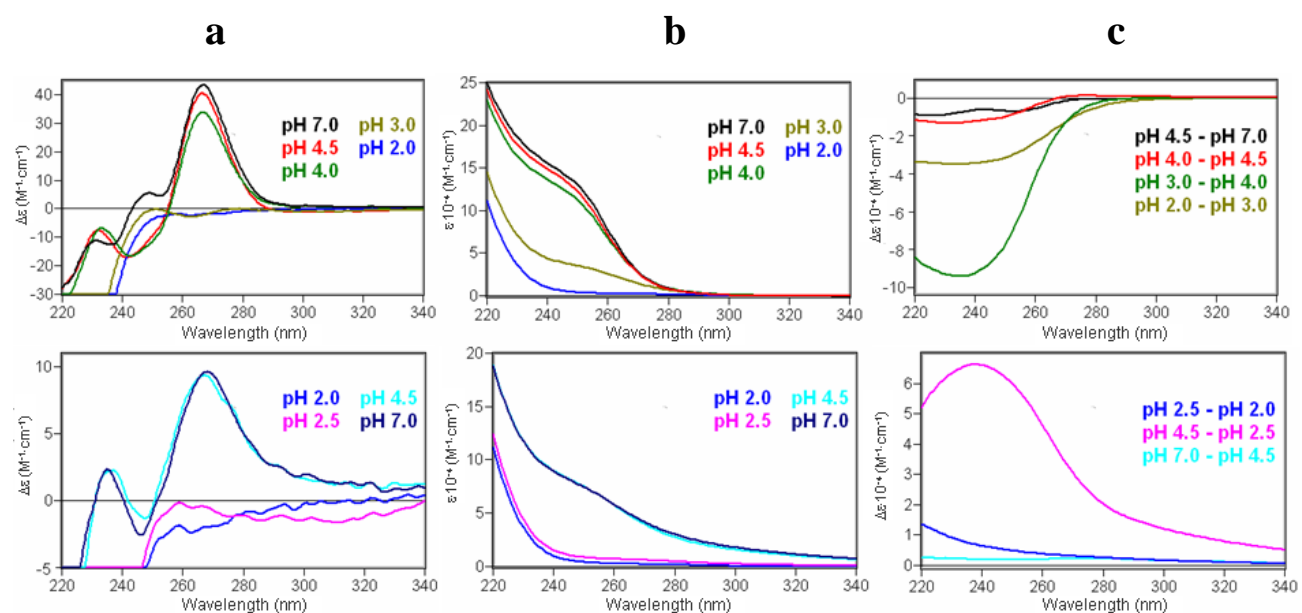


Fig. S3. **a** CD, **b** UV-vis, and **c** UV-vis difference spectra corresponding to the acidification (first row) and reneutralization (second row) of a 10 μM solution of $\text{Cd}_7\text{-MeMT}$.

ARTICLE 2

The Cd^{II}-binding abilities of recombinant *Quercus suber* metallothionein: bridging the gap between phytochelatins and metallothioneins

Journal of Biological Inorganic Chemistry, (2007), 12, 867-882

The Cd^{II}-binding abilities of recombinant *Quercus suber* metallothionein: bridging the gap between phytochelatins and metallothioneins

Jordi Domènec · Rubén Orihuela · Gisela Mir · Marisa Molinas · Sílvia Atrian · Mercè Capdevila

Received: 2 November 2006 / Accepted: 12 April 2007 / Published online: 15 May 2007
© SBIC 2007

Abstract In this work, we have analyzed both at stoichiometric and at conformational level the Cd^{II}-binding features of a type 2 plant metallothionein (MT) (the cork oak, *Quercus suber*, QsMT). To this end four peptides, the wild-type QsMT and three constructs previously engineered to characterize its Zn^{II}- and Cu^I-binding behaviour, were heterologously produced in *Escherichia coli* cultures supplemented with Cd^{II}, and the corresponding complexes were purified up to homogeneity. The Cd^{II}-binding ability of these recombinant peptides was determined through the chemical, spectroscopic and spectrometric characterization of the recovered clusters. Recombinant synthesis of the

four QsMT peptides in cadmium-rich media rendered complexes with a higher metal content than those obtained from zinc-supplemented cultures and, consequently, the recovered Cd^{II} species are nonisostructural to those of Zn^{II}. Also of interest is the fact that three out of the four peptides yielded recombinant preparations that included S²⁻-containing Cd^{II} complexes as major species. Subsequently, the in vitro Zn^{II}/Cd^{II} replacement reactions were studied, as well as the in vitro acid denaturation and S²⁻ renaturation reactions. Finally, the capacity of the four peptides for preventing cadmium deleterious effects in yeast cells was tested through complementation assays. Consideration of all the results enables us to suggest a hairpin folding model for this typical type 2 plant Cd^{II}-MT complex, as well as a nonnegligible role of the spacer in the detoxification function of QsMT towards cadmium.

Electronic supplementary material The online version of this article (doi:10.1007/s00775-007-0241-y) contains supplementary material, which is available to authorized users.

J. Domènec · S. Atrian (✉)
Departament de Genètica,
Facultat de Biologia,
Universitat de Barcelona,
Av. Diagonal, 645,
08028 Barcelona, Spain
e-mail: satrian@ub.edu

R. Orihuela · M. Capdevila
Departament de Química,
Facultat de Ciències,
Universitat Autònoma de Barcelona,
08193 Bellaterra Barcelona, Spain

G. Mir · M. Molinas
Departament de Biologia,
Universitat de Girona,
Campus Montilivi,
17071 Girona, Spain

S. Atrian
Institut de Biomedicina de la Universitat de Barcelona,
Barcelona, Spain

Keywords Cadmium–His binding · Phytochelatins · Plant metallothionein · Sulfide ligands · Yeast complementation

Introduction

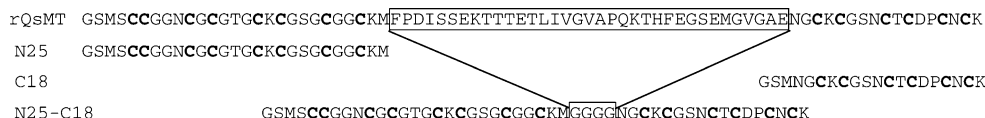
Cadmium is a metal that is well known for being toxic to organisms, in general, and to plants, in particular, where it causes severe metabolic malfunctions leading to intense chlorosis and growth impairment. Consequently, plants have developed efficient defence systems against cadmium toxicity, which mainly consist of chelating polypeptides that immobilize metal ions inside the cell. Two types of plant (including algae) metal-chelating peptides have been reported, enzymatically synthesized phytochelatins (PCs) and gene-encoded metallothioneins (MTs) [1]. Plant PCs, such as yeast cadystins, are polymers of glutamic acid–Cys

γ -dipeptide linked to a terminal glycine residue, the number of units in the polymer ranging from 5 to 17 [2]. They bind Cd^{II} through metal–thiolate bonds, forming Cd^{II} PC complexes of variable size [3]. These complexes typically include acid-labile sulfide ligands, also in a variable metal to sulfide to peptide ratio, which contribute to the formation of semicrystal particles known as *crystallites*, analogous to those extensively studied in yeasts [4]. *Arabidopsis* mutants lacking PC synthase have a definite cadmium-sensitive phenotype [5], and cadmium tolerance has been related to Cd^{II} PC accumulation in tobacco [6], tomatoes [7] and maize [8].

PCs were considered the only metal-defence mechanism in plants until 1980, when an MT-like peptide was first isolated in copper-treated *Agrostis* (reddish bent) roots [9], more than 20 years after the discovery of MT in animals. MTs are ubiquitous, small, Cys-rich proteins that chelate heavy-metal ions through metal–thiolate bonds. Currently, MTs have been extensively identified as a multigenic family in angiosperms (*A. thaliana* as a model [1]), in gymnosperms [10] and in algae (*Fucus*) [11], constituting family 15 of the global MT Kägi classification [12]. Plant MTs are considerably longer than their animal counterparts owing to the exclusive presence of a 30–50-residue-long, Cys-devoid region, between the N- and C-terminal Cys-rich domains (four to eight Cys each). Specifically, the distribution of the Cys residues and the length of the spacer region have been used to further classify plant MTs into four subtypes [1, 13]. Although plant MTs have been extensively related to housekeeping functions in physiological zinc and copper metabolism [14, 15] and in reactive oxygen species scavenging [1, 16, 17], early studies report that plant MT synthesis also responds to cadmium induction [17, 18]. Confirmation of the putative cadmium detoxification role of plant MTs was primarily achieved by yeast complementation studies [19]. More recently, it has been directly shown in plant cells that MTs mediate resistance and tolerance to cadmium [20, 21]. Strikingly, very little is known about the Cd^{II}-MT complexes that are formed upon plant MT synthesis in response to cadmium, mainly owing to the high level of proteolysis associated with native protein purification. Consequently and in comparison with the structural knowledge of animal MT complexes [22], there is an appalling lack of data about the interaction between heavy-metal ions and plant MTs. Unfortunately, many initial efforts in recombinant (*Escherichia coli*) plant MT synthesis did not make it possible to overcome this drawback [23, 24], and MT complexes were directly characterized as fusion proteins [25], which is of dubious biological relevance. Fortunately, this scenario is beginning to change, and the characterization of recombinant *Triticum aestivum* (wheat, [26]) and *Musa acuminata* (banana, [27]) MT complexes was recently reported.

Some time ago, we adapted our glutathione S-transferase based MT expression system in *E. coli*, which we have fully validated for animal MTs [28, 29], to obtain highly homogeneous preparations of undigested, full-length metal complexes from a typical dicot angiosperm MT (*Quercus suber* MT, QsMT) [30]. QsMT is a type 2 plant MT isolated in our laboratory from a cork oak (*Q. suber*) phellem complementary DNA (cDNA) library of oxidative stress induced genes. Protein expression and purification from *E. coli* cells grown in the presence of zinc, cadmium or copper enabled us to determine the Zn^{II}-, Cd^{II}- and Cu^I-binding properties of the full-size peptide. Our results showed that when expressed in the presence of cadmium, recombinant QsMT (rQsMT) binds a surprisingly high content of Cd^{II} in comparison with Zn^{II}, confirming that this protein could play an important role in the heavy-metal detoxification of plants [30]. Interestingly, our results also suggested the presence of acid-labile sulfide ligands in the Cd^{II}-rQsMT complexes, concordantly with the sulfide anions mediating the formation of the Cd^{II} PC crystallites. This was the first time that the participation of sulfide ligands was suspected in any MT preparation, and led to the significant discovery that, although at different ratio, all MT recombinant complexes with divalent metal ions may contain these nonproteic ligands [31]. To gain some insight into the metal cluster structure and protein folding of plant MTs we then engineered three QsMT-derived peptides: the N-terminal Cys-rich domain (N25), the C-terminal Cys-rich domain (C18) and a chimera where both Cys-rich domains were linked by a four-Gly bridge (N25-C18) instead of the original linker region of 39 amino acids (Scheme 1). Expression of these constructs in the presence of copper or zinc allowed us to analyse the binding properties for these metal ions, and to propose a protein folding model in a single metal cluster formed by the interaction of both Cys-rich domains where the linker domain, though not participating in metal coordination, is important for the stability and function of the protein [32].

In the current study, we applied the same rationale to analyse the Cd^{II}-binding features of rQsMT at stoichiometric and conformational levels. This is especially interesting owing to the participation of sulfide ions in Cd^{II}-rQsMT. Thus, the four QsMT peptides (wild-type rQsMT, N25-C18, N25 and C18) were purified from *E. coli* cells grown in the presence of cadmium, and their in vivo Cd^{II}-binding ability was determined through the chemical, spectroscopic and spectrometric characterization of the corresponding clusters. Then, the in vitro Zn^{II}/Cd^{II} replacement reactions were studied, as well as the in vitro acid denaturation and sulfide renaturation reactions. Finally, to test the capacity of the four peptides for preventing cadmium deleterious effects in yeast cells, a



Scheme 1 Amino acid sequences of the wild-type recombinant *Quercus suber* metallothionein (*rQsMT*) and of the three deletion mutants as constructed in [32]: *N25*, the *rQsMT* N-terminal region, containing the first eight Cys; *C18*, the *QsMT* C-terminal region,

functional approximation was performed through yeast complementation assays. All the results enable us to suggest, for the first time, a metal-binding and folding model for a typical plant Cd^{II}-MT complex.

Materials and methods

Recombinant synthesis and purification of the Zn^{II} and Cd^{II} complexes of wild-type QsMT, N25-C18, N25 and C18

Isolation of the QsMT cDNA, construction of the N25, C18 and N25-C18 coding sequences, and cloning into the pGEX expression vector have been previously described [30, 32]. *E. coli* BL21 cells transformed with the respective recombinant plasmids pGEX-QsMT, pGEX-N25, pGEX-C18 and pGEX-N25-C18 were grown in the presence of 300 μM ZnCl₂ or CdCl₂ and hence used for recombinant syntheses. Expression and purification were performed as reported in [31], so all MT complexes were recovered in 50 mM tris(hydroxymethyl)aminomethane hydrochloride pH 7.0 solution, and were kept at –70 °C until used.

Chemical, spectroscopic and spectrometric characterization of the metal peptide complexes

Following the procedures already described by our group [31, 32], acid inductively coupled plasma atomic emission spectroscopy (ICP-AES) and amino acid analysis were used to determine the protein concentration of the different Zn^{II}- or Cd^{II}-containing preparations. Their metal-to-protein ratios were also deduced from the acid ICP-AES measurements and their mean sulfide-to-protein contents were estimated by gas chromatography–flame photometric detection (GC-FPD) [31]. The use of Na₂SO₄ as an ICP-AES standard for the Cys- and Met-derived sulfur quantification in MTs was validated by Bongers et al. [33]. However, as we reported in [31], Na₂SO₄ cannot be used as a standard for sulfide sulfur determinations as both types of sulfur enter into the plasma phase differently. Consequently, the S²⁻-to-protein ratios cannot be obtained by direct subtraction of the acid from the conventional ICP-AES values, although both types of data are included

containing six Cys; and *N25-C18*, the fusion of N25 and C18 through a flexible bridge of four Gly (box), thus devoid of the spacer region of QsMT. Additional Gly and Ser are present in the N-terminus of the four peptides owing to the recombinant synthesis strategy [28]

in Tables 1 and 2. A Polyscan 61 E (Thermo Jarrell Ash) spectropolarimeter and an Alpha Plus amino acid auto-analyser (Pharmacia LKB Biotechnology) were respectively used for the ICP-AES measurements and amino acid analysis. An HP 5890 series II gas chromatograph coupled to an FPD80 CE detector (Thermo Finnigan) was employed for the GC-FPD sulfide quantifications.

The in vitro Cd^{II}-binding analyses were performed by Cd^{II} titration of the Zn^{II} peptides as described elsewhere [28], and were monitored spectroscopically and spectropolarimetrically. Electronic absorption measurements were performed using an HP-8453 diode array UV-vis spectrophotometer. A JASCO spectropolarimeter (J-715) interfaced to a computer (GRAMS/AI 7.02 software) was used for circular dichroism (CD) determinations. All manipulations involving metal ion and protein solutions were performed under an argon atmosphere, and titrations were carried out at least in duplicate to ensure reproducibility. The pH for all experiments remained constant throughout, without further addition of buffers, and the temperature was kept constant at 25 °C by means of a Peltier PTC-351S apparatus.

The molecular mass of the metal peptide species was determined by electrospray ionization (ESI) mass spectrometry (MS) performed either with a Fisons Platform II instrument (VG Biotech) controlled by MassLynx software following the same conditions previously described [32] or with an Ultima Micromass quadrupole time of flight (QTOF) instrument (ESI-QTOF), also controlled by MassLynx software and calibrated with NaI (0.2 g NaI dissolved in 100 ml of a 1:1 H₂O/2-propanol mixture). In the ESI-TOF analysis of the metallopeptides, 5 μl of the sample was injected at 40 μl/min under the following conditions: source temperature, 150 °C; desolvation temperature, 250 °C; capillary counter electrode voltage, 3.0 kV; cone potential, 80 V. Spectra were collected throughout an *m/z* range from 950 to 2,150 at a rate of 2 s per scan with an interscan delay of 0.1 s. The liquid carrier was a 10:90 mixture of acetonitrile and 5 mM ammonium acetate, pH 7. For analysis of the apo form, the samples were demetalated by acidification with HCl at pH 1.5 and MS measurements were carried out as explained for the holo forms, except that the liquid carrier was a 10:90 mixture of methanol and ammonium formate/

Table 1 Analytical characterization of the recombinant Zn^{II} complexes of *Quercus suber* metallothionein (QsMT) and the three QsMT-derived peptides (N25-C18, N25 and C18)

Peptide	Peptide concentration ($\times 10^{-4}$) Zn ^{II} -to-peptide molar ratio			S ²⁻ /peptide ^c	ESI-MS ^d			
	ICP ^a	Acid ICP ^b	Amino acid analysis		Major species	Minor species	M_r expected	M_r found
QsMT	1.3 ± 0.10	0.9 ± 0.05	0.9 ± 0.10	1.3 ± 0.40	Zn ₄ -QsMT		8,070.4	8,070.0 ± 0.6
	2.7 ± 0.04	3.5 ± 0.06			Zn ₃ -QsMT	8,007.1	8,007.4 ± 1.2	
					Zn ₄ S ₂ -QsMT	8,138.6	8,138.2 ± 1.4	
N25-C18	1.5 ± 0.08	1.3 ± 0.07	1.3 ± 0.11	1.0 ± 0.30	Zn ₄ -N25-C18		4,622.6	4,620.0 ± 0.6
	3.6 ± 0.05	3.6 ± 0.08			Zn ₄ S ₁ -N25-C18	4,656.7	4,660.2 ± 0.8	
					Zn ₃ S ₁ -N25-C18	4,593.3	4,592.7 ± 0.6	
N25	3.8 ± 0.12	3.2 ± 0.08	3.2 ± 0.23	0.3 ± 0.10	Zn ₂ -N25		2,535.6	2,534.0 ± 0.5
	2.0 ± 0.09	2.2 ± 0.10			Zn ₃ -N25	2,599.0	2,600.5 ± 0.7	
					Zn ₇ S ₁ -(N25) ₂	5,295.4	5,295.5 ± 0.7	
C18	3.5 ± 0.11	3.4 ± 0.09	3.3 ± 0.38	0.0 ± 0.00	Zn ₂ -C18		2,152.1	2,150.0 ± 0.7
	1.9 ± 0.10	1.8 ± 0.08			Zn ₁ -C18	2,088.7	2,086.4 ± 0.8	
					Zn ₅ -(C18) ₂	4,367.6	4,367.8 ± 1.9	

ICP inductively coupled plasma, ESI-MS electrospray ionization mass spectrometry

^a Peptide concentration and Zn^{II}-to-peptide ratio calculated from conventional ICP atomic emission spectroscopy (AES) results

^b Peptide concentration and Zn^{II}-to-peptide ratio calculated from acid ICP-AES results

^c S²⁻-to-peptide ratio measured by gas chromatography–flame photometric detection (GC-FPD)

^d Experimental and theoretical molecular weights corresponding to the Zn^{II} peptides. Zn^{II} contents were calculated from the mass difference between holo and apo proteins

Table 2 Analytical characterization of the recombinant Cd^{II} complexes of QsMT and the three QsMT-derived peptides (N25-C18, N25 and C18)

Peptide	Peptide concentration ($\times 10^{-4}$ M) Cd ^{II} -to-peptide molar ratio			S ²⁻ /peptide ^c	ESI-MS ^d			
	ICP ^a	Acid ICP ^b	Amino acid analysis		Major species	Minor species	M_r expected	M_r found
QsMT(1)	1.5 ± 0.20	0.8 ± 0.03	0.8 ± 0.11	2.9 ± 0.80	Cd ₆ S ₄ -QsMT		8,615.5	8,617.2 ± 0.3
	2.9 ± 0.07	6.7 ± 0.05			Cd ₇ S ₄ -QsMT	8,725.9	8,723.7 ± 1.1	
QsMT(2)	1.5 ± 0.22	0.6 ± 0.05	0.6 ± 0.09	2.4 ± 0.60	Cd ₆ S ₄ -QsMT		8,615.5	8,619.1 ± 0.8
	2.5 ± 0.08	6.3 ± 0.08			Cd ₇ S ₄ -QsMT	8,725.9	8,726.0 ± 0.7	
QsMT(3)	2.3 ± 0.31	1.3 ± 0.07	1.3 ± 0.18	2.2 ± 0.70	Cd ₅ -QsMT		8,368.8	8,370.1 ± 0.6
	3.7 ± 0.10	5.3 ± 0.08			Cd ₆ S ₄ -QsMT	8,615.5	8,618.2 ± 1.2	
N25-C18	2.4 ± 0.26	1.0 ± 0.04	1.0 ± 0.20	2.4 ± 0.60	Cd ₆ S ₄ -N25-C18		5,167.7	5,169.6 ± 0.5
	2.4 ± 0.09	5.9 ± 0.07			Cd ₅ -N25-C18	4,921.1	4,922.1 ± 0.2	
N25	3.0 ± 0.35	1.2 ± 0.04	1.2 ± 0.21	2.8 ± 0.60	Cd ₇ S ₄ -(N25) ₂		5,726.8	5,730.5 ± 1.9
	1.4 ± 0.13	3.8 ± 0.09			Cd ₆ -(N25) ₂	5,480.1	5,478.7 ± 2.0	
C18	2.9 ± 0.12	2.8 ± 0.10	2.7 ± 0.30	0.5 ± 0.40	Cd ₄ -(C18) ₂		4,492.3	4,490.9 ± 0.6
	2.1 ± 0.12	2.3 ± 0.10			Cd ₅ -(C18) ₂	4,602.7	4,600.9 ± 1.2	

^a Peptide concentration and Cd^{II}-to-peptide ratio calculated from conventional ICP-AES results

^b Peptide concentration and Cd^{II}-to-peptide ratio calculated from acid ICP-AES results

^c S²⁻-to-peptide ratio measured by GC-FPD

^d Experimental and theoretical molecular weights corresponding to the Cd^{II} peptides. Cd^{II} contents were calculated from the mass difference between holo and apo proteins

ammonia at pH 1.5. In all cases, the theoretical molecular masses were calculated according to [32] except for the sulfide-containing species, where two additional protons were added per sulfide anion.

Demetalation and reconstitution of the Cd^{II} complexes of rQsMT and the three derived peptides

Two different strategies were used for the demetalation of the MT complexes in this work: acidification and EDTA treatment. For acidification, and according to equivalent experiments with Cd^{II} PC complexes [34], the four Cd^{II} peptide preparations were acidified from neutral pH to a pH lower than 1 with 1–10⁻³ M HCl depending on the stage of the titration, and were renaturalized afterwards to pH 7.0 with 1–10⁻³ M NaOH, also depending on the stage of the titration. After renaturalization, several molar equivalents of a standard solution of Na₂S prepared as described in [31] were added. All the CD and UV-vis changes experienced by the samples during these pH variations and sulfide additions were recorded and corrected for dilution effects. When possible, ESI-MS analyses of the intermediate and resulting final solutions were also performed.

According to procedures reported in the literature [35], a 16 μM solution of Cd^{II}-rQsMT at pH 7.5 was treated with 10–50 mM EDTA, depending on the stage of the titration, and the spectropolarimetric changes were recorded.

Yeast functional complementation assays

Following the details reported in [32], two MT-deficient, copper-sensitive *Saccharomyces cerevisiae* strains were used, *cup1*^S: DTY3 (*MATA*, *leu2-3*, *112his3*^A*1*, *trp1-1*, *ura3-50*, *gal1 CUP1*^S), harbouring only one copy of the *CUP1* MT gene; and *cup1*^A: DTY4 (same with *cup1::URA3*), thus with no copy of *CUP1* [36]. The growth of yeast cells transformed with the plasmids p424-QsMT, p424-N25-C18, p424-N25 or p424-C18, constructed as previously described [30, 32, 37], was assayed in culture media supplemented with or without CdCl₂ (1.5, 2.5 or 3.5 μM for the plate).

Results and discussion

The metal complexes rendered by the three QsMT-derived peptides (N25-C18, N25 and C18) when biosynthesized in zinc- or cadmium-enriched media were analysed and characterized by spectroscopic and spectrometric methods, and the data were compared with those of the full-length rQsMT [30, 32]. Independently of the metal ions supplemented in the media, acidification to pH 1.0 of each

recombinant peptide yielded single apo forms whose molecular masses were in accordance with the values calculated from their amino acid composition [32], this confirming their identity and integrity. None of the CD spectra of the four demetalated peptides exhibited absorptions in the 220–400-nm range, which is especially significant in the case of apo-QsMT, as this indicates that the aromatic residues of the spacer region are CD-silent. However, the UV-vis spectrum of apo-QsMT showed absorptions in the range 260–280 nm (Fig. 3j) attributable to the two Phe residues of the spacer.

The Zn^{II}-binding features of rQsMT and derived peptides: a deeper insight

The in vitro Zn^{II}/Cd^{II} replacement studies of the four recombinant peptides required biosynthesis and analytical characterization of the corresponding Zn^{II} complexes, previously characterized in [32]. However, our current knowledge of the presence of sulfide ligands in the recombinant MT species [31] together with the use of ESI-QTOF allowed refining of our previous data [32], particularly their metal and S²⁻ contents (Table 1). The present results revealed that Zn^{II}-C18 was the only case where S²⁻ ligands were not detected by GC-FPD. In contrast, rQsMT, N25-C18 and N25 gave rise to minor S²⁻-containing species. It should be noted that, as already reported in [31], we have found that GC-FPD always overestimates the S²⁻ content of the MT samples. Consequently, there is a discordance between the S²⁻/protein quantification achieved by GC-FPD and the stoichiometries and relative abundances of the MT species detected by ESI-MS.

Analysis of the Cd^{II}-binding features of rQsMT

Multiple recombinant syntheses of the full-length QsMT in cadmium-rich medium yielded three kinds of in vivo preparations, namely rQsMT types 1, 2 and 3, which could not be related to specific culture conditions. According to the MS data shown in Table 2, Cd^{II}-rQsMT(1) and Cd^{II}-rQsMT(2) showed identical speciation: Cd₆S₄ and Cd₇S₄ as the most abundant species, while Cd^{II}-rQsMT(3) yielded major Cd₅ and minor Cd₆S₄ complexes. Therefore, the unknown ligand of [30] could be readily identified as four S²⁻ anions. In any case, none of the Cd^{II}-rQsMT complexes were either isostoichiometric or isostructural to their Zn^{II}-rQsMT counterpart. Although all Cd^{II}-rQsMT types consisted of Cd^{II} homometallic samples of close speciation, their CD fingerprints were markedly dissimilar (Fig. 1a). Interestingly, these CD features were exchangeable by in vitro acidification or demetalation treatments, as explained further below.

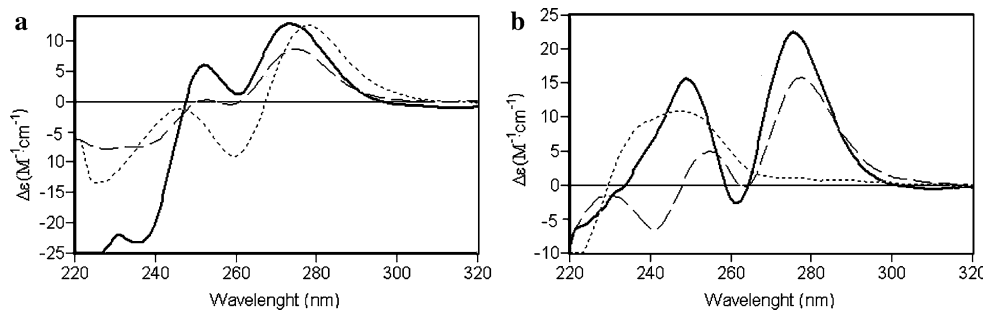


Fig. 1 Comparison of the normalized circular dichroism (CD) spectra of the following recombinant metallothionein (MT) preparations: **a** Cd^{II}-rQsMT(1) (dotted line), Cd^{II}-rQsMT(2) (dashed line),

Cd^{II}-rQsMT(3) (solid line) **b** Cd^{II}-N25-C18 (solid line), Cd^{II}-N25 (dashed line), Cd^{II}-C18 (dotted line). rQsMT recombinant *Quercus suber* MT

Overall analysis of the in vitro Zn^{II}/Cd^{II} replacement in Zn^{II}-rQsMT led us to propose Cd₄-QsMT (major), Cd₅-QsMT, and several minor S²⁻-containing complexes of close metal stoichiometry, as the final products of this reaction, even in the presence of excess Cd^{II} (whole spectroscopic and spectrometric data included in Fig. 2, Table S1). These species were similar to those of the Cd^{II}-rQsMT(3) preparation, but were absent in Cd^{II}-rQsMT(1) and Cd^{II}-rQsMT(2) samples (Table 2). Notably, none of the CD fingerprints of the three Cd^{II}-rQsMT types were reproduced during the Cd^{II} titration (Figs. 1a, 2a, b). As the main difference between the in vivo and in vitro Cd^{II}-binding abilities of QsMT was the presence of S²⁻-rich Cd₆S₄-rQsMT complexes (in the in vivo samples), we extended the Cd^{II} titration by gradually adding Na₂S after 7 equiv Cd^{II} had been added to Zn^{II}-rQsMT. This gave rise to an absorption increase in the 260–320-nm region (Fig. 2c, d, g, h, k, l), in accordance with the S²⁻ anions being incorporated into the Cd^{II} complexes [34]. The final CD fingerprints (Fig. 2d) clearly evolved towards the envelopes recorded for Cd^{II}-rQsMT (Fig. 1a). Despite the drawbacks associated with generation of Na⁺ adducts, ESI-MS analysis of the final samples revealed the presence of S²⁻-containing species with higher nuclearity than those present before Na₂S addition (i.e. Cd₇S₉-QsMT and Cd₆S₆-QsMT, Table S1). All these data reinforce the hypothesis of S²⁻ as a determinant of (1) the nuclearity of Cd^{II}-rQsMT complexes and (2) the differences between the biosynthesized Cd^{II}-rQsMT samples and the in vitro constituted Cd^{II}-QsMT complexes.

Finally, acidification/reneutralization of the three Cd^{II}-rQsMT preparation types shed light on their different nature. Acidification of Cd^{II}-rQsMT(3) from pH 7 to 4.5 caused a decrease in the intensity of the CD shoulder at approximately 250 nm, to give rise to a CD profile very similar to that of Cd^{II}-rQsMT(1) (whose CD spectrum remains invariable between pH 7.0 and 4.3, Fig. S1), with one intermediate step corresponding to the CD of

Cd^{II}-rQsMT(2) (Fig. 3a). Thus, at pH 4.5 any of the three Cd^{II}-rQsMT types exhibited the same CD spectrum [i.e. that of Cd^{II}-rQsMT(1)], which remained unaltered between pH 4.5 and 3.5 (Fig. 3b), to render at pH 1 the typical CD and UV spectra of an apo-MT with aromatic amino acids (Fig. 3c, d, i, j). The H₂S odour was perceptible during the three acidifications, confirming the acid-labile character of the S²⁻ ligands of the original complexes. Renutralization up to pH 7 of the resulting S²⁻-devoid samples (Fig. 3e, k, q) gave rise to Cd₄-QsMT (major) and Cd₅-QsMT (minor) species (ESI-MS data not shown) whose CD envelopes evidently did not reproduce those of any of the Cd^{II}-rQsMT preparations. As before, addition of Na₂S to these solutions caused dramatic changes to their spectroscopic features (Fig. 3f, l, r) and rendered S²⁻-containing complexes (Cd₈S₆ and Cd₇S₂) whose CD fingerprint resembled that of Cd^{II}-rQsMT(3) (Fig. 4a). Interestingly, during the de-metalation of Cd^{II}-rQsMT(1) by EDTA (Fig. 4b, c), the addition of the first EDTA equivalent (Fig. 4b) increased chirality at approximately 280 nm, while not altering that at approximately 250 nm. Afterwards, increasing molar ratios of EDTA led to samples showing CD spectra similar to that of Cd^{II}-rQsMT(3) (Fig. 4c).

The comprehensive consideration of all these data suggests that the heterogeneity of the Cd^{II}-rQsMT samples (types 1–3) was due to two main factors: (1) the already mentioned relative abundance of S²⁻-containing complexes in the sample and (2) the putative participation of the His of the spacer in cadmium coordination, as suggested by the following hints. First, preliminary Raman data revealed the presence of metal-His bonds in the Cd^{II}-rQsMT complexes, and their absence in Zn^{II}-rQsMT [38]. Second, literature data suggest that CD shoulders at approximately 250 nm can be attributed to Cd^{II}-His coordination [39, 40], which we have corroborated with studies in mammalian MT1 mutants [41] and chicken MT [42]. And third, a differential His participation in Cd^{II} binding would be consistent with the

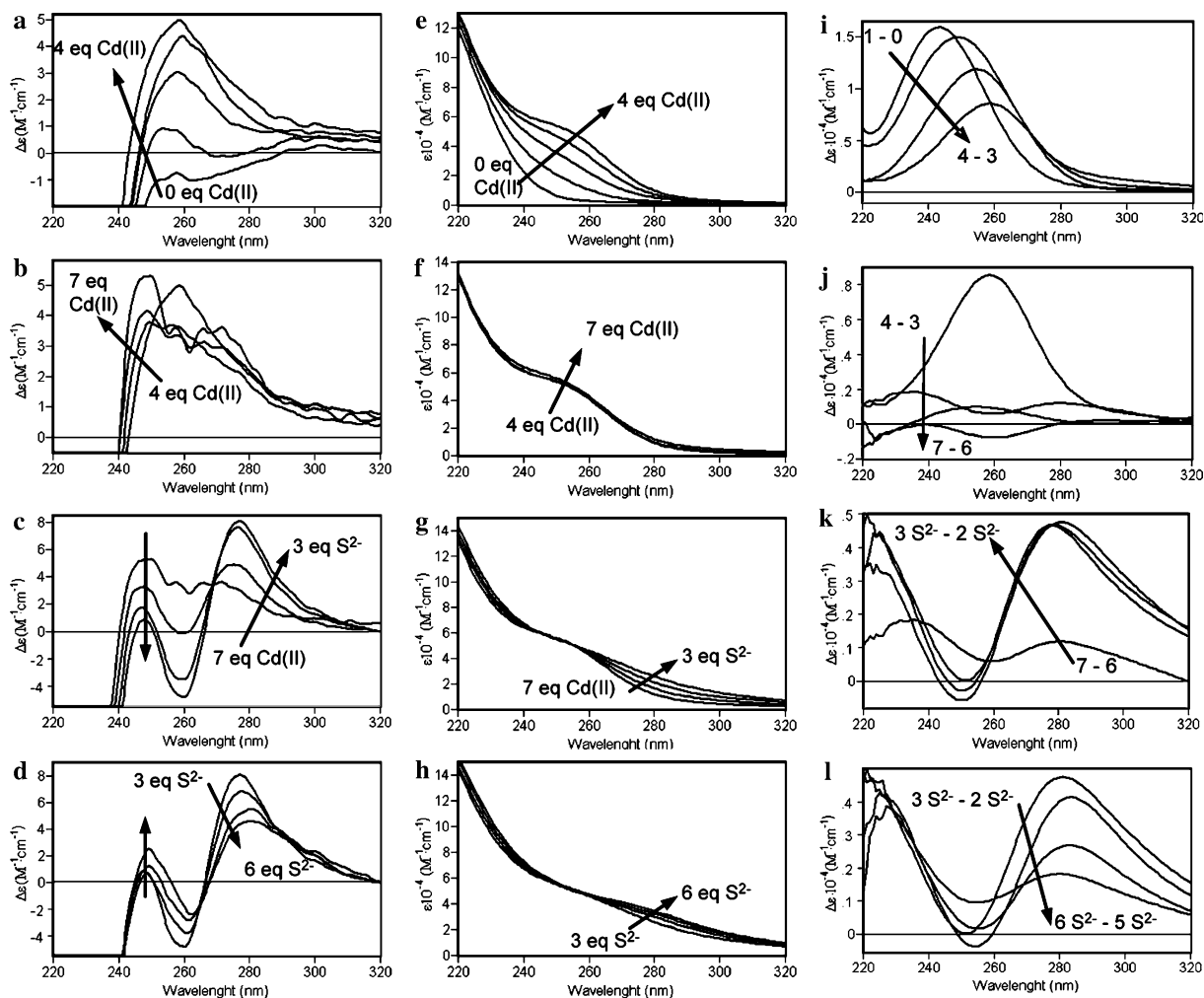


Fig. 2 CD (a–d), UV–vis (e–h) and UV–vis difference (i–l) spectra corresponding to the titration of a 20 μ M solution of Zn-rQsMT with Cd(II) at pH 7.0 followed by the addition of several equivalents of

Na₂S. Arrows show the evolution of the spectra when the indicated number of Cd(II) or S²⁻ equivalents were added

initially different CD spectra of the three types of Cd^{II}-rQsMT converging to an identical CD fingerprint at pH 4.5, after His protonation. Finally, the EDTA-induced Cd^{II} displacement from the rQsMT complexes could cause conformational rearrangements allowing His participation in Cd^{II} coordination. This hypothesis is highly consistent with the fact that the lower the Cd^{II} content, the higher the chirality at approximately 250 nm [cf. rQsMT(3), Table 2, Fig. 1a].

Thus, all our data are in concordance with rQsMT(3) being mainly composed of S²⁻-devoid Cd₅ complexes where His may participate in cadmium coordination; rQsMT(1) containing S²⁻-rich Cd₆ and Cd₇ complexes with no His participation; and rQsMT(2) being a mixture of rQsMT(1) and rQsMT(3). Therefore, when Cd^{II}-rQsMT is synthesized in *E. coli*, and depending on the folding that the protein adopts when binding the Cd^{II} ions, the His

residue of the spacer may or may not participate in Cd^{II} binding, with this determining the stoichiometry and the conformation of the final complexes.

Analysis of the Cd^{II}-binding features of N25-C18

N25-C18 synthesized in cadmium-rich medium yielded homometallic Cd^{II} complexes, among which Cd₆S₄-N25-C18 and Cd₅-N25-C18 were the most abundant species (Table 2). Thus, the Cd^{II}-N25-C18 complexes were neither isostoichiometric nor isostructural to their Zn^{II}-N25-C18 counterparts, as neither were the rQsMT species. Cd^{II}-N25-C18 showed a characteristic CD spectrum composed of two Gaussian bands centred at approximately 250 (Cd^{II} thiolate) and 280 nm (Cd^{II} sulfide) chromophores (Fig. 1b), which was clearly different from those of the diverse Cd^{II}-rQsMT types (Fig. 1).

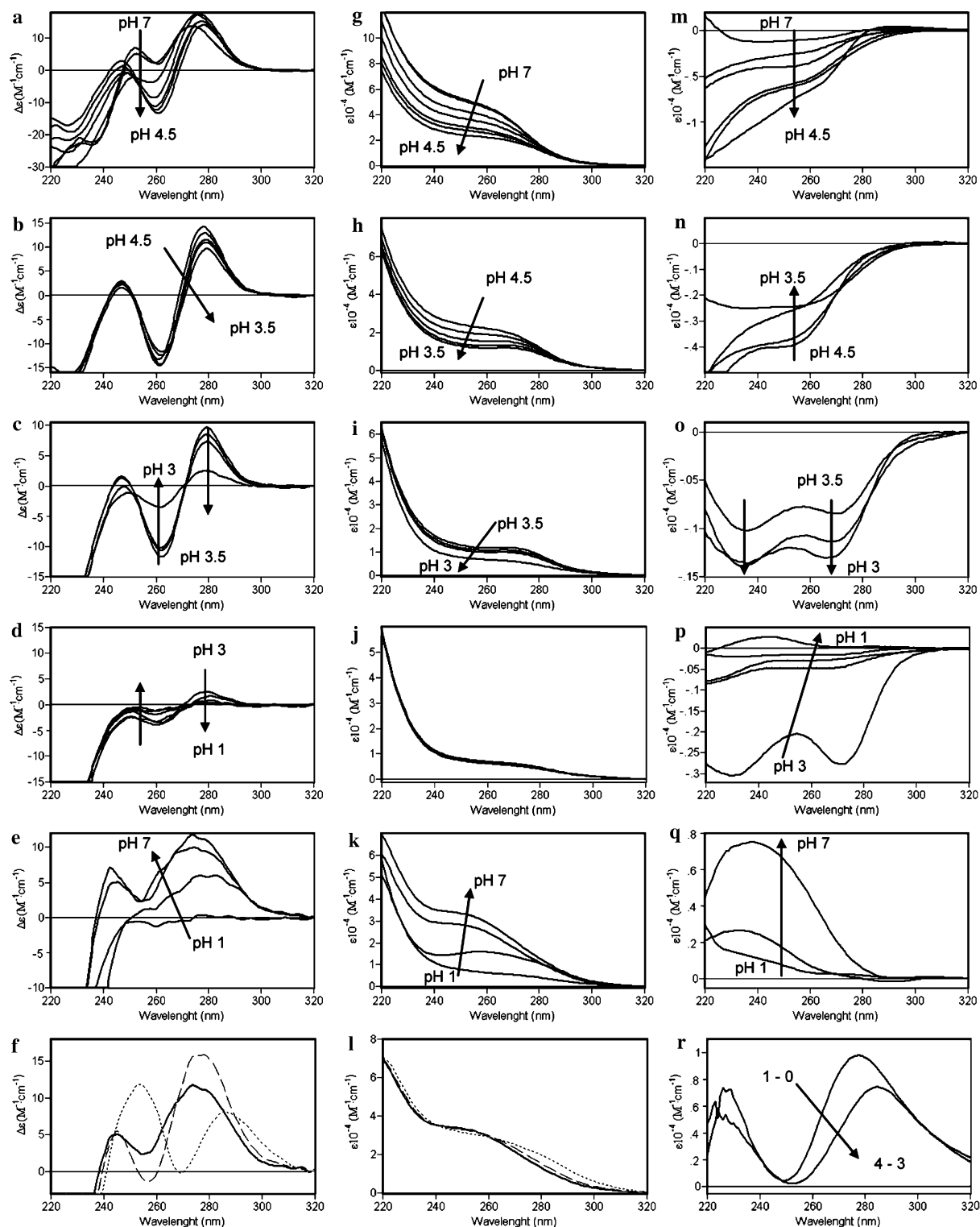


Fig. 3 CD (a–f), UV-vis (g–l) and UV-vis difference (m–r) spectra corresponding to the acidification (a–d, g–j, m–p) and reneutralization (e, k, q) of a 20 μM solution of Cd^{II} -rQsMT(3); and addition of several Na_2S equivalents (f, l, r) to the final reneutralized solution. Arrows show the evolution of the spectra during acidification and

renaturalization processes. Curves in f, l and r correspond to the reneutralized Cd^{II} -QsMT solution of e (solid line) and those recorded after addition of 1 equiv (dashed line) and 4 equiv (dotted line) S^{2-} to the former

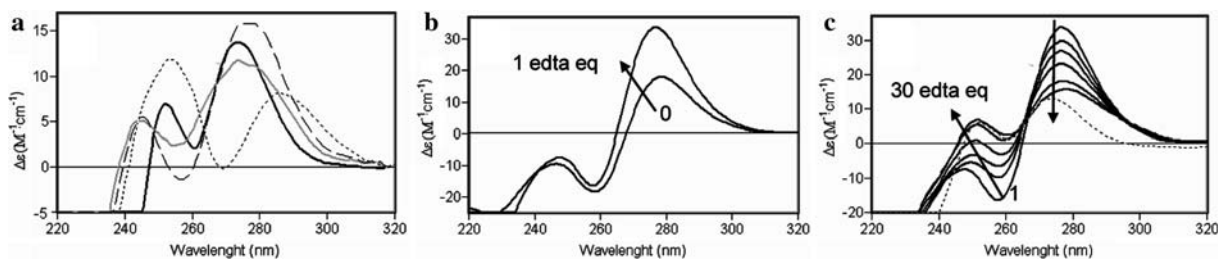


Fig. 4 **a** Comparison of the CD spectra of Cd^{II}-rQsMT(3) (solid black line), the acidified/reneutralized Cd^{II}-QsMT sample (solid grey line) and with addition of 1 equiv (dashed line) and 4 equiv (dotted line) S²⁻ to the previous sample. **b, c** CD spectra corresponding to the addition of the first EDTA equivalent and of 1, 1.5, 2, 3, 9 and

30 equiv EDTA to a 16 μM Cd^{II}-rQsMT(1) sample. The dotted line in **c** corresponds to the CD spectrum of the Cd^{II}-rQsMT(3) preparation. Arrows show the evolution of the spectra during the demetalation process

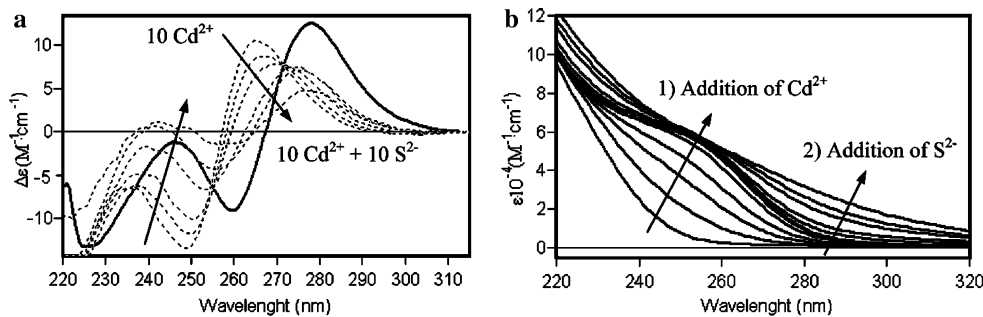


Fig. 5 **a** Comparison between the CD spectra of Cd^{II}-rQsMT(1) (solid line) and those recorded after the addition of 1, 2, 5, 7 and 10 equiv Na₂S at the end of the titration of Zn^{II}-N25-C18 with Cd(II), i.e. after 10 equiv Cd^{II}. **b** UV-vis spectra recorded during the addition of 1–10 equiv Cd^{II} to Zn₄-N25-C18, leading to the formation of Cd₅-

N25-C18, followed by the addition of 1, 2, 5, 7 and 10 equiv Na₂S. The difference in CD intensities between Cd^{II}-rQsMT(1) and the final Cd^{II}-N25-C18 sample and the deviations of the baseline of the UV-vis spectra are due to the turbulence of the final stages of Na₂S additions, caused by precipitation of the excess Cd^{II} as CdS

Titration of Zn₄-N25-C18 with Cd^{II} (full data in Fig. S2, Table S2) rendered Cd₅-N25-C18 as the major species even for an excess of Cd^{II} and resulted in a different CD spectrum from that of the in vivo sample. Surprisingly, although blueshifted it resembled that of Cd^{II}-rQsMT(1) (Fig. 5a). Addition of Na₂S after the final titration step further increased this resemblance, with a clear indication of S²⁻–Cd^{II} coordination (Fig. 5). These results are fully consistent with the previous hypothesis about the Cd^{II}-coordinating behaviour of His in rQsMT. Hence, N25-C18 that is devoid of this residue can reproduce the features of Cd^{II}-rQsMT(1), where we presume no Cd^{II}–His contributions, and never those of rQsMT(3).

It is especially worth noting that titration of Zn^{II}-N25-C18 with Cd^{II} and S²⁻ yielded complexes more similar to Cd^{II}-rQsMT than to Cd^{II}-N25-C18. However, a process of acidification/reneutralization/S²⁻ addition of the biosynthesized Cd^{II}-N25-C18 ended up with a CD fingerprint very similar to the initial one (Fig. S3). The interpretation of the spectroscopic data of these reactions was more straightforward than for Cd^{II}-rQsMT owing to the absence of His and Phe in the N25-C18 polypeptide. Thus, it could

be deduced that acidification of Cd₆S₄-N25-C18 from pH 7 to 4.5 promoted an important structural rearrangement. The 250-nm Gaussian band became a derivative-shaped band at the same wavelength, so some Cd^{II} thiolate chromophores could be lost, while S²⁻ would remain bound to the Cd^{II} ions. We cannot discard the migration of some thiolate-bound Cd^{II} to S²⁻-rich environments, as suggested by the UV-vis difference spectra in Fig. S3c. It was not until pH between 4 and 2 that CD absorptions at approximately 280 nm—together with those remaining at approximately 250 nm—disappeared, to generate a characteristic apo-MT spectrum. At this point, a strong H₂S odour was perceptible and the Cd^{II} ions released to the solution visibly precipitated as CdS. In spite of the turbidity of the sample, it was reneutralized to pH 7. Reincorporation of the Cd^{II} ions to N25-C18 gave rise to an intense and very wide CD signal centred at approximately 260 nm and that was very different from that of the initial in vivo Cd^{II}-N25-C18 (Fig. 6a), as expected from the loss of most of the S²⁻ ligands. This new CD fingerprint could be interpreted as being composed of one absorption centred at about 250 nm—attributable to Cd^{II}(SCys)₄—and other absorp-

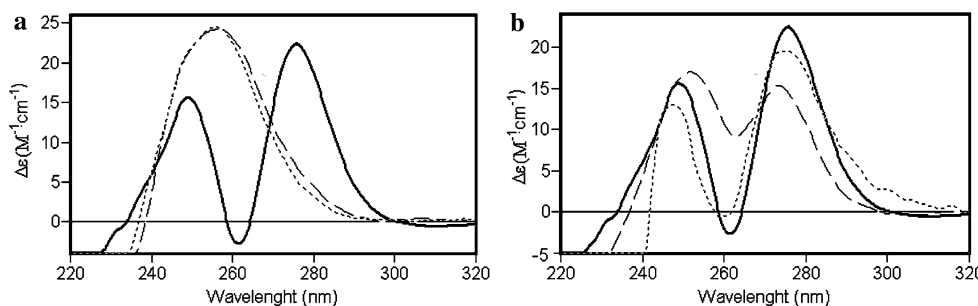


Fig. 6 **a** Comparison between the normalized CD spectra of recombinant Cd^{II}-N25-C18 (solid line), Zn^{II}-N25-C18 after the addition of 3 equiv Cd^{II} (dotted line) and the reneutralized Cd^{II}-N25-C18 sample (dashed line). **b** Comparison between the CD

spectra of recombinant Cd^{II}-N25-C18 (solid line), the reneutralized Cd^{II}-N25-C18 sample after the addition of 4 equiv S²⁻ (dashed line) and the reneutralized Cd^{II}-QsMT sample after the addition of 1 equiv S²⁻ (dotted line)

tions in the 270–320-nm range—due to Cd^{II}-S²⁻ if it is assumed that some CdS particles became trapped by some Cys residues. Although this may appear speculative, it is consistent with the observations that (1) the envelope of the CD spectrum of the reneutralized sample perfectly matched that recorded for the addition of 3 equiv Cd^{II} to Zn₄-N25-C18 (Fig. 6a), a preparation that contained one S²⁻ per MT (Table 1), and (2) that the tail of the CD absorptions extending until 300 nm could only be attributed to Cd^{II}-S²⁻ chromophores. Subsequent Na₂S addition to the reneutralized sample caused dramatic changes in the CD spectra already from the first step (Fig. 6b) to practically reproduce, for 3–4 equiv S²⁻ added, the spectrum of the initial in vivo Cd^{II}-N25-C18. This final CD profile was not too different from that achieved by Cd^{II}-rQsMT(1) after a similar acidification/reneutralization/S²⁻ addition process (Fig. 6b), which indicates that both polypeptides can, depending on the conditions, show similar Cd^{II}-binding behaviour when His does not contribute to Cd^{II} coordination.

Analysis of the Cd^{II}-binding features of the separate N25 and C18 peptides

The syntheses of the separate N25 and C18 peptides in cadmium-rich media yielded dimeric Cd^{II} homometallic complexes (Table 2). Cd₇S₄-(N25)₂ and Cd₆-(N25)₂ were the main species of a Cd^{II}-N25 preparation exhibiting high sulfide content (2.8 S²⁻ per peptide). Conversely, Cd^{II}-C18 was mainly composed of major Cd₄-(C18)₂ and minor Cd₅-(C18)₂ complexes (Fig. 7), in concordance with the very low S²⁻ content detected by GC-FPD (0.5 S²⁻ per peptide). The CD spectra of these samples (Fig. 1b) also reflected their differential S²⁻ content, since Cd^{II}-N25, unlike Cd^{II}-C18, gave rise to CD absorptions at approximately 280 nm.

The in vitro Zn^{II}/Cd^{II} replacement followed by S²⁻ addition, and the acidification/reneutralization/S²⁻ addition studies were also undertaken for the separate N25 and C18

peptides (results summarized in Fig. 8, and full data included in Figs. S4–S7, Tables S3, S4). In vivo Cd^{II}-N25 aggregates could not be reproduced in vitro by any of the methods assayed. Starting from major monomeric Zn₂-N25 species with a very low S²⁻ content, the dimeric Cd₇S₄-(N25)₂ complexes could hardly be obtained, considering that species with a maximum of three Cd^{II} ions were obtained at the end of the titration. Remarkably, acidification and reneutralization of in vivo Cd₇S₄-(N25)₂ did not lead to the original complexes. However, the addition of Na₂S either at the end of the Cd^{II} titration or after reneutralization gave rise to CD envelopes that practically coincided with that obtained for the acidification at pH 4 of in vivo Cd^{II}-N25 (Fig. 8a). This suggests that N25 is unable to achieve in vitro the same folding as in in vivo conditions, which basically implies dimerization and participation of S²⁻ ligands.

In a completely different scenario, the monomeric Zn₂-C18 complexes, where S²⁻ was not detected by GC-FPD, easily rendered, after addition of 2 equiv Cd^{II}, Cd₄-(C18)₂ dimers that exactly reproduced the CD fingerprint of the in vivo Cd^{II}-C18 preparation (Fig. 8b). As acidification and reneutralization of the in vivo Cd^{II}-C18 sample required just a small amount of Na₂S to regenerate the initial CD envelope, it is sensible to assume the presence of minute amounts of S²⁻ in Zn^{II}-C18, enough to yield in vitro the S²⁻-containing Cd^{II}-C18 complexes.

Finally, the Cd^{II} titration of an equimolar mixture of Zn^{II}-N25 and Cd^{II}-C18, hereafter referred to as cotitration, was performed to analyse possible interactions between the separate N25 and C18 peptides (Fig. 9, Table S5). The CD spectrum of the initial mixture perfectly matched the sum of the spectra of both separated Zn^{II} complexes (Fig. 10a), which suggests that they do not interact in solution. As this CD fingerprint was clearly different from that of Zn^{II}-N25-C18, a dumbbell fold for this chimeric Zn^{II} peptide could already be ruled out. The Zn^{II}-N25 plus Zn^{II}-C18 mixture (Fig. 9) saturated for 7 equiv Cd(II) added, yielding a CD

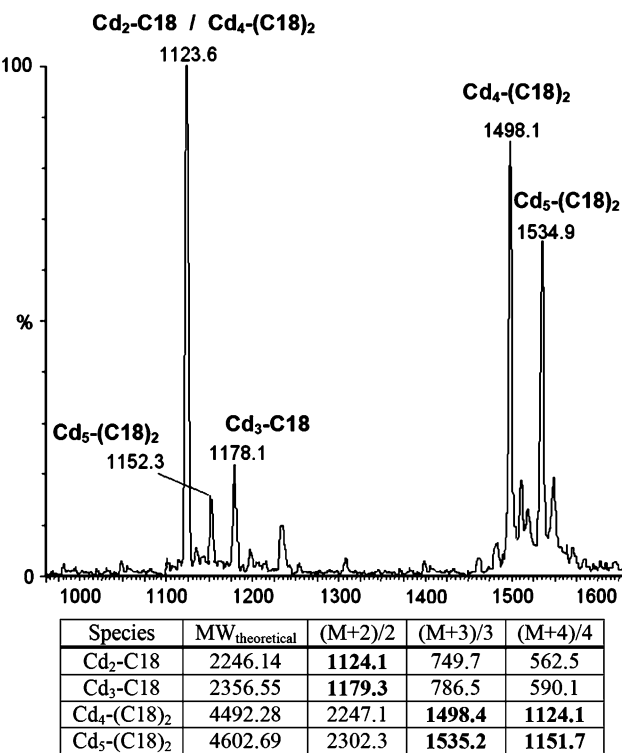


Fig. 7 Electrospray ionization (ESI) mass spectrometry (MS) spectrum of the recombinant Cd^{II}-C18 preparation with indication of the theoretical molecular weights of the Cd^{II}-C18 species and the MS peaks expected for each charge state. The assessment of the presence of C18 dimers was made on the basis of a deconvolution method [32] allowing us to identify two types of ESI-MS peaks corresponding to dimeric forms: (1) peaks that match the *m/z* charge states of a (Cd_{*n*}-MT)₂ form (*n* being an odd value); (2) peaks that only match the molecular weight of two peptide chains binding an odd number of Cd^{II} ions. Furthermore, some peaks could be either interpreted as corresponding to a monomer of *m/z* or to a dimer of 2*m/z* ratio

fingerprint (Fig. 10b) practically coincident with the sum of the final spectra of the separate Cd^{II} titrations of Zn^{II}-N25 and Zn^{II}-C18. In these reactions, major Cd₃-N25 and Cd₄-(C18)₂ complexes were respectively formed; the same

species that were detected as major products of the cotitration (ESI-MS analysis in Table S5). Thus, both separate peptides behaved equally when titrated alone or in each other's presence: N25 evolving from monomeric Zn₂ to monomeric Cd₃ species, and C18 from monomeric Zn₂ to dimeric Cd₄ complexes. The difference between the final CD fingerprint of the cotitration and those of the *in vivo* Cd^{II}-N25-C18 (Fig. 10b) or those reached at the end of the Zn^{II}-N25-C18 titration with Cd^{II} (Fig. S2) implies a dependent behaviour of both regions in the N25-C18 polypeptide when coordinating Cd^{II}. It is worth noting that heterodimers (N25/C18) were also detected at the end of the cotitration, although as minor species (Table S5), which is highly significant in order to support a hairpin model for Cd^{II}-N25-C18 (discussed later). The small amount of heterodimers is consistent with the low peptide concentration at which the cotitration was performed to allow monitoring by CD, and with the fact that N25 seems not to require interaction with other peptides (same N25 or C18) to form Cd^{II} complexes in solution.

QsMT cadmium detoxification capacity in yeast

To test whether the QsMT-derived peptides provided protection against cadmium toxicity, and to what extent, N25, C18 or N25-C18 were expressed in *CUP1*-deficient yeast cells (*cup1*^Δ). Cells transformed with the nonrecombinant plasmid or cells synthesizing the full-length QsMT were used as negative and positive controls, respectively. In the absence of supplemented cadmium, all the strains yielded colonies of similar size (Fig. 11a), this showing that the presence of the QsMT peptides had no inherent effect on growth. Phenotype recovery was then evaluated in terms of capacity for growing in the presence of cadmium. Control p424 *cup1*^Δ cells were sensitive to Cd^{II} concentrations as low as 1.5 μM, whereas the same cells synthesizing QsMT were able to grow at a similar rate as *cup1*^S at 1.5 μM Cd^{II},

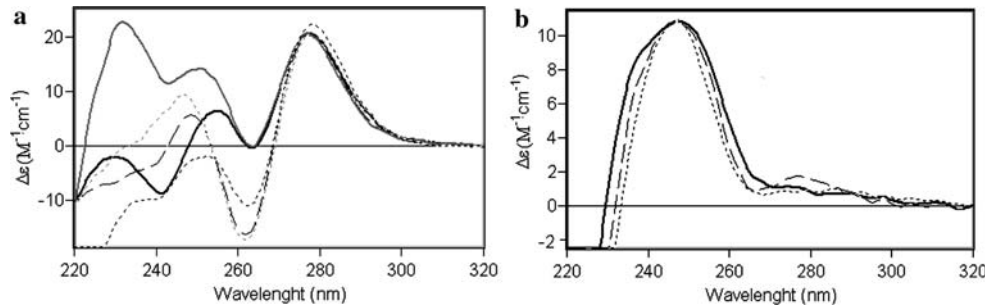


Fig. 8 **a** Comparison between the normalized CD spectra of recombinant Cd^{II}-N25 (solid black line), Zn^{II}-N25 after the addition of 9 equiv Cd^{II} (solid grey line), Zn^{II}-N25 after the addition of 10 equiv Cd^{II} and 4 equiv S²⁻ (dotted grey line), the Cd^{II}-N25 sample acidified to pH 4 (dashed black line) and the reneutralized Cd^{II}-N25

sample after the addition of 1 equiv S²⁻ (dotted black line). **b** Comparison between the CD spectra of recombinant Cd^{II}-C18 (solid black line), the reneutralized Cd^{II}-C18 sample after the addition of 2 equiv S²⁻ (dashed line) and the Zn^{II}-C18 sample after the addition of 2 equiv Cd^{II} (dotted line)

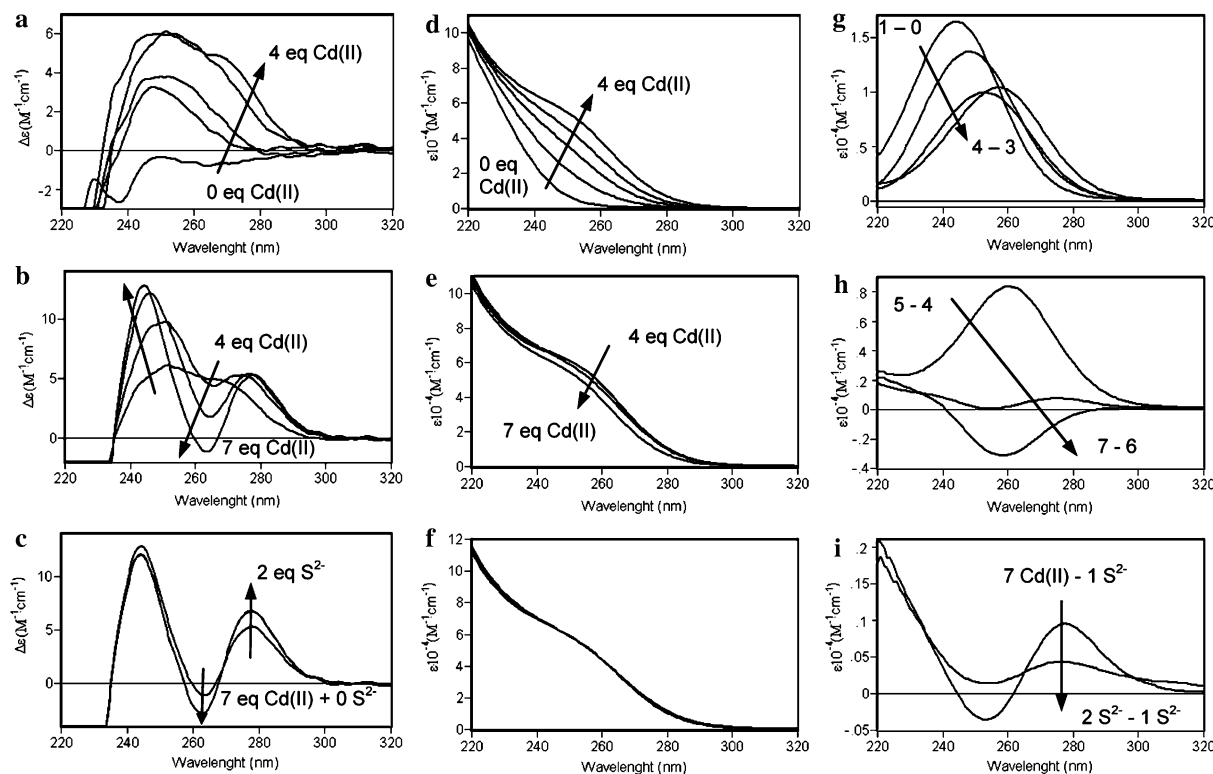


Fig. 9 CD (a–c), UV–vis (d–f) and UV–vis difference (g–i) spectra corresponding to the titration of a solution of 20 μ M Zn^{II}-N25 and 20 μ M Zn^{II}-C18 with Cd^{II} at pH 7.0 followed by the addition of 1 and

2 equiv Na₂S. Arrows show the evolution of the spectra when the indicated number of Cd^{II} or S²⁻ equivalents were added

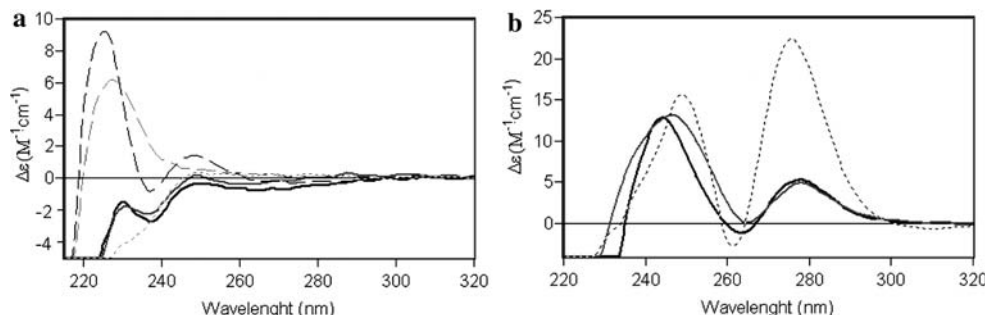


Fig. 10 **a** Comparison between the CD spectra of the mixture of equimolar amounts of Zn^{II}-N25 and Zn^{II}-C18 (solid black line) with the sum of the CD spectra of Zn^{II}-N25 and Zn^{II}-C18 (solid grey line). The CD spectra of Zn^{II}-N25 (dotted line), Zn^{II}-C18 (dashed grey line) and Zn^{II}-N25-C18 (dashed black line) are also included. **b** Comparison between the CD spectra of the mixture obtained in the

cotitration of Zn^{II}-N25 and Zn^{II}-C18 after the addition of 7 equiv Cd^{II} (solid black line) and the sum of the final CD spectra of the separate titrations of Zn^{II}-N25 and Zn^{II}-C18 with Cd^{II} (solid grey line). The CD spectrum of recombinant Cd^{II}-N25-C18 (dotted line) is also included

which is definitely better than the parental strain at 2.5 and 3.5 μ M Cd^{II} (Fig. 11b). This is highly consistent with the copper thionein character of the endogenous yeast MT, since we have shown that the single copy of *CUP1* present in the *cup1^S* strain is able to exhibit fairly normal growth under copper stress [32]. Cells synthesizing the QsMT-derived peptides exhibited a markedly reduced growth rate in relation to cells synthesizing QsMT. The higher the Cd^{II}

concentration, the greater the disparity in growth rate between the pQsMT-transformed strain and the other three strains. This result is especially significant for N25-C18, which has the same number of Cys as QsMT and which yields aggregates of equivalent Cd^{II} and S²⁻ content (Table 2), with the only difference being the lack of the spacer region. This finding fully corroborates the same behaviour we previously reported for copper stress [32]. The obser-

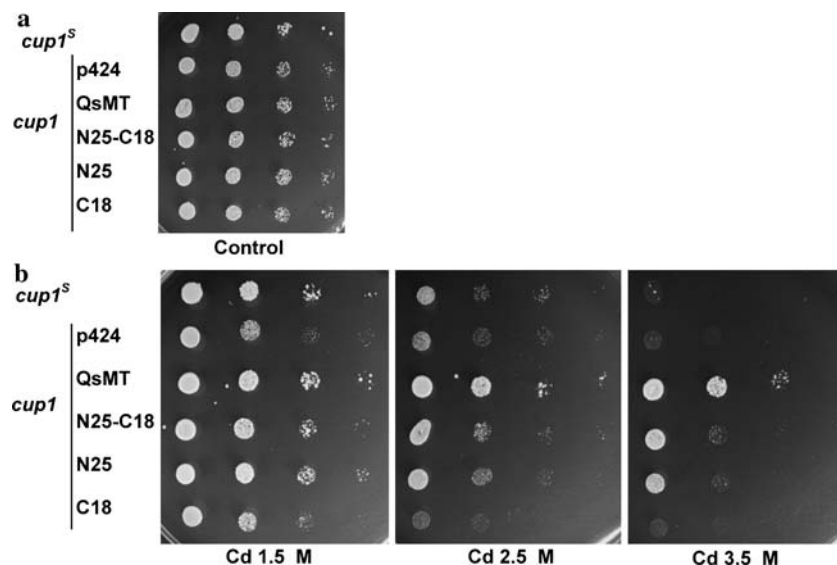


Fig. 11 Yeast functional complementation assays. The *cup1^S* strain presents only one copy of the *CUP1* gene, coding for an MT, while the *cup1^A* strain includes no copy of this gene. *cup1^A* cells have been transformed with the plasmid p424 without insertion, or with the constructions p424-QsMT, p424-N25-C18, p424-N25 or p424-C18. For the metal tolerance tests, transformed *cup1^A* cells were initially grown in selective SC-Trp-Ura medium and *cup1^S* strain in SC medium, both at 30 °C and 220 rpm to an optical density at 600 nm of 0.5–0.7. Cultures were then tenfold serially diluted three times, and

3 ml of each final sample was spotted on SC medium plates, supplemented or not supplemented with cadmium. Plates were incubated for 3 days at 30 °C and photographed. **a** Control SC medium without cadmium, to assess the viability of all the transformants. **b** The same medium supplemented with 1.5, 2.5 or 3.5 mM CdCl₂. The first column of each assay corresponds to the original culture, and each of the subsequent columns to its sequential tenfold dilution, as explained before

vation that the plant MT spacer is crucial for its in vivo metal detoxification function was already reported in [19] after comparison of the cadmium tolerance exhibited by yeast cells expressing different *Arabidopsis* MTs: MT1, an isoform naturally devoid of a spacer region, and MT2, an isoform with the typical plant MT sequence. The differences were then attributed either to the presence of the central domain or to the different arrangement of the Cys residues between both *Arabidopsis* MTs, but this second possibility can be now fully ruled out.

Conclusion

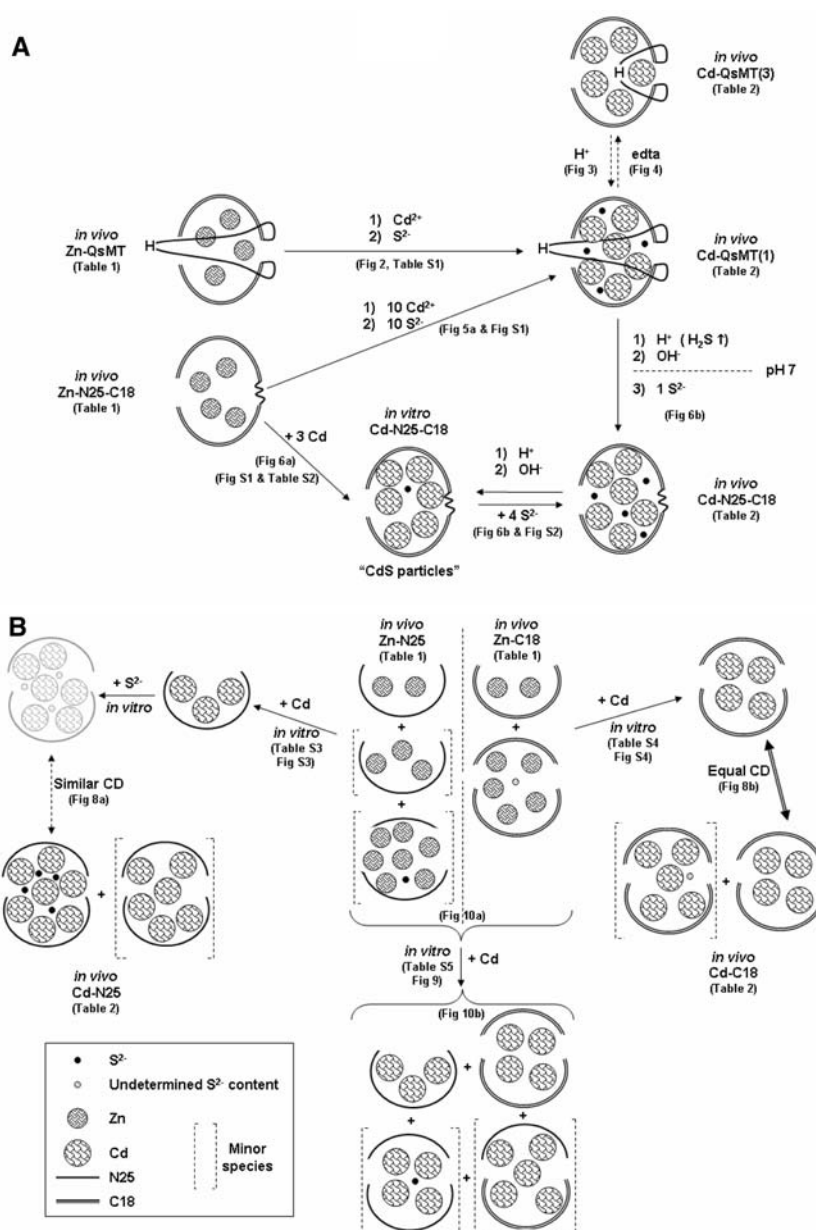
A comprehensive evaluation of all the data gathered provides a first approach to the structure/function relationship in a typical type 2 plant MT (QsMT) when coordinating Cd^{II}, which completes our previous studies of the Zn^{II}- and Cu^I-binding abilities of this same MT [30, 32]. For the sake of clarity, a synopsis of the stoichiometric and spectroscopic results is included (Scheme 2) with indication of the precise figure and/or table where they are shown.

All our current results are in full concordance with our previous assumption of rQsMT folding into a hairpin structure upon Zn^{II} coordination, enclosing four Zn^{II} ions and a low number of S²⁻ ligands, with no hint of partici-

pation of either the spacer region or, consequently, its His residue [32]. A hairpin model can now be also proposed for the in vivo folded Cd^{II}-rQsMT complexes. The ready dissimilarity between the rQsMT Cd^{II}-binding capacity and that deduced from the addition of those of N25 and C18 clearly rules out domain independence, thus discarding a dumbbell-like fold. Furthermore, the major species in the Cd^{II}-N25 and Cd^{II}-C18 preparations were dimeric Cd^{II} complexes, which further supports a hairpin model for Cd^{II}-rQsMT, as a dumbbell fold would rely on the ability of each Cys-rich region to fold into a monomeric metal complex. Consistently with the stoichiometric data, the CD analyses clearly reveal that the sum of Cd^{II}-N25 and Cd^{II}-C18 spectra is far from reproducing the CD fingerprint of any of the Cd^{II}-rQsMT types.

The unexpected recovery of distinct Cd^{II}-rQsMT types (Table 2) can be fully explained by assuming two alternative global conformations for the same hairpin fold. Hence, Cd^{II}-rQsMT(1) would be mainly composed of complexes containing six Cd(II) ions, with participation of four S²⁻ ligands but with no indication of the spacer His residue contribution. Conversely, Cd^{II}-rQsMT(3) would mainly consist of complexes of lower Cd^{II} content, (five Cd^{II}) and devoid of S²⁻ ligands, in which there are indications of Cd^{II}-His coordination, and therefore of the contribution of the spacer to the cluster architecture. This

Scheme 2 The proposed composition and fold of the Zn^{II} and Cd^{II} complexes of recombinant **a** QsMT and N25-C18 and **b** N25 and C18. *In vivo* indicates a complex directly purified from recombinant synthesis, and *in vitro* refers to complexes obtained by the *in vitro* reaction indicated. For the sake of clarity the sulfide anions are shown reduced. When possible, the interrelationship between species has also been shown, as well as all the figures and tables from which the results have been drawn. The symbols used are detailed in the inset to *b*. H⁺ sample acidification, OH⁻ sample reneutralization, S²⁻ sulfide addition, grey species of uncertain metal-to-protein stoichiometry, dashed arrows equivalences deduced from similar CD spectra



hypothesis is fully supported by the *in vitro* interconvertibility between both Cd^{II}-rQsMT types, inducible by slight acidification or demetalation treatments (Scheme 2a). Furthermore, it is also consistent with the facts that (1) complexes with at most five Cd^{II}, analogous to those of Cd^{II}-rQsMT(3), are obtained from the low-S²⁻-containing Zn^{II}-rQsMT species by *in vitro* Zn^{II}/Cd^{II} replacement and (2) the subsequent addition of S²⁻ to the end of this titration renders species similar to those of Cd^{II}-rQsMT(1).

Following a similar reasoning to that used for rQsMT, our current data also suggest a hairpin model when N25-C18 binds Zn^{II} or Cd^{II} *in vivo*, although we rated this possibility as second best for Zn^{II}-N25-C18 in previous

studies [32]. Cd^{II}-N25-C18 shares metal and sulfide content with Cd^{II}-rQsMT, but exhibits chirooptical properties different from those of all Cd^{II}-rQsMT types, which suggests that even if the spacer does not contribute to metal coordination, its presence determines some structural features that lead to different CD fingerprints for Cd^{II}-rQsMT(1) and Cd^{II}-N25-C18. This is exactly the same situation we observed for the Zn^{II}-binding features of these two polypeptides [32]. The lack of S²⁻ anions in the Zn^{II}-N25-C18 preparations also caused the Cd^{II}-N25-C18 complexes obtained from *in vitro* replacement to clearly differ from the *in vivo* recovered species, but again the spectroscopic features of both Cd^{II}-N25-C18 samples could

be mutually reproduced after the Acidification/reneutralization/sulfide-addition processes, thus highlighting their close relationship (Scheme 2a).

Finally, the analysis of the separate N25 and C18 peptides provided further evidence for a hairpin folding model of Cd^{II}-rQsMT (Scheme 2b). C18, the smallest, six-Cys domain, yielded in vivo major monomeric complexes containing two Zn^{II}, but Cd^{II} coordination induced its dimerization both in vivo and in vitro, rendering Cd₄-(C18)₂ dimers. This tendency was already observed in Zn^{II} coordination by the presence of minor Zn₅-(C18)₂ forms, containing small amounts of S²⁻ (Table 1). Therefore, and probably owing to the cadmium ionic radius, formation of dimeric Cd^{II}-C18 complexes is favoured. The behaviour of N25 was more complex than that of C18, most likely because its greater length and higher Cys content enable it to alternate between monomers and dimers when binding Cd^{II}. In vivo, N25 basically folds into Zn₂ and Zn₃ monomers, although as for C18, the presence of minor S²⁻-containing species already evidences a dimerization tendency. But, unlike C18, N25 gives completely different results for in vivo and in vitro Cd^{II} binding. Hence, in vivo, S²⁻-containing Cd₇S₄-(N25)₂ or S²⁻-devoid Cd₆-(N25)₂ dimers were recovered. This was in major concordance with the results for rQsMT and N25-C18, the two additional Cys in the N25 dimer easily accounting for the extra Cd^{II} bound (Cd₇S₄ and Cd₆ for dimeric N25, compared with Cd₆S₄ and Cd₅ for rQsMT and N25-C18). But in vitro, the Zn^{II}-N25 monomers evolve to Cd₃-N25 monomers, with once again subsequent S²⁻ addition at the end of this titration bringing the CD features of the sample close to those of the in vivo complexes. Therefore, the overall results of N25 analysis pointed to the tendency for dimerization being directly related to the availability of S²⁻ ligands, both conditions concomitantly enhancing the metal content of the clusters. If S²⁻ is absent or scarce, the dimeric Cd^{II} complexes are always a minor species. The result of the cotitration experiment further corroborates this hypothesis, both peptides behaving independently in low-sulfide conditions. In conclusion, if the tendency of both peptides is to dimerize when binding Cd^{II} in vivo, the most likely scenario is that N25-C18 and rQsMT fold into hairpin structures, to fully accomplish this requirement.

In summary, to our knowledge, this is the first characterization of type 2 plant MT Cd^{II}-binding behaviour, including a molecular dissection of its functional regions. Other studies were carried out with undigested fusion constructs and/or with other types of plant/algae MTs [23–27, 43]. We have shown that Cd^{II}-rQsMT most probably adopts a hairpin structure that increases its metal-binding capacity with the aid of S²⁻ ligands. The S²⁻-devoid complexes always exhibit a lower Cd^{II} content and the data

suggest that in this case the His residue from the spacer region most likely contributes to Cd^{II} coordination. The major participation of S²⁻ ligands in Cd^{II}-rQsMT complexes accounts for two uncommon features among MTs: the recovery of nonisostoichiometric Zn^{II} and Cd^{II} complexes, and the tendency for dimerization of the separate Cys-rich domains to enhance Cd^{II} coordination. Globally, all these attributes recall those of the well-known plant PCs, revealing similar molecular strategies of both Cys-rich polypeptides for Cd^{II} coordination.

Acknowledgements This work was supported by the Spanish Ministerio de Ciencia y Tecnología grants BIO2006-14420-C02-01 for S.A., BIO2006-14420-C02-02 for M.C. and AGL2003-00416 for M.M. G.M. and R.O. received predoctoral fellowships from the Pla de Formació de Personal Investigador del DURSI, Generalitat de Catalunya, and the Departament de Química, Universitat Autònoma de Barcelona, respectively. We especially want to acknowledge technical support from Roger Bofill and fruitful scientific discussions with Armida Torreggiani. We also thank the Serveis Científico-Tècnics de la Universitat de Barcelona (GC-FPD, ICP-AES, ESI-MS) and the Servei d'Anàlisi Química de la Universitat Autònoma de Barcelona (CD, UV-vis) for allocating instrument time.

References

- Cobbett CS, Goldsbrough PB (2002) Annu Rev Plant Biol 53:159–182
- Grill E, Winnacker E-L, Zenk M (1985) Science 230:674–676
- Grill E, Winnacker E-L, Zenk M (1987) Proc Natl Acad Sci USA 84:439–443
- Dameron CT, Winge DR (1990) Inorg Chem 29:1343–1348
- Cobbett C, Goldsbrough P (2000) In: Raskin I, Ensley BD (eds) Phytoremediation of toxic metals: using plants to clean up the environment. Wiley, New York, pp 247–269
- Reese RN, Wagner GJ (1987) Biochem J 241:641–647
- Steffens JC, Hunt DF, Williams BG (1986) J Biol Chem 261:13879–13882
- Rauser WE (2000) J Plant Physiol 156:545–551
- Rauser WE, Curvetto NR (1980) Nature 287:563–564
- Chatthai M, Kaukinen KH, Tranbarger TJ, Gupta PK, Misra S (1997) Plant Mol Biol 34:243–254
- Morris CA, Nicolaus B, Sampson V, Harwood JL, Kille P (1999) Biochem J 338:553–560
- Binz PA, Kägi JHR (2001) Metallothionein. <http://www.bioc.uzh.ch/mtpage/MT.html>
- Robinson NJ, Tommey AM, Kuske C, Jackson PJ (1993) Biochem J 295:1–10
- Murphy A, Taiz L (1995) Plant Physiol 109:945–954
- van Hoof NA, Hassinen VH, Hakvoort HWJ, Ballintijn KF, Schat H, Verkleij JAC, Ernst WHG, Karenlampi SO, Tervahauta AI (2001) Plant Physiol 126:1519–1526
- Guo W-J, Bundithya W, Goldsbrough PB (2003) New Phytol 159:369–381
- Navabpour S, Morris K, Allen R, Harrison E, Mackerness SAH, Buchanan-Wollaston V (2003) J Exp Bot 54:2285–2292
- Ma M, Lau P-S, Jia Y-T, Tsang W-K, Lam SKS, Tam NFY, Wong Y-S (2003) Plant Sci 164:51–60
- Zhou J, Goldsbrough PB (1994) Plant Cell 6:875–884
- Lee J, Shim D, Song W-Y, Hwang I, Lee Y (2004) Plant Mol Biol 54:805–815

21. Zimeri AM, Dhankher OP, McCaig B, Meagher RB (2005) *Plant Mol Biol* 58:839–855
22. Gonzalez-Duarte P (2003) In: McCleverty J, Meyer TJ (eds) *Metallothioneins, comprehensive coordination chemistry II*, vol. 8. Elsevier, Amsterdam, pp 213–228
23. Tommey AM, Shi J, Lindsay WP, Urwin PE, Robinson NJ (1991) *FEBS Lett* 292:48–52
24. Kille P, Winge DR, Harwood JL, Kay J (1991) *FEBS Lett* 295:171–175
25. Bilecen K, Ozturk UH, Duru AD, Sutlu T, Petoukhov MV, Svergun DI, Koch MHJ, Sezerman UO, Cakmak I, Sayers Z (2005) *J Biol Chem* 280:13701–13711
26. Peroza EA, Freisinger E (2007) *J Biol Inorg Chem* (in press). doi: 10.1007/s00775-006-0195-5
27. Freisinger E (2007) *Inorg Chim Acta* 360:369–380
28. Cols N, Romero-Isart N, Capdevila M, Oliva B, González-Duarte P, González-Duarte R, Atrian S (1997) *J Inorg Biochem* 68:157–166
29. Capdevila M, Cols N, Romero-Isart N, González-Duarte R, Atrian S, González-Duarte P (1997) *Cel Mol Life Sci* 53:681–688
30. Mir G, Domènech J, Huguet G, Guo WJ, Goldsbrough PB, Atrian S, Molinas M (2004) *J Exp Bot* 55:2483–2493
31. Capdevila M, Domènech J, Pagani A, Tío L, Villarreal L, Atrian S (2005) *Angew Chem Int Ed Engl* 44:4618–4622
32. Domènech J, Mir G, Huguet G, Capdevila M, Molinas M, Atrian S (2006) *Biochimie* 88:583–593
33. Bongers J, Walton CD, Richardson DE, Bell JU (1988) *Anal Chem* 60:2683–2686
34. Reese RN, Winge DR (1988) *J Biol Chem* 262:12832–12835
35. Gan T, Muñoz A, Shaw III CF, Petering DH (1995) *J Biol Chem* 270:5339–5345
36. Longo VD, Gralla EB, Valentine JS (1996) *J Biol Chem* 271:12275–12280
37. Mumberg D, Müller R, Funk M (1995) *Gene* 156:119–122
38. Domènech J, Tinti A, Capdevila M, Atrian S, Torreggiani A (2007) *Biopolymers* (in press). doi 10.1002/bip.20729
39. Maret W, Vallee BL (1993) *Methods Enzymol* 226:52–71
40. Lever ABP (1986) *Inorganic electronic spectroscopy*, 2nd edn. Elsevier, Amsterdam
41. Romero-Isart N, Cols N, Termansen MK, Gelpí JL, González-Duarte R, Atrian S, Capdevila M, González-Duarte P (1999) *Eur J Biochem* 259:519–527
42. Villarreal L, Tío L, Capdevila M, Atrian S (2006) *FEBS J* 273:523–535
43. Merrifield ME, Chaseley J, Kille P, Stillman MJ (2006) *Chem Res Toxicol* 19:365–375

The Cd^{II}-binding abilities of recombinant *Quercus suber* metallothionein, QsMT: bridging the gap between phytochelatins and metallothioneins

J. Domènec, R. Orihuela, G. Mir, M. Molinas, S. Atrian, M. Capdevila

SUPPLEMENTARY MATERIAL

Tables

Table S1 Distribution of the metal complexes present in solution, according to ESI-MS data, during the titration of Zn^{II}-rQsMT with CdCl₂ at pH 7 as a function of the number of Cd^{II} or S²⁻ eq added.

Table S2 Distribution of the metal complexes present in solution, according to ESI-MS data, during the titration of Zn^{II}-N25-C18 with CdCl₂ at pH 7 as a function of the number of Cd^{II} eq added.

Table S3 Distribution of the metal complexes present in solution, according to ESI-MS data, during the titration of Zn^{II}-N25 with CdCl₂ at pH 7 as a function of the number of Cd^{II} eq added.

Table S4 Distribution of the metal complexes present in solution, according to ESI-MS data, during the titration of Zn^{II}-C18 with CdCl₂ at pH 7 as a function of the number of Cd^{II} eq added.

Table S5 Distribution of the metal complexes present in solution, according to ESI-MS data, during the co-titration of Zn^{II}-C18 and Zn^{II}-N25 with CdCl₂ at pH 7 as a function of the number of Cd^{II} eq added.

Figures

Fig. S1 CD spectra corresponding to the acidification of a 20 μM solution of Cd^{II}-rQsMT(1) from pH 7.0 to pH 1.0.

Fig. S2 CD (A), UV-vis (B) and UV-vis difference (C) spectra corresponding to the titration of a 20 μM solution of Zn^{II}-N25-C18 with Cd^{II} at pH 7.0 followed by the addition of several Na₂S eq.

Fig. S3 CD (A), UV-vis (B) and UV-vis difference (C) spectra corresponding to the acidification (first two rows), reneutralization (third row) and addition of several Na₂S eq (fourth row) of a 20 μM solution of Cd^{II}-N25-C18.

Fig. S4 CD (A), UV-vis (B) and UV-vis difference (C) spectra corresponding to the titration of a 20 μM solution of Zn^{II}-N25 with Cd^{II} at pH 7.0 followed by the addition of several Na₂S eq.

Fig. S5 CD (A), UV-vis (B) and UV-vis difference (C) spectra corresponding to the titration of a 20 μM solution of Zn^{II}-C18 with Cd^{II} at pH 7.0 followed by the addition of several Na₂S eq.

Fig. S6 CD (A), UV-vis (B) and UV-vis difference (C) spectra corresponding to the acidification (first two rows), reneutralization (third and fourth row) and addition of several Na₂S eq (fifth row) of a 20 μM solution of Cd^{II}-N25.

Fig. S7 CD (A), UV-vis (B) and UV-vis difference (C) spectra corresponding to the acidification (first three rows), reneutralization (fourth row) and addition of several Na₂S eq (fifth row) of a 20 μM solution of Cd^{II}-C18.

	Cd ^{II} and/or S ²⁻ eq added to Zn ^{II} -rQsMT			
	4 Cd ^{II}	7 Cd ^{II}	7 Cd ^{II} + 3 S ²⁻ *	7 Cd ^{II} + 4 S ²⁻ *
Zn ₁ Cd ₃ -QsMT	♦	♦		
Zn ₁ Cd ₄ -QsMT	♦	♦		
Zn ₁ Cd ₅ -QsMT	♦			
Cd ₃ -QsMT	♦	♦		
Cd ₃ S ₂ -QsMT	♦			
Cd ₄ -QsMT	✓	✓	✓	
Cd ₅ -QsMT	✓	x	x	
Cd ₆ -QsMT	x	♦		
Cd ₆ S ₆ -QsMT				x
Cd ₇ S ₃ -QsMT			x	
Cd ₇ S ₉ -QsMT				✓

Table S1 Distribution of the metal complexes present in solution, according to ESI-MS data, during the titration of Zn^{II}-rQsMT with CdCl₂ at pH 7 as a function of the number of Cd^{II} or S²⁻ eq added.

(Code: ✓ denotes the major species; x species of intermediate abundance and ♦, the minor species)

* The high signal-to-noise ratio due to the numerous Na-adducts formed hampers a more detailed interpretation of the MS data.

	Cd ^{II} eq added to Zn ^{II} -N25-C18		
	5 Cd ^{II}	6 Cd ^{II}	10 Cd ^{II}
Cd ₅ -N25-C18	✓	✓	✓
Cd ₄ -N25-C18	x	x	x
Cd ₆ -N25-C18	♦	x	x
Cd ₅ S ₁ -N25-C18	x		

Table S2 Distribution of the metal complexes present in solution, according to ESI-MS data, during the titration of Zn^{II}-N25-C18 with CdCl₂ at pH 7 as a function of the number of Cd^{II} eq added.

(Code: ✓ denotes the major species; x species of intermediate abundance and ♦, the minor species)

Note: ESI-MS data corresponding to the addition of sulfide anions are not included due to the difficulties encountered when interpreting the spectra because of the Na-adducts detected.

	Cd ^{II} eq added to Zn ^{II} -N25			
	2 Cd ^{II}	4 Cd ^{II}	8 Cd ^{II}	10 Cd ^{II}
Zn ₁ Cd ₂ -N25	x			
Zn ₁ Cd ₃ -N25	♦	♦		
Cd ₂ -N25	♦	✓	♦	♦
Cd ₃ -N25	✓	✓	✓	✓
Cd ₃ S ₂ -N25			♦	x
Cd ₄ -N25				♦

Table S3 Distribution of the metal complexes present in solution, according to ESI-MS data, during the titration of Zn^{II}-N25 with CdCl₂ at pH 7 as a function of the number of Cd^{II} eq added.

(Code: ✓ denotes the major species; x species of intermediate abundance and ♦, the minor species)

Note: ESI-MS data corresponding to the addition of sulfide anions are not included due to the difficulties encountered when interpreting the spectra because of the Na-adducts detected.

	Cd ^{II} eq added to Zn ^{II} -C18		
	1 Cd ^{II}	2 Cd ^{II}	3 Cd ^{II}
Zn ₂ Cd ₂ -(C18) ₂ / Zn ₁ Cd ₁ -C18	✓	x	
Cd ₄ -(C18) ₂ / Cd ₂ -C18	x	✓	✓
Cd ₂ -(C18) ₂	x		
Zn ₁ Cd ₂ -(C18) ₂		♦	
Cd ₄ S ₁ -(C18) ₂			♦
Cd ₃ Zn ₃ -(C18) ₂			x

Table S4 Distribution of the metal complexes present in solution, according to ESI-MS data, during the titration of Zn^{II}-C18 with CdCl₂ at pH 7 as a function of the number of Cd^{II} eq added.

(Code: ✓ denotes the major species; x species of intermediate abundance and ♦, the minor species)

Note: ESI-MS data corresponding to the addition of sulfide anions are not included due to the difficulties encountered when interpreting the spectra because of the Na-adducts detected.

	Cd ^{II} eq added to Zn ^{II} -N25 + Zn ^{II} -C18		
	2 Cd ^{II}	4 Cd ^{II}	6 Cd ^{II}
Zn ₁ Cd ₁ -C18 / Zn ₂ Cd ₂ -(C18) ₂	✓	x	
Cd ₁ -C18 / Cd ₂ -(C18) ₂	x	✓	
Cd ₄ -(C18) ₂	♦	x	✓
Cd ₂ -C18			
Zn ₂ Cd ₅ -(N25) ₂ / Cd ₅ S ₁ -(N25) ₂	✓	✓	
Cd ₃ -(N25)		✓	✓
Cd ₄ S ₁ -(N25) ₂	x		
Cd ₅ -(N25-C18)			♦

Table S5 Distribution of the metal complexes present in solution, according to ESI-MS data, during the co-titration of Zn^{II}-C18 and Zn^{II}-N25 with CdCl₂ at pH 7 as a function of the number of Cd^{II} eq added.

(Code: ✓ denotes the major species; x species of intermediate abundance and ♦, the minor species)

Note: ESI-MS data corresponding to the addition of sulfide anions are not included due to the difficulties encountered when interpreting the spectra because of the Na-adducts detected.

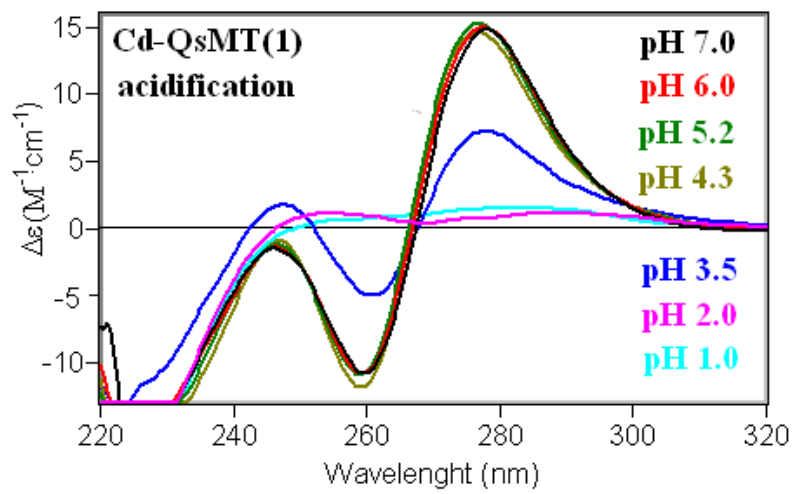


Fig. S1 CD spectra corresponding to the acidification of a 20 μM solution of Cd^{II}-rQsMT(1) from pH 7.0 to pH 1.0.

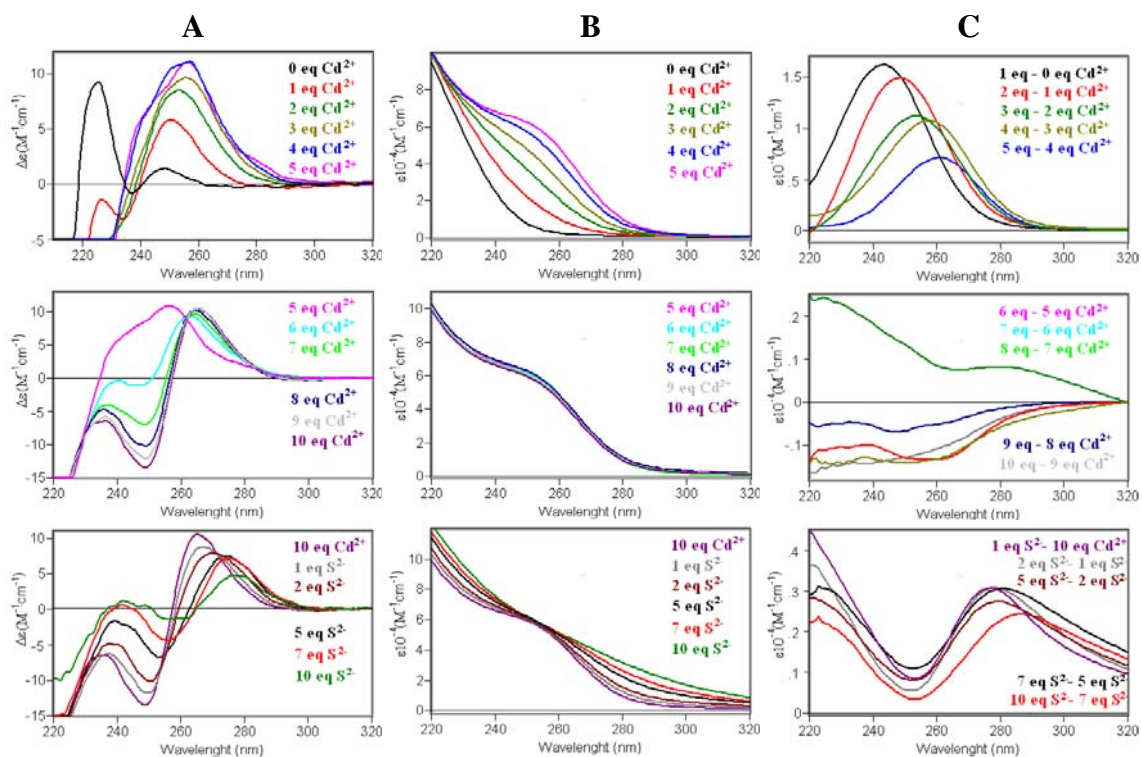


Fig. S2 CD (A), UV-vis (B) and UV-vis difference (C) spectra corresponding to the titration of a 20 μM solution of Zn^{II}-N25-C18 with Cd^{II} at pH 7.0 followed by the addition of several Na₂S eq. The Cd^{II} or S²⁻ to MT molar ratio are indicated within each frame.

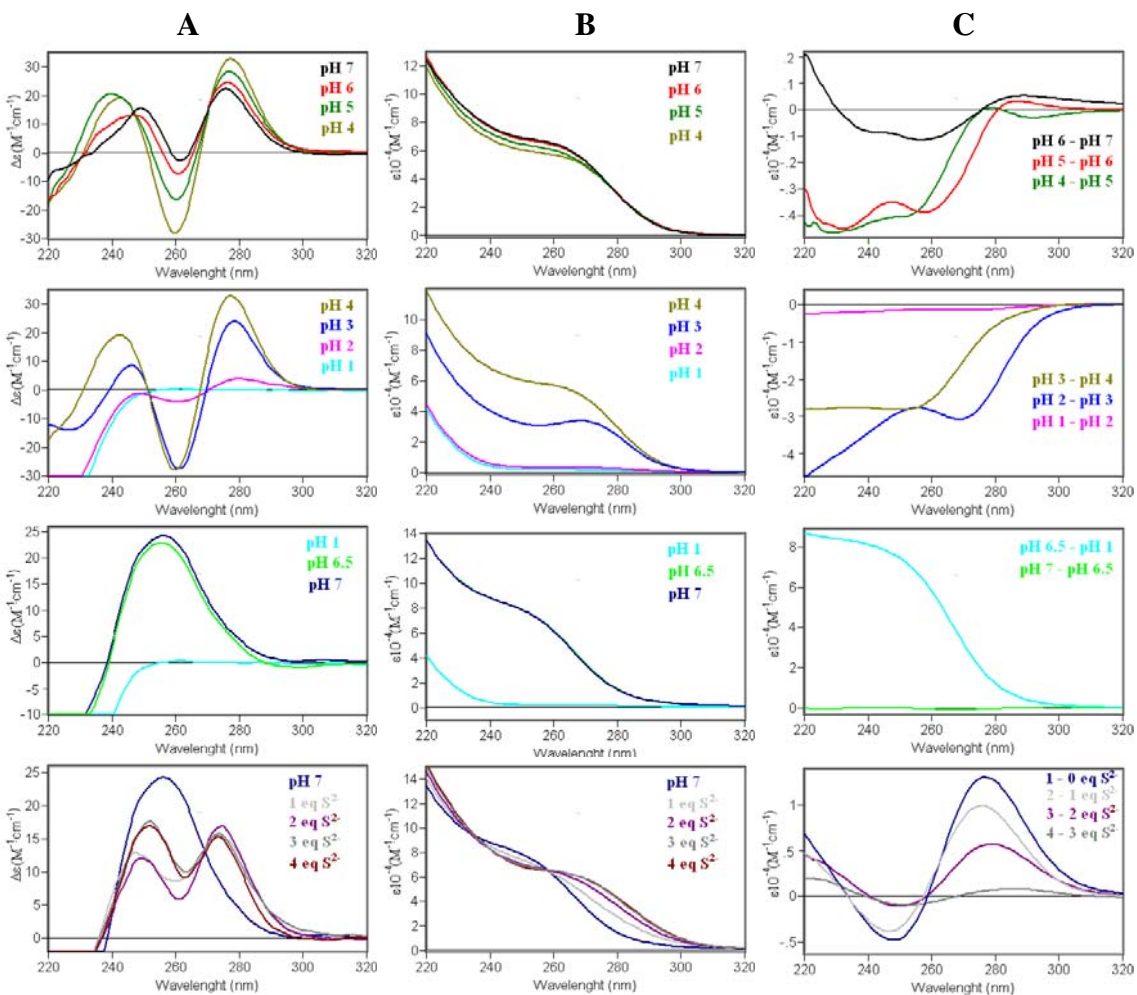


Fig. S3 CD (A), UV-vis (B) and UV-vis difference (C) spectra corresponding to the acidification (first two rows), reneutralization (third row) and addition of several Na_2S eq (fourth row) of a $20 \mu\text{M}$ solution of Cd^{II} -N25-C18. The pH and S^{2-} to MT molar ratio are indicated within each frame.

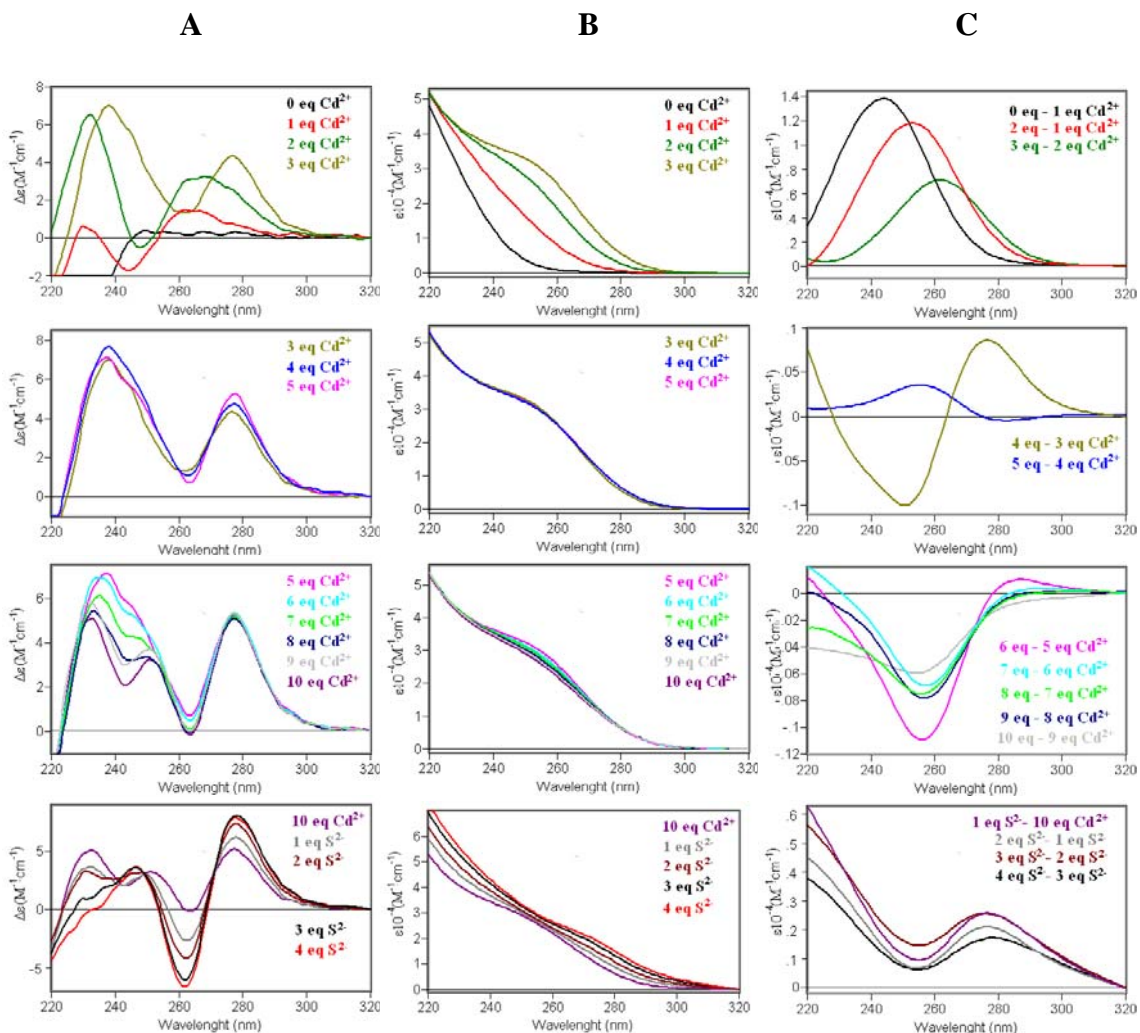


Fig. S4 CD (A), UV-vis (B) and UV-vis difference (C) spectra corresponding to the titration of a 20 μ M solution of Zn^{II}-N25 with Cd^{II} at pH 7.0 followed of the addition of several Na₂S eq. The Cd^{II} or S²⁻ to MT molar ratio are indicated within each frame.

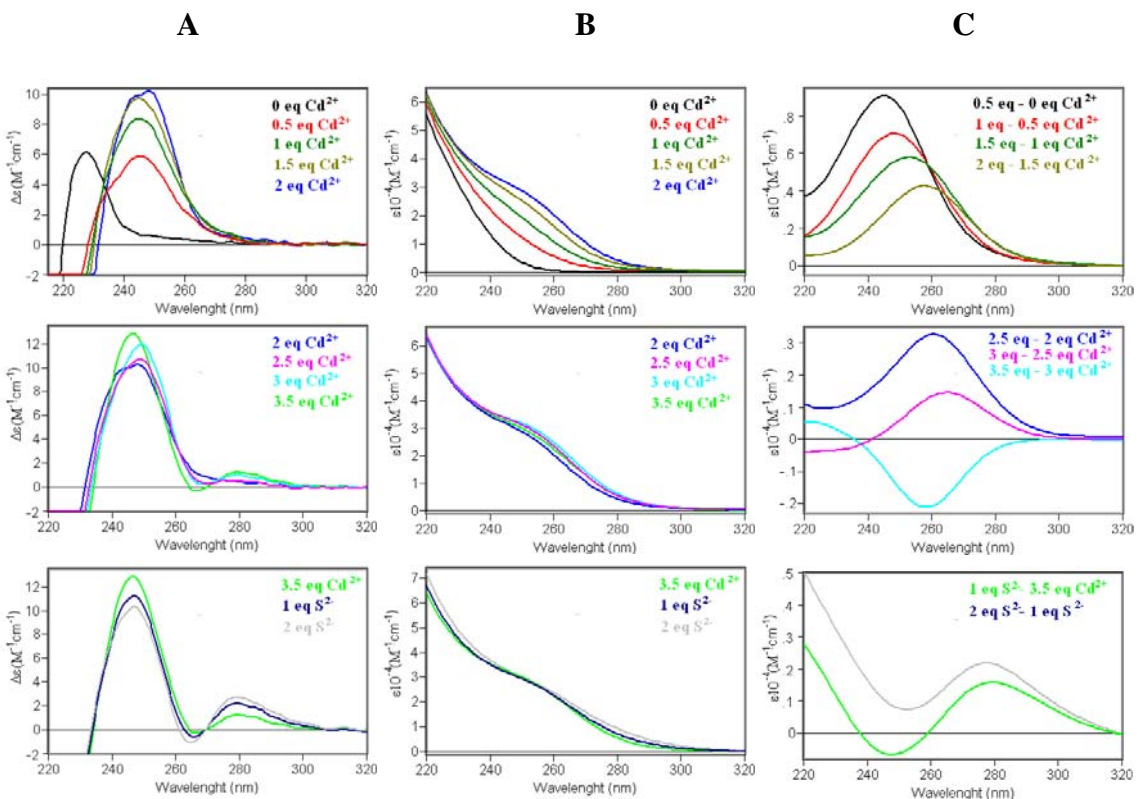


Fig. S5 CD (A), UV-vis (B) and UV-vis difference (C) spectra corresponding to the titration of a 20 μM solution of $\text{Zn}^{\text{II}}\text{-C18}$ with Cd^{II} at pH 7.0 followed by the addition of several Na_2S eq. The Cd^{II} or S^{2-} to MT molar ratio are indicated within each frame.

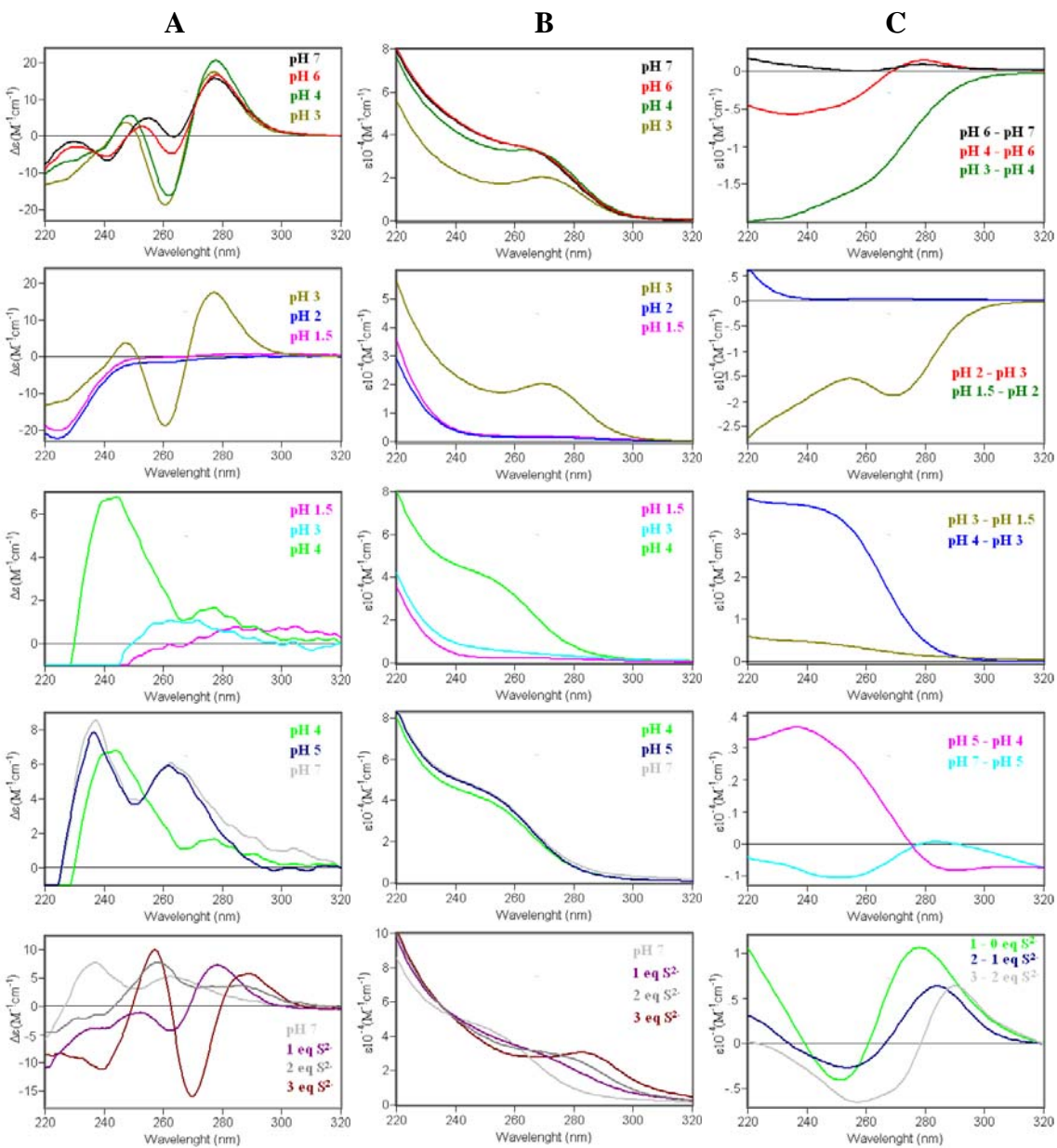


Fig. S6 CD (A), UV-vis (B) and UV-vis difference (C) spectra corresponding to the acidification (first two rows), reneutralization (third and fourth row) and addition of several Na_2S eq (fifth row) of a $20 \mu\text{M}$ solution of Cd^{II} -N25. The pH and S^{2-} to MT molar ratio are indicated within each frame.

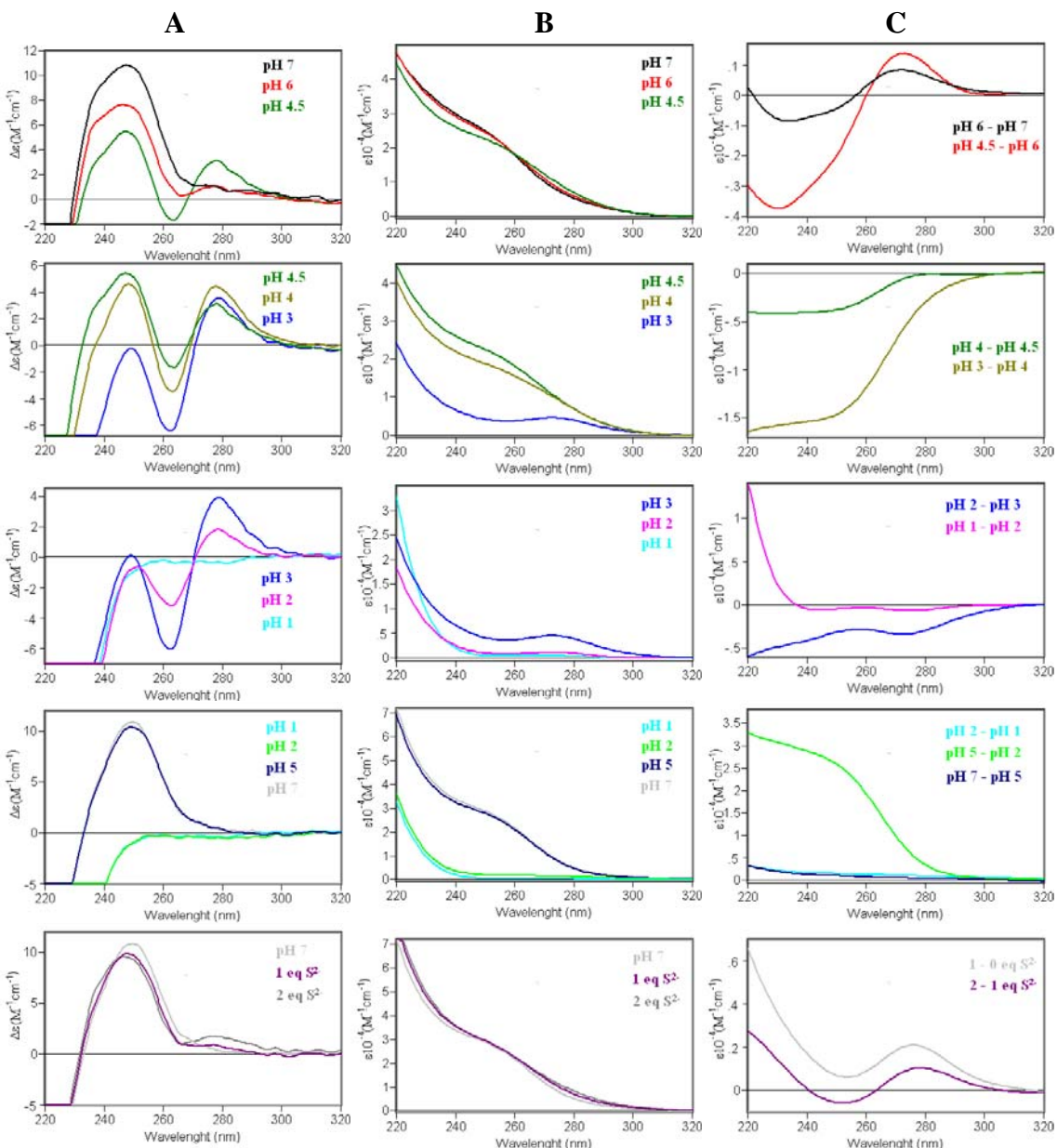


Fig. S7 CD (A), UV-vis (B) and UV-vis difference (C) spectra corresponding to the acidification (first three rows), reneutralization (fourth row) and addition of several Na_2S eq (fifth row) of a $20 \mu\text{M}$ solution of Cd^{II} -C18. The pH and S^{2-} to MT molar ratio are indicated within each frame.

ARTICLE 3

C.elegans metallothionein isoform specificity: metal-binding abilities and histidine role in CeMT1 and CeMT2

FEBS Journal, (2009), eniat

***C. elegans* metallothionein isoform specificity: metal binding abilities and histidine role in CeMT1 and CeMT2**

**R. Bofill,^{1,*} R. Orihuela,^{1,*} M. Romagosa,^{2,*} J. Domènech,^{2,*} S. Atrian,²
M. Capdevila¹**

¹ Departament de Química, Facultat de Ciències, Universitat Autònoma de Barcelona, 08193
Barcelona (Bellaterra) (Spain)

² Departament de Genètica, Facultat de Biologia, Universitat de Barcelona and IBUB (Institut
Biomedicina de la Universitat de Barcelona), Av. Diagonal 645, 08028 Barcelona (Spain)

* These authors contributed equally to this work

Keywords: Metallothionein – metal-histidine coordination – isoform specificity – differentiation – *Caenorhabditis elegans*

Abstract

Two metallothionein (MT) isoforms have been identified in the model nematode *Caenorhabditis elegans*, CeMT1 and CeMT2, two 75- and 63-residues long polypeptides, respectively. Both isoforms encompass a conserved cysteine pattern (19 in CeMT1 and 18 in CeMT2) and, most significantly, due to their coordinative potential, CeMT1 includes four histidines, while CeMT2 only one. We here present a comprehensive and comparative analysis of the metal (Zn(II), Cd(II) and Cu(I)) binding abilities of CeMT1 and CeMT2, performed through spectroscopic and spectrometric characterization of the recombinant metal-MT complexes synthesized for wild-type isoforms (CeMT1 and CeMT2), their separate N- and C-terminal moieties (NtCeMT1, CtCeMT1, NtCeMT2 and CtCeMT2), and a ΔHisCeMT2 mutant. The corresponding *in vitro* Zn/Cd- and Zn/Cu-replacement and acidification/renaturalization processes have also been studied, as well as protein modification strategies that allow to identify and quantify the contribution of His residues to metal coordination. Overall, our data indicate that both isoforms exhibit a clear preference for divalent metal ion binding, rather than for copper coordination, but this preference is more pronounced towards cadmium for CeMT2, while it is markedly clearer towards zinc for CeMT1. The presence of histidines in these MTs is revealed as decisive for their coordination performance: in CeMT1, they contribute to the binding of a 7th Zn(II) ion in relation to the M(II)₆-CeMT2 complexes, both when synthesized in the presence of supplemented Zn(II) or Cd(II); and in CeMT2, the unique C-terminal histidine abolishes the Cu-thionein character that otherwise would exhibit this isoform.

Abbreviations

DEPC, diethyl pyrocarbonate; MT, metallothionein

INTRODUCTION

C. elegans is one of the foremost model organisms in molecular and development biology studies and consequently, their Metallothionein (MT) system has also been object of special attention [1]. MTs are a large superfamily of cysteine-rich, small metal-binding polypeptides, present in all Eukaryota [2] and recently reported also in Eubacteria [3]. They probably evolved through a tangle of duplication, functional differentiation and convergence events that yielded the existing scenario, particularly complicated in terms of molecular evolution and physiological function assignment [4], beyond the universally accepted role in metal detoxification. Their putative *basic function*, globally assumed as related to metal homeostasis and/or metal-redox metabolism, may have been in the root of the appearance of MTs in life [5], and also one of the factors driving MT differentiation and specialization events through evolution. In an attempt to relate MT functional performance at molecular level (metal-binding abilities) and MT roles at physiological level (metabolic role), we proposed consideration of two groups of MTs: Zn-thioneins (or *divalent-metal-thioneins*) vs. Cu-thioneins [6], a classification we recently extended to a stepwise gradation between these two extreme types [7]. The sorting criteria are based in the stoichiometric and spectroscopic features of the Zn-, Cd- and Cu-MT complexes rendered by MT recombinant synthesis, which result indicative of the ability to coordinate one specific type of metal ion. Most significantly, this classification is fully coincident with the particular induction pattern (type of metal-inducer) of each MT gene, highlighting that MT functional specialization was most probably achieved both through promoter responsiveness and MT function properties towards a given metal. The most interesting examples of MT specialization are found among Invertebrates and unicellular Eukaryota, and so far, we have defined the MT metal binding features of *Arthropoda* (crustacea [6] and diptera [8]), *Mollusc* (bivalve [9]), *Protozoa* (ciliates [10]) and yeast (*S. cerevisiae* [11]) MTs following this approach.

In *C. elegans*, two distinct MT peptides were isolated after cadmium exposure, CeMT1 and CeMT2 [12], and recently the *C. elegans* genome project confirmed that no further MTs were encoded in this organism [13]. The *CeMT1* (*mtl-1*) and *CeMT2* (*mtl-2*) genes appear to share a common origin if considering the equivalent position of their small intron [14]. The corresponding cDNAs were shown to code for the CeMT1

and CeMT2 polypeptides, 75 and 63-residues long respectively [15,16], this dissimilarity being mainly due to 15 additional amino acids in the C-terminal region of CeMT1 (Table 1). Both peptides exhibit extremely conserved cysteines (19 in CeMT1 and 18 in CeMT2), contain one tyrosine, a rather uncommon trait in MTs, and most worth noting in view of their coordinative potential, CeMT1 includes four histidines, while CeMT2 has only a terminal one. In the absence of a comprehensive analysis of CeMT1 and CeMT2 metal-binding abilities, the information currently available is provided by three lines of evidence: the expression pattern of the *CeMT* genes, some scattered data on metal-CeMT complexes, and the analysis of the phenotypes exhibited by CeMT-devoid knockouts. Hence, both *CeMT* genes are strongly induced by cadmium in intestinal cells [17], which already points to a preference for divalent metal binding (Zn-thionein character), but detailed analyses of the regulation patterns of the two genes yielded interesting differential behavior hints [15]. On the one hand, *CeMT1* is also transcribed constitutively, from a TATA-less promoter, in pharyngeal cells. On the other hand, a strictly cadmium-inducible promoter controls *CeMT2* expression, restricted to intestinal cells. Significantly, *CeMT* promoters show almost no response in front of zinc or copper [18]. Regarding the purified CeMT polypeptides, stable, native Cd-CeMT1 and Cd-CeMT2 complexes were recovered upon cadmium feeding, although significantly the former contained a 20% of Zn(II) [12], somehow suggesting some metal coordination differential trends between isoforms. For CeMT2, the native homometallic species were identified as Cd₆-CeMT2 complexes [15] and their recombinant synthesis yielded complexes spectroscopically and stoichiometrically equivalent to the native species, exhibiting the common spectroscopic features of Cd-MT complexes [19, 20]. Additionally, Zn₆-CeMT2 species were identified as resulting from *in vitro* reconstitution of the corresponding CeMT2 apo-form. Finally, the construction of single and double MT-knockout *C. elegans* strains revealed that the MT-null organisms showed an unexpected decrease in biological fitness, with reduced body volume and litter size, even in the absence of any metal surplus [21]. Furthermore, the alteration of these phenotypical effects, even more acute than the increased cadmium sensitivity, was more marked in ΔCeMT1 than in ΔCeMT2. Thus, overall available information suggests that (i) *C. elegans* MTs are probably involved in basic biological processes, and (ii) the role of CeMT1 in global metabolism is more critical than that of CeMT2. Noteworthy,

Peptide	Sequence	Cys	His	Tyr
NtCeMT1	GSMACKC DCKNKQCKC --GDK- C ECSGD KCCE	9	0	0
CtCeMT1	GSKY C CE EASEKKCCPAGCKGDC KCANC H CAEQKQC GDKTHQHQGTAAAHAAH	10	4	1
CeMT1	GSMACKC DCKNKQCKC --GDK- C ECSGD KCCE KY CE EASEKKCCPAGCKGDC KCANC H CAEQKQC GDKTHQHQGTAAAHAAH	19	4	1
CeMT2	GSMV C K DCKKNQNCS CNTGTD CD CSDAK CCE Q Y CCPTASE EKKCC KSGCAGG GCKC ANC ECAQ -----AA-	18	1	1
ΔHis-CeMT2	GSMV C K DCKKNQNCS CNTGTD CD CSDAK CCE Q Y CCPTASE EKKCC KSGCAGG GCKC ANC ECAQ -----AA-	18	0	1
NtCeMT2	GSMV C K DCKKNQNCS CNTGTD CD CSDAK CCE	9	0	0
CtCeMT2	GSQ Y CCPTASE EKKCC KSGCAGG GCKC ANC ECAQ -----AAH	9	1	1

Table 1.- Amino acid sequences of the wild type and mutant forms of CeMT1 and CeMT2 studied in this work. The coordinating, or putative coordinating residues have been highlighted (Cys in grey shadow, His and Tyr in bold), and the total content in each peptide indicated. The initial GlySer dipeptide derives from the expression system used for recombinant synthesis and has been shown not to influence the MT binding properties.

MTs seem to be only one of the three strategies developed by *C. elegans* to prevent cadmium intoxication, additionally to phytochelatins [22], and to the selective pumping of Cd(II) ions to lysosomes that generate the deposit granules known as cadmosomes [23].

In this scenario, we considered the study of the *C. elegans* MT system at protein function level of the up most interest, in order to shed light on the possible physiological functions of MTs in this organism and to progress in the understanding of the forces driving MT isoform differentiation, both aspects recently claimed to await analysis [1]. Consequently, we here present a thorough characterization of the metal binding abilities of the two CeMT isoforms according to our rationale, which includes the comparative spectroscopic and spectrometric analysis of the Zn-, Cd- and Cu-complexes recombinantly synthesized in *E. coli*, for wild-type isoforms (CeMT1 and CeMT2), their separate N- and C-terminal moieties (NtCeMT1, CtCeMT1, NtCeMT2 and CtCeMT2), and a ΔHisCeMT2 mutant. Additionally, we also present the analysis of the *in vitro* Zn/Cd- and Zn/Cu-replacement processes undergone by the corresponding Zn-peptides, as well as the study of the putative contribution of their His residues to metal coordination. Overall, all our data indicate that both isoforms exhibit a clear preference for divalent metal ion binding, rather than for copper(I). Nevertheless, this preference is more pronounced towards cadmium for CeMT2, while it is markedly clearer towards zinc for CeMT1. These metal-binding features are in full concordance with an involvement of CeMT1 in the global metabolism of physiological zinc, and a contribution of CeMT2 to ingested cadmium detoxification.

RESULTS AND DISCUSSION

Identity and integrity of the recombinant CeMT1 and CeMT2 polypeptides

Recombinant synthesis from the pGEX expression constructs yielded CeMT1 and CeMT2 whose identity, purity and integrity was confirmed by ESI-MS of the respective apo-forms obtained by acidification at pH 2.4 of the Zn-MT complexes. In all cases, a single polypeptide, of the expected molecular mass was detected: 3108.6 for NtCeMT1, 5287.9 for CtCeMT1, 8262.4 for CeMT1, 3397.0 for NtCeMT2, 3502.0 for CtCeMT2, 6737.7 for CeMT2 and 6600.6 for ΔHisCeMT2. The boundaries between two putative metal binding domains were defined according to the alignment with mammalian MT1, considering that the two moieties kept an equivalent number of cysteines (*cf.* sequences in Table 1). None of the CD spectra of the seven apo-peptides exhibited absorptions in the 220-400 nm range, which is especially significant since it indicates that the CeMT1 and CeMT2 Tyr residue is CD silent. Equally, and as reported in the literature [19], the Tyr presence caused an absorption maximum at *ca.* 280 nm in the corresponding UV-vis spectra of both isoforms (data not shown). The metal-CeMT complexes were recovered at a concentration range of 0.5 to 2 × 10⁻⁴ M for Zn- and Cd-CeMT, and 0.5 to 1 × 10⁻⁴ M for Cu-CeMT, this meaning an average of 1 mg of pure metal-MT complex per liter of *E. coli* culture.

Zn(II) binding abilities of CeMT1 and CeMT2

Recombinant synthesis of CeMT1 yielded a unique Zn₇-CeMT1 species. Conversely, at the same conditions, CeMT2 and ΔHisCeMT2 gave rise to

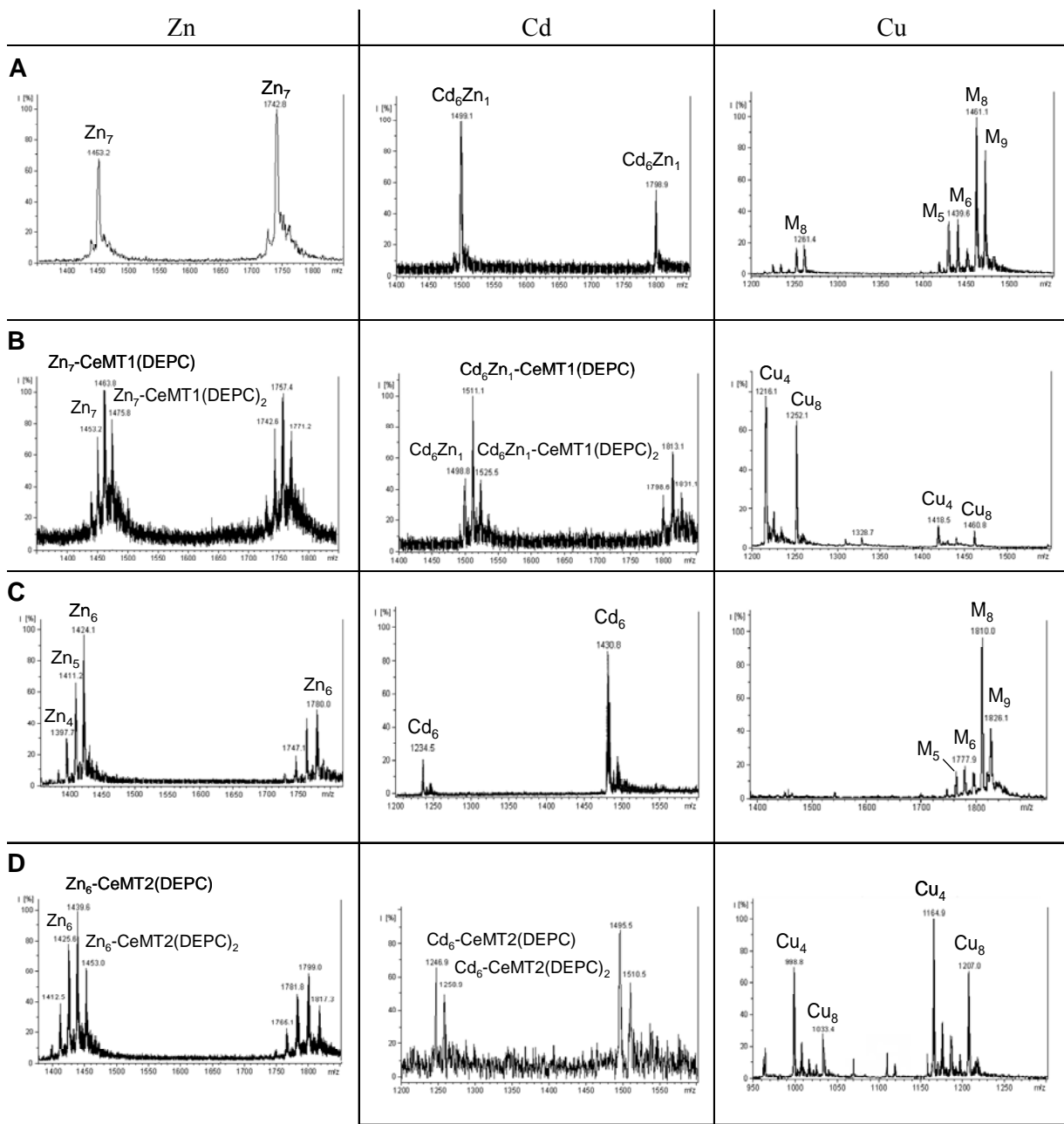


Figure 1.- ESI-TOF-MS spectra recorded at pH 7.0 of the recombinant CeMT1 (A) and CeMT2 (C) synthesized in Zn, Cd and Cu-supplemented *E. coli* cultures. Spectra recorded after incubation with DEPC are shown for Zn- and Cd-CeMT1 (B) and Zn- and Cd-CeMT2 (D). In the last column of panels (B) and (D), the spectra of the Cu-CeMT preparations recorded at pH 2.8 are shown.

mixtures of homonuclear Zn(II)-complexes with Zn₆- as the major species -in concordance with the results of *in vitro*-reconstitution of apo-CeMT2 [19]- but also with significant contribution of Zn₅- and Zn₄-CeMT2 (*cf.* Table 2, Fig. 1). The three preparations showed similar, although atypical, CD profiles since the exciton coupling centered at *ca.* 240 nm associated to the Zn-Cys chromophores exhibited an inverse chirality in relation to conventional Zn-MTs [24] (Fig. 2). To our knowledge, Zn(II)-MTO is the only case with a

similar CD fingerprint [25]. As both Zn(II)-CeMT2 and Zn(II)-ΔHisCeMT2 preparations rendered identical stoichiometries, it is clear that the C-terminal CeMT2 histidine does not enhance its metal binding ability. However, as small differences in their CD spectra (Fig. 2), together with Raman results [26] suggest that this residue participates in Zn(II)-binding, it is sensible to conclude that this would only apply to a subset of the Zn(II)-CeMT2 complexes present in the preparation.

Table 2.- Analytical characterization of the recombinant preparations of the Zn-complexes yielded by CeMT1, CeMT2, their N-term and C-term moieties and the ΔHisCeMT2 mutant.

Peptide	Zn-peptide molar ratio (ICP-AES)	ESI-MS ^a		
		Major species Minor species	MW theoretical	MW experimental
CeMT1	6.5 Zn	Zn₇-CeMT1	8706.0	8708.1 ± 0.4
CeMT2	5.0 Zn	Zn₆-CeMT2 Zn ₅ -CeMT2 Zn ₄ -CeMT2	7118.1 7054.7 6991.3	7117.2 ± 0.8 7051.2 ± 1.4 6986.4 ± 0.2
CtCeMT1	2.1 Zn	Zn₄-CtCeMT1 Zn ₂ -CtCeMT1 Zn ₁ -CtCeMT1	5541.4 5414.7 5351.3	5541.4 ± 0.6 5411.2 ± 0.5 5344.4 ± 0.3
NtCeMT1	1.8 Zn	Zn₃-NtCeMT1 Zn ₁ -NtCeMT1	3298.7 3172.0	3298.0 ± 0.1 3166.2 ± 0.2
CtCeMT2	2.2 Zn	Zn₃-CtCeMT2 Zn ₂ -CtCeMT2	3692.2 3628.8	3691.8 ± 0.4 3626.8 ± 0.7
NtCeMT2	2.6 Zn	Zn₃-NtCeMT2 Zn ₂ -NtCeMT2	3587.2 3523.8	3587.1 ± 0.1 3522.4 ± 0.2
ΔHisCeMT2	4.7 Zn	Zn₆-ΔHisCeMT2 Zn ₅ -ΔHisCeMT2 Zn ₄ -ΔHisCeMT2	6981.0 6917.6 6854.2	6980.7 ± 0.3 6917.6 ± 0.1 6854.0 ± 0.1

^a Theoretical and experimental molecular masses of the Zn-CeMT peptides. Zn contents were calculated from the mass difference between holo- and apo-proteins.

The higher Zn(II) binding capacity of CeMT1 *vs.* CeMT2 correlates very well with the results obtained for their separate putative metal-binding domains. The highly similar N-terminal moieties (NtCeMT1 and NtCeMT2) rendered equivalent mixtures of species, with major Zn₃-complexes. Conversely, the C-terminal peptides (CtCeMT1 and

CtCeMT2) yielded mixtures with different major species: Zn₄-CtCeMT1 *vs.* Zn₃-CtCeMT2 (Table 1). The CD fingerprints of the Zn(II)-complexes of NtCeMT1 and NtCeMT2 (Fig. 3) were highly atypical and difficult to interpret, specially the absence of a CD signal at *ca.* 240 nm for Zn(II)-NtCeMT2, while those of CtCeMT1 and CtCeMT2

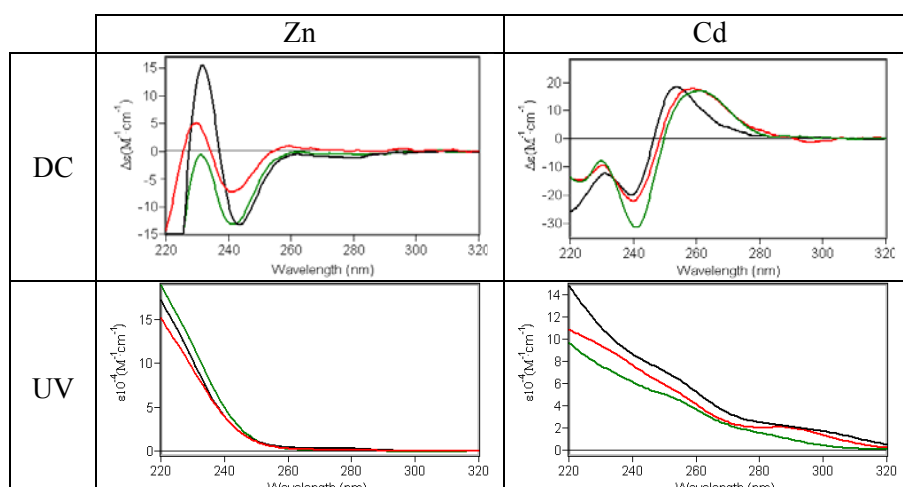


Figure 2.- Comparison between the CD and UV-vis spectra of recombinant CeMT1 (black), CeMT2 (red) and ΔHisCeMT2 (green) synthesized in Zn and Cd supplemented media.

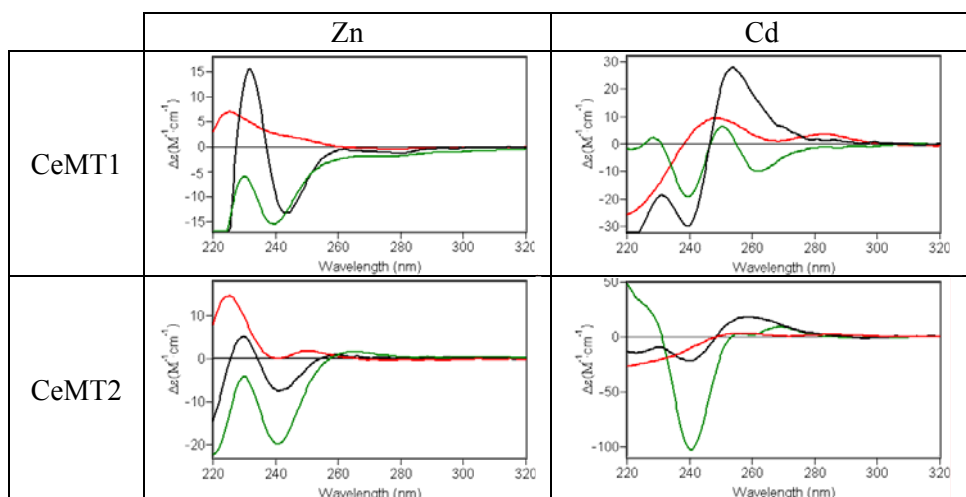


Figure. 3.- Comparison between the CD spectra of recombinant CeMT1 and CeMT2 (black), NtCeMT1 and NtCeMT2 (red), and CtCeMT1 and CtCeMT2 (green) synthesized in Zn and Cd supplemented media.

displayed a Gaussian band centered at *ca.* 240(-) nm, resembling more those of the respective entire MTs. Finally, it is worth noting that despite the apparent additivity of the stoichiometries of the complexes rendered by the separate moieties of CeMT1 and CeMT2, summation of their CD spectra did not give rise in any case to spectra close to those of the entire Zn(II)-CeMT preparations, which is indicative, for both CeMTs, of a strong moiety interaction when binding Zn(II) ions.

Overall, the differences between Zn(II)-CeMT1 and -CeMT2 put forward a higher zinc binding capacity of the former, reflected both in the stoichiometry and the homogeneity of their preparations. These differences are due to the different coordination capacity of the respective C-terminal moieties and attributable to the total of four additional putative coordinating residues (1 Cys and 3 His) of CtCeMT1 in relation to CtCeMT2. These results strongly suggest participation of the histidine residues of CeMT1 in Zn(II) coordination, allowing a MT peptide with only 19 Cys to stably coordinate up to 7 Zn(II). But, unfortunately, the similarities between the CD spectra of Zn(II)-CeMT1 and Zn(II)-CeMT2 preclude the assignment of the putative His-Zn(II) chromophores to defined CD absorptions, which would have resulted highly informative about the presence of Zn-His bonds.

In vivo and in vitro Cd(II) binding abilities of CeMT1 and CeMT2

Differing from the results for Zn(II) coordination, the biosynthesis in Cd supplemented cultures of the two wild type CeMT1 and CeMT2 forms, as well as of ΔHisCeMT2, gave invariably rise to single species, although of different stoichiometry, for

each isoform (Table 3, Fig. 1). Most interestingly, CeMT1 rendered an heterometallic Cd₆Zn₁-CeMT1 species, in contrast to the homometallic Cd₆-CeMT2 and Cd₆-ΔHisCeMT2 complexes. ESI-MS results for the separate CeMT moieties were here highly informative, since they revealed formation of a unique Cd₃Zn₁-complex for CtCeMT1, while a major Cd₃-NtCeMT1 species (Table 3), which nicely suggest that the Zn(II) ion of Cd₆Zn₁-CeMT1 is located within its C-terminal domain. In contrast, synthesis of NtCeMT2 and CtCeMT2 gave rise to practically pure Cd₃-species, also fully concordant with the entire Cd₆-CeMT2 complex. The CD and JV-vis fingerprints of the Cd(II)-CeMT1, Cd(II)-CeMT2 and Cd(II)-ΔHisCeMT2 preparations (Fig. 2) were highly similar, showing the typical absorptions at *ca.* 250 nm of conventional Cd-SCys chromophores, which additionally discarded the presence of sulfide-containing aggregates. Our data were coincident with the UV-vis absorption spectra previously reported for the native and recombinant Cd(II)-CeMT2 isoform [15,19]. The slight blue-shift of the spectrum of Cd₆Zn₁-CeMT1 in relation to that of Cd₆-CeMT2 is attributable to the influence of the Zn(II) ion present in the complex. The four CeMT moiety peptides showed atypical CD envelopes (Fig. 3), whose summation in no case reproduced that of the corresponding full-length proteins, in spite of the additivity of their metal contents (Table 3), suggesting, as for Zn(II), clear interactions between domains when binding Cd(II). The two N-terminal segments, of similar sequence and comparable speciation, gave also rise to nearly equivalent CD fingerprints although of different intensity, which could be interpreted by assuming the characteristic Cd-SCys signals at 250 nm, plus the possible contribution of weak absorptions of minor sulfide-containing species at

Table 3.- Analytical characterization of the recombinant preparations of the Cd-complexes yielded by CeMT1, CeMT2, their N-term and C-term moieties and the ΔHisCeMT2 mutant.

Peptide	Metal-peptide molar ratio (ICP-AES)	ESI-MS ^a		
		Major species Minor species	MW theoretical	MW experimental
CeMT1	0.9 Zn 6.5 Cd	Cd₆Zn₁-CeMT1	8988.2	8989.1 ± 0.5
CeMT2	5.7 Cd	Cd₆-CeMT2	7400.2	7399.0 ± 0.5
CtCeMT1	0.6 Zn 2.9 Cd	Cd₃Zn₁-CtCeMT1	5682.5	5683.2 ± 0.9
NtCeMT1	0.1 Zn 2.9 Cd	Cd₃-NtCeMT1 Cd ₃ Zn ₁ -NtCeMT1	3439.8 3503.2	3438.9 ± 0.6 3502.4 ± 0.5
CtCeMT2	2.9 Cd	Cd₃-CtCeMT2	3833.2	3833.1 ± 0.1
NtCeMT2	0.1 Zn 2.3 Cd	Cd₃-NtCeMT2 Cd ₃ Zn ₁ -NtCeMT2	3728.2 3791.6	3729.0 ± 0.1 3790.8 ± 0.1
ΔHisCeMT2	5.5 Cd	Cd₆-ΔHisCeMT2	7263.0	7262.5 ± 0.1

^a Theoretical and experimental molecular masses of the Cd-peptides. Zn and Cd contents were calculated from the mass difference between holo- and apo-proteins.

ca. 280 nm. Oppositely, the CD envelopes of the C-terminal moieties are difficult to rationalize, especially in the case of Cd₃Zn₁-CtCeMT1, where we expected the influence of Zn(II) to be similar than in the full-length CeMT1. Although the CD profiles of these two Cd(II) complexes coincide in the 240-250 nm region (Fig. 3), Cd₃Zn₁-CtCeMT1 shows absorptions at 260(-) nm that is absent in the full length protein spectrum. One possible explanation for this, as well as for the faint shoulder observed at ca. 270(+) for CeMT1, would be the contribution of the multiple histidines to metal binding (see below). Finally, the comparison of the CD spectra of the *in vivo* Zn(II)-CeMT1 and Zn(II)-CeMT2 complexes with the respective Cd(II)-complexes show their inverse chirality, which allows to postulate that they do not share the same 3D architecture, albeit their equivalent stoichiometry (M₇-CeMT1 and M₆-CeMT2; M= Zn or Cd) (Fig. 2).

Besides recombinantly, Cd(II)-complexes of all the studied CeMT peptides were obtained *in vitro* by two different procedures: (a) Cd(II) titration of the recombinant Zn(II)-MT forms and (b) acidification plus subsequent reneutralization of the recombinant Cd(II)-MT preparations. The key results of these experiments show that in all cases, the titration of the Zn(II)-CeMT preparations with Cd(II) allowed reproduction of the spectrometric

and spectropolarimetric features of the biosynthesized Cd(II)-MT forms, after the addition of the *expected* number of Cd(II) equivalents, *i.e.* 6 Cd(II) eq for the full length proteins (Fig. 4) and 3 Cd(II) eq for the fragments (data not shown). Most interestingly, the Zn/Cd replacement process on CeMT1 yielded Cd₆Zn₁-CeMT1, even after the addition of a significant excess of Cd(II). Also, the *in vivo* heteronuclear Cd₆Zn₁-CeMT1 complex did not exchange the Zn(II) ion upon excess Cd(II) addition. Acidification/reneutralization of all biosynthesized Cd(II)-CeMT complexes revealed that the initial species were recovered after this process. For CeMT1, these experiments also supported the participation of His residues in metal coordination since acidification of Cd₆Zn₁-CeMT1, as well as of Cd₃Zn₁-CtCeMT1, (from pH 7.0 to pH 1.0) did not induce important variations in the respective CD envelopes precisely until ca. pH 4.5, this coinciding with the pK_a value for this amino acid. Furthermore, after this acidification stage, UV-vis difference spectra revealed a loss of absorbance at wavelengths ca. 240 nm (Fig. 5), while ESI-MS data indicated that at pH 4.2 most of the complexes lost their Zn(II) ion, as the major species present in the sample were Cd₆-CeMT1 and Cd₃-CtCeMT1, respectively. Consequently, it is sensible to deduce that the coordination of the Zn(II) ion bound at the C-terminal moiety of CeMT1 is

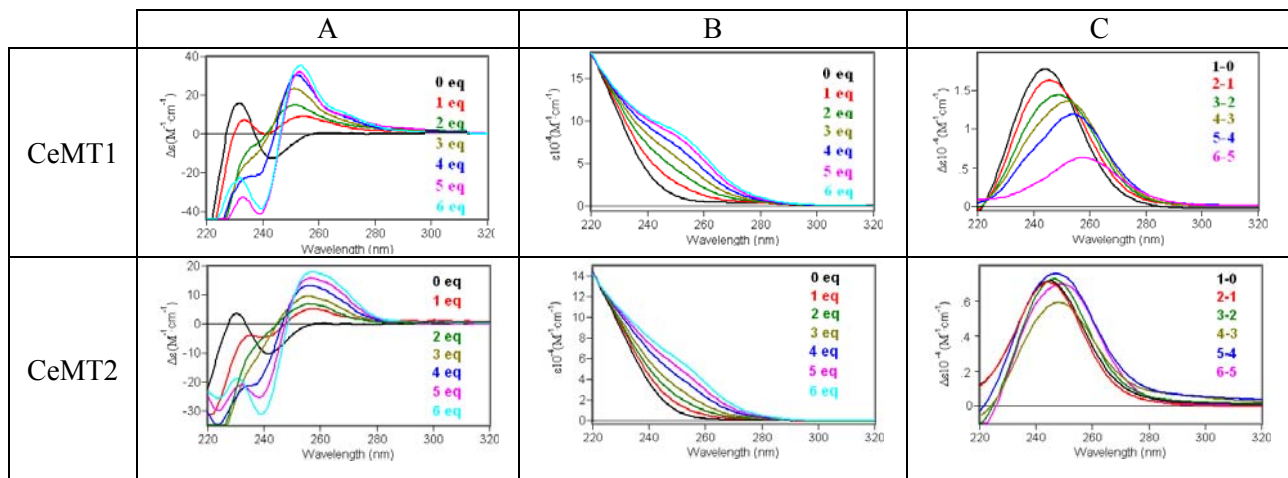


Figure 4.- CD (A), UV-vis (B) and UV-Vis difference (C) spectra corresponding to the titration of a 10 μM solution of Zn-CeMT1 and Zn-CeMT2 with Cd(II) at pH 7

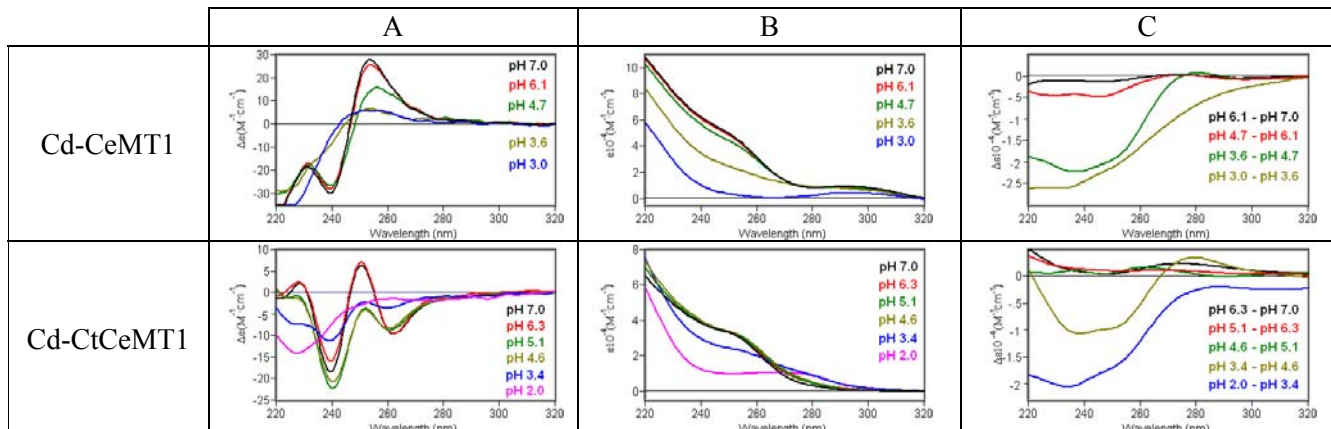


Figure 5.- CD (A), UV-vis (B), and UV-vis difference (C) corresponding to the acidification of a 10 μM solution of Cd-CeMT1 and 20 μM solution of Cd-CtCeMT1.

contributed by histidines, the number of them involved in metal binding being analyzed in the next section.

Thus, overall results reveal that equivalent Cd-complexes of CeMT1 and CeMT2, as well as those of their putative domains, are obtained *in vivo* (by recombinant synthesis) and *in vitro* (by Zn/Cd replacement or acidification/reneutralization). Our data also demonstrates that CeMT1 forms heteronuclear Cd₆Zn₁-complexes when folding in the presence of high cadmium, and that this Zn(II) ion is bound into its C-terminal moiety, in a coordination environment most probably contributed by His residues. On the contrary CeMT2 folds into homonuclear, canonical Cd₆-complexes, of equivalent features whatever their origin, recombinant synthesis, or *in vitro* Zn/Cd

replacement, acidification/reneutralization or Cd(II) reconstitution of apo-forms (this last, J. H. R. Kägi, personal communication). Therefore, a marked preference for Zn(II) binding (Zn-thionein character) is put forward for CeMT1 in contrast to the more optimal performance of CeMT2 for Cd(II) binding [7], which also accounts for the presence of Zn(II) in the metal-CeMT1 complexes purified from cadmium intoxicated organisms [12].

Quantification of the His residues involved in metal coordination in the Zn- and Cd- CeMT1 and CeMT2 complexes

Diethyl pyrocarbonate (DEPC) modification allows identification and quantification of the His residues of proteins that are not somehow protected [27]. In

the case of reaction with His, DEPC produces a 72.06-Da carboxyethyl adduct at the imidazole (γ)-NH position [28] and although DEPC also reacts with other nucleophilic residues (Cys, Lys, Tyr, Ser, Thr, Arg) and α -amino groups, this reaction proceeds with a marked lower efficiency [29,30]. Therefore, to evaluate the number of CeMT1 and CeMT2 histidines contributing to divalent metal ion coordination, the Zn- and Cd-preparations of both *C.elegans* CeMT1 and CeMT2, and the Cd-complexes of CtCeMT1 and CtCeMT2 were incubated with DEPC and the respective results evaluated by ESI-TOF-MS (Fig. 1), using the Zn(II)- Δ HisCeMT2 and Cd(II)-NtCeMT1 peptides as negative controls, since they do not encompass any histidine.

The results indicated that both Zn(II)- Δ HisCeMT2 and Cd(II)-NtCeMT1 were mono-carboxyethylated. Consequently, at the conditions assayed the reaction of their free terminal α -NH₂ groups with DEPC should be assumed since these two peptides highly differ in the number of other potentially modifiable residues (Cys, Lys, Tyr, Ser and Thr), this highlighting that their N-terminal group are the most effectively DEPC reactants. For the His-containing peptides (Zn- and Cd-complexes of CeMT1, CeMT2 and respective CtCeMT moieties), ESI-MS revealed two carboxyethylations. One of them should be assigned to their terminal amino group, and for the CeMT2 and CtCeMT2 complexes, the second modification is then attributable to their unique, C-terminal histidine. The formation of the second adduct for the metal complexes of CeMT1 and CtCeMT1 indicates that one of their four histidines remains free to react with DEPC. Consequently, and by analogy to CeMT2, it is sensible to assume the reaction of DEPC with their C-terminal His residue. In any case, these results demonstrate that three of the four histidines of M(II)-CeMT1 are unreachable to DEPC, the most sensible explanation being their involvement in metal coordination, in view of the results reported in the last section.

In vivo and in vitro Cu(I) binding abilities of CeMT1 and CeMT2

The synthesis of CeMT1 and CeMT2 in copper-supplemented cultures rendered equivalent results: a mixture of heteronuclear Zn,Cu-complexes, with major M₈- and M₉-species, which were identified as Cu₄- and Cu₈-containing complexes by ESI-MS at pH 2.4, in full concordance with the mean Cu(I) and Zn(II) content per MT measured by ICP-AES (Table 4, Fig. 1). Conversely, Δ HisCeMT2 synthesized at the same conditions yielded homometallic Cu-complexes with a major Cu₈-

Δ HisCeMT2 species. Both NtCeMT moieties also gave rise to homonuclear Cu₅- preparations. Under these conditions, low zinc contents were detected in the preparations of the copper complexes of the CtCeMT segments, which rendered major M₄- (Cu₄- for CtCeMT2) and additional minor M₅- (Cu₄Zn₁- for CtCeMT1). To further extend the

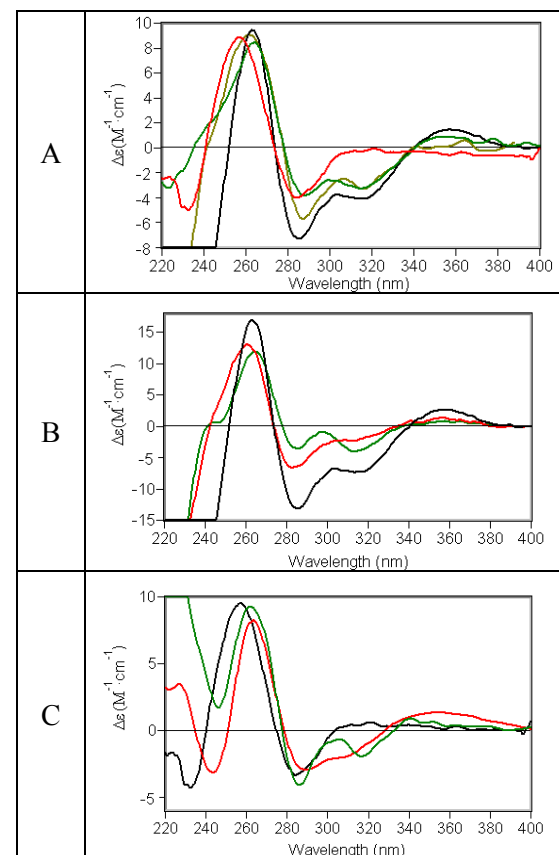


Figure 6.- Comparison between the CD spectra of recombinant CeMT1 (black), CeMT2 under normal oxygenation conditions (red), CeMT2 under low oxygenation conditions (green), Δ HisCeMT2 (kaki) (A); CeMT1 (black), NtCeMT1 (red), and CtCeMT1 (green) (B); and CeMT2 (black), NtCeMT2 (red), and CtCeMT2 (green) (C) synthesized in Cu supplemented media.

copper binding preference analyses of the two isoforms, their synthesis were repeated in copper supplemented media but at low aeration conditions. Interestingly, while the results for CeMT2 were fully comparable to those obtained for Δ HisCeMT2 at regular oxygenation (*i.e.* homonuclear Cu-complexes), the resulting Cu-CeMT1 preparations showed extremely poor spectroscopic and spectrometric data revealing indiscernible mixtures of Cu-species. This data were consistent with a more pronounced character of Zn-thionein for CeMT1 and partial Cu-thionein for CeMT2, which

Table 4- Analytical characterization of the recombinant preparations of the Cu-complexes yielded by CeMT1, CeMT2, their N-term and C-term moieties and the Δ HisCeMT2 mutant, obtained under normal aeration conditions.

Peptide	Metal-peptide molar ratio (ICP-AES)	ESI-MS ^a			
		Major species Minor species		MW theoretical	MW experimental
CeMT1	2.2 Zn 4.6 Cu	pH 7.0	M₈-CeMT1	8762.7-8769.4	8761.6 \pm 1.4
			M₉-CeMT1	8825.3-8832.8	8823.2 \pm 0.7
		pH 2.4	M₆-CeMT1	8637.7-8642.7	8635.0 \pm 4.4
			M₅-CeMT1	8575.1-8579.3	8573.4 \pm 9.3
CeMT2	2.5 Zn 4.3 Cu	pH 7.0	Cu₄-CeMT1	8512.6	8506.4 \pm 1.1
			Cu₈-CeMT1	8762.7	8758.2 \pm 0.3
		pH 2.4	M₈-CeMT2	7238.1-7245.0	7237.5 \pm 1.5
			M₉-CeMT2	7300.7-7308.4	7300.4 \pm 5.5
CtCeMT1	0.8 Zn 3.7 Cu	pH 7.0	M₆-CeMT2	7113.0-7118.2	7107.6 \pm 1.8
			M₅-CeMT2	7050.4-7054.8	7046.0 \pm 2.0
		pH 2.4	Cu₄-CeMT2	6987.9	6976.2 \pm 0.1
			Cu₈-CeMT2	7238.1	7232.4 \pm 4.0
NtCeMT1	0.0 Zn 4.4 Cu	pH 7.0	M₄-CtCeMT1	5538.1-5541.4	5534.4 \pm 0.4
			M₅-CtCeMT1	5600.7-5604.8	5598.0 \pm 0.5
		pH 2.4	Cu₄-CtCeMT1	5538.1	5534.5 \pm 0.5
			Cu₅-NtCeMT1	3421.3	3419.3 \pm 0.5
CtCeMT2	0.5 Zn 3.5 Cu	pH 7.0	M₄-CtCeMT2	3752.2-3755.7	3753.0 \pm 2.0
			Cu₄-CtCeMT2	3752.2	3753.2 \pm 1.5
		pH 2.4	Cu₅-NtCeMT2	3709.8	3706.5 \pm 0.1
			Cu₅-NtCeMT2	3709.8	3707.5 \pm 0.6
Δ HisCeMT2	0.0 Zn 8.7 Cu	pH 7.0	Cu₈-ΔHisCeMT2	7101.0	7096.8 \pm 0.3
			Cu₉-ΔHisCeMT2	7163.5	7160.8 \pm 0.4
		pH 2.4	Cu₈-ΔHisCeMT2	7101.0	7099.6 \pm 0.3
			Cu₉-ΔHisCeMT2	7163.5	7163.8 \pm 1.2

^a Theoretical and experimental molecular masses corresponding to the Cu-peptides. In the case of Zn,Cu mixed-metal species, the theoretical molecular masses correspond to the homometallic Cu_x and Zn_x species, respectively, and the metal-to-protein stoichiometries deduced at pH 7.0 are indicated as M_x (M is Zn or Cu). Cu contents at pH 2.4 were calculated from the mass difference between holo- and apo-proteins.

would behave as a proper Cu-thionein but for its C-terminal His. The CD fingerprints of all these preparations (Fig. 6) showed the characteristic signals associated to the Cu-MT species although the complexity of their envelopes is difficult to rationalize in view of the mixtures of complexes obtained and the distinct coordination environments that Cu(I) ions can show.

Both for CeMT1 and CeMT2, the different behavior of the separate fragments with respect to the full length peptides is in accordance with the non additivity of their respective CD fingerprints (Fig. 6), which suggests the existence of cooperativity between moieties when binding Cu(I), as described both for Zn(II) and for Cd(II) binding.

But significantly, this dependence entails here a striking consequence, as the clear Cu-binding preference of the N-terminal moieties is turned into a definite Zn-thionein character for the full-length proteins.

Concerning the *in vitro* studies, it is noteworthy to highlight that the addition of Cu(I) to either Zn₇-CeMT1, Zn₆-CeMT2 or Zn₆- Δ HisCeMT2 gave rise to a continued increase in absorbance at the studied wavelength range until 8-9 Cu(I) eq added, when the spectra (Fig. 7) become invariable indicating saturation and in nice concordance with the Cu(I) contents observed in the *in vivo* preparations. It is difficult to correlate the variations in the CD envelopes observed during the titrations with the

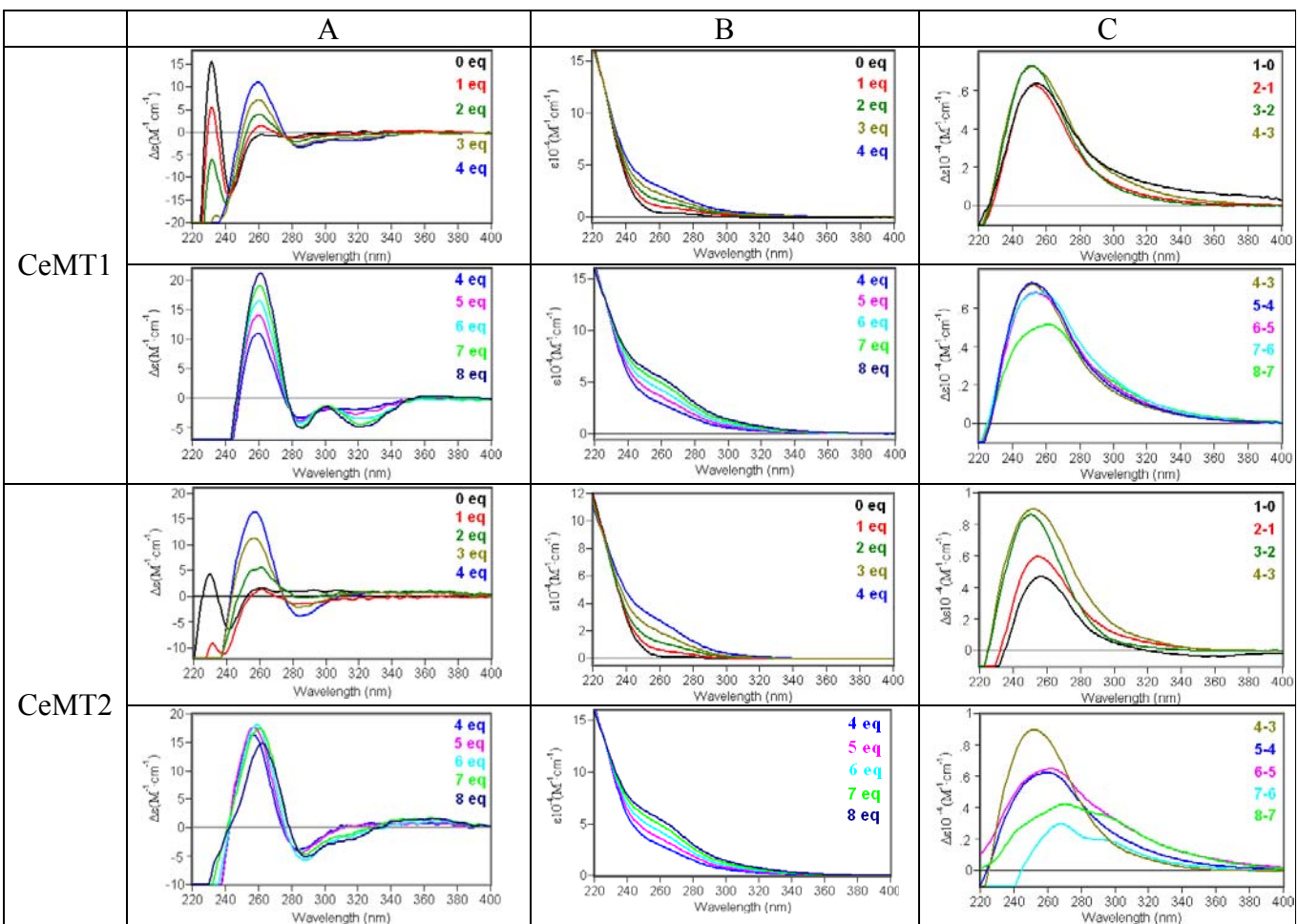


Figure 7- CD (A), UV-vis (B) ad UV-Vis difference (C) spectra corresponding to te titration of a 10 μM solution of Zn(II)-CeMT1 and Zn(II)-CeMT2 with Cu(I) at pH 7.0.

corresponding ESI-MS data, since the later revealed the coexistence of multiple metal-MT species at all stages of the titrations, with the presence of major M₈- and M₉-CeMT already from the beginning, which resulted in Cu₄- and Cu₈-CeMT species when acidified at pH 2.4, and which probably retained Zn(II) ions even after addition of an excess of Cu(I).

CONCLUDING REMARKS

All the data reported in this work are indicative of a differential metal binding behavior for the two *C. elegans* MT isoforms. Although they exhibit a clear preference for divalent-metal binding rather a copper-thionein character, CeMT1 shows an optimal behavior when binding Zn(II), while CeMT2 is highly proficient for Cd(II) coordination. In fact, CeMT1 occupies the more extreme position in our recent proposal of a step gradation from Zn- to Cu-thioneins [7]. These results are in full concordance with CeMT1 being constitutively expressed in pharyngeal cells, where it would develop some background role related to

physiological metal -mainly zinc- metabolism, while CeMT2 unique synthesis after cadmium induction confers to this isoform a basic detoxification role. This hypothesis is also concordant with the effects observed in the fitness of *C. elegans* MT-knockout organisms, where the lack of CeMT1 is more deleterious in the absence of metals than that of CeMT2. No response has been described for the *CeMT* promoters in front of copper overload, neither seem that MTs are a major system for copper tolerance in this organism [31], and this is also in agreement with the fact that according to our classification, none of the CeMT isoforms display proper Cu-thionein features, although certainly Cu(I)-CeMT2 complexes are more stable than Cu(I)-CeMT1 species.

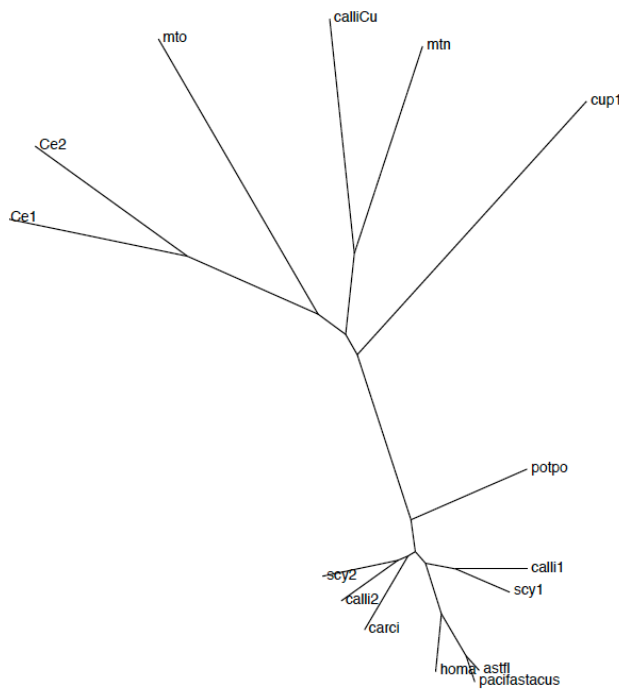
In relation to the metal complex architecture, our results are compatible with a two-domain folding when coordinating Zn(II), Cd(II), or Cu(I) ions, defining N-terminal and C-terminal segments with additive metal binding capacity but not additive structural features, in relation to the full-length polypeptides. It is worth noting that, the precise differences in metal binding abilities

between isoforms arise from their highly dissimilar C-terminal moieties, in concordance with their amino acid sequence differences and peculiarities, *i.e.* a longer CtCeMT1 with one Cys and three His extra residues in relation to CtCeMT2. Hence, CeMT1 is able to bind seven divalent metal ions, while CeMT2 only yields M(II)₆-species. In the case of zinc, this implies Zn₇-CeMT1 *vs.* major Zn₆-CeMT2 complexes, but significantly, for cadmium this entails Cd₆Zn₁-CeMT1 *vs.* Cd₆-CeMT2 species. This Zn(II) ion in Cd₆Zn₁-CeMT1 probably plays a structural role, because even a clear excess of Cd(II) is unable to remove it from the complex. A step further of our results allows proposing that CeMT1 and CeMT2 histidine residues not only participate in metal coordination, but are the main responsible of their metal binding behavior. In CeMT1, all data points to the contribution of three out of four histidines,

probably excluding the C-terminal His, in the coordination of the seventh M(II) ion, precisely the Zn(II) of Cd₆Zn₁-CeMT1. Unfortunately, this Zn-NHis coordination is not detectable by spectropolarimetric methods. In the case of CeMT2, the unique C-terminal histidine seems to have no major role for divalent metal coordination, although some hints suggest a partial participation in a subset of the metal complexes present in our preparations.

Discussion of the Cu(I) coordination behavior becomes more complex in view of the difficulties to calculate the exact Zn(II) and Cu(I) stoichiometry of the corresponding species by ESI-MS. However, and in spite of this drawback, the sole analysis of the presence/absence of Zn(II) ions in the recombinant complexes synthesized in copper supplemented cultures provides enough information to confirm that histidines are determinants of the presence of Zn(II), and

A)



B)

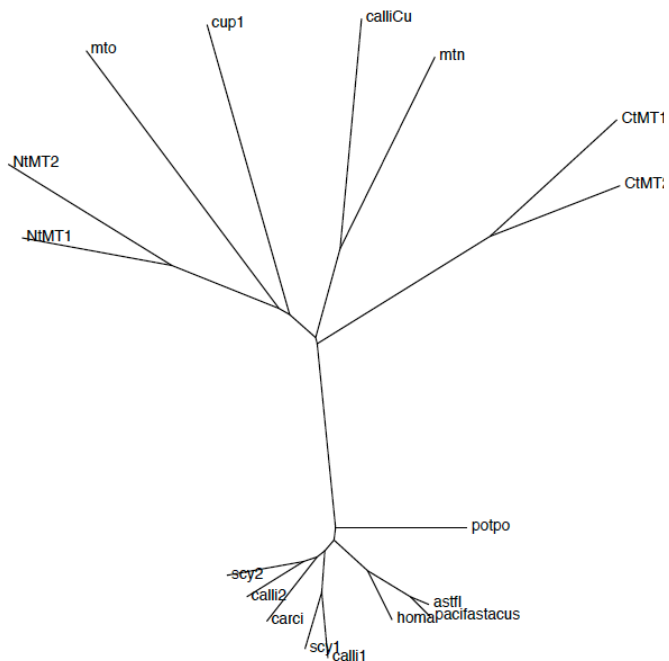


Figure 8- Protein distance trees of CeMT1, CeMT2 and N-terminal and C-terminal separate moieties. Neighbor-Joining trees constructed with the entire CeMT1 (Ce1) and CeMT2 (Ce2) polypeptides (A) and with their N-terminal and C-terminal separate moieties (NtMT1, NtMT2, CtMT1 and CtMT2) (B). Protein sequences were aligned by ClustalW, and the alignments were used as inputs to construct Neighbor-Joining trees, by the Fitch-Margoliash algorithm (Phylip package), as described in [33]. MT abbreviations are: Call1, Call2 and CalliCu, *Callinectes sapidus*, 1, 2 and copper isoforms, respectively; Scy1 and Scy2, *Scylla serrata* isoforms 1 and 2; Carci, *Carcinus maenas*; Astfl, *Astacus astacus*; Pacifastacus, *Pacifastacus leniusculus*; Homa, *Homarus americanus*; Potpo, *Potamon potamios*; Cup1, *Saccharomyces cerevisiae* Cup1; Mtn, *Drosophila melanogaster* MtnA; and Mto, *Drosophila melanogaster* MtnB.

therefore of the Zn- or Cu-thionein character of the polypeptides. Hence, the two full-length peptides, CeMT1 and CeMT2 give rise to mixtures of complexes, with major species of relative low nuclearity (M_8 - and M_9 -CeMT). The behavior of the respective N-terminal moieties is clear and similar, yielding homonuclear Cu₅-complexes, and thus the N-terminal peptides constitute typical Cu-thioneins although of low Cu(I):MT ratio (5:1 for a 9-Cys MT). Contrarily, the His-containing CtCeMT moieties both render Zn,Cu-heteronuclear complexes, even of lower Cu(I):MT ratio than the N-terminal segments (4:1 for 14 or 10 coordinating residues in CtCeMT1 and CtCeMT2, respectively), therefore tending to a Zn-thionein behavior. The presence of Zn(II) in CtCeMT1 was clearly evidenced after detection of a Cu₄Zn₁-CtCeMT1 species. This is a new case, comparable to the mammalian MT1 isoform, where the combination of a Cu-thionein domain (β MT1) with a Zn-thionein fragment (α MT1) renders a full-length MT with Zn-thionein character [32]. Furthermore, the character of Zn-thionein of CeMT2 could be neatly attributable to its C-terminal histidine, since the corresponding Δ HisCeMT2 mutant was capable of folding into homonuclear Cu(I) complexes in the presence of supplemented copper, which the wild type form was not. In conclusion, the presence of their His residues precludes these MTs of behaving as Cu-thioneins, as would otherwise correspond to them according to their global protein sequence similarities. Precisely these analyses (Fig. 8), which we have shown to yield consistent results with the metal binding preferences of other MTs [6,33] position both entire CeMT1 and CeMT2 peptides, as well as their moieties, in the subset of Cu(I)-thioneins. According to our metal binding preference analysis, this is true for the N-terminal fragments and Δ HisCeMT2, nearly true for the C-terminal moieties, but is obviously not the case for the entire CeMTs. Definitely, the CeMT system analysis has revealed noteworthy metal-coordination peculiarities, mainly derived from the unusual presence of histidines in their protein sequences, which enlarges the list of MTs where this amino acid plays a decisive role [34,35]. Therefore, the ultimate details will be undoubtedly revealed when the 3D structures of the corresponding metal complexes are available.

MATERIALS & METHODS

Construction of the expression vectors for the *C. elegans* MT1 (CeMT1) and MT2 (CeMT2) wild type and mutant forms

All the metal-MT complexes studied in this work were recombinantly synthesized in *E. coli* through cloning of their cDNAs into the pGEX-4T2 plasmid (GE Healthcare), to yield primary GST-MT fusions from which the corresponding metal-MT complexes were subsequently purified [24].

Three λ ZAPII phage clones (yk120h8, yk364c6 and yk656b5), including cDNAs for *C. elegans* MT1, were kindly provided by Dr. Y. Kohara, from the Genome Biology unit of the National Institute of Genetics, Mishima, Japan. For the expression of the whole length CeMT1 peptide, the corresponding ORF was amplified by a PCR reaction that respectively added a *Bam*H I and a *Sall* site to the 5' and 3' ends of the coding sequence, using purified CeMT1- λ ZAPII DNA as template and the following primers: 5'-GGCGGATCCATGGCTG-CAAGTGT-3' (upstream) and 5'-GTTTCGTCG-ACTT AATGAGCCGCAGCAGT-3' (downstream). cDNAs encoding for the independent CeMT1 moieties were obtained by PCR amplification with the following primers: for the N-terminal fragment (residues 1 to 27), 5'-CGTG-GATCCATGGCTTGCAAGTGT-3' (upstream) and 5'-GCTCGAGTCGACTTACTCACAAACA-CTTGTC-3' (downstream); and for the C-terminal fragment (residues 28 to 75), 5'-CCGCGT-GGATCCAAGTACTGCTGT-3' (upstream) and 5'-CGACTCGAGTTAATGAGCCGCAGC-3' (downstream). Note that the C-terminal fragment was inserted in pGEX by a 3'-introduced *Xho*I site instead of *Sall* due to repeated cloning problems when using the latter.

The synthetically constructed CeMT2 cDNA [19] was kindly provided by Prof. J. H. R. Kägi, from the Institute of Biochemistry of the University of Zürich, Switzerland, and used also as a template for the construction of regions coding for the deletion mutant Ce Δ His and the independent N-terminal and C-terminal CeMT2 domains. All the PCR reactions were designed to introduce 5' *Bam*H I and 3' *Sall* restriction sites for subcloning purposes. The wild type CeMT2 cDNA was amplified using as upstream primer: 5'-CGGGGATCCATGGTCTGC-AAG-3' and as downstream primer: 5'-ACGCG-TCGACC TAATGAGCAGC-3'. The region coding for the N-terminal CeMT2 segment, encompassing from Met1 to Glu30, was amplified using as upstream primer 5'-CGGGGATCCATGGTCTGC-AAG-3' and as downstream primer 5'-ACGCGTC-GACCTACTCACAGCACTG-3'. The region coding for the C-terminal CeMT2, which comprises from the Gln31 to the His63 CeMT2 residues, was amplified with the upstream primer 5'-CGGGGATCCCAGTACTGCTGC-3' and the downstream primer 5'-ACGCGTCGACCTAATG-

AGCAGC-3'. For the construction of a cDNA encoding the CeMT2 peptide lacking its C-terminal His residue, the wild type cDNA was amplified using the same upstream primer than for the entire cDNA (5'-CGGGGATCCATGGTCTGCAAG-3') but 5'-ACGCCTCGACCTAACGAGCCTG-3' as downstream primer.

All the PCR reactions consisted in 30-cycle amplifications, performed with 1 U of thermo resistant Vent DNA polymerase (New England Biolabs), 0.2 mM dNTPs and 100 pmols of the required primers at 2 mM MgCl₂ (final concentration), in a final 100 µl volume, under the following conditions: 45 s at 95 °C (denaturation), 30 s at 55-60 °C (hybridization) and 45 s at 72 °C (elongation). Elongation conditions were maintained during 5 minutes after the 30 cycles. The final products were analyzed by agarose gel electrophoresis/ethidium bromide staining; the band with the expected size was excised and subcloned into the pGEX-4T2 vector. Before recombinant protein synthesis, all coding sequences were confirmed by automated DNA sequencing. To this end, the pGEX-derived constructions were transformed in *E. coli* DH5α cells, and sequenced using the ABI PRISM Dye Terminator-Cycle Sequencing Ready reaction kit (Perkin Elmer) in an Applied Biosystems ABI PRISM 310 Automatic Sequencer. In all cases the expected sequence was corroborated, but for the position 26 of CeMT1 peptide, which corresponded to an AGG (Arg) instead of the reported AAG (Lys) codon. All the CeMT1 clones sequenced showed the same alteration, this suggesting that a polymorphism, in relation to the published sequence is the most likely explanation. Taking into account the conservative nature of this change and the fact that we had recently established that an opposite charge substitution (Lys for Glu, position 34) had no effect at all in the binding abilities of the Crs5 MT of *S. cerevisiae* [11], we decided to continue our studies with the obtained clones.

Recombinant synthesis and purification of the *C. elegans* MT1 (CeMT1) and MT2 (CeMT2) wild type and mutant forms

The obtained pGEX constructs were transformed into *E. coli* BL21 cells for the expression of the cloned cDNAs as fusions with Glutathione-S-Transferase (GST). The recombinant peptides were biosynthesized in 3 l-LB cultures, inoculated with 300 ml of overnight pre-cultures. Induction with isopropyl β-D-thiogalactopyranoside (IPTG) was performed at OD₆₀₀= 0.8, and cultures were further grown for 3 h in the presence of 500 µM CuSO₄, 300µM ZnCl₂, or 300µM CdCl₂, in order to recover

the corresponding Cu-, Zn- or Cd-MT complexes, respectively. Copper-supplemented cultures were grown in two different conditions (normal and low aeration), in view of the reported influence of oxygenation in the recovered final complexes (see [11] for details). Cells were harvested by centrifugation (Sorvall RC5C, 15 min at 9600 x g), resuspended in PBS x1 and lysed by sonication (Branson Sonifier 250, 0.6Hz) in the presence of 0.5% β-mercaptoethanol, to avoid protein oxidation. From this step on, all procedures were carried out using Ar (pure grade 5.6)-saturated buffers. After sonication, cellular debris was pelleted by centrifugation (20 min at 20000 x g) and the GST-MT fusions isolated from the supernatant by Glutathione-Sepharose 4B (GE Healthcare) affinity chromatography. Metal-MT complexes were excised from the fusion constructs by thrombin cleavage and batch affinity chromatography. Sample concentration was attained by several rounds of centrifugation in Centriprep Microcon 3 (Amicon). The metal-MT complexes were finally purified through FPLC in a Superdex75 (GE Healthcare) column equilibrated with 50 mM Tris-HCl, pH 7.0. Selected fractions were kept at -70 °C until further use.

Analysis and characterization of the recombinant metal peptide complexes

The S, Zn, Cd and Cu content of the Zn-, Cd- and Cu-CeMT preparations was analyzed by means of Inductively Coupled Plasma Atomic Emission Spectroscopy (ICP-AES) in a Polyscan 61E (Thermo Jarrell Ash) spectrometer, measuring S at 182.040 nm, Zn at 213.856 nm, Cd at 228.802 and Cu at 324.803 nm. Samples were prepared following the method described elsewhere [36], and in parallel were also incubated in 1 M HCl at 65 °C for 5 min prior to measurements in order to eliminate possible traces of labile sulfide ions [37]. In all cases, protein concentration was calculated from the acid ICP-AES sulfur measure, assuming that the sulfur content of the sample was contributed by the MT peptides, that is, 20 S/mol for CeMT1 (1 Met, 19 Cys), 19 S/mol for CeMT2 or ΔHisCeMT2 (1 Met, 18 Cys), 10 S/mol for NtCeMT1 and NtCeMT2 (1 Met, 9 Cys), 10 S/mol for CtCeMT1 (10 Cys) and 9 S/mol for CtCeMT2 (9 Cys).

***In vitro* Zn-, Cd- and Cu-binding studies of CeMT1 and CeMT2**

The titration of all Zn-CeMT complexes with Cd(II) or Cu(I) at pH 7 were carried out following the procedures previously described [38,39]. The *in*

vitro acidification/reneutralization experiments were also performed adapting a previously reported procedure [40]. Essentially, 10 µM preparations of the Cd-peptides were acidified from neutral pH (7.0) to acid pH (2.0) with 1–10⁻³ M HCl depending on the stage of the titration. CD and UV-vis spectra were recorded at pH 7.0, 4.5, 4.0, 3.0 and 2.0 both immediately after acid addition and 10 min later, always with identical results. Finally, the samples were kept at pH 2.0 for 20 min and then they were reneutralized to pH 7.0 with 1–10⁻³ M NaOH, also depending on the stage of the titration. CD and UV-vis spectra were recorded at pH 2.0, 2.5 and 7.0. All the results were corrected for dilution effects. During all experiments strict oxygen-free conditions were kept by saturation of the solution with Ar.

Spectroscopic measurements

A Jasco spectropolarimeter (Model J-715) interfaced to a computer (J700 software) was used for CD measurements at a constant temperature of 25 °C maintained by a Peltier PTC-351S apparatus. Electronic absorption measurements were performed on an HP-8453 Diode array UV-visible spectrophotometer. All spectra were recorded with 1 cm capped quartz cuvettes, corrected for the dilution effects and processed using the GRAMS 32 programme.

ElectroSpray Ionization Time-Of-Flight Mass Spectrometry (ESI-TOF-MS) analyses

Molecular mass determinations were performed by ESI-TOF-MS in a MicroTof-Q instrument (Bruker). Calibration was attained with NaI (0.2 g NaI in 100 mL of a 1:1 H₂O/isopropanol mixture). Divalent metal-protein samples were analyzed under the following conditions: 20 µL of the sample were injected through a PEEK (polyether heteroketone) column (1.5 m x 0.18 mm i.d.) at 40 µL/min at the following conditions: capillary counterelectrode voltage, 5000 V; dry temperature, 90–110 °C; dry gas, 6 L/min; m/z range, 800–2000. The running buffer was a mixture of 5:95 mixture of acetonitrile and 15 mM ammonium acetate/ammonia, pH 7. The monovalent metal-protein samples were analyzed as follows: 20 µL of sample were injected at 30 µL/min at the following conditions: capillary counterelectrode voltage, 4000 V; dry temperature, 80 °C; dry gas, 6 L/min; m/z, range 800–2000. The running buffer was a mixture of 10:90 mixture of acetonitrile and 15mM ammonium acetate/ammonia, pH 7. It is worth noting that while it is possible to determine the Zn:Cd:MT ratio in the heterometallic Zn,Cd-CeMT

species, the proximity between the atomic weights of zinc and copper and the ESI-MS experimental error range prevents the determination of the Zn:Cu ratio in the heterometallic Zn,Cu-CeMT species, although ESI-MS analysis of the samples at acid pH allows to delimit the Cu-species present in the sample. For the analysis of the apo-MT forms, obtained from recombinant Zn-MT forms, and of the heterometallic Zn,Cu-MT species, 20 µL of the sample at pH 7 were injected under the same conditions described for the holo-forms, with the following exceptions in order to release Zn(II) ions but not Cu(I) ions from the complexes: the liquid carrier was a 5:95 mixture of acetonitrile and ammonium formate/ammonia at pH 2.4. All samples were injected at least twice in order to ensure reproducibility. In all cases, molecular masses were calculated in accordance with [11,41].

Diethyl pyrocarbonate protein modification assays

Covalent modification experiments with DEPC were performed for 30–120 min at pH 7 under a molar excess of DEPC in order to avoid both the hydrolysis of DEPC (half time of 9 min at 25 °C and pH 7) and/or additional carboxyethylation of His at (δ)-N position, following [42]. Therefore, a fresh DEPC solution in absolute ethanol (DEPC:ethanol 1:200) was allowed to react with a 100 µL solution of the tested metal-CeMT complexes (ranging from 0.2x to 2.1x10⁻⁴ M) in 50 mM Tris-HCl buffer, pH 7.0, for 20 min at room temperature. The resulting DEPC:protein ratios used were 8:1 for Zn(II)-CeMT1 and Cd(II)-CeMT1 and 5:1 for Zn(II)-and Cd(II)-CeMT2, Zn(II)- and Cd(II)-CtCeMT1 and Zn(II)- and Cd(II)-CtCeMT2. Additionally, Zn(II)-ΔHisCeMT2 and Cd(II)-NtCeMT1 were also incubated with 5 molar equivalents of DEPC under the same conditions and used as negative controls, due to the lack of His in their sequence. After incubation, all samples were immediately analyzed by ESI-TOF MS, as described above.

Note: Any further information about the spectroscopic and/or spectrometric data recorded on the study of the CeMT peptides and not included in the manuscript, are available upon e-mail request to the authors.

Acknowledgements

This work was supported by Spanish Ministerio de Ciencia y Tecnología grants BIO2006-14420-C02-

01 to S. Atrian, and BIO2006-14420-C02-02 to M. Capdevila. R.O. received a pre-doctoral fellowship from the *Departament de Química, Universitat Autònoma de Barcelona*. We are grateful to Dr. Y. Kohara (Genome Biology, National Institute of Genetics, Mishima, Japan) for sending us the CeMT1 cDNA. We are deeply indebted to Prof. J. Kägi (Institute of Biochemistry of the University of Zürich, Switzerland) for the CeMT2 cDNA, as well as for communication of unpublished results and fruitful discussions. We thank the *Serveis Científico-Tècnics de la Universitat de Barcelona* (GC-FPD, ICP-AES, DNA sequencing) and the *Servei d'Anàlisi Química (SAQ) de la Universitat Autònoma de Barcelona* (CD, UV-vis, ESI-MS) for allocating instrument time. We are also grateful to Prof. Claudio Fernández (Universidad Nacional de Rosario, Argentina) who advised us for DEPC modification of His residues.

REFERENCES

- 1 Stürzenbaum SR (2009) Earthworm and nematode metallothioneins. In: *Metal Ions in Life Sciences: Metallothioneins and Related Chelators* (Sigel A, Sigel H & Sigel RKO, eds.), pp 183-198. RSC, Cambridge, U.K.
- 2 Metal Ions in Life Sciences; vol 5: Metallothioneins and Related Chelators, (2009) (Sigel A, Sigel H & Sigel RKO, eds.), pp 1-514. RSC, Cambridge.
- 3 Gold B, Deng H, Bryk R, Vargas D, Eliezer D, Roberts J, Jiang X & Nathan C (2008) Identification of a copper-binding metallothionein in pathogenic mycobacteria. *Nature Chem Biol* **4**, 609-616.
- 4 Palmiter R (1998) The elusive function of metallothioneins. *Proc Natl Acad Sci USA* **95**, 8428-8430.
- 5 Robinson NJ (2008) A bacterial copper metallothionein. *Nature Chem Biol* **4**, 582-583.
- 6 Valls M, Bofill R, Gonzalez-Duarte R, Gonzalez-Duarte P, Capdevila M & Atrian S (2001) A new insight into metallothionein (MT) classification and evolution. The *in vivo* and *in vitro* metal binding features of *Homarus americanus* recombinant MT. *J Biol Chem* **276**, 32835-32843.
- 7 Bofill R, Capdevila M & Atrian S (2009) Independent metal-binding features of recombinant metallothioneins convergently draw a step gradation between Zn- and Cu-thioneins. *Metallomics*, DOI:10.1039/B904953C.
- 8 Egli D, Domènech J, Selvaraj A, Balamurugan K, Hua H, Capdevila M, Georgiev O, Schaffner W & Atrian S (2006) The four members of the *Drosophila* metallothionein family exhibit distinct yet overlapping roles in heavy metal homeostasis and detoxification. *Genes to Cells* **11**, 647-658.
- 9 Orihuela R, Domènech J, Bofill R, You C, Mackay EA, Kägi JHR, Capdevila M & Atrian S (2008) Metal-binding features of a polyvalent metallothionein: the recombinant mussel *Mytilus edulis* MT-10-IV. *J Biol Inorg Chem* **13**, 801-812.
- 10 Domènech J, Bofill R, Tinti A, Torreggiani A, Atrian S & Capdevila M (2008) Comparative insight into the Zn(II)-, Cd(II)- and Cu(I)-binding features of the protozoan *Tetrahymena pyriformis* MT1 metallothionein. *Biochim Biophys Acta* **1784**, 693-704.
- 11 Pagani A, Villarreal L, Capdevila M & Atrian S (2007) The *Saccharomyces cerevisiae* Crs5 metallothionein metal-binding abilities and its role in response to zinc overload. *Molec Microbiol* **63**, 256-269.
- 12 Maruyama K, Hori R, Nishihara T & Kondo M (1986) Isolation and characterization of metallothionein from nematode (*Caenorhabditis elegans*). *Eisei Kagaku* **32**, 22-27.
- 13 The *C. elegans* Sequencing Consortium (1998) Genome sequence of the nematode *C. elegans*: a platform for investigating biology. *Science* **282**, 2012-2018.
- 14 Freedman JH, Slice LW, Dixon D, Fire A & Rubin CS (1993) The novel metallothionein genes of *Caenorhabditis elegans* – Structural organization and inducible, cell-specific expression. *J Biol Chem* **268**, 2554-2564.
- 15 Slice LW, Freedman JH & Rubin CS (1990) Purification, characterization, and cDNA cloning of a novel metallothionein-like, cadmium binding protein from *Caenorhabditis elegans*. *J Biol Chem* **265**, 256-263.
- 16 Imagawa M, Onozawa T, Okumura K, Osada S, Nishihara T & Kondo M (1990) Characterization of metallothionein cDNAs induced by cadmium in the nematode *Caenorhabditis elegans*. *Biochem J*, **268**, 237-240.
- 17 Liao VHC & Freedman JH (1998) Cadmium-regulated genes from the nematode *Caenorhabditis elegans* –identification and cloning of new cadmium-responsive genes by differential display. *J Biol Chem* **273**, 31962-31970.
- 18 Swain SC, Keusekotten K, Baumeister R & Stürzenbaum SR (2004) *C. elegans* metallothioneins: new insights into the phenotypic effects of cadmium toxicosis. *J Mol Biol* **341**, 951-959.
- 19 You C, Mackay EA, Gehrig PM, Hunziker PE & Kägi JHR (1999) Purification and characterization of recombinant *Caenorhabditis elegans* metallothionein. *Arch Biochem Biophys* **372**, 44-52.
- 20 Gehrig PM, You C, Dallinger R, Gruber C, Brouwer M, Kägi JHR & Hunziker PE (2000) Electrospray ionization mass spectrometry of Zn, Cd and Cu

- metallothioneins: Evidence for metal-binding cooperativity. *Protein Science* **9**, 395-402.
- 21 Hugues S & Stürzenbaum SR (2007) Single and double metallothionein knockout in the nematode *C. elegans* reveals cadmium dependant and independent toxic effects on life history traits. *Environ Pollut* **145**, 395-400.
- 22 Vamataniuk OK, Bucher EA, Ward JT & Rea PA (2001) A new pathway for heavy metal detoxification in animals. Phytochelatin synthase is required for cadmium tolerance in *Caenorhabditis elegans*. *J Biol Chem* **276**, 20817-20820.
- 23 Liao VHC, Dong J & Freedman JH (2002) Molecular Characterization of a novel, cadmium-inducible gene from the nematode *Caenorhabditis elegans*. A new gene that contributes to the resistance to cadmium toxicity. *J Biol Chem* **277**, 42049-42059.
- 24 Cols N, Romero-Isart N, Capdevila M, Oliva B, González-Duarte P, González-Duarte R & Atrian S (1997) Binding of excess cadmium(II) to Cd₇-metallothionein from recombinant mouse Zn₇-metallothionein 1. UV-VIS absorption and circular dichroism studies and theoretical location approach by surface accessibility analysis. *J Inorg Biochem* **68**, 157-166.
- 25 Domènech J, Palacios O, Villarreal L, González-Duarte P, Capdevila M & Atrian S (2003) MTO: the second member of a *Drosophila* dual copper-thionein system. *FEBS Lett.* **533**, 72-78.
- 26 Torreggiani A, Domènech J, Atrian S, Capdevila M & Tinti A (2008) Raman study of *in vivo* synthesized Zn(II)-metallothionein complexes: structural insight into metal clusters and protein folding. *Biopolymers* **89**, 1114-1124.
- 27 Li C & Rosenberg RC (1993) Carbethoxylation of coordinated histidine by diethylpyro-carbonate. *J Inorg Biochem* **51**, 727-735.
- 28 Miles EW (1977) Modification of histidyl residues in proteins by diethylpyrocarbonate. *Methods Enzymol* **47**, 431-442.
- 29 Qin K, Yang Y, Mastrangelo P & Westaway D (2002) Mapping Cu(II) binding sites in prion proteins by diethyl pyrocarbonate modification and matrix-assisted laser desorption ionization-time of flight (MALDI-TOF) mass spectrometric footprinting. *J Biol Chem* **277**, 1981-1990.
- 30 Binolfi A, Lamberto GR, Duran R, Quintanar L, Bertoncini CW, Souza JM, Cerveñansky C, Zweckstetter M, Griesinger C & Fernández CO (2008) Site-specific interactions of Cu(II) with alpha and beta-synuclein: bridging the molecular gap between metal binding and aggregation. *J Am Chem Soc* **130**, 11801-11812.
- 31 Calafato S, Swain S, Hughes S, Kille P & Stürzenbaum S (2008) Knock down of *Caenorhabditis elegans* cutc-1 exacerbates the sensitivity toward high levels of copper. *Toxicol Sci* **106**, 384-391.
- 32 Bofill R, Capdevila M, Cols N, Atrian S, González-Duarte P (2001) Zn(II) is required for the *in vivo* and *in vitro* folding of mouse Cu-metallothionein in two domains. *J Biol Inorg Chem* **6**, 405-417.
- 33 Tio L, Villarreal L, Atrian S & Capdevila M (2004) Functional differentiation in the mammalian Metallothionein gene family. *J Biol Chem* **279**, 24403-24413.
- 34 Leszczyszyn OI, Schmid R & Blindauer CA (2007) Toward a property/function relationship for metallothioneins: histidine coordination and unusual cluster composition in a zinc-metallothionein from plants. *Proteins* **68**, 922-935.
- 35 Villarreal L, Tio L, Capdevila M & Atrian S (2006) Comparative metal binding and Genomics analysis of the avian (chicken) Metallothionein vs. mammalian forms. *FEBS J* **273**, 523-535.
- 36 Bongers J, Walton CD, Richardson DE & Bell JU (1988) Micromolar protein concentrations and metalloprotein stoichiometries obtained by inductively coupled plasma. Atomic emission spectrometric determination of sulfur. *Anal Chem* **60**, 2683-2686.
- 37 Capdevila M, Domènech J, Pagani A, Tío L, Villarreal L & Atrian S (2005) Zn- and Cd-metallothionein recombinant species from the most diverse phyla may contain sulfide (S²⁻) ligands. *Angew Chem Int Ed* **44**, 4618-4622.
- 38 Capdevila M, Cols N, Romero-Isart N, Gonzalez-Duarte R, Atrian S & Gonzalez-Duarte P (1997) Recombinant synthesis of mouse Zn₃-β and Zn₄-α metallothionein 1 domains and characterization of their cadmium(II) binding capacity. *Cell Mol Life Sci* **53**, 681-8.
- 39 Bofill R, Palacios O, Capdevila M, Cols N, González-Duarte R, Atrian S & González-Duarte P (1999) A new insight into the Ag⁺ and Cu⁺ binding sites in the metallothionein β domain. *J Inorg Biochem* **73**, 57-64.
- 40 Domènech J, Orihuela R, Mir G, Molinas M, Atrian S & Capdevila M (2007) The Cd(II)-binding abilities of recombinant *Quercus suber* metallothionein, QsMT: bridging the gap between phytochelatins and metallothioneins. *J Biol Inorg Chem* **12**, 867-882.
- 41 Fabris D, Zaia J, Hathout Y & Fesenlau C (1996) Retention of thiol protons in two classes of protein zinc ion coordination centers. *J Am Chem Soc* **118**, 12242-12243.
- 42 Mendoza VL & Vachet RW (2008) Protein Surface Mapping Using Diethylpyrocarbonate with Mass Spectrometric Detection. *Anal Chem* **80**, 2895-2904.

ARTICLE 4

Cup1 revisited: divalent metal ion binding analysis unveils the presence of acid labile (S^{2-}) ligands in native complexes

Manuscrit in preparació

CUP1 REVISITED: DIVALENT METAL ION BINDING ANALYSIS UNVEILS THE PRESENCE OF ACID-LABILE SULFIDE (S^{2-}) LIGANDS IN NATIVE COMPLEXES**

Rubén Orihuela⁺, Freddy Monteiro⁺, Ayelen Pagani, Sílvia Atrian and Mercè Capdevila*

Abstract

Metallothioneins (MTs) are ubiquitous, small, cysteine-rich metal-binding proteins, (1) which can be differentiated in two types according to their metal preferences: Zn-thioneins (extensively, *divalent-metal ion-thioneins*) and Cu-thioneins (2). The expression of their genes is also differently regulated, in accordance with the function that the encoded product will have to deal with: the former being commonly cadmium-inducible and the latter either constitutive or copper-inducible. In a previous work we demonstrated that acid-labile sulfide ligands (S^{2-}) are present in divalent-metal-MT complexes when recombinantly constituted in *E.coli* (3). From these studies it was clear that S^{2-} ligands were only detected in the complexes formed with divalent metals and not with monovalent metal ions (Cu) and that the amount of S^{2-} was always much higher in the Cd- than in the Zn-complexes. Also, and in concordance with data gathered when studying distinct MTs, the higher the Cu-thionein character of an MT, the richer in S^{2-} ligands will be their complexes with divalent metals, which could be interpreted as that the sequence is optimized for Cu(I) binding and it needs of additional ligands to fulfill the requirements of tetrahedral coordination (4). About the effects of the presence of sulfide, there are some possibilities to be considered; either it is beneficial and has a metabolic function, for example homeostasis and/or transport of S^{2-} in the organisms that would be carried out by zinc-containing complexes of Cu-thioneins synthesized in basal conditions; or it could be harmful and, for this reason, the synthesis of Cu-thioneins is strictly regulated and they are not synthesized upon cadmium induction (*cf.* yeast, snail, others...). In this sense, we have published a recent work showing that S^{2-} -containing Cd-MT complexes under reductive stress could cause damage to the cell membrane (5).

The significance of this finding remained

[*] Dr. M. Capdevila*, R. Orihuela⁺
Departament de Química
Facultat de Ciències
Universitat Autònoma de Barcelona
08193 Bellaterra, Barcelona (Spain)
Fax: +93 581 31 01
e-mail: merce.capdevila@uab.es

Prof. S. Atrian, Dr. A. Pagani, F. Monteiro⁺
Departament de Genètica
Facultat de Biologia
Universitat de Barcelona
Av. Diagonal 645, 08028 Barcelona (Spain)

[+] These two authors contributed equally to this work

[**] This work was financially supported by the Spanish Ministerio de Ciencia e Innovación, through the grants BIO2006-14420-C02-01 and BIO2006-14420-C02-02 to S. Atrian and M. Capdevila, respectively. We are indebted to Prof. Dennis Winge (University of Utah, USA) for providing us with the *S. cerevisiae* N301 strain (first isolated in Prof. Tetsuo Murayama's laboratory, Matsuyama, Japan), as well as for continuous exchange of ideas.

questionable, due to the possibility that the sulfide ligands could be merely due to the synthesis in heterologous prokaryotic environments. For this reason it should be investigated whether MTs exhibited this behavior also when synthesized in their native organisms. Thus, and in relation of the above exposed statements, a case of an extreme copper-thionein should be the ideal system to demonstrate if S²⁻ ligands are also present in native metal-MT complexes. The yeast *S. cerevisiae* Cup1 peptide, isolated in the seventies (6,7), has been accepted, by general assent, as the paradigmatic Cu-thionein. It was sequenced in the eighties, their copper-binding abilities deeply characterized (8,9) and the 3D structure of the Cu-Cup1 complexes finally solved few years ago, settling what the authors qualified as a *long lasting enigma* (10). Since wild-type yeasts only synthesize Cup1 under Cu excess, we used a yeast mutant strain (301N), where a transcription factor mutation enables a high Cup1 expression in cells grown in excess of cadmium (11,12). Hence, we undertook the global goal of studying the Zn(II), Cd(II) and Cu(I) binding abilities of Cup1 through the characterization of the Zn-, Cd- and Cu-complexes formed both *in vivo* (recombinantly in *E. coli*) and *in vitro* (by metal replacement), and the comparison with the native Cd-Cup1 complexes also purified in this work (from N301 *S. cerevisiae*). Therefore, this study allowed us also to answer the long-standing question about the universality of S²⁻ ligands in metal-MT complexes: is it a mere consequence of recombinant *E. coli* synthesis, or is it also a *native* trait, unnoticed before?

EXPERIMENTAL PROCEDURES

Recombinant Synthesis and Purification of Metal-Cup1 Complexes in E. coli- The CUP1 coding region was amplified by direct PCR on genomic *Saccharomyces cerevisiae* DNA extracted from the VC-sp6 strain (*MATa trp1-1 ura3-52 ade- his- CAN^R gall leu2-3,112 cup1^S*) (13), using the following primers: upstream 5' ATTGGATCCAAAATGAAGGT 3' and downstream 5' AGACTAGTCGACTCATTTCCAGA 3'. The former introduced a *BamHI* site immediately before the CAA codon (Gln), while the latter created a *SalI* site immediately after the translation stop codon. Thus, the amplified cDNA coded for a polypeptide equivalent to the mature, N-term processed form of Cup1. The 35-cycle PCR amplification -30 s at 94 °C

(denaturing), 30 s at 58 °C (annealing) and 30 s 72 °C (extension) was carried out in a total volume of 100 µl, comprising 2 µL of 25 mM dNTP mixture, 2 µl of 20 µM primer solution, 1 u of GoTaq Flexi DNA polymerase (Promega) and 100 ng of the template DNA. The PCR product was isolated from a 2% agarose gel, digested with *BamHI-SalI* (New England Biolabs), and directionally inserted in the pGEX-4T-1 (Amersham GE Healthcare) expression vector for the synthesis of a glutathione-S-transferase fusion protein (GST-Cup1). Ligations were performed with the TAKARA DNA ligation kit (v2.1), and the ligation mixture was used to transform first *E. coli* DH5α cells. The GST-CUP1 construct was prepared from these transformants in order to be automatically sequenced (Applied Biosystems ABIPRISM 310; PerkinElmer), using the BigDye terminator v3.1 kit (ABI Biosystems). Hereafter, the expression plasmid was transformed into the *E. coli* BL21 protease-deficient strain for recombinant over expression. Cultures for preparative purposes were grown in 1.5-L Erlenmeyer flasks. To this end, overnight, saturated cultures of transformed BL21 cells served to inoculate (at 10% v/v) 3-liter or 5-liter of fresh LB medium (0.5% Bacto yeast extract, 1% Bacto tryptone (Becton, Dickinson and Co.), 1% NaCl (Merck), pH 7.3) supplemented with 100 mg/l ampicillin (Roche). Induction with isopropyl β-D-thiogalactopyranoside (IPTG) (Promega) at 200 µM final concentration was performed at OD600=0.6, and cultures were grown for 30 min before the addition of either 300 µM ZnCl₂, 300 µM CdCl₂ or 500 µM CuSO₄ (Merck). After 3 h of incubation at 37 °C, cells were harvested by 7-min centrifugation at 9644 xg (Sorvall RC5C). For protein purification, cells were resuspended in 5% of the original volume of ice-cold PBS buffer (1.4 M NaCl, 27 mM KCl, 101 mM Na₂HPO₄ and 18 mM KH₂PO₄) and 0.5% (v/v) β-mercaptoethanol (Sigma) was added to avoid protein oxidation. Cells were lysed by sonication (Branson Sonifier 250, 0.6 Hz) at 4 °C with 0.6 s pulses for 8 min. From this step onwards, all procedures were carried out on Argon (pure grade 5.6) saturated buffers. After sonication, cell debris was pelleted by centrifugation (45 min at 17212 xg) and the supernatant was recovered to purify the GST-Cup1 fusion by batch affinity chromatography, with Glutathione-Sepharose 4B (GE Healthcare Bio-Sciences) at a 1:10 matrix/sample volume ratio. The mixture was gently agitated at room temperature for 1 h

and washed three times in PBS. A 10 μ g/ml solution of thrombin in PBS was added to the matrix bed to separate the Cup1 portion from the fusion protein, and digestion was allowed to occur overnight at 22–25 °C. Since the GST portion of the fusion protein remained bound to the matrix, the supernatant contained the metal-Cup1 complexes and thrombin. This solution was concentrated with Centriprep Concentrators (Amicon) with a 3-kDa cut-off and the Cup1 complexes were finally purified to homogeneity by Fast Performance Liquid Chromatography (FPLC) using a Superdex75 10/300 GL column (Pharmacia), equilibrated with 50 mM Tris-HCl pH 7.0, and run at 0.7 ml/min. The eluate absorbance was followed at 254 nm, protein-containing fractions were pooled, and aliquots of 200 μ L were kept at -80 °C until further use. More details on recombinant Cup1 synthesis can be found in our previous manuscript reporting the characterization of Crs5, the other yeast MT (14).

Purification of native Cd(II)-Cup1 complexes- The cadmium-resistant 301N *Saccharomyces cerevisiae* strain (MAT α , ura1, *CUP1*^r) (15), kindly provided by Dr. Dennis Winge (Utah University, USA), was used to obtain natively conformed Cd(II)-Cup1 complexes, suitable to undergo spectroscopic and spectrometric characterization. In this strain, *CUP1* expression is not restricted to copper induction, and therefore high-Cd(II) cultures yield native Cd(II)-complexes synthesis that accumulate in yeast cytoplasm. Hence, 301N was streaked on YPD plates (1% Bacto yeast extract, 2% Bacto tryptone, 2% Bacto Agar, 5% Glucose (Panreac), pH 5.7) supplemented with 500 μ M CdSO₄ (Merck), and one of the grown colonies was used to inoculate 100-ml liquid YPD that, after 48 h growth at 30 °C was added to 10-liter fresh YPD medium supplemented with 500 μ M CdSO₄. This culture was grown also for 48 h in a Microferm Fermentor (New Brunswick) coupled to a Westfalia CSA-1-06-475 centrifuge controlled by a TVE-OP 76/0 programmer (Braun Biotech), at constant temperature (30 °C), pH (5.7) and O₂ saturation (76–87%). Approximately 100 g of cells (wet weight) were obtained after centrifugation, which were subsequently submitted 3 cycles of washing in mili-Q water, plus centrifugation (Sorvall RC5C) at 10000 xg for 5 min, at 4 °C. Aliquots of 20 g and 40 g were stored at -20 °C until use. For protein purification, 20 g of cell mass were resuspended in 60 ml of

20 mM TrisHCl, 0.5mM β -mercaptoethanol, pH 8.0, Argon saturated buffer, and disrupted by 10 rounds of 1-min vortexing in glass beads, followed by 1 min on ice. Complete cell lysis was corroborated under the microscope. Total protein cell extract was cleared by centrifugation at 47800 xg for 1 h at 4 °C, and the recovered final volume was approximately of 50 ml. All further steps were performed at 4 °C and in Argon saturated buffers. 10 ml of the initial homogenate were first fractionated by size exclusion chromatography in a Sephadex G75 (Amersham GE Healthcare) column (2.5x40 cm, equilibrated with 20 mM Tris-HCl, 5 mM β -mercaptoethanol, 100 mM NaCl buffer, pH 8.0). The column was eluted at 0.6 ml/min with continuous monitoring of absorbance at 254 nm, and collection of 6-ml fractions, which were submitted ICP-AES in order to measure their cadmium content (see details below). Two alternative strategies were followed from this step on. The first option was a second fractionation of the G75 fraction pool exhibiting the main cadmium content (G3 peak) by means of ion exchange chromatography. To this end, the G3 pool was concentrated with Centriprep concentrators to a final volume of 5 ml, and loaded into a DEAE-Sepharose (Amersham GE Healthcare) column (1.5 x 13 cm, equilibrated with 20 mM Tris-HCl, 5 mM β -mercaptoethanol buffer, pH 8.0) with a flow rate of 0.6 ml/min. After 2 void volumes washing, elution was performed with a linear gradient of 20-to-500 mM NaCl in the same buffer, and 3-ml fractions were collected and analyzed. The second option of purification was designed to avoid the use of ion exchange chromatography. Consequently, the G3 fraction pool was subdivided in three parts (F1, F2, F3), according to their cadmium content, and each of them was further fractionated by subsequent FPLC. For this, 15 ml of each F pool were concentrated to a final volume of 0.5 ml to be loaded into a Superdex75 (Pharmacia) column integrated in an Äkta equipment (GE Healthcare) controlled by a computer running Unicorn v5.1, equilibrated with 20 mM Tris-HCl, 5 mM β -mercaptoethanol buffer, pH 8.0. Fractionation was run at a flow rate of 0.8 ml/min, at 20 °C and fractions were pooled according to their 254 nm absorbance and their Cd(II) content, measured by ICP-AES analysis.

Preparation by metal replacement of “in vitro-folded” Cd(II)-Cup1 and Cu(I)-Cup1 complexes- The so-called “*in vitro* complexes” were

prepared by titration at pH 7.0 of the recombinant Zn(II)-Cup1 complexes with Cd(II) (CdCl_2 in mili-Q purified water) or Cu(I) ($[\text{Cu}(\text{MeCN})_4]\text{ClO}_4$ complex in 30% (v/v) MeCN/H₂O) solutions, at equivalent molar ratios. Detailed description of this procedure has been previously reported (16, 17). The *in vitro* complexes were spectroscopically and spectrometrically characterized, following the same methodology explained below for *in vivo*-conformed complexes. All the titrations were carried out in Ar atmosphere and, for the all experiments, the pH remained constant throughout, without the addition of any extra buffers.

Acidification/reneutralization experiments- 20 μl aliquots of Cd-Cup1 preparations were acidified from neutral (7.0) to acid (2.0) pH with 10^{-3} -1 M HCl. CD and UV-vis spectra were recorded at pH 7.0, 4.5, 4.0, 3.0 and 2.0, both immediately after acidification and at different incubation times at pH 2.0. For reneutralization, the pH was restored to 7.0 with 10^{-3} -1 M NaOH. CD and UV-vis spectra were recorded at several pH intervals during reneutralization. Once the solution had reached a neutral pH, different equivalents of $\text{Na}_2\text{S}\cdot\text{H}_2\text{O}$ were added stepwise, in order to test if sulfide was incorporated into the reconstituted Cd-Cup1 complexes. All experiments were performed under strict oxygen-free conditions by saturation of solutions with Ar.

Analytical characterization of metalated-Cup1 preparations- When required, the S, Zn, Cd and Cu content of the samples was analyzed by Inductively Coupled Plasma Atomic Emission Spectroscopy (ICP-AES) on a Polyscan 61E (Thermo Jarrell Ash, Franklin, MA, USA) spectropolarimeter at suitable wavelengths (S, 182.040 nm; Zn, 213.856 nm; Cd, 228.802 nm; Cu, 324.803 nm). Routinely, samples were prepared as described in (18), thus treated with 2% (v/v) HNO_3 . Alternatively, a pre-incubation in 1M HCl at 65°C for 5 min prior to ICP measurements guaranteed the elimination of the acid-labile sulfide ligands putatively present in the sample, as shown in (19). This strategy guaranteed that all the sulfur remaining in the sample corresponded to Cys and Met residues, and therefore the ICP-AES measures of sulfur content could be used to quantify the Cup1 concentration in the preparations. Additionally, average metal-to-Cup1 ratios were calculated from these ICP-AES measurements.

When necessary, the mean S²⁻-to-protein content was quantified by Gas Chromatography-Flame Photometric Detection (GC-FPD) using an HP-5890 series II gas chromatograph coupled to an FPD80 CE detector (Thermo Finnigan). The calibration curve was determined with diluted standards of S²⁻ from 0.25 to 3 ppm. Sample aliquots were transferred to airtight vials and after strong acidification with H₂SO₄, pH 0.0, the generated H₂S was allowed to evolve to the gaseous phase for 2 h. Equilibrated head-space gas was subjected to chromatography as reported before (19).

Electronic absorption measurements were performed on a HP-8453A Diode array UV-visible spectrometer, and the temperature was kept at 25 °C by means of a Peltier PTC-351S apparatus. For Circular Dichroism (CD) spectra determinations, a Jasco spectropolarimeter (Model J-715) interfaced to a computer (GRAMS 32 Software) was used. All the spectra were recorded in 1 cm-capped quartz cuvettes and they were finally corrected for dilution effects.

Mass Spectrometry analysis of metal-Cup1 species- Molecular mass determinations were performed by electrospray ionization time-of-flight mass spectrometry (ESI-TOF MS) on a Micro Tof-Q instrument (Bruker) interfaced with a Series 1100 HPLC Agilent pump, equipped with an autosampler both controlled by the Compass Software. Calibration was attained with 0.2 g NaI dissolved in 100 mL of a 1:1 H₂O:isopropanol mixture. Samples containing divalent metal ion-Cup1 complexes were analyzed under the following conditions: 20 μl of protein solution injected through a PEEK (polyether heteroketone) column (1.5 m x 0.18 mm i.d.), at 40 $\mu\text{l}/\text{min}$; capillary counter-electrode voltage 5 kV; desolvation temperature 90-110 °C; dry gas 6 l/min; spectra collection range 800-2000 m/z. The carrier buffer was a 5:95 mixture of acetonitrile:ammonium acetate/ammonia (15 mM, pH 7.0). Alternatively, the Cu(I)-Cup1 samples were analyzed as follows: 20 μl of protein solution injected at 30 $\mu\text{l}/\text{min}$; capillary counter-electrode voltage 3.5 kV; lens counter-electrode voltage 4 kV; dry temperature 80 °C; dry gas 6 l/min. Here, the carrier was a 10:90 mixture of acetonitrile:ammonium acetate/ammonia, 15 mM, pH 7.0. For the corroboration of the apo-Cup1 expected molecular mass, 20 μl of the recombinant Zn(II)-Cup1 preparation was injected under the same

Table 1. Analytical characterization of the recombinant and native Cup1 complexes

Metal-MT	Metal/MT (ICP-AES)	S ²⁻ /MT ^[a] (GC-FPD)	ESI-MS ^[b]
rCu-Cup1 ^[c]	8.0 Cu	n.d.	Cu₈-Cup1 Cu ₁₆ -(Cup1) ₂
rCu-Cup1 ^[d]	7.0 Cu	n.d.	Cu₈-Cup1 Cu ₄ -Cup1 Cu ₅ -Cup1 Cu ₆ -Cup1
rZn-Cup1	2.8 Zn	n.d.	Zn₄-Cup1 Zn ₃ -Cup1 Zn ₅ -Cup1
rCd-Cup1	5.9 Cd	1.7	Cd₅-Cup1 Cd ₆ S ₁ -Cup1 Cd ₆ S ₄ -Cup1
n1Cd-Cup1 ^[e]	4.2 Cd	n.d.	Cd₅-Cup1 Cd ₄ Zn ₁ -Cup1 Cd ₆ -Cup1
n2Cd-Cup1 ^[f]	4.4 Cd	2.3	Cd₅-Cup1 Cd ₆ S ₁ -Cup1 Cd ₆ S ₄ -Cup1 Cd ₄ Zn ₁ -Cup1

[a] n.d.= not detectable. [b] Species shown in bold correspond to the major components of the preparation. M represents Zn(II) or Cu(I) ions. [c] Recombinant Cu-Cup1 synthesized in normally aerated cultures. [d] Recombinant Cu-Cup1 synthesized in at low aerated cultures. [e] Native Cd-Cup1 purified using anionic exchange chromatography. [f] Native Cd-Cup1 purified avoiding anionic exchange chromatography.

conditions described before, but using a 5:95 mixture of acetonitrile:formic acid pH 2.5, as liquid carrier, which caused the complete demetalation of the Cup1 peptide.

RESULTS & DISCUSSION

Metal Binding Abilities of Cup1

Analysis of the monovalent and divalent metal binding capabilities of recombinant Cup1 was attained through a three-step strategy. First, the *in vivo* synthesized M-Cup1 (where M represents zinc, cadmium and copper) complexes were characterized by spectroscopic and spectrometric means. Second, the reaction pathways of the *in vitro* Zn/Cd and Zn/Cu replacement processes undergone by the Zn-Cup1 peptide at pH 7 were determined. Detailed analysis of the spectroscopic (CD and UV-vis electronic absorption) and spectrometric (ESI-MS-TOF) sets of data recorded during these titrations provided information on the number of metal-MT species generated at each point of the titration, their stoichiometry and their degree of folding. And third, the recombinant Cd-Cup1 complexes were acidified/reneutralized and,

afterwards, several Na₂S equivalents were added. Finally, the native Cd-Cup1 preparations purified from the *S. cerevisiae* mutant strain 301N, grown in excess cadmium, were characterized and compared to the *in vivo* and *in vitro* generated recombinant Cd-Cup1 complexes.

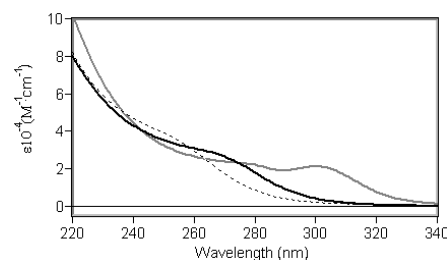


Figure 1. Comparison of the UV-vis spectra of the initial recombinant Cd-Cup1 preparation just after purification (solid black line), the recombinant Cd-Cup1 complex after 15 days (solid grey line), and the Cd-Cup1 reneutralized (dotted line).

In vivo Zn(II) and Cd(II) Binding Abilities of Recombinant Cup1

Despite its Cu-thionein character, Cup1 is perfectly capable of binding zinc or cadmium ions (8). Although some data on Zn- and Cd-Cup1 *in vitro* folded species are available, until now, none had been reported for complexes assembled intracellularly.

Cup1 is biosynthesized in zinc-supplemented cultures as a mixture of homometallic species, being Zn₄-Cup1 the most abundant (Table 1) and with a very low chiral CD (data not shown). This suggest that Zn(II) coordination induces a poor degree of folding, according with the Cu-thionein character of Cup1. On the other hand, the Cd-Cup1 preparation, constituted a mixture of species of variable Cd(II) stoichiometries, mainly Cd₅-Cup1, together with several minor sulfide-containing complexes (i.e. Cd₆S₁-, Cd₆S₄- or Cd₇S₄-Cup1) detected by ESI-MS (Table 1). GC-FPD data were totally consistent with the sulfide presence. Unlike for Zn-Cup1, Cd-Cup1 spectra is mainly composed of two Gaussian bands, one centered *ca.* 250 nm related with the Cd-SCys chromophores and another at *ca.* 280 nm in concordance with the Cd-S²⁻ absorptions (Fig. 4). Curiously, we have observed that the CD spectra and the relative abundance of the initial species varies with time, the more time elapsed, the more rich in sulfide species became, as it can be observed both spectroscopically (DC and UV-vis) and spectrometrically (ESI-MS). Possibly this fact is due to the aggregation of the Cd-S particles contained in the sample as a red-shift displacement can be observed in the UV spectra (Fig. 1).

In vitro Cd(II) Binding Abilities of Recombinant Cup1

The Cd(II) titration of Zn-Cup1 (Fig. 2) and the acidification/reneutralization of the recombinant Cd-Cup1 complexes provided a further insight into the Cd-binding abilities of Cup1. As a consequence of the absence of sulfide in the Zn-Cup1 preparation, the final species obtained from the Zn/Cd replacement reaction are also sulfide-devoid complexes, and consequently the preparations showed spectropolarimetric features different to those of Cd-Cup1 obtained *in vivo*. When an excess of cadmium has been added to Zn-Cup1, the major complex obtained is Cd₅-Cup1, and, in any case, the addition of several sulfide equivalents at the end of the titration, leads to their incorporation in the final complexes as it can be observed in the UV spectra (Fig. 2).

The same Cd₅-Cup1 species is obtained after the acidification/reneutralization of the recombinant Cd-Cup1 complexes (data not shown). During the acidification, the acid-labile sulfide present in the sample is lost, as it can be observed in the decrease of the absorption at 280 nm in the UV-vis spectra (Fig. 1.). Just as described for the Zn/Cd replacement studies, the addition of sulfide after the reneutralization of Cd-Cup1, leads to the formation of sulfide-rich species

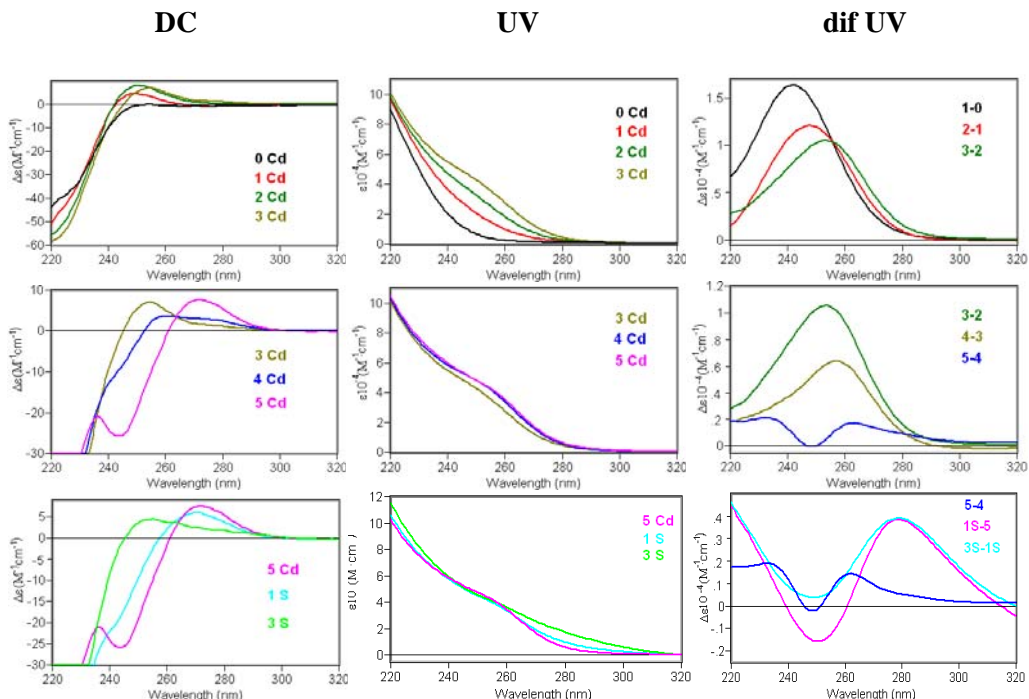


Figure 2. CD, UV-vis and difference UV spectra corresponding to the titration of a 20 μ M solution of Zn-Cup1 with Cd(II).

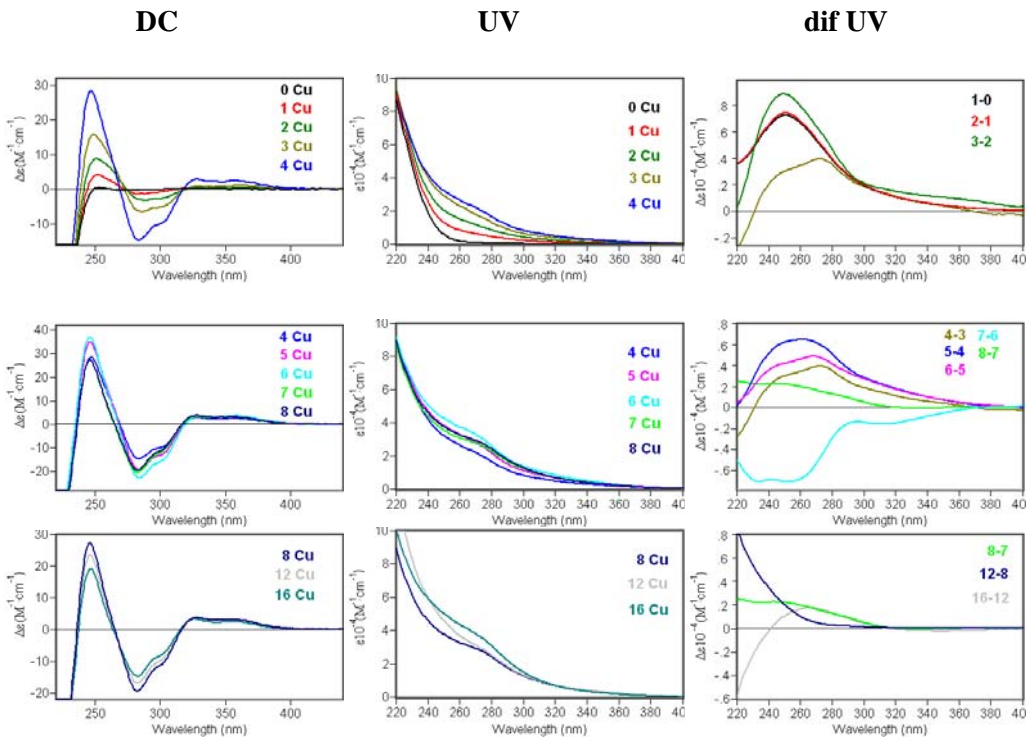


Figure 3. CD, UV-vis and difference UV spectra corresponding to the titration of a 20 μM solution of Zn-Cup1 with Cu(I).

detected by ESI-MS.

In vivo Cu(I) Binding Abilities of Recombinant Cup1

The recombinant synthesis of Cup1 in copper enriched cultures at low oxygenation rendered a major homometallic Cu₈-Cup1 complex accompanied of very minor Cu₁₆- dimeric forms. The presence of these dimeric Cup1 complexes has been already proposed in the literature for native preparations (20). Although in the biosynthesis of Cup1 in normal aeration cultures the major species is also an homometallic Cu₈-Cup1 complex, in these conditions some other minor Cu-Cup1 complexes have been detected. Both productions showed similar CD fingerprints but those from the low aeration synthesis exhibited a higher intensity. It is worth noting that our recombinant Cu-Cup1 spectra are totally coincident with those Cu-Cup1 spectra shown in other reports for native preparations (21).

In vitro Cu(I) Binding Abilities of Recombinant Cup1

The titration of Zn-Cup1 with Cu(I) (Fig. 3) allowed the reproduction of the CD fingerprint of the recombinant preparations but, although Cu₈-

Cup1 was the major species, in no step a single species was obtained. However it is remarkable that the Zn/Cu displacement shows certain cooperative character, as described in the literature (22), since the 4th Cu(I) equivalent added already forms the highly stable Cu₈-Cup1 complex. The titrations of Zn-Cup1 with Cu(I) suggest the impossibility of this isoform to yield an unique Cu₈-Cup1 species starting from a Zn-loaded polypeptide. Consequently, and as happens for another extreme Cu-thioneins, such is the Cu-MT isoform of the roman snail *H. pomatia*, it is sensible to propose that the Cu₈-Cup1 is directly produced *de novo*, instead of being product of a Zn/Cu replacement.

Purification and Characterization of Native Cd-Cup1 Complexes

Traditionally, the native MT purification schemes include chromatography fractionations both through gel filtration and ion exchange column (23). We hypothesized that, if present in native preparations, S²⁻-metal-MT complexes could be probably retained in the anionic exchange matrix. For this reason, we applied two different purification strategies for the purification of the native Cd-Cup1 complexes, using and avoiding anion exchange

chromatography. In the first case, when gel filtration (Superdex) and anion exchange columns (DEAE) were used, the final preparation (called here n1Cd-Cup1) contained a major Cd₅-Cup1 complex accompanied by other minor species, some of them being Zn,Cd-Cup1 heterometallic species (Fig. 5). These samples were sulfide-devoid, and their CD features very similar to those resulting from the Zn/Cd replacement carried out with recombinant Zn-Cup1 (Fig. 4). Conversely, when only gel filtration (size exclusion) was used, the results from recombinants syntheses and native purifications (called here n2Cd-Cup1) were spectroscopically and spectrometrically equivalent (Figs. 4 & 5), this including a major Cd₅-Cup1 complex and another minor S²⁻ containing Cd-Cup1 complexes (*i.e.* Cd₆S₁⁻, Cd₆S₄⁻) in addition of the same minor heterometallic Zn,Cd-complexes detected after the first purification strategy.

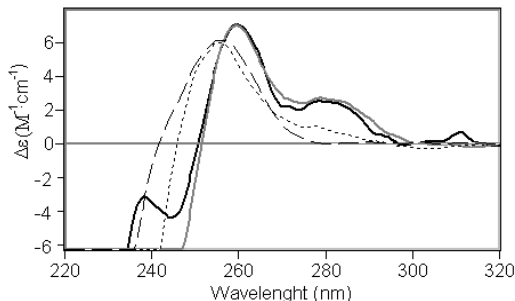


Figure 4. CD spectra of recombinant and native Cd-Cup1 preparations. Spectra have been grouped as: recombinant Cd-Cup1 (solid black line), native Cd-Cup1 avoiding the use of anionic exchange columns (solid grey line), native Cd-Cup1 using anionic exchange columns (dashed line) and CD spectra of Zn-Cup1 after the addition of 3 Cd^{II} equivalents (dotted line). Intense absorptions at 280 nm could be attributed to the presence of Cd-S²⁻ bonds.

CONCLUDING REMARKS

The data presented herein support the hypothesis that native metal-MT preparations can include sulfide-containing complexes, in addition to the expected canonical non-sulfide-containing species. This is the first demonstration that native MTs have the capacity to form Cd-thiolate complexes in which labile sulfide contribute to the Cd(II) binding when folded in native, intracellular environments. Thus, this answers the question about sulfide ligands in metal-MT

complexes being a native trait rather than a mere artifact of *E. coli* recombinant synthesis.

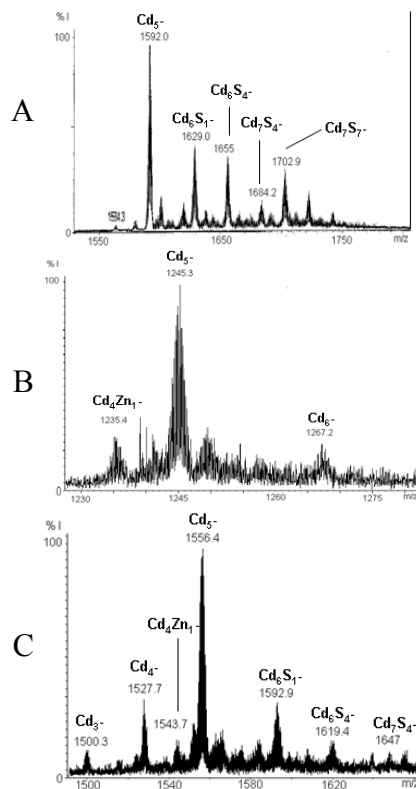


Figure 5. ESI-MS spectra of Cd-Cup1: a) recombinant, b) native preparation using anion exchange columns (n1-Cd-Cup1), and c) native preparation recovered only using size exclusion columns (n2-Cd-Cup1).

It has to be noted that ion exchange chromatography is commonly used for native MT purification and precisely this could explain why the S²⁻ ligands remained so long unnoticed. In addition, the fact that for nearly half a century most of the MT research has been carried out using *in vitro* reconstituted metal-MT species, obtained after heavy acidification of the purified metal-MT forms and the effort of obtaining pure chromatographic fractions, which may involve discarding other minor metal-MT species present in the initial homogenate and assumed to be impurities, could be another explanation to this fact.

In conclusion the presence of S²⁻ ligands in metal-MT complexes, and the particular properties of the corresponding crystallite-like particles, would be highly significant for structural, nanobiological, and biotechnological applications, all these aspects being now under further consideration.

REFERENCES

-
- [1] A. Sigel, H. Sigel, R. K. O. Sigel, Eds. Metallothioneins and related peptides. *Metal ions in Life Sciences*, Vol. 5 (Royal Society of Chemistry, Cambridge, **2009**, pp. 1-514.
- [2] M. Valls, R. Bofill, R. Gonzalez-Duarte, P. Gonzalez-Duarte, M. Capdevila, S. Atrian, *J. Biol. Chem.* **2001**, 276, 32835-32843.
- [3] M. Capdevila, J. Domènec, A. Pagani, L. Tio, L. Villarreal, S. Atrian, *Angew. Chem. Int. Ed. Engl.* **2005**, 44, 4618-4622.
- [4] R. Bofill, M. Capdevila, S. Atrian, *Metallomics* **2009**, 229-234
- [5] A. Torreggiani, J. Domènec, R. Orihuela, C. Ferreri, S. Atrian, M. Capdevila, C. Chatgilialoglu, *Chem. Eur. J.* **2009**, DOI
- [6] R. Prinz, U. Weser, *FEBS Lett.* **1975**, 54, 224-229
- [7] R. Premakumar, D. R. Winge, R. D. Wiley, K. V. Tajagopalan, *Arch. Biochem. Biophys.* **1975**, 170, 278-288
- [8] D. R. Winge, W. R. Nielson, W. R. Gray, D. H. Hamer, *J. Biol. Chem.* **1985**, 260, 14464-14469.
- [9] Z. Sayers, P. Brouillon, C. E. Vorgias, H. F. Nolting, C. Hermes, M. H. J. Koch, *Eur. J. Biochem.* **1993**, 212, 521-528.
- [10] V. Calderone, B. Dolderer, H. J. Hartmann, H. Echner, C. Luchinat, C. Del Bianco, S. Mangani, U. Weser, *Proc. Natl. Acad. Sci. USA* **2005**, 102, 51-56.
- [11] M. Inouhe, H. Hiyama, H. Tohoyama, M. Joho, T. Murayama, *Biochim. Biophys. Acta* **1989**, 993, 51-55.
- [12] M. Inouhe, A. Inagawa, M. Morita, H. Tohoyama, M. Joho, T. Murayama, *Plant Cell Physiol.* **1991**, 32, 475-482.
- [13] V.C. Culotta, W. R. Howard, X. F. Liu, *J. Biol. Chem.* **1994**, 269, 25295-25302
- [14] A. Pagani, L. Villarreal, M. Capdevila, S. Atrian, *Mol. Microbiol.* **2007**, 63, 256-269.
- [15] H. Tonoyama, T. Murayama, *Agric. Biol. Chem.* **1977**, 41, 1523-1524
- [16] M. Capdevila, N. Cols, N. Romero-Isart, R. Gonzalez-Duarte, S. Atrian, P. Gonzalez-Duarte, *Cell. Mol. Life Sci.* **1997**, 53, 681-688.
- [17] R. Bofill, O. Palacios, M. Capdevila, N. Cols, R. Gonzalez-Duarte, S. Atrian, P. Gonzalez-Duarte, *J. Inorg. Biochem.* **1999**, 73, 57-64
- [18] J. Bongers, C. D. Walton, D. E. Richardson, J. U. Bell, *Anal. Chem.* **1988**, 60, 2683-2686
- [19] M. Capdevila, J. Domènec, A. Pagani, L. Tio, L. Villarreal, S. Atrian, *Angew. Chem. Int. Ed. Engl.* **2005**, 44, 4618-4622.
- [20] C. W. Peterson, S. S. Narula, I. M. Armitage, *FEBS Lett.* **1996**, 379, 85-93.
- [21] C. Luchinat, B. Dolderer, C. del Bianco, M. Echner, H.-J. Hartmann, W. Voelter, U. Weser, *J. Biol. Inorg. Chem.* **2003**, 8, 353-359.
- [22] J. Byrd, R. M. Berger, D. R. McMillin, C. F. Wright, D. Hamer, D. N. Winge, *J. Biol. Chem.* **1988**, 263, 6688-6694.
- [23] U. Weser, H. J. Hartmann, A. Fretzdorff, G. J. Strobel, *Biochim. Biophys. Acta* **1979**, 493, 465-477.

ARTICLE 5

Zinc and cadmium complexes of a plant metallothionein under radical stress: desulfurization reactions associated with the formation of *trans* lipids in model membranes

Chemistry- A European Journal, (2009), 15, 6015-6024

Zinc and Cadmium Complexes of a Plant Metallothionein under Radical Stress: Desulfurisation Reactions Associated with the Formation of *trans*-Lipids in Model Membranes

Armida Torreggiani,^{*[a]} Jordi Domènech,^[a, b] Ruben Orihuela,^[c] Carla Ferreri,^[a] Sílvia Atrian,^[b, d] Mercè Capdevila,^[c] and Chrysostomos Chatgilialoglu^{*[a]}

Abstract: Metallothioneins (MTs) are sulfur-rich proteins capable of binding metal ions to give metal clusters. The metal-MT aggregates used in this work were Zn- and Cd-QsMT, where QsMT is an MT from the plant *Quercus suber*. Reactions of reductive reactive species (H^+ atoms and e_{aq}^-), produced by γ irradiation of water, with Zn- and Cd-QsMT were carried out in both aqueous solutions and vesicle suspensions, and were characterized by different approaches. By using a biomimetic model based on unsaturated lipid vesicle suspensions, the occurrence of tandem protein/lipid damage was shown. The

reactions of reductive reactive species with methionine residues and/or sulfur-containing ligands afford diffusible sulfur-centred radicals, which migrate from the aqueous phase to the lipid bilayer and transform the *cis* double bond of the oleate moiety into the *trans* isomer. Tailored experiments allowed the reaction mechanism to be elucidated in some detail. The formation of sulfur-centred radicals is accom-

panied by the modification of the metal-QsMT complexes, which were monitored by various spectroscopic and spectrometric techniques (Raman, CD, and ESI-MS). Attack of the H^+ atom and e_{aq}^- on the metal-QsMT aggregates can induce significant structural changes such as partial deconstruction and/or rearrangement of the metal clusters and breaking of the protein backbone. Substantial differences were observed in the behaviour of the Zn- and Cd-QsMT aggregates towards the reactive species, depending on the different folding of the polypeptide in these two cases.

Keywords: biomimetic chemistry · liposomes · metalloproteins · radical reactions · reaction mechanisms

Introduction

Metallothioneins (MTs) are intracellular, low molecular weight, sulfur-rich proteins, present in virtually all living organisms. Metallothioneins exhibit high capacity for binding both biologically essential (Zn^{II} and Cu^{I}) and xenobiotic (Cd^{II} , Hg^{II} and Ag^{I}) metal ions, giving rise to metal clusters in which the metal ions can show tetrahedral, trigonal or diagonal coordination environments.^[1] In native metal-MT complexes, disulfide bonds are almost completely absent because all thiol groups of cysteine residues (ca. 30% of the amino acid residues) are deprotonated and bound to metal ions. Although metal-MT coordination is mainly achieved by formation of metal-thiolate bonds, recently the contribution of non-protein ligands, such as chloride and/or sulfide anions, has been also reported.^[2,3] Thus, acid-labile sulfide ions (S^{2-}) have been detected in nearly all recombinant Zn^{II} -MT and Cd^{II} -MT complexes synthesized in *E. coli*, that is, in an *in vivo*, physiological, but heterologous, environment. The amount of S^{2-} depends on the MT and on the co-

[a] Dr. A. Torreggiani, Dr. J. Domènech, Dr. C. Ferreri, Dr. C. Chatgilialoglu
ISOF, Consiglio Nazionale delle Ricerche
Via P. Gobetti 101, 40129 Bologna (Italy)
Fax: (+39)051-639-8349
E-mail: chrys@isof.cnr.it
torreggiani@isof.cnr.it

[b] Dr. J. Domènech, Prof. S. Atrian
Departament de Genètica, Facultat de Biologia
Universitat de Barcelona
Av. Diagonal 645, 08028 Barcelona (Spain)

[c] Dr. R. Orihuela, Prof. M. Capdevila
Departament de Química, Facultat de Ciències
Universitat Autònoma de Barcelona
08193 Bellaterra, Barcelona (Spain)

[d] Prof. S. Atrian
Institut de Biomedicina de la
Universitat de Barcelona (IBUB) (Spain)

 Supporting information for this article is available on the WWW under <http://dx.doi.org/10.1002/chem.200802533>.

ordinated metal ion, but generally its presence does not increase the chelating potential of the MT. This conclusion is based on two facts: 1) the divalent metal content of the aggregates remains the same although the sulfide content is usually higher in the Cd^{II} than in the Zn^{II} complexes, and 2) sulfide-containing and sulfide-devoid complexes exhibiting the same metal stoichiometry are usually found in the same preparation.

Although MTs do not appear to be essential for life, there is mounting evidence for their contribution to stress resistance, including exposure to radicals and toxic metals.^[4] Accordingly, multifunctional roles such as chelators of harmful heavy metals and excess essential metals (detoxification and metal-homeostasis processes) and scavengers of various radicals and reactive oxygen species (ROS) have been proposed for MTs. In support of a function of MTs in control of oxidative stress, many studies have showed that MT expression increases dramatically in response to tissue injury, inflammation and tumours, and it appears to reduce controlled cell death (apoptosis).^[5,6] Thus, the ability of MTs to act as antioxidants may provide a survival advantage at a time of major infection and inflammation, conditions under which a large increase in radical-mediated tissue damage takes place. On the other hand, the protective role of MT appears to be reversed in other studies whereby apoptosis is precisely promoted after exposure of cells to a nitric oxide (NO) donor.^[7]

In the context of free-radical damage, the fate of radical species derived from protein damage has been the subject of many investigations, although a clear picture of the degradation paths and their influence on the aetiology of the disease is far from being achieved.^[8,9] Recently, tandem radical damage involving aqueous and lipid domains was evidenced by using sulfur-containing proteins in the presence of unsaturated membrane phospholipids.^[10–14] Thus, it has been shown that damage starts from specific radical attack on sulfur moieties of proteins, leading to release of diffusible thiyl radicals that can migrate from the aqueous phase to the membrane bilayer. At this site, these radicals react with the *cis* double bond of the phospholipid fatty acids and result in its transformation into the corresponding *trans* geometrical isomer.^[15,16] Incorporation of *trans* lipid is known to affect membrane properties as well as being correlated with health problems.^[17–20]

It has been proved that lipid isomerisation is promoted very efficiently by thiyl radicals originating from methionine (Met) and cysteine/cystine (Cys) residues of proteins and, recently, by sulphydryl radicals (HS[·]/S²⁻) from hydrogen sulfide, an endogenously generated gas species with roles in the nervous and cardiovascular systems and in pathological conditions such as inflammation.^[21,22] The presence of sulfur-containing amino acids (Met and Cys) and sulfide ligands in metal-MT complexes makes them a very interesting case

for studying this tandem lipid damage. In particular, the acid-labile sulfide ligands (S²⁻) could generate diffusible sulphydryl radicals and thus promote isomerisation of double bonds in membrane lipids. Connecting MT reactivity with membrane lipid transformation may contribute insight into radical stress to biomolecules and their role in biological signalling.

The metal-MT aggregates analysed in this work were derived from the metallothionein of the cork oak *Quercus suber* (QsMT). Like most plant MTs, it has a peculiar organization of its amino acid sequence, consisting of two short cysteine-rich terminal domains (containing 6 and 8 Cys residues) linked by a cysteine-devoid spacer region (Figure 1), which includes an additional putative ligand (His).^[23] Previous characterization of the Zn- and Cd-binding abilities of QsMT and its separate domains supports the dependence on the two Cys-rich domains,^[24,25] together with participation of the spacer region in the in vivo folding of Zn- and Cd-QsMT, and in overcoming Cd toxicity in yeast.^[25] Comparative study of the Zn- and Cd-QsMT aggregates has indicated differences in their metal and sulfide contents, which suggests structural differences depending on coordinated metal ion,^[23,25] in contrast with the isomorphism commonly assumed for animal MTs.^[26]



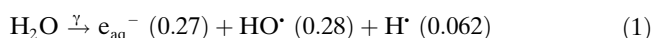
Figure 1. Amino acid sequence of the type 2 plant MT from *Quercus suber* (QsMT). QsMT contains 77 amino acid residues including 14 cysteine (C), 3 methionine (M) and 1 histidine (H).^[23] Cysteine and histidine residues are in bold.

Here we present a detailed study on the behaviour of Zn- and Cd-QsMT aggregates under conditions of reductive radical stress.^[27] In particular, we modelled tandem radical damage involving protein and lipid domains by γ irradiation of lipid vesicle suspensions containing these two types of metal-QsMT complexes. Different experimental conditions were considered in order to obtain some insights into the contribution of the different primary reactive species (hydrated electrons, hydroxyl radicals and hydrogen atoms) to the processes determining secondary molecular damage in another target site such as a lipid compartment. The use of different spectroscopic techniques allowed the changes induced on the proteins by γ irradiation to be determined and underline the involvement of the sulfur-containing moieties, most interestingly the metal-sulfur clusters.

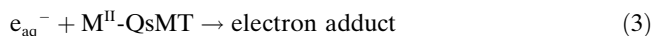
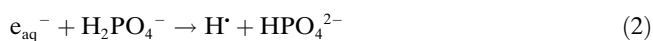
Results and Discussion

Radiolytic production of transients:^[30,31] γ Radiolysis of neutral water leads to e_{aq}^- , HO[·] and H[·] [Eq. (1)]. The values in parentheses represent the radiation chemical yields *G* in units of micromoles per joule. From available literature ki-

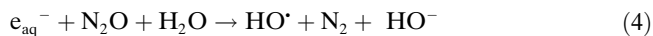
netic data on MTs,^[29] all three reactive species are expected to react very fast with the M^{II}-QsMT complexes (M^{II}=Zn^{II} or Cd^{II}). Radical stress on M^{II}-QsMT was stimulated by using by two experimental procedures: 1) the three reactive species (in different proportions) are allowed to react with M^{II}-QsMT (Method A); 2) the hydroxyl radicals are scavenged by tBuOH (Method B).



Method A1: Oxygen-free (Ar-flushed) 10 mM H₂PO₄⁻ solutions containing 30 μM M^{II}-QsMT. Under these conditions, e_{aq}⁻ can be converted to H[·] [Eq. (2), k₂=1.5×10⁷ M⁻¹s⁻¹], depending on the pH [pK_a(H₂PO₄⁻)=7.21] and the reactivity of e_{aq}⁻ with the substrate. Assuming a rate constant of 1×10¹⁰ M⁻¹s⁻¹ for the reaction of e_{aq}⁻ with MT [Eq. (3)], about 20% of e_{aq}⁻ will be converted to H[·] at pH 7, giving G(H[·])≈0.13 μmolJ⁻¹.



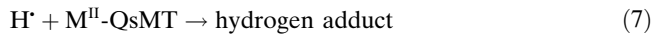
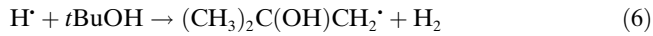
Method A2: N₂O-saturated 10 mM H₂PO₄⁻ solutions containing 30 μM M^{II}-QsMT. Under these conditions, e_{aq}⁻ are efficiently transformed into HO[·] radicals by the approximately 0.02 M of N₂O [Eq. (4), k₄=9.1×10⁹ M⁻¹s⁻¹], affording G(HO[·])=0.55 μmolJ⁻¹, that is, H[·] and HO[·] accounted for 10 and 90%, respectively, of the reactive species. With this method G(H[·]) is approximately half that of Method A1.



Method B1: Oxygen-free (Ar-flushed) aqueous solutions containing 0.2 M tBuOH and 30 μM M^{II}-QsMT. In the presence of 0.2 M tBuOH, HO[·] radicals are scavenged efficiently [Eq. (5), k₅=6.0×10⁸ M⁻¹s⁻¹], although the rate constant of HO[·] with MT is 1.7×10⁹ M⁻¹s⁻¹.^[28,29]



Since H[·] react with tBuOH only slowly [Eq. (6), k₅=1.7×10⁵ M⁻¹s⁻¹], it is expected that H[·] are partitioned between the reaction with tBuOH and M^{II}-QsMT [Eqs. (6) and (7)].



Method B2: N₂O-saturated aqueous solutions containing 0.2 M tBuOH and 30 μM M^{II}-QsMT. In N₂O-saturated solutions (ca. 0.02 M), e_{aq}⁻ are efficiently transformed into HO[·] radicals [Eq. (4)]. Under these conditions, H[·] and HO[·] radi-

cals accounted for 10 and 90%, respectively, of the reactive species. As described above, HO[·] radicals are scavenged by Equation (4), whereas H[·] atoms are partitioned between the reaction with tBuOH and MT [Eqs. (6) and (7)]. Therefore, Methods B1 and B2 should afford similar G(H[·]) values that are slightly smaller than that of Method A2.

γ Radiolysis of M^{II}-QsMT complexes in POPC-LUVET suspensions (Method A): The biomimetic model of a cell membrane consisted of 2 mM suspensions of 1-palmitoyl-2-oleoyl-phosphatidylcholine (POPC) liposomes containing large unilamellar vesicles (LUVET) of a *cis* monounsaturated fatty acid, to which solutions of Zn- or Cd-QsMT (30 μM) in phosphate buffer at pH 7 were added.^[32–34] The mixtures were flushed with Ar (Method A1) or saturated with N₂O (Method A2) prior to γ irradiation. Aliquots of the suspension (100 μL) were withdrawn at different irradiation times for lipid isolation and derivatization to the corresponding fatty acid methyl esters,^[35] and the *cis/trans* lipid isomer ratio was determined by GC analysis.^[32–34] In all experiments, the geometrical isomerization of the lipid chains of the POPC vesicles occurred and the formation of elaidate (*trans* isomer) increased linearly with the dose. Control experiments in the absence of metal-QsMT confirmed that under these conditions elaidate formation is less than 0.2% after exposure to 500 Gy.

Figure 2 shows the irradiation-dose profiles for formation of *trans* isomer in the Ar-flushed (Method A1) and N₂O-saturated (Method A2) experiments. Both sets of experiments clearly indicate that Cd-QsMT has a higher capacity to induce *cis-trans* isomerization than Zn-QsMT. For a particular aggregate, Method A1 (solid lines) is more effective than Method A2 (dashed lines), which suggests an important contribution of the reducing species in the *cis-trans* isomerization process. Indeed on going from Method A1 to A2, G(H[·]) is almost halved and e_{aq}⁻ are transformed into HO[·] radicals. Under similar conditions, it is reported that HO[·] radicals react rapidly with MT to produce disulfide bridges via their radical anions.^[27–29]

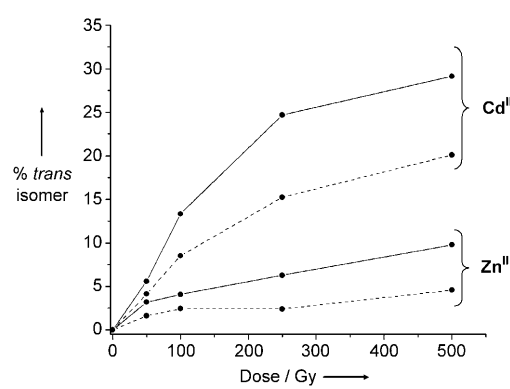
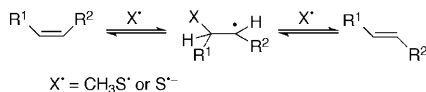


Figure 2. Dose dependence of the formation of elaidate (*trans* isomer) residues from γ irradiation of POPC vesicles (2 mM) containing Zn-QsMT or Cd-QsMT aggregates (30 μM) in Ar-flushed (solid line) or N₂O-saturated (dashed lines) 10 mM H₂PO₄⁻ solutions at pH 7.

Based on our previous investigation on tandem protein-lipid damage,^[11–14] these findings can be explained by the occurrence of desulfurization processes at the level of sulfur-containing residues of the proteins, which generate diffusible sulfur-centred radicals X^\bullet (e.g., $\text{CH}_3\text{S}^\bullet$ from methionine residues or $\text{HS}^\bullet/\text{S}^\bullet$ from disulfide bridges) that can migrate from the aqueous phase to the membrane bilayer and transform the double bond of the oleate moiety by the catalytic addition-elimination mechanism shown in Scheme 1.^[15,16]



Scheme 1. Reaction mechanism for *cis-trans* isomerization catalyzed by $\text{CH}_3\text{S}'$ or S' radicals.

γ Radiolysis of M^{II} -QsMT complexes in POPC-LUVET suspensions in the presence of *t*BuOH (Method B): In order to evaluate more deeply the role of each reactive species in the above-described reactions, we reformulated the experiments under slightly different conditions including 0.2 M *t*BuOH as additive. This amount of *t*BuOH is needed to scavenge efficiently HO^\bullet radicals and thus prevent their attack on M^{II} -QsMT.^[27–29] The experiments involved 2 mM POPC-LUVET suspensions to which Zn- or Cd-QsMT solutions (30 μM) and 0.2 M *t*BuOH were added. The mixtures were flushed with Ar (Method B1) or saturated with N_2O (Method B2) prior to γ irradiation.

Progressive isomerization paralleling irradiation dose is shown in Figure 3, from low doses up to 500 Gy. In both Ar-flushed (Method B1) and N_2O -saturated (Method B2) protein-lipid suspensions, *cis-trans* isomerization was higher in comparison to the analogous experiments in the absence of *t*BuOH (cf. Figure 2). This behaviour further indicates that H' atoms and perhaps e_{aq}^- are indeed very specific damaging agents for sulfur-containing residues, and that this is the process that can cause secondary molecular damage. Again it is found that Cd-QsMT has a higher capacity to induce *cis-trans* isomerization than Zn-QsMT. For a particular aggregate, the fact that Method B1 (solid lines) was more effective than Method B2 (dashed lines) indicates a synergic contribution of hydrogen and electron adducts on M^{II} -QsMT to the formation of diffusible species responsible for *cis-trans* isomerization.

Reaction mechanism: Under similar experimental conditions using other peptides and proteins, we have previously shown that methanethiyl radicals ($\text{CH}_3\text{S}'$) are produced by the attack of H' on methionine residues promoting isomerization in an extremely efficient way.^[11–14] Also, post-translational modification of methionine to α -aminobutyric acid (Aba) in peptides and proteins has been demonstrated. Diffusible sulfur-centred radicals are not limited only to those produced by methionine desulfurization. Indeed, we have recently shown that H' and the e_{aq}^-/H^+ couple react with di-

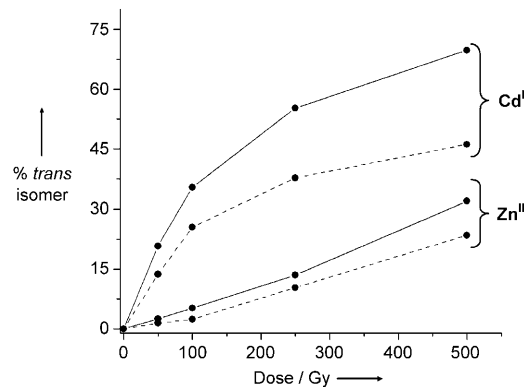
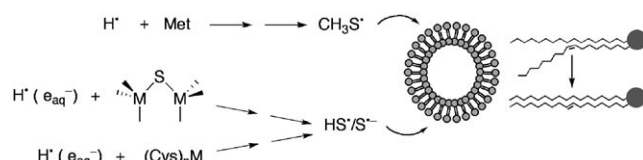


Figure 3. Dose dependence of the formation of elaidate (*trans* isomer) residues from γ irradiation of POPC vesicles (2 mM) containing Zn-QsMT or Cd-QsMT aggregates (30 μM) in Ar-flushed (—) or N_2O -saturated (----) solutions containing 0.2 M *t*BuOH.

sulfide moieties of the bovine RNase A sequence to produce alanine and H_2S as products.^[14] Since QsMT contains cysteine and sulfide ligands bound to metal ions, we suggest that H' atoms and/or the e_{aq}^-/H^+ couple also react with M^{II} -QsMT to produce sulphydryl radical ($\text{HS}^\bullet/\text{S}^\bullet$) which are known to be very efficient *cis-trans* isomerising agents.^[22] In this respect, the higher isomerization yields obtained in the presence of Cd-QsMT, an MT preparation that contains a larger number of acid-labile sulfide ligands than Zn-QsMT (3 instead of 1, Table S1 in the Supporting Information), suggests a possible major role of the S^{2-} present in the metal clusters as a precursor of diffusible isomerising radicals ($\text{HS}^\bullet/\text{S}^\bullet$).

By comparing these results with our previous experiments on Met-containing peptides,^[13] and normalising the data on the basis of the Met content, the Cd-QsMT system shows a strong increment of the isomerisation efficiency (>30%). This suggests that the other sulfur-containing moieties of the protein come into play in addition to Met residues, and can be connected with this tandem protein-lipid damage.

In Scheme 2 the possible desulfurization mechanisms connected to lipid isomerization are summarized. We suggest that both the reaction of H' with the methionine residue, affording the diffusible thiyl radical $\text{CH}_3\text{S}'$, and the reaction of H' (and/or e_{aq}^-) with sulfide and cysteine ligands bound to metals ions, affording diffusible $\text{HS}^\bullet/\text{S}^\bullet$ radicals, are operative. These sulfur-centred intermediates can migrate from



Scheme 2. Methionine residues (Met) or sulfur-containing ligands bound to metals moieties (sulfide and cysteine) are modified by attack of H' and/or e_{aq}^- with formation of diffusible sulfur-centered radicals such as $\text{CH}_3\text{S}'$ or S' that can migrate to the lipid bilayer and induce *cis-trans* isomerization of unsaturated fatty acid residues.

the aqueous phase to the lipid bilayer and transform the double bond of the oleate moiety, according to the catalytic mechanism shown in Scheme 1.^[10,15] Even very low levels of protein modification produced by H[•] and/or e_{aq}⁻ can be detected, since an amplification effect is given by the catalytic cycle of the thiyl radical-based *cis-trans* isomerization.^[15] In other words, amplified membrane damage is the final effect of these reductive pathways. The smaller isomerization efficiency of Method A with respect to Method B (cf. Figures 2 and 3) suggests that the reaction of HO[•] radicals with M^{II}-QsMT (Method A) leads to the formation of oxidation products that do not influence the parallel desulfurization processes by the action of H[•] and e_{aq}⁻.

To gain further confirmation of our proposal, it was imperative to determine whether simpler metal-sulfur complexes could produce *cis-trans* isomerization of the lipid vesicles under similar experimental conditions. First, we tested zinc sulfide (ZnS) and cadmium sulfide (CdS) suspensions, and Figure 4 shows four representative experiments

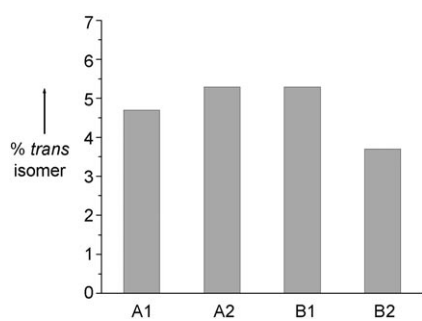


Figure 4. Formation of elaidate (*trans* isomer) residues from 100 Gy of irradiation of POPC vesicles (2 mM) containing CdS (30 µM) by the various methods: A1) Ar-flushed, A2) N₂O-saturated, B1) Ar-flushed and 0.2 M tBuOH, B2) N₂O-saturated and 0.2 M tBuOH.

performed under the various methods described above with CdS (30 µM) at a dose of 100 Gy. In all experiments, geometrical isomerization of the lipid chains of the POPC vesicles occurred with the formation of *trans* isomer in about 5% yield. Control experiments showed that *trans* isomer is not formed in the absence of CdS. Analogous results were obtained with ZnS. These findings strongly support the contribution of the reaction of H[•] and/or e_{aq}⁻ with sulfide ligands bound to metal ions to afford a diffusible isomerising agent (cf. Scheme 2). Next we checked the correspondent reactivity of metal cysteine complexes in producing isomerising species, also in comparison with an analogous experiment carried out with free cysteine. The Zn-Cys complex was chosen as representative example, because of the insolubility of the corresponding complex with Cd. Under the conditions of Method B1 with Zn-Cys complex or free cysteine (30 mM), 4.1 and 7.7% of *trans* isomer were formed, respectively, after 100 Gy of irradiation. Interestingly, free cysteine is more effective in the *cis-trans* isomerisation than the Zn-Cys complex; the latter gave identical results to the analogous experiment carried out with ZnS.

M^{II}-QsMT modification associated with reductive stress: To obtain information on protein modifications on H[•] and e_{aq}⁻ attack, we used various spectroscopic techniques (Raman, CD, and ESI-MS) to examine the changes produced in the metal-QsMT complexes under the above-described conditions.

Argon-flushed aqueous solutions of M^{II}-QsMT containing 0.2 M tBuOH were irradiated at different doses, lyophilised and analysed by Raman spectroscopy, a technique that provides valuable information on preferential sites of radical attack.^[11,14,36-38] Figure 5 shows Raman spectra in the 250–800 cm⁻¹ region for experiments with Zn-QsMT and Cd-QsMT at 0, 50 and 100 Gy. This region provides information on the involvement of sulfur-containing ligands such as cysteine (SCys) and sulfide (S²⁻) in metal binding, with several bands attributable to metal-S stretching modes at low wavenumbers (<500 cm⁻¹).^[39-41] Previous studies enable assignment of the metal-S bridging vibrations essentially to the highest wavenumber bands (395–430 cm⁻¹), whereas both S-terminal and S-bridging ligands contribute to the lowest wavenumber modes (280–370 cm⁻¹).^[42,43] The lack of S-H stretching at about 2570 cm⁻¹ (data not shown) is in accordance with the absence of free SH groups, as already observed for other MTs.^[42] Before irradiation, the weak intensity of the disulfide bands (510–540 cm⁻¹ region) indicated that almost all the 14 Cys residues present in QsMT are involved in metal coordination.^[41,44] Different metal cluster architectures in the two metallated QsMTs (a binuclear ZnS centre in Zn-QsMT and a cubane-type cluster for Cd^{II} ions), in addition to metal centres M^{II}(Cys)₄ with a probable tetrahedral geometry have previously been suggested.^[41]

Exposure of the metal-QsMT aggregates to a 50 Gy dose [Figure 5, spectra b)] led to changes in the metal-S stretching bands suggesting the occurrence of radical-induced modifications in the metal-MT clusters. The decrease in intensity of some metal-S stretching bands, particularly evident in the Zn-QsMT spectrum (i.e., 310 and 330 cm⁻¹), indicates partial destructuring of tetrahedral metal coordination environments (Figure 5A). Also, the higher intensity of the bands in the 410–440 cm⁻¹ region indicates a higher percentage of metal-S_b-metal (S_b: bridging sulfur) bonds in both metal-QsMT aggregates, which could be attributed to a larger number of bridging Cys residues than in the native structure. On increasing the irradiation dose to 100 Gy [Figure 5, spectra c)], further changes in the bands due to S-metal vibrations confirmed that they are one of the preferential sites of reductive radical attack. For Zn-QsMT, a significant increase in intensity of the band at about 520 cm⁻¹ due to the S-S stretching mode of disulfide bridges was observed, as well as the appearance of a band at about 480 cm⁻¹ that could be due to the formation of polysulfides (S_n).^[45] These spectral modifications are in accordance with oxidation of the protein upon irradiation, which can be a consequence of partial deconstruction of the Cys-Zn clusters. Similar behaviour has been observed for rabbit Zn-MT and Zn/Cd-MT undergoing oxidative stress.^[28,46]

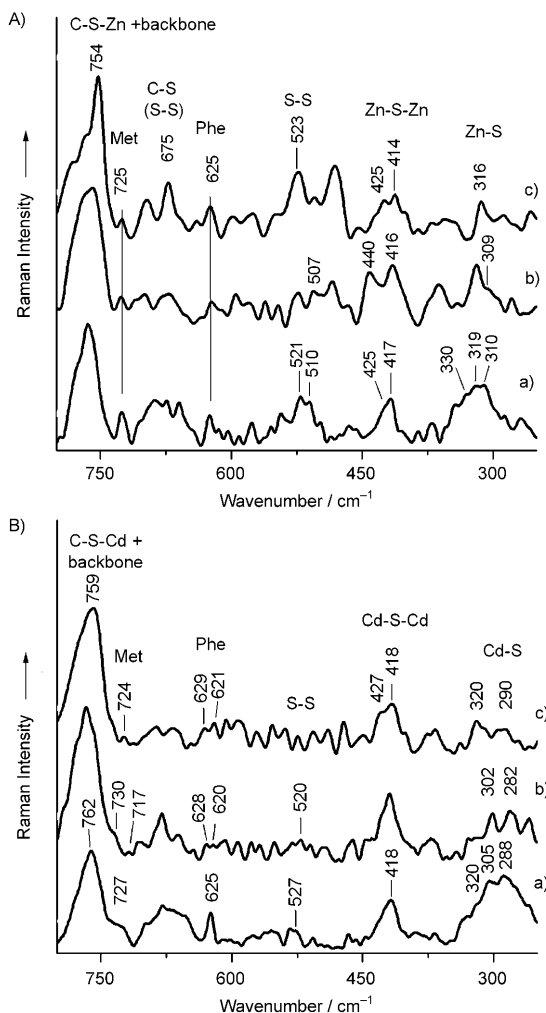


Figure 5. Raman spectra of A) Zn-QsMT and B) Cd-QsMT in the 800–250 cm^{-1} region for Ar-flushed aqueous solutions containing 0.2 M *t*BuOH at different irradiation doses: a) 0, b) 50 and c) 100 Gy.

In the primary structure of QsMT, the Met residues, which are not involved in metal binding, proved to be the most sensitive residues towards γ radiolysis when the protein binds Cd^{II} ions. In fact, after a 50 Gy dose exposure the splitting of the 727 cm^{-1} band (730 and 717 cm^{-1}) due to the C–S bonds of the Met residues was visible [Figure 5B, spectrum b)]. On the contrary, only a very weak intensity decrease of the 725 cm^{-1} band was observed in Zn-QsMT under the same conditions. It is well known that H⁺ atoms selectively attack Met.^[14] Therefore, the different sensitivity to reductive attack displayed by the Met residues of the two metallated QsMT forms is easily rationalized by taking into account the already proposed different folding of the protein when binding Zn^{II} or Cd^{II}.^[23,25] Hence, H⁺ atom attack on Met could be partially limited by the polypeptide folding in the Zn-QsMT complexes, and then other moieties could become the preferential sites of attack (i.e., metal–thiolate and/or metal–sulfide bonds). Since reductive radical attack on Met residues was recently found to yield diffusible sulfur radicals that can induce damage in cellular membranes, this

result can be related to the lower capability of Zn–QsMT to induce *cis-trans* isomerisation than Cd–QsMT (cf. Figure 2 and 3).

Analogously to Met, Phe residues are significantly attacked by reductive species only when QsMT is bound to Cd^{II}. In fact, irradiation of the Cd–QsMT complexes induced splitting of the 625 cm^{-1} band due to Phe side chain (ca. 630 and ca. 620 cm^{-1}),^[44] whereas no significant spectral changes in this band were visible in the Zn–QsMT system (Figure 5).

Distinct polypeptide folding of the Zn^{II} and Cd^{II} complexes of QsMT^[25] was also concordant with the bands afforded by the His residue of the QsMT spacer (cysteine-devoid region). The two nitrogen atoms of His are potential donors for transition metal ions, and their participation in metal-binding can be detected by using Raman marker bands, such as the C₄=C₅ stretching band. In fact, this band appears at different wavenumbers depending on the tautomeric form of His and its involvement in coordination.^[40,47–49] Eventual His participation in the metal binding was evaluated by curve-fitting analysis of the 1630–1565 cm^{-1} spectral range that allows the contribution of overlapped weak bands generated by His and Phe residues to be distinguished (see Supporting Information). This analysis revealed that 95 and 10 % of His is involved in metal binding in the Cd–QsMT and Zn–QsMT native structures, respectively, whereas His becomes completely involved in both Cd^{II} and Zn^{II} coordination after 100 Gy irradiation. Thus, the attack of reductive reactive species is able to induce a significant structural rearrangement of the metal aggregates, as indicated by the necessity of new metal ligands such as His to stabilize the overall structure of the metal–MT complexes.

Analysis of CD spectra recorded before and after irradiation can be informative if compared with the distinct CD fingerprints that recombinant Cd–QsMT preparations show, depending on the participation of sulfide ligands in Cd coordination.^[25] The variations observed in the CD fingerprint of the Cd–QsMT sample after irradiation at 50 and 100 Gy (Figure 6) suggest a decrease in Cd–SCys chromophores and an increase in Cd–S²⁻ chromophores, in agreement with Raman data. The low intensity and chirality of the CD spec-

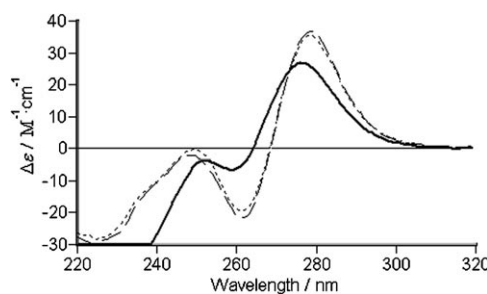


Figure 6. Comparison of the CD spectra of different recombinant Cd–QsMT preparations: Cd–QsMT before irradiation (black); Cd–QsMT irradiated at 50 Gy (dashed) and Cd–QsMT irradiated at 100 Gy (dotted) of Ar-flushed aqueous solutions containing 0.2 M *t*BuOH.

trum of Zn–QsMT^[24] precluded a parallel analysis to that made with Cd–QsMT. However, the UV/Vis spectra recorded after increasing irradiation doses also confirmed the increased number of Zn–S²⁻ chromophores in this case.

The different behaviour observed between Cd–QsMT and Zn–QsMT upon irradiation is not only explained by their different sulfide content, but also by recalling the already proposed non-isostructural^[25] of the two complexes, and consequently by assuming that the reactive species have slightly different targets. In case of Cd–QsMT the attack could enhance the occurrence of a desulfurisation process starting from sulfide ions and leading to diffusible sulphydryl radicals (HS[•]/S^{•-}). On the contrary, in the case of Zn–QsMT, the attack of reactive species seems to occur mainly on metal thiolate clusters and thus induces a significant structural rearrangement, as also indicated by the formation of new disulfide bridges, and by the necessity of new metal ligands (i.e., His) to stabilize the metal–MT aggregates (see above). This conclusion was further confirmed by the radical-induced modifications observed in the 730–800 cm⁻¹ region of the Raman spectrum, where the contribution from both the vibrational modes of the C–S bonds originating from Cys–metal bonds^[50] and the backbone vibrations are visible [Figure 5 A, spectrum c)].^[51] In particular, the appearance of a strong component at 754 cm⁻¹ in Zn–QsMT, as opposed to Cd–QsMT, indicated a relevant increase in the β-turn content of the Zn-containing aggregates after the highest irradiation dose [Figure 5, spectra c)].^[52] Thus, the contribution of this process to the formation of diffusible radical species could explain the higher capacity of the Cd–QsMT aggregates to induce *cis-trans* isomerisation than the Zn-containing complexes.

An ESI-MS analysis allowed us to establish that the attack of reductive species on Cd–QsMT leads to breaking of the protein backbone. To illustrate this, Figure 7 shows ESI-MS spectra recorded at pH 7 (Cd^{II} bound to QsMT) and at pH 2 (Cd^{II} displaced from QsMT; therefore, only apo-peptides) before and after irradiation of the Cd–QsMT samples at 100 Gy. Interestingly, ESI-MS data recorded at pH 7 clearly suggest that irradiation induces two kinds of

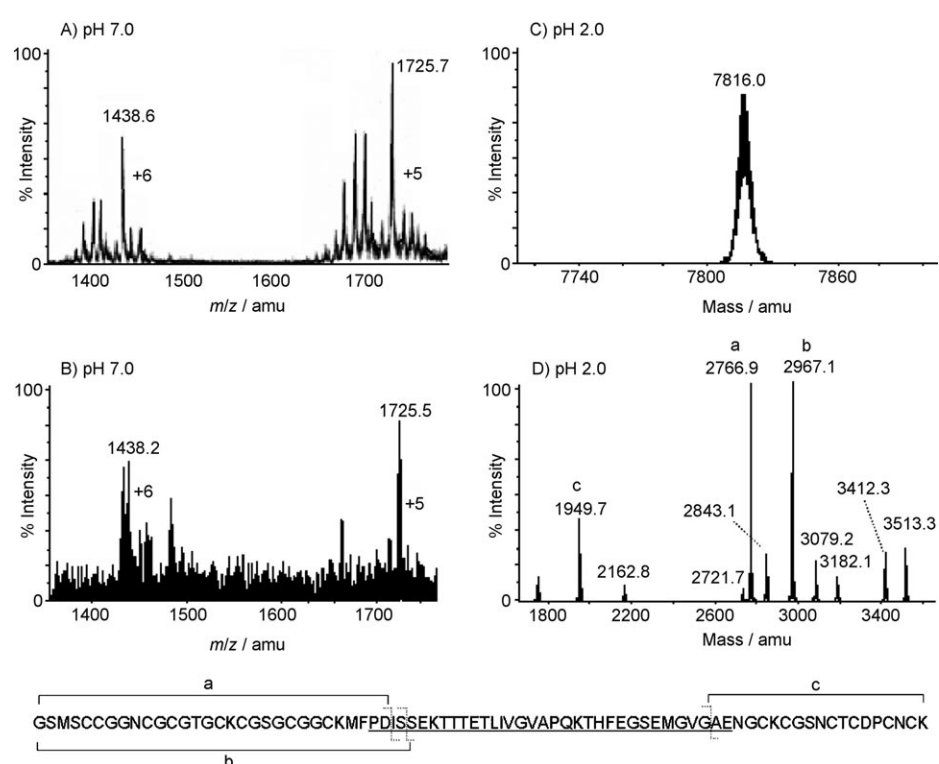
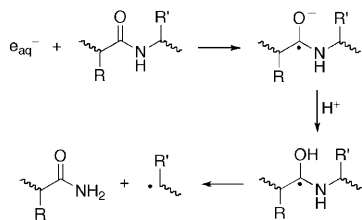


Figure 7. ESI-MS spectra at pH 7.0 (A, B) and deconvoluted spectra at pH 2.0 (C, D) of the recombinant Cd–QsMT sample before (A, C) and after (B, D) irradiation of Ar-flushed aqueous solutions containing 0.2 M *t*BuOH at 100 Gy. In A) the major species before irradiation is Cd₆S₄–QsMT (1725.7 and 1438.6 peaks with charges of +5 and +6, respectively) together with several minor species. In B), after the irradiation of the sample at 100 Gy the major species in solution is still Cd₆S₄–QsMT. In the deconvoluted spectra at pH 2.0 before irradiation (C), the species with mass 7816.0 corresponds to apo-QsMT. After irradiation at 100 Gy the deconvoluted spectrum at pH 2.0 (D) shows the resulting fragments of the protein. Letters a, b and c correspond to the most abundant fragments. Their sequences, identified by using FindPept (<http://www.expasy.org/tools/findpept.html>), are displayed at the bottom of the figure.

changes in the Cd–QsMT preparations: 1) small variations of their mass compatible with desulfurisation of some Cys or Met residues to Ala or Aba, respectively, and 2) variations in the speciation, so that only the major species (Cd₆S₄–QsMT) is resistant at 100 Gy. Moreover, ESI-MS data recorded at acid pH revealed that, even at the lowest irradiation dose (50 Gy), the protein backbone is cleaved; the stronger the irradiation, the shorter the generated peptide fragments. Analysis of the detected peptide fragments revealed that the cleavage sites can be located in the cysteine-devoid spacer, probably due to the greater exposure of this part of the polypeptide to reactive species attack. In conclusion, data at both pH 7 and pH 2 revealed that in irradiated Cd₆S₄–QsMT, the Cd–SCys bonds are precisely what maintains the integrity of the initial complex, even after breaking of some peptide bonds of the spacer. This observation nicely corroborates our previous proposal that Zn– and Cd–QsMT aggregates are folded into a hairpin rather than a dumbbell.^[25]

Cleavage of the polypeptide backbone may be due to the addition of solvated electrons to the peptide carbonyl group. In fact, in proteins the number of carbonyl groups is much higher than that of other active sites (i.e., disulfide bridges,



Scheme 3. A possible mechanism for peptide backbone breaking caused by e_{aq}^- attack.

His) and thus the probability that e_{aq}^- react with them is higher. Electron capture by carbonyl groups can give rise to a reaction similar to deamination, causing main-chain cleavage and formation of α -carbon-centred radicals (Scheme 3).^[8,9]

Conclusions

A biomimetic model of unsaturated lipid vesicle suspensions containing metal-MT complexes proved to be an effective system for studying the reaction of reductive reactive species (H^- and e_{aq}^-) with Met residues or sulfur-containing ligands. Desulfurization of these residues occurs with generation of sulfur-centred radicals, which in turn are catalysts of the *cis-trans* isomerisation in liposomes. These results help to envisage the identity of the real culprits in the endogenous formation of *trans* lipids, and thus suggest a comprehensive chemical biology approach to fully evaluate the proteomic and lipidomic changes associated with cellular stress. Tandem lipid–protein damage consists of changes in the natural *cis* lipid geometry to the corresponding *trans* isomer, together with disruption of the protein backbone and/or of the metal clusters, mutation of the protein Cys or Met amino acid residues and formation of Ala or Aba, respectively. These findings can be important in the puzzling biological questions connected to radical stress and molecular signalling derived therefrom, in particular the role of the metal-sulfur clusters in the oxidoreductive biological environment and the general antioxidant activity attributed to these ubiquitous metalloprotein structures.^[52] Other interesting relations can be found in the change in redox potential^[53] and in the mechanisms of mobilization of sulfur that are adaptation processes linked to their reactivity.^[54]

Experimental Section

Preparation and characterisation of recombinant M^{II} -QsMT aggregates ($M^{II}=Zn^{II}$ or Cd^{II}): QsMT was obtained in its Zn-, or Cd-complexed forms by heterologous synthesis in *E. coli*, followed by purification by affinity chromatography and fast protein liquid chromatography (FPLC). The clone containing the pGEX-QsMT plasmid was previously constructed as reported.^[23] Protein synthesis was performed in 6 L Lucia Bertani cultures inoculated with 600 mL of an overnight culture and grown at 37°C during 1.5 h, until an OD_{600} of 0.8–1.0 was reached. QsMT biosynthesis was induced at this moment with 100 μM isopropyl β -D-thiogalacto-

pyranoside (IPTG; final concentration), and 300 μM $ZnCl_2$ or 300 μM $CdCl_2$ was added 30 min thereafter (final concentration). Cells were grown for 3 h and lysed by sonication. From this step on, all processes were performed in Ar-saturated atmosphere. M^{II} -QsMT aggregates were purified in phosphate buffer saline (PBS $\times 1$) by batch-affinity chromatography (Glutathione-Sepharose 4B) followed by a digestion with thrombin. The resulting samples were concentrated by centrifugation with Centriprep Microcon 3 (Amicon) and subsequently purified in 50 mM Tris HCl pH 7 by FPLC on a Superdex 75 column. Selected fractions were kept at -70°C until further use. Further details of the synthesis and purification steps can be found in the literature.^[23–25]

Following the procedures already described for other MTs,^[3,24] the protein concentrations and metal-to-protein ratio of the different M^{II} -QsMT preparations were determined by inductively coupled plasma atomic emission spectroscopy (acid ICP-AES) on a Polyscan 61 E (Thermo Jarrell Ash) spectropolarimeter. The mean sulfide-to-protein ratios were estimated by GC-FPD (FDP = flame photometric detector) measurements of the sulfide content of the samples on an HP 5890 Series II gas chromatograph coupled to a FPD80 CE Instruments (Thermo Finnigan) detector, which were referred to the protein concentration measured by acid ICP-AES.^[3] The metal complexes present in the Zn-QsMT and Cd-QsMT preparations were analysed and characterised by spectroscopic and spectrometric methods. The average contents of metal ions and acid-labile sulfide (S^{2-}) of the recombinant QsMT preparations proved to be higher in Cd- than in Zn-QsMT (Table S1, Supporting Information), consistent with the previously reported data.^[23,25]

$M^{II}\text{S}$ and $M^{II}\text{-Cys}$ complexes ($M^{II}=Zn^{II}$ or Cd^{II}): ZnS and CdS were commercially available and used without further purification. The Zn^{II} -cysteine complex was obtained by mixing aqueous solutions of $ZnCl_2$ and L-cysteine in the 1/2 metal/ligand ratio following a literature method,^[55] whereas the corresponding complex with Cd is reported to be water-insoluble.^[56]

Irradiation of the M^{II} -QsMT complexes ($M^{II}=Zn^{II}$ or Cd^{II}): M^{II} -QsMT (30 μM) were prepared in aqueous 0.2 M $t\text{BuOH}$ or 10 mM phosphate buffer at pH 7. Aliquots of the solutions were transferred to different vials, flushed with $N_2\text{O}$ or Ar, and then irradiated. $t\text{BuOH}$ concentration was 2% (v/v). One of the vials was not irradiated and directly analysed spectroscopically, whereas the other vial was irradiated for different times in the range of 9–10 Gym^{-1} . Continuous radiolysis was performed by using a ^{60}Co Gammacell (Atomic Energy of Canada Ltd., Canada) at a dose rate of 10–12 Gym^{-1} . The exact absorbed radiation dose was determined with a Fricke chemical dosimeter, by taking $G(\text{Fe}^{3+})=1.61 \mu\text{mol J}^{-1}$.^[57]

Irradiation of M^{II} -QsMT, $M^{II}\text{S}$ and $M^{II}\text{-Cys}$ complexes ($M^{II}=Zn^{II}$ or Cd^{II}) in large unilamellar vesicles: Our biomimetic model of a cell membrane consisted of 1-palmitoyl-2-oleoylphosphatidylcholine (POPC) liposomes containing a *cis* monounsaturated fatty acid, in the form of large unilamellar vesicles (LUVET) approximately 100 nm in diameter, prepared by the extrusion technique.^[32–34] LUVET were prepared as previously described^[33] by using POPC in aqueous solution. Water was purified with a Millipore (Milli-Q) system. POPC-LUVET suspensions were prepared to a final concentration of 2 mM in a 4 mL vial equipped with an open-top screw cap and a Teflon-faced septum. M^{II} -QsMT, $M^{II}\text{S}$ and $M^{II}\text{-Cys}$ samples were added until a final 30 μM concentration. $t\text{BuOH}$ or phosphate buffer at pH 7 were added when necessary to respective final concentrations of 0.2 M and 10 mM. In all cases, the total volume of the reaction sample was 0.5 mL. The suspension was flushed with argon or $N_2\text{O}$ prior to γ irradiation. During irradiation, aliquots of the reaction mixture were withdrawn at various time intervals. Workup and analysis of the irradiated reaction mixture were carried out as previously reported.^[11,12,14]

Spectroscopic and spectrometric analysis of Zn- and Cd-QsMT complexes: As in previous work, a Jasco spectropolarimeter (J-715) interfaced to a computer (GRAMS/AI (7.02) Software) was used for circular dichroism (CD) determinations.^[25] Electronic absorption measurements were performed on an HP-8453 diode-array UV/Visible spectrophotometer. All spectra were recorded in 1 cm capped quartz cuvettes, and all

manipulations involving QsMT solutions were performed under argon atmosphere.

The molecular mass of the Cd–QsMT species was determined by electrospray ionisation time of flight mass spectrometry (ESI-TOF-MS) on a MicroToF-Q Instrument (Bruker), calibrated with NaI (0.2 g of NaI dissolved in 100 mL of a 1:1 H₂O:2-propanol mixture). In the ESI-TOF-MS analysis of the metallopeptides, 20 µL of the sample was injected at 40 µL min⁻¹ under the following conditions: source temperature, 150°C; desolvation temperature, 250°C; capillary-counterelectrode voltage, 3.0 kV; cone potential, 80 V. Spectra were collected throughout the *m/z* range from 950 to 2150 at a rate of 2 s per scan with an interscan delay of 0.1 s. The liquid carrier was a 10/90 mixture of acetonitrile and 5 mM ammonium acetate, pH 7. For apo-form analysis, the samples were demetalated by acidification with HCl at pH 2, and mass spectrometry was carried out as explained for the holo forms, except that the liquid carrier was a 10/90 mixture of methanol and ammonium formate/ammonia at pH 1.5. In all cases, the theoretical molecular masses were calculated according to ref. [24], except for the sulfide-containing species, for which two additional protons were added per sulfide anion.

For Raman analysis and to overcome the spectroscopic masking effect of the Tris HCl buffer in Raman and IR spectroscopy, samples were subjected to a dialysis and lyophilisation protocol prior to irradiation.^[41] 1 mL of each Zn- or Cd–QsMT sample containing 1 mg of protein was subjected to 6 h of dialysis against (200 mL) of 5 mM Tris HCl buffer pH 7 by using dialysis membranes from Medicell International (Ø 6.3 mm). The 5 mM Tris HCl solution was changed after 2 h of dialysis. Freezing at 80°C for 1 h and lyophilisation of the samples for 6 h followed the dialysis process. The resulting solid precipitates were redissolved in 200 µL of deionised water and subjected to an additional dialysis/lyophilisation cycle. The final lyophilised product was kept frozen at -80°C until analysis. Raman spectra were obtained on lyophilised samples with a Bruker IFS 66 spectrometer equipped with an FRA-106 Raman module and a cooled Ge-diode detector. The excitation source was a Nd³⁺:YAG laser (1064 nm) in backscattering configuration. The spectral resolution was 4 cm⁻¹, and the total number of scans for each spectrum 6000. The laser power on the sample was 100 mW. A linear correction brought the base line of the Raman spectra to approximately zero intensity. The derivative spectra were calculated according to the Savitzky–Golay method. Curve-fitting analysis was implemented with OPUS/IR version 2.0 program, which uses the Levenberg–Marquardt algorithm. The Raman component profiles were described as a linear combination of Lorentzian and Gaussian functions, whereas the IR components were described as Gaussian functions.

Acknowledgements

The support and sponsorship by COST Action CM0603 on “Free Radicals in Chemical Biology (CHEMBIORADICAL)” are kindly acknowledged. Work supported in part by the European Community’s Marie Curie Research Training Network under contract MRTN-CT-2003-505086 [CLUSTOXDNA]. S.A. and M.C. are indebted to the Ministerio de Educacion y Ciencia (BIO2006-14420-C02/01 and BIO2006-14420-C02/02, respectively) for financial support.

- [1] J. H. R. Kägi in *Metallothionein III, Biological Roles and Implications* (Eds.: K. T. Suzuki, N. Imura, M. Kimura), Birkhäuser, Basel, 1993, pp. 29–55.
- [2] L. Villarreal, L. Tío, S. Atrian, M. Capdevila, *Arch. Biochem. Biophys.* **2005**, *435*, 331–335.
- [3] M. Capdevila, J. Domènech, A. Pagani, L. Tío, L. Villarreal, S. Atrian, *Angew. Chem.* **2005**, *117*, 4694–4698; *Angew. Chem. Int. Ed.* **2005**, *44*, 4618–4622.
- [4] J. H. Beattie, A. M. Wood, A. M. Newman, I. Bremner, K. H. A. Choo, A. E. Michalska, J. S. Duncan, P. Trayhurn, *Proc. Nat. Acad. Sci. USA* **1998**, *95*, 358–363.

- [5] D. X. Deng, S. Chakrabarti, M. P. Waalkes, M. G. Cherian, *Histopathology* **1998**, *32*, 340–347.
- [6] G. W. Wang, Z. Zhou, J. B. Klein, Y. J. Kang, *Am. J. Physiol. Heart Circ. Physiol.* **2001**, *280*, H2292–H2299.
- [7] S. Liu, K. Kawai, V. A. Tyurin, Y. Y. Tyurina, G. G. Borisenko, J. P. Fabisiak, P. J. Quinn, B. R. Pitt, V. E. Kagan, *Biochem. J.* **2001**, *354*, 397–406.
- [8] W. M. Garrison, *Chem. Rev.* **1987**, *87*, 381–398.
- [9] C. L. Hawkins, M. J. Davies, *Biochim. Biophys. Acta Bioenerg.* **2001**, *1504*, 196–219.
- [10] S. Atrian, K. Bobrowski, M. Capdevila, C. Chatgilialoglu, C. Ferreri, C. Houée-Levin, A. M. Salzano, A. Scaloni, A. Torreggiani, *Chimia* **2008**, *62*, 721.
- [11] C. Ferreri, I. Manco, M. R. Faraone-Mennella, A. Torreggiani, M. Tambo, S. Manara, C. Chatgilialoglu, *ChemBioChem* **2006**, *7*, 1738–1744.
- [12] V. Kadlecik, C. Sicard-Roselli, C. HouPe-Levin, M. Kodicek, C. Ferreri, C. Chatgilialoglu, *Angew. Chem.* **2006**, *118*, 2657–2660; *Angew. Chem. Int. Ed.* **2006**, *45*, 2595–2598.
- [13] O. Mozziconacci, K. Bobrowski, C. Ferreri, C. Chatgilialoglu, *Chem. Eur. J.* **2007**, *13*, 2029–2033.
- [14] C. Ferreri, C. Chatgilialoglu, A. Torreggiani, A. M. Salzano, G. Reznicek, A. Scaloni, *J. Proteome Res.* **2008**, *7*, 2007–2015.
- [15] C. Chatgilialoglu, C. Ferreri, *Acc. Chem. Res.* **2005**, *38*, 441–448.
- [16] C. Ferreri, C. Chatgilialoglu, *ChemBioChem* **2005**, *6*, 1722–1734.
- [17] T. L. Roberts, D. A. Wood, R. A. Riemsma, P. J. Gallagher, F. C. Lampe, *Lancet* **1995**, *345*, 278–282.
- [18] F. A. Kummerow, Q. Zhou, M. M. Mahfouz, *Am. J. Clin. Nutr.* **1999**, *70*, 832–838.
- [19] R. N. Lemaitre, I. B. King, T. E. Raghunathan, R. M. Pearce, S. Weinmann, R. H. Knopp, M. K. Copass, L. A. Cobb, D. S. Siscovich, *Circulation* **2002**, *105*, 697–701.
- [20] D. Mozaffarian, M. B. Katan, A. Ascherio, M. J. Stampfer, W. C. Willett, *N. Engl. J. Med.* **2006**, *354*, 1601–1613.
- [21] C. Chatgilialoglu, C. Ferreri, I. N. Lykakis, P. Wardman, *Bioorg. Med. Chem.* **2006**, *14*, 6144–6148.
- [22] I. N. Lykakis, C. Ferreri, C. Chatgilialoglu, *Angew. Chem.* **2007**, *119*, 1946–1948; *Angew. Chem. Int. Ed.* **2007**, *46*, 1914–1916.
- [23] G. Mir, J. Domènech, G. Huguet, W. J. Guo, P. Goldsbrough, S. Atrian, M. Molinas, *J. Exp. Bot.* **2004**, *55*, 2483–2493.
- [24] J. Domènech, G. Mir, G. Huguet, M. Molinas, M. Capdevila, S. Atrian, *Biochimie* **2006**, *88*, 583–593.
- [25] J. Domènech, R. Orihuela, G. Mir, M. Molinas, S. Atrian, M. Capdevila, *J. Biol. Inorg. Chem.* **2007**, *12*, 867–882.
- [26] J. H. R. Kägi, Y. Kojima in *Metallothionein II, Proceedings of the 2nd International Meeting on Metallothionein and Other Low Molecular Weight Metal-Binding Proteins*, Birkhäuser, Basel, 1987.
- [27] The reaction of HO[·] radicals with MT in the absence and presence of molecular oxygen has been previously reported by radiolytic methods.^[28,29] Evidence for formation of disulfide radical anion by pulse radiolysis and formation of disulfide bridges as the main products by γ radiolysis are reported.
- [28] X. Fang, J. Wu, G. Wei, *Radiat. Res.* **1994**, *138*, 165–170.
- [29] X. Fang, J. Wu, G. Wei, H.-P. Schuchmann, C. von Sonntag, *Int. J. Radiat. Biol.* **1995**, *68*, 459–466.
- [30] G. V. Buxton, C. L. Greenstock, W. P. Helman, A. B. Ross, *J. Phys. Chem. Ref. Data* **1988**, *17*, 513–886.
- [31] A. B. Ross, W. G. Mallard, W. P. Helman, G. V. Buxton, R. E. Huie, P. Neta, NDRL-NIST Solution Kinetic Database—Version 3, Notre Dame Radiation Laboratory, Notre Dame, IN and NIST Standard Reference Data, Gaithersburg, 1998.
- [32] C. Chatgilialoglu, C. Ferreri, M. Ballestri, Q. G. Mulazzani, L. Landi, *J. Am. Chem. Soc.* **2000**, *122*, 4593–4601.
- [33] C. Ferreri, C. Costantino, L. Perrotta, L. Landi, Q. G. Mulazzani, C. Chatgilialoglu, *J. Am. Chem. Soc.* **2001**, *123*, 4459–4468.
- [34] C. Ferreri, A. Samadi, F. Sassatelli, L. Landi, C. Chatgilialoglu, *J. Am. Chem. Soc.* **2004**, *126*, 1063–1072.
- [35] J. F. K. Kramer, V. Fellner, M. E. R. Dugan, F. D. Sauer, M. M. Mossova, M. P. Yurawecz, *Lipids* **1997**, *32*, 1219–1228.

- [36] A. Torreggiani, M. Tamba, I. Manco M. R. Faraone-Mennella, C. Ferreri, C. Chatgilialoglu, *J. Mol. Struct.* **2005**, 744/747, 767–773.
- [37] A. Torreggiani, M. Tamba, I. Manco, M. R. Faraone-Mennella, C. Ferreri, C. Chatgilialoglu, *Biopolymers* **2006**, 81, 39–50.
- [38] A. Torreggiani, M. Tamba, C. Ferreri, *Protein Pept. Lett.* **2007**, 14, 716–722.
- [39] A. I. Boldyrev, J. Simons, *Mol. Phys.* **1997**, 92, 365–380.
- [40] T. Miura, T. Satoh, H. Takeuchi, *Biochim. Biophys. Acta* **1998**, 1384, 171–179.
- [41] J. Domènech, A. Tinti, M. Capdevila, S. Atrian, A. Torreggiani, *Biopolymers* **2007**, 86, 240–248.
- [42] J. Domènech, R. Bofill, A. Tinti, A. Torreggiani, S. Atrian, M. Capdevila, *Biochim. Biophys. Acta* **2008**, 1784, 693–704.
- [43] A. Torreggiani, J. Domènech, S. Atrian, M. Capdevila, A. Tinti, *Biopolymers* **2008**, 89, 1114–1124.
- [44] A. T. Tu in *Spectroscopy of Biological Systems, Vol. 13* (Eds.: R. J. H. Clark, R. E. Hester), Wiley, New York, **1986**, pp. 47–112.
- [45] C. Kraff, R. Pigorsch, B. Weber, F. Ott, S. Brennecke, G. E. Krammer, R. Salzer, *Vib. Spectrosc.* **2007**, 43, 49–52.
- [46] L. P. Thomas, G. J. Bachowski, A. W. Girotti, *Biochim. Biophys. Acta* **1986**, 884, 448–461.
- [47] A. Torreggiani, S. Bonora, G. Fini, *Biopolymers* **2000**, 57, 352–364.
- [48] H. Takeuchi, *Biopolymers* **2003**, 72, 305–317.
- [49] A. Torreggiani, A. D. Esposti, M. Tamba, G. Marconi, G. Fini, *J. Raman Spectrosc.* **2006**, 37, 291–298.
- [50] J. Pande, C. Pande, D. Gilg, M. Vasak, R. Callender, J. H. R. Kägi, *Biochemistry* **1986**, 25, 5526–5532.
- [51] S. Krimm, J. Bandekar, *Biopolymers* **1980**, 19, 1–29.
- [52] R. D. Palmiter, *Proc. Natl. Acad. Sci. USA* **1998**, 95, 8428–8430.
- [53] S. E. Iismaa, A. E. Vasquez, G. M. Jensen, P. J. Stephens, J. N. Butt, F. A. Armstrong, B. K. Burgees, *J. Biol. Chem.* **1991**, 266, 21563–21571.
- [54] B. Campanini, F. Schiaretti, S. Abbruzzetti, D. Kessler, A. Mozzarelli, *J. Biol. Chem.* **2006**, 281, 38769–38780.
- [55] S. Foley, M. Enescu, *Vib. Spectrosc.* **2007**, 44, 256–265.
- [56] O. G. Faget, J. Felcman, T. Giannerini, S. C. A. Tellez, *Spectrochim. Acta Part A* **2005**, 61, 2121–2129.
- [57] J. W. T. Spinks, R. J. Woods, *An Introduction to Radiation Chemistry*, 3rd ed., Wiley, New York, **1990**, p. 100.

Received: December 3, 2008

Revised: February 17, 2009

Published online: May 5, 2009

CHEMISTRY

A EUROPEAN JOURNAL

Supporting Information

© Copyright Wiley-VCH Verlag GmbH & Co. KGaA, 69451 Weinheim, 2009

Zinc and Cadmium Complexes of a Plant Metallothionein under Radical Stress: Desulfurization Reactions Associated with the Formation of *Trans* Lipids in Model Membranes

Armida Torreggiani,^{*[a]} Jordi Domènech,^[a,b] Ruben Orihuela,^[c] Carla Ferreri,^[a] Sílvia Atrian,^[b,d] Mercè Capdevila,^[c] and Chrysostomos Chatgilialoglu^{*[a]}

[a] Dr. C. Chatgilialoglu, Dr. J. Domènech, Dr. C. Ferreri, Dr. A. Torreggiani
ISOF, Consiglio Nazionale delle Ricerche
Via P. Gobetti 101, 40129 Bologna (Italy)
Fax: (+39)051-639-8349
E-mail: chrys@isof.cnr.it and torreggiani@isof.cnr.it

[b] Prof. S. Atrian, Dr. J. Domènech
Departament de Genètica, Facultat de Biologia
Universitat de Barcelona
Av. Diagonal 645, 08028-Barcelona (Spain)

[c] Prof. M. Capdevila, Dr. R. Orihuela
Departament de Química, Facultat de Ciències,
Universitat Autònoma de Barcelona,
E-08193 Bellaterra, Barcelona (Spain)

[d] Prof. S. Atrian
Institut de Biomedicina de la Universitat de Barcelona (IBUB),
Spain.

Table S1. Analytical Characterisation of the Zn- and Cd-QsMT preparations

Metal-QsMT	Acid ICP-AES ^a	GC-FPD
	Mean metal content	Mean sulfide content
Zn-QsMT	3.8 Zn	1.3
Cd-QsMT	5.7 Cd	2.8

^a Metal/QsMT ratio calculated from the S, Zn, Cd concentrations from acid ICP-AES measurements. The protein content, and thus the metal-to-protein ratio values, were calculated assuming that all the S measured corresponded to the 14 Cys and 3 Met residues of the QsMT polypeptide (17 mol S = 1 mol QsMT).

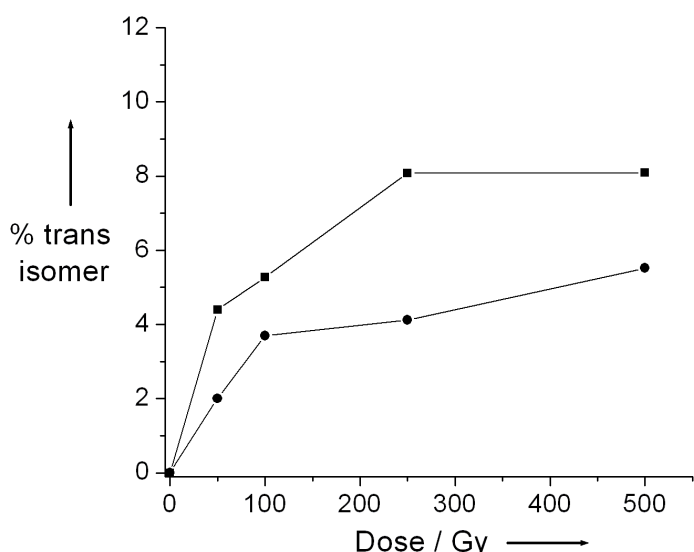


Figure S1. Dose dependence of the formation of elaidate (trans isomer) residues from γ irradiation of POPC vesicles (2 mM) containing CdS (30 μ M) in N_2O -saturated 10 mM $H_2PO_4^-$ solutions at pH 7 (■) or N_2O -saturated (●) solutions containing 0.2 M *t*BuOH.

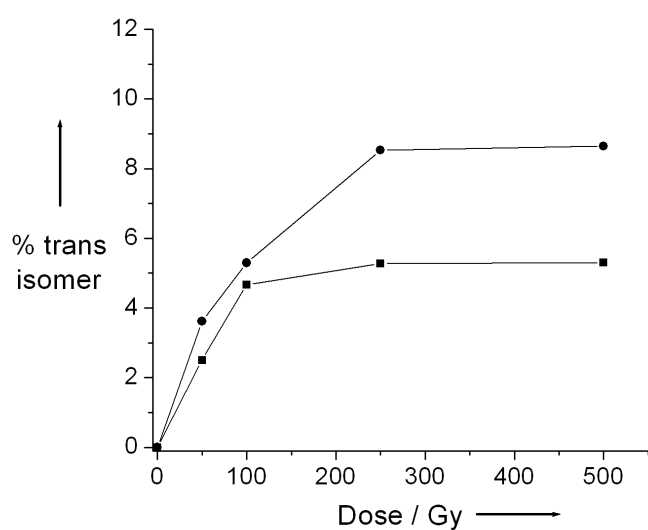


Figure S2. Dose dependence of the formation of elaidate (trans isomer) residues from γ irradiation of POPC vesicles (2 mM) containing CdS (30 μ M) in Ar-flushed 10 mM $H_2PO_4^-$ solutions at pH 7 (■) or Ar-flushed (●) solutions containing 0.2 M *t*BuOH.

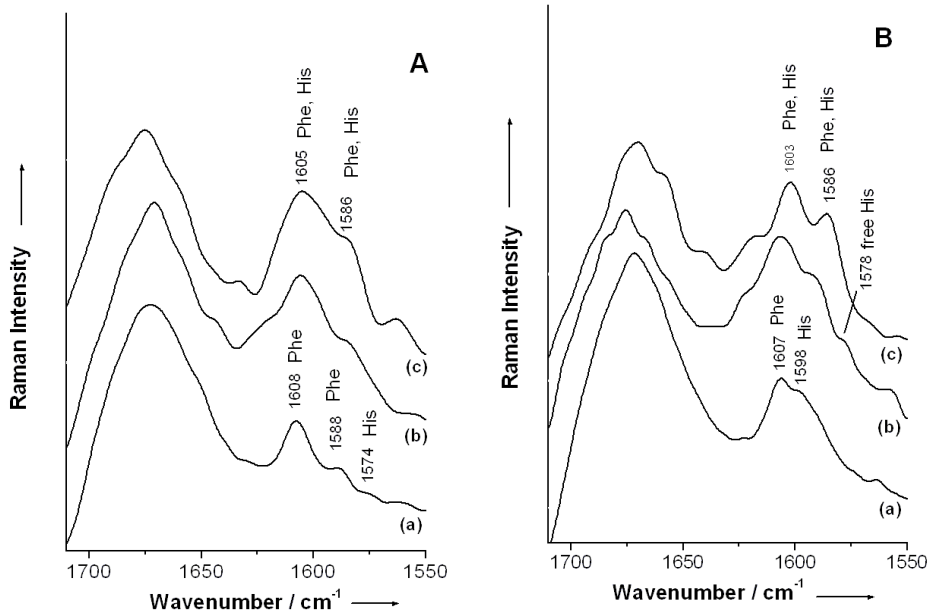


Figure S3. Raman spectra of (A) Zn-QsMT and (B) Cd-QsMT in the 1710-1550 cm^{-1} region before (a) and after irradiation exposure: 50 (b) and 100 Gy (c). If aromatic residues are present in a low percentage, as in MTs, in this spectral region it is possible to identify the weak band due to the C=C stretching vibration of His residues, whose frequency is strongly dependent by the tautomeric form of His (tautomer I or II, also referred as $\text{N}_\tau\text{-H}$ or $\text{N}_\pi\text{-H}$) and its involvement in metal ion chelation

RELACIÓ DE TAULES

1. Introducció

Taula 1.- MTs amb l'estructura tridimensional inclosa en el PDB.	6
Taula 2.- MTs de planta	10

3. Resultats i discussió

3.1 Estudi de la capacitat coordinant de la metal-lotioneïna MeMT del mol·lusc *M.edulis*

Taula 3.- Dades de la síntesi de MeMT en medis rics en Zn(II) i Cd(II)	33
Taula 4.- Dades de les síntesis de MeMT en medis rics en Cu(II)	35

3.2 Estudi de la capacitat coordinant de la metal-lotioneïna QsMT de l'alzina surera *Q.suber*

Taula 5.- Dades de la síntesi de QsMT, N25-C18, N25 i C18 en medis rics en Zn(II)	38
Taula 6.- Dades de les síntesis de QsMT i N25-C18 en medis rics en Cd(II)	38
Taula 7.- Dades de la síntesi de N25 i C18 en medis rics en Cd(II)	41

3.3 Estudi de la capacitat coordinant de les metal-lotioneïnes CeMT1 i CeMT2 del nematode *C.elegans*

Taula 8.- Dades de la síntesi de CeMT1, NtCeMT1 i CtCeMT1 en medis rics en Zn(II) i Cd(II)	44
Taula 9.- Dades de la síntesi de CeMT2, NtCeMT2 i CtCeMT2 en medis rics en Zn(II) i Cd(II)	46
Taula 10.- Dades de la síntesi de CeMT1, NtCeMT1 i CtCeMT1 en medis rics en Cu(II)	48
Taula 11.- Dades de la síntesi de CeMT2, NtCeMT2 i CtCeMT2 en medis rics en Cu(II)	49
Taula 12.- Dades de la síntesi de CeMT2 i Δ HisCeMT2 en medis rics en Zn(II) i Cd(II)	51
Taula 13.- Dades de la síntesi de CeMT2 i Δ HisCeMT2 en medis rics en Cu(II)	51
Taula 14.- Resultats dels experiments d'incubació de MTs amb DEPC	53

3.4 Estudi de la capacitat coordinant de la metal-lotioneïna Cup1 del llevat *S.cerevisiae*

Taula 15.- Dades de la síntesi de Cup1 en medis rics en Zn(II) i Cd(II).	55
Taula 16.- Dades de les síntesis de Cup1 en medis rics en Cu(II)	57

3.5 Estudi del comportament de les metal-lotioneïnes envers l'estrés reductor

Taula 17.- Caracterització de les metal-lotioneïnes natives Cd-Cup1	59
---	----

3.6 Vers una nova proposta de classificació de les MTs

Taula 18.- Esquema de la gradació de les MTs	67
Taula 19.- Propietats comparades de les Zn-tioneïnes i les Cu-tioneïnes genuïnes	69

RELACIÓ DE FIGURES

1. Introducció

Figura 1.- Esquema general d'obtenció i purificació d'una proteïna recombinant	5
Figura 2.- Estructura tridimensional de MTs enllaçades a ions divalents	7
Figura 3.- Estructura tridimensional de Cu ₈ -Cup1 de llevat	8
Figura 4.- Agregats metall-proteïna de les fitoquelatines	9
Figura 5.- Espectres de DC representatius de Cd-MTs amb lligands sulfur	12
Figura 6.- Representació esquemàtica del cicle redox proposat per a les MT	14
Figura 7.- Alineament de les seqüències de les MTs de <i>M.edulis</i> i <i>M.galloprovincialis</i>	16
Figura 8.- Connectivitat dels clústers metall-MT de Cd ₇ -MT10 de <i>M.galloprovincialis</i>	17
Figura 9.- Models estructurals proposats per a les MTs de planta	19
Figura 10.- Alineament de les seqüències de CeMT1 i CeMT2	20
Figura 11.- Alineament de les seqüències de Cup1 i Crs5	22

3. Resultats i discussió

<i>3.1 Estudi de la capacitat coordinant de la metal-lotioneïna MeMT del mol·lusc <i>M.edulis</i></i>	
Figura 12.- Espectres de DC de la MT10 de <i>M.galloprovincialis</i> i de <i>M.edulis</i>	33
<i>3.2 Estudi de la capacitat coordinant de la metal-lotioneïna QsMT de l'alzina surera <i>Q.suber</i></i>	
Figura 13.- Estructura primària de QsMT, N25 i C18	37
Figura 14.- Espectres de DC de Cd-N25-C18 i Cd-QsMT	39
Figura 15.- Expressió de QsMT, N25-C18, N25 i C18 en soques de llevat	39
Figura 16.- Espectres de DC de les acidificacions de les produccions de Cd-QsMT	40
<i>3.3 Estudi de la capacitat coordinant de les metal-lotioneïnes CeMT1 i CeMT2 del nematode <i>C.elegans</i></i>	
Figura 17.- Estructura primària de CeMT1, CeMT2, i els seus pèptids derivats	43
Figura 18.- Alineament de les seqüències de CtCeMT1 i CtCeMT2	50
Figura 19.- Esquema de la reacció entre el DEPC i la histidina	50
<i>3.4 Estudi de la capacitat coordinant de la metal-lotioneïna Cup1 del llevat <i>S.cerevisiae</i></i>	
Figura 20.- Variacions espectroscòpiques i espectromètriques de Cd-Cup1 amb el temps	56
Figura 21.- Esquema general de les purificacions de la MT Cd-Cup1 nativa	58
Figura 22.- Espectres de DC de Cd-Cup1 nativa i recombinant	60

3.5 Estudi del comportament de les metal-lotioneïnes envers l'estrès reductor

Figura 23.- Esquema general dels danys produïts per radicals reductors	61
Figura 24.- Radiòlisi de l'H ₂ O i mecanisme de reacció de la <i>trans</i> -isomerització	62
Figura 25.- Esquema general dels diferents experiments realitzats amb radicals i MTs	63

3.6 Vers una nova proposta de classificació de les MTs

Figura 26.- <i>Trans</i> -isomerització del POPC produït per Zn-QsMT i Cd-QsMT	64
Figura 27.- Alineament de les seqüències de HpCuMT i HpCdMT	70

